MANTÆ

The Next Generation Firefighting Aircraft

Group 24

Technische Universiteit Delft

TU Delft

This page is intentionally left blank.

MANTÆ

The Next Generation Firefighting Aircraft

by

Group 24

Controlled copies	Name	Organisation
Tutor	P. Lancelot	ASCM
Coaches	D. Van Baelen	C&S
	M. Nijemeisland	NOVAM
Teaching Assistant	M. Seoane Álvarez	
All members of group 24	I. H. de Boer	4499034
	P. A. Decormis Leon	4661486
	H. H. Erwich	4543696
	D. J. Hélant Muller	4357019
	F. V. Hoogeboom	4553462
	L. M. Middendorp	4559649
	M. A. J. Maurer	4683455
	J. N. P. Post	4363426
	H.M. Rutten	4466446
	K. B. Wessendorp	4651162

Change Record

Issue	Date	Pages affected	Brief description of change
1	June 22, 2020	all	Draft
2	June 26, 2020	all	Final

Project duration: April 20, 2020 – July 2, 2020

TU Delft

Preface

This report is the final of four reports on the design of a Next Generation Firefighting Aircraft to be delivered for completion of the Design Synthesise Exercise, also known as the DSE. The DSE is the final project for students concluding their Bachelors degree in Aerospace Engineering at the Delft University of Technology.
After a short overview of the project given in Chapter 3, the detailed design is explored on a subsystem basis. Readers especially interested in the performance of the design compared to existing aircraft can find this in Chapter 2. Moreover, the operation and capabilities of the design are explained in Chapter 15.
The group would like to thank our tutor Paul Lancelot and coaches Dirk Van Baelen and Marlies Nijemeisland for their valuable guidance and advice throughout the project. In addition, we would like to thank our teaching assistant María Seoane for her help and insight. Finally, we would like to thank Marcel Pond from Conair Aerial Firefighting for providing helpful information.

Group 24

Delft, June 26, 2020

Executive Overview

Forest fires are one of the most destructive forces and pollution source on the planet. The steady increase in temperatures due to climate change has a dangerous effect on nature. Wildfire increase in frequency and in size. People, flora, fauna and infrastructure can be affected by these fires.

Aerial fire fighting is a very effective way of battling large forest fires that cannot be contained by a ground brigade alone. To tackle this problem the MANTÆ is designed. The **M**ulti-purpose **A**mphibious **N**ext-Generation **T**actical **A**erial **E**xtinguisher has as main mission to be able to outperform and replace an ageing fleet, to improve aerial support during firefighting operations. In this report, a walk through the design process of the MANTÆ is explained. This includes detailed analyses of the relevant systems and subsystems, as well as an operations and manufacturing description and a cost estimation for the final product. This executive overview summarises the main design decisions and their conclusions.

Market Analysis

An overview of all the wildfires in the world was shown in the market analysis. Over the past few years more regions have become susceptible to wildfires, while regions that were already susceptible have been hit by more extensive fires. A map of airports and water sources was also shown to relate water scooping workflows to different regions of the world. Next firefighting tactics were discussed. A common misconception is that waterbombers directly extinguish fires. In reality these aircraft mostly support firefighters on the ground by laying down firelines. There are multiple tactics for this which are discussed. Finally the performance of the main competitors of the MANTÆ ; the Canadair CL-415, The Beriev Be-200 and the ShinMaywa US-2, was laid out.

Project Overview

The project consists of six phases: project organisation, project familiarisation, concept development, trade-off phase, detailed design and closing out phase. The phase described in this report is the detailed design phase, containing the design and integration all the relevant subsystems. In the previous phase, a number of viable concepts were analysed and traded off against each other to come to a superior design. The winning design was a blended wing body amphibious aircraft, with propellers as propulsion. The subsystems of this design have to adhere to a number of requirements set by the stakeholders and the team. These requirements were translated into a functional analysis of the systems. A functional flow diagram along with a functional breakdown structure help visualise the necessary functional outcome of the systems. A Gantt chart was constructed to provide a detailed planning for all the required tasks during the design process.

Wing Fuselage

The primary structure for the aircraft is the wing/fuselage combination. Since the aircraft is a blended wing body, the wings are now referred to as the outer wings and the fuselage is refereed to as the inner wing. A preliminary sizing already provided a geometry for the inner and outer wing, after which a Class I weight estimation could be done to find an estimate for the MTOW and OEW. The Class I estimation is used as an input for the Class II weight estimation, which outputs the weight of the operational items and weight penalties for the special structure of blended wing bodies. To provide proper support for the entire aircraft, the inner and outer wing are connected through a wing box construction. The wing box comprises of 3 continuous spars, ribs, stringers and skin. The weight of these components are obtained after calculating all the stresses the structure has to endure, design eventually for the ultimate load factor the aircraft will experience. The weight penalty for the blended wing body was added to the weight of the inner wing to come to the total airframe mass, which is later used for the stability.

Hull Design

The hull has been designed to work in both the hydrostatic and the hydrodynamic regimes. In the hydrostatic regime the hull is ruled purely by displacement and must displace the same amount of water as its own weight. This lead to a displacement of $59 m^3$. Once the plane begins to pick up speed the hull will transition from displacement to planing; the hydrodynamic regime. While planing only the underside of the hull will be in contact with the water, producing hydrodynamic lift. A step was added to the hull to make the transition from planing to flying easier. Unlike older flying boats the step on the aircraft is a straight fairing instead of a direct step, decreasing aerodynamic drag.

Extinguishing System

The general idea of the extinguishing system is based on water scooping (also called water skimming). By extending probes down from the bottom of the aircraft water can be redirected upwards into the water tanks, while the thrust provides a forward velocity. When the tanks are full the pilot retracts the probes and the aircraft takes off. The design contains four water tanks. The whole system is 3.5 metres wide and have a length of 4.5 metres. Next, the height of the tanks will be ranging between 1 and 1.5 metres to provide a total 15019.6 litres per drop.

For fire line construction the choice of retardant is significant. Retardant can be categorised into: long-term retardants, foams and water enhancing gels. The candidates are 'Phos-Chek MVP-FX', 'Phos-Chek WD881' and 'Thermo-Gel 200L' respectively. Foams and water enhancing gels provide better properties to suppress fire whereas long-term retardants stand out since long-term retardant have the capability to extinguishing fire. Depending on which retardant is used the additional cost per drop can differ between 90 to 8000 euro. To benefit the amphibious properties of the aircraft, the retardant is bought as concentrate and mixed via eight access hole that penetrate through the cabin flow. Water is effective for direct attacks at low cost and environmental impact. But to make efficient fire lines, retardant are more effective. However this increases cost and impact on the environment. Since this choice for water or retardant is dependent on the mission and operative region the tank design is adapted for retardant addition.

The material used for the tanks is Al 2024 T4 for its high strength and low weight properties. Additional structural plate are is installed inside the tank to prevent negative effect on stability caused by baffling water. Other features are overflow tanks for better scooping and dropping performance. Next, the tanks can be refilled at the airport by ground-fill adaptors. Lastly, each tank will contain its own probe, so choice can be made for only filling the inboard tanks and leaving the outboard tanks empty.

Propulsion

The propulsion system of the aircraft consists of four turboprop engines. These four engines must deliver the required shaft power to perform in cruise, climb, take-off and manoeuvring. With a tool that determines what power is required in each of these cases the feasible engine options are obtained. However, from these engines some perform better than others in terms of power to cost, power to mass and power to volume performance. Performing a trade-off of these options it is determined that the Pratt & Whitney P150A engine is the best turboprop engine for the design. Along with this engine the Dowty R408 propeller system is used. This is the same powerplant used in other aircraft such as the Q400 and Antonov AN-132.

Using this powerplant the fuel consumption at different stages of the operation is determined. This fuel performance allows the aircraft to meet its performance requirements such as water delivery, cruise range and ferry range. From a sustainability perspective, the engine contributes to two main sources of pollution: noise and emissions. The powerplant has proven to emit low noise levels, as seen with aircraft using it, comparatively to jet aircraft, which are usually less noisy than turboprop aircraft. The engine is also proven to fly on bio-fuels such as Camelina HRJ. Finally, a risk analysis including mitigation strategies for the most likely failures to occur during the operation of the turboprop engine is performed.

Aerodynamics

The aerodynamics of the aircraft are integral to many its subsystems, therefore a careful analysis of the aerodynamic characteristics is essential. Using an automatised analysis for the airfoil and planform selection, the Wortmann FX69-274 airfoil is chosen for integration in the inner wing and the Martin Hepperle MH78 airfoil is used for the outer wing.

Stability and Control

According to requirements **FFA-CTRL-001** and **FFA-CTRL-002**, the aircraft shall be controllable and stable. A controllable aircraft is ensured by the control surfaces on the aircraft capable of adjusting the pitch, roll and yaw angle of the aircraft.

Ground stability is assured by correct placement of the landing gear. The landing gear itself will be capable of folding into the aircraft during flight. Furthermore, requirement **FFA-GRO-001** requires the aircraft to have a turn radius of a maximum of $20m$. This requirement is also fulfilled.

Static stability is also ensured, by having the centre of gravity always in front of the neutral point. Dynamic stability is, however, not guaranteed. Therefore, a full state feedback loop is introduced, that makes the aircraft stable by using the control surfaces on the aircraft.

Communication

Communication is an essential part of aviation. It does not only include voice and data communication from the aircraft to other relevant parties, but also the exchange of data between the systems and subsystems of the aircraft. Most of the hardware for communication can be found in the cockpit, where there is a system of interconnected avionics. The avionics include means for voice and data communication, navigation, flight management, collision avoidance, data storage and data processing. All data is gathered through sensors, antennas and transceivers, that are fitted on the outside and inside of the aircraft. After processing the data, an output can be shown through the pilots via the glass cockpit after which then can give new inputs to the flight controls, or the fly-by-wire system can make slight stability adjustments without human input.

Performance

The performance of the aircraft in firefighting scenarios is heavily dependent on the minimum speed at which the aircraft can be operated. The stall speeds were recalculated to take into account all aerodynamic effects of the BWB aircraft, including the occurrence of ground effect when approaching the water. Although the stall speed in clean

configuration had less than 2% deviation from the initial estimate, the stall speed in takeoff and landing configuration was reduced by 14% due to the addition of belly flaps. This means a safe skimming speed of 52.7m/s and a drop speed between 65m/s and 70m/s. The water delivery per hour of operation was evaluated for five different mission scenarios, with an overall performance of 31500L/h for the primary mission delivered over a total of 10 drops. The manoeuvrability of the aircraft has also been evaluated, yielding a turn radius of 288.5m and a rate of descent of at least 23.94m/s at drop speed.

Approach to Sustainability

Sustainability is a very important aspect of any design that satisfies all stakeholders of the design. These stakeholders can be assigned to three categories: Social, economical and environmental. It is important that all these must be satisfied for a design to be successful. In the current aircraft design, many steps have been taken to ensure a sustainable design. These include the possibility to perform secondary missions (search & rescue, medical evacuation or cargo transport) and a well known propulsion system for easy maintenance that is capable to run on bio-fuel. Finally, it is worth mentioning that there are some things to improve upon in the future. This includes a thorough analysis of the production of the aircraft, a revised hull design and the use of more reusable materials.

RAMS Characteristics

There are four characteristics of the aircraft which must be analysed to determine whether the aircraft is not only feasible, but also satisfies the requirements and objective. These are reliability, availability, maintainability and safety. In order to achieve a reliable and safe design redundancy in fail prone components is used. This makes for a fault tolerant design which, in the case of failure of a component, is able to still be fully operational. At the same time, this characteristic of the design makes it more available, meaning that it is operational and ready to perform a mission much more than the time it spends under maintenance or in-operational for another reason. To achieve this high availability and maintain safety standards the design is highly maintainable. This is reached through modular components and a set of preventive maintenance procedures. This prevents the failure of parts which would require a longer time under a corrective maintenance. The use of a well-known power-plant and other characteristics allow the aircraft to be widely deployable and maintain a safe and reliable operation.

Risk Assessment

For a safe and reliable design the risk assessment is performance. The main risks were first determine into their categories. Then each risk was rated on likelihood of occurrence and impact together the amount of risk which is the multiplication. To reduce the risk either the likelihood or impact can be decreased. Risk mitigation is performed to reduced the amount of risk. Scenarios that retain to pose high risk are related to smoke, collision on waterways and failures that are caused by corrosion.

Operations and Manufacturing

As the aircraft is multipurpose, different operations had to be specified. Takeoff and landing operations for both water and airfield operations were specified. Special care was taken to describe limiting cases like STOL, soft airfields, crosswind, and high waves. Furthermore the operations during all missions; firefighting, ferrying, search and rescue, medical evacuation and transporting cargo were described. Firefighting was discussed in more detail relative to the other missions as this is the primary mission of the aircraft. Firefighting mission phases include cruise, scooping, and the drop of the payload. Ground operations were also discussed. These include startup procedures and checklists, refilling and refuelling, and maintenance. Finally the delivery of aircraft and what happens at the end of the aircraft's lifetime were laid out.

Careful consideration of existing manufacturing equipment and knowledge will have to taken to ensure optimal production efficiency. Assuming everything will be built "in-house", use of large expensive machinery will need to be minimised, such as by extensively using stamped parts and rolled sheets, which can all be made with the same machines irrelevant of their size. Assembly of the parts should be done using rivets if those parts will not need to be disassembled during the service life of the aircraft. In areas that require regular maintenance, bolts should be used to allow the parts to be removed and reattached with only basic tooling. If possible, outsourcing the production or treatment of certain parts should be evaluated, as this can improve part quality and decrease cost and weight. The disadvantages of outsourcing can be reduced by carefully choosing the location of the factory to be close to workshops or adequate transportation systems.

Resource Allocation

The resource allocation consists of a weight and cost breakdown. After a Class I weight estimation, purely based on statistics of amphibious aircraft and passenger blended wing bodies, a maximum take-off weight of 54000kg and a planform was established. After designing components of the aircraft a more precise weight was estimated, resulting in a final maximum take-off weight of 59000kg, which is a 8% increase. This is expected as there was insufficient data on aircraft of similar design as it is one of the first amphibious blended wing bodies. Next to a weight breakdown, a cost estimation was also performed. Similar to the weight estimation, a Class I cost estimation was made based on method described in [1] and a cost of 39 million euro was estimated. However, this method is based on conventional

aircraft. Therefore a more detailed cost estimation is performed. This included manufacturing, material (including the airframe, propulsion, avionics and electronics), operation and maintenance cost. A final cost of the aircraft was determined to be 20.5 million euro. After looking at the market of the CL-415 an Beriev 200 it was estimated that 40 MANTÆ are needed in 20 years. However, to avoid bankruptcy a market price of 38 million euro was determined to break even when selling 22 aircraft. Finally the performance-to-cost ratio of the aircraft was compared to its main competitors and it was found to outperform them at ranges less than 400 km.

Sensitivity Analysis

A sensitivity analysis was performed by considering a different airfoil used for the centre section, as well as an increase in manufacturing costs. These have been chosen since they are parameters that would likely still change as the design process develops. Use of the MH78 airfoil instead of the Workman69 resulted in benefits of low speed performance, however stability issues hinder the benefits of the airfoil and introduce other difficulties for the pilots.
Additionally, after implementing an increase in manufacturing costs of 50%, the MANTÆ aircraft still performs better than its competitors for the main mission of 250 km to water and 30 km to the water source.

Verification and Validation

With a final design developed for the firefighting aircraft, it is necessary to determine whether it meets the requirements set out and if it can perform the required mission. Through design review and analysis methods the design is found to meet all subsystem, system and stakeholder requirements. The aircraft is able to meet the performance, safety & reliability, cost, sustainability, control and other parameters which are presented on a compliance matrix. Validation of the design must be carried out by performing a wind tunnel test, since no other BWB amphibious aircraft have been built or tested to validate the design.

Conclusion

Figure 1 shows the final design of this project: the MANTÆ. It is able to deliver $31,000 L/h$ of water or a retardant mix to a fire that is situated $250 km$ from the main base and $30 km$ from the nearest useable water source. It has the ability to operate in remote areas with small runways and has an operational range of $2184 km$. The ferry range is $5224 km$, allowing the aircraft to be deployed anywhere in the world in less than a week. Next to the main fire fighting mission, the aircraft also has secondary mission capabilities. The long operational range can aid in search missions. For medical evacuation, there is enough space to install a medical bay and a rescue rib can also be included for rescue missions.

The performance of the MANTÆ compared to its competitors is very good. It has a very high water delivery rate, a large retardant capacity and a higher performance-to-cost ratio than the well known CL-415.

While this report concludes the final design, there are some recommendations for further analysis of this aircraft. The powerplant can be up for review if turbofan engines become a more common option for mass production. The design of the hull was done with a minimal amount of knowledge on hydrostatics and -dynamics. Without a time constraint, further analysis could be done for different configurations like a catamaran or trimaran. The use of AVL for the airfoil choice does not take into account flow separation, which decreases the accuracy of results and could have causes preliminary elimination of suitable airfoils.

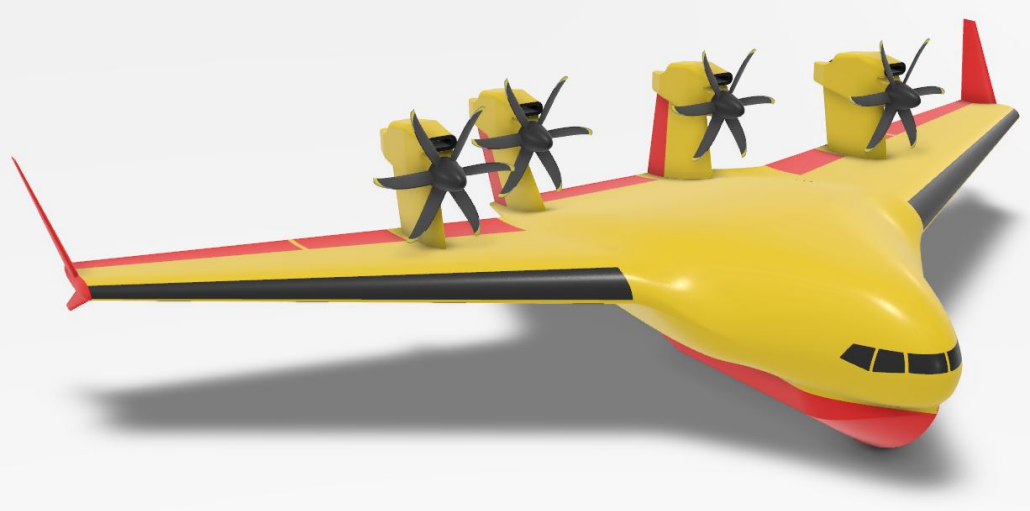

Figure 1: Final design

Contents

Nomenclature

List of Abbreviations

ATC	Air Traffic Control
ADS-B	Automatic Dependent Surveillance-Broadcast
AHRS	Attitude and Heading Reference System
AVL	Athena Vortex Lattice
CML	Continous Mold-line Link
CVDR	Cockpit Voice and Data Recorder
DME	Distance Measuring Equipment
EFIS	Electronic Flight Instrument System
FBS	Functional Breakdown Structure
FFD	Functional Flow Diagram
FMS	Flight Management System
GLONASS	GLObalnaja NAvigatsionnaja Spoetnikovaja Sistema
GNSS	Global Navigation Satellite System
GPS	Global Positioning System
HF	High Frequency
HUD	Head-Up Display
ILS	Instrument Landing System
MANTÆ	Multi-purpose Amphibious Next-generation Tactical Aerial Extinguisher
MNS	Mission Need Statement
MTOW	Maximum Take-Off Weight
OEW	Operational Empty Weight
POS	Project Objective statement
TAWS	Terrain Avoidance and Warning System
UHF	Ultra High Frequency
VHF	Very High Frequency
VLM	Vortex Lattice Method

List of Symbols

a	acceleration
A	Area
α	Angle of attack
$\dot{\alpha}$	Time derivative of angle of attack
$\bar{A}$	State space state matrix
ac	Aerodynamic centre
A_{CL}	State space closed loop state matrix
A_p	Contact area of tire with the ground
AR	Aspect Ratio
b	length between two boom points
$\bar{B}$	State space input matrix
B	Track width
β	Side-slip angle
$\dot{\beta}$	Time derivative of side-slip angle
B_i	Boom area of point i
B_{max}	Maximum track width
B_{min}	Minimum track width
C	Capacity
c	chord
$\bar{C}$	State space output matrix
C_D	Drag coefficient
C_{D_0}	Zero-lift drag coefficient
cg	Centre of gravity
CGR	Climb gradient
C_L	Lift coefficient
C_{m_α}	Derivative of moment coefficient w.r.t. the angle of attack
$C_{m_{c/4}}$	Moment coefficient at quarter chord
c_P	Specific fuel consumption propeller engine
$c_{P_{eq}}$	Equivalent specific fuel consumption for a propeller engine
d	Diameter of tire
D	Drag
$\bar{D}$	State space feed-through matrix
δ_a	Aileron deflection angle
Δ_α	Change in angle of attack
Δ_β	Change in side-slip angle
δ_e	Elevator deflection angle
δ_r	Rudder deflection angle
$\dot{\delta}$	Deflection rate
D_e	Hourly water delivery
d_{fire}	Distance from base to the fire
$\frac{d\theta}{dz}$	The angle of twist
ds	the length of the intragrated section
d_{water}	Distance from the fire to a water source
dx	Devitation in x-direction from the leading edge
dz	Deviation in z-direction from the camberline
e	Oswald efficiency factor
η_j	Propulsive efficiency
η_p	Propeller efficiency
$\dot{\phi}$	Time derivative roll angle
$F_{actuator}$	Actuator force
$F_{aerodynamic}$	Aerodynamic force
f_{power}	Power setting during cruise
f_{thrust}	Thrust setting during cruise
$f_{weight_{land}}$	Weight fraction between take-off and landing
$f_{weight_{cruise}}$	Weight fraction between take-off and cruise
g	Gravitational acceleration
G	Shear Modulus
H	Distance between the Z-coordinate of the centre of gravity and the ground
θ	Pitch angle
$\dot{\theta}$	Time derivative of pitch angle
$H_\#$	Vertical length as defined in fig. 4.13
I_{ii}	Moment of Inertia
J	Propeller advance ratio
k	Specific fuel consumption factor
K	Gain vector
L	Lift
$L_\#$	Horizontal length as defined in fig. 4.13
$L_{actuator}$	Moment arm actuator
$L_{aerodynamic}$	Moment arm aerodynamic force
l_{rib}	ribspacing
M_1	Mass before dropping
M_2	Mass after dropping
M_a	Longitudinal distance between main landing gear and most aft centre of gravity position
MAC	Mean aerodynamic chord
M_f	Longitudinal distance between main landing gear and most forward centre of gravity position
M_{ff}	Fuel fraction
M_{MTO}	Take-off mass
n	Load factor
N	Number of engines
n_{man}	Manoeuvring load factor
$n.p.$	Neutral point
N_{trips}	Number of trips between fire and water source

p	Yaw rate
$\dot{p}$	Time derivative yaw rate
ρ	Air density
P_a	Power available
P_{br}	Shaft power
$P_{br_{TO}}$	Maximum take-off shaft power
P_{eq}	Equivalent power
P_{nose}	Loading on nose landing gear
P_{TO}	Take-off power
q	Pitch rate
$\dot{q}$	Time derivative pitch rate
q_{b_i}	Shear flow in an open section
$\frac{q_H}{S}$	Shear flow as defined in fig. 4.14
$\bar{q}_D$	Dynamic pressure at design diving speed
q_{s_i}	Shear flow due to shear
q_{T_i}	Shear flow due to torque
r	Roll rate
$\dot{r}$	Time derivative roll rate
$rate_{refill}$	Refill rate on airports
R_{jet}	Cruise range jet aircraft
$R_{operational}$	Operational range
ROC	Rate of Climb
$R_{propeller}$	Cruise range propeller aircraft
R_r	Rim radius of tire
$R_{turn_{ground}}$	Ground turning radius
S	Wing surface area
σ	Structural stress
σ	Air density ratio
s_a	Airborne take-off distance
SF	Safety Factor
s_g	Ground take-off distance
S_{land}	Landing distance
$S_{take-off}$	Take-off distance
t	thickness
τ	Shear stress
T_j	Jet thrust
T_{MBM}	Mean Time Between Maintenance
T_{MF}	Mean Time Between Failures
$T_{mission}$	The total mission time
T_{MLD}	Mean Logistics Down Time
T_{MTM}	Mean Time To Maintain
T_{MTR}	Mean Time To Repair
TOP	Take-off parameter
T_{TO}	Take-off Thrust
$\frac{T}{W}$	Thrust loading
u	Forwards velocity in body reference frame
$\dot{u}$	Forwards acceleration in body reference frame
$\bar{u}$	Input vector
Δ_u	Change in forward velocity in body reference frame
υ	Poison ratio
V	Velocity
V_0	Free-stream velocity
V_2	Minimum Climb speed
$V_{approach}$	Approach speed
V_{cruise}	Cruise speed
$V_{landing}$	Landing speed
$V_{no-load}$	No-load speed of an actuator
$V_{stall_{take-off}}$	Take-off stall speed
$V_{stall_{land}}$	Landing stall speed
$V_{stall_{clean}}$	Clean configuration stall speed
$V_{take-off}$	Take-off speed
V_z	The shear force in the z direction
w	Width of tire
w	Upwards velocity in body reference frame
$\dot{w}$	Upwards acceleration in body reference frame
W_{api}	Air-conditioning and anti-icing system weight
W_{aux}	Auxiliary gear weight
W_{els}	Electronic system weight
W_f	Fuel weight
W_{fc}	Flight control system weight
W_{fur}	Furnishing weight
W_{hps}	Hydraulic and pneumatic system
W_{MTO}	Maximum take-off weight
W_{OE}	Operative empty weight
W_{ox}	Oxygen system weight
$\frac{W}{P}$	Power loading
$W_{pl_{max}}$	Maximum payload weight
W_{pt}	Paint weight
$\frac{W}{S}$	Wing loading
W_{TO}	Take-off weight
$\bar{x}$	State vector
$\dot{x}$	Time derivative of state vector
$X0$	Initial disturbance vector
x_{cg}	X-position of the mean aerodynamic chord
$X_{min_{main}}$	Most forward allowable position main landing gear
$\bar{y}$	State space output vector
$\frac{dW_p}{dR}$	Change in payload with a change in range
$\angle_{rotate}$	Rotation angle of nose wheel

1 Introduction

In recent years, forest fires have been increasing and growing.[1,2] Fires are destructive and the only way to stop them is by controlling or extinguishing them. The damage caused by the fire can have economic consequences, such as destroying a crop or demolish buildings and houses. In addition, fires also emit gases that affect air quality and climate change because some of these gases are greenhouse gases.[3] People and animals are affected by these fires, which not only destroy their territory, but can also enclose them, leading to casualties. The increase in forest fires, combined with the increase in the length and intensity of the fire seasons, makes it extremely important to develop an effective way to fight these fires.
The best method to deal with these wildfires is aerial firefighting. Aerial firefighting can not only reach the most remote areas, but also gives a wide view of the area, including the fire. This can help the ground firefighters and prevent them from being trapped by the fire. The current fleet is relatively old and therefore not as effective as it could be. The current fleet consists for the most part of converted, but also some purpose-built aircraft. The most recently developed converted aircraft for firefighting missions is the 737 – 300.[4] This aircraft was introduced in 1980 and therefore does not contain the innovations of recent years. [5] The Beriev 200 is the last specially developed aircraft for firefighting missions and had its first flight in 1998.[6] This shows that there has not been a newly developed firefighting aircraft in more than 20 years. Over the past two decades, the aviation industry has developed with many innovations in the field of technology, sustainability and safety. This can ensure more efficient and effective aerial firefighting without causing further damage. As a result, an important efficient, effective and safety aircraft can be developed that can also be more environmentally friendly. This will result in a reduction of fire and aircraft emissions and a better protection of both wildlife and human life.
Therefore MANTÆ was developed, the **M**ulti-purpose **A**mphibious **N**ext-Generation **T**actical **A**erial **E**xtinguisher. In order to successfully develop the MANTÆ, the Mission Need Statement and Project Objective Statement were established and these are as follows:

Mission Need Statement
"Develop the next generation firefighting aircraft, able to outperform and replace an ageing fleet, to improve aerial support during firefighting operations."

Project Objective Statement
"Design or convert an aircraft for a firefighting role which can be widely deployable, with 4000 manhours."

First a Market analysis is performed and described in Chapter 2. To achieve the mission need and the project objective statement a project overview is established which is explained in Chapter 3, including project organisation, the important requirement and constraints and a recap of design options which are considerd. After choosing the design, the **amphibious multi propeller engine blended wingbody** a Class I weight estimation was performed to design the initial planform. The steps from the Class I weight estimation to a more detailed structural design is described in Chapter 4. Hereafter, Chapter 5 explains the hull design, including the integration of the hull in the main body. After integrating the hull with the main body, a aerodynamic analysis can be performed, which is described in Chapter 6. Chapter 7 discusses the sizing and choice of the engine used in the design. As our aircraft main mission is firefighting, a detailed design of the extinguishing system of the aircraft is explained in Chapter 8. Chapter 9 discusses the stability of the aircraft together with the controls of the aircraft. The performance of the final design is discussed in Chapter 10. The communication capabilities of the aircraft is discussed in Chapter 11, including the avionics and the internal relations. The sustainability and the RAMS analysis is discussed in Chapter 12 and Chapter 13, respectively. Chapter 14 evaluates the risks of the design and how these can be mitigated. The operations and manufacturing process of the final design is discussed in Chapter 15. A resource allocation, where the weight and cost breakdown is displayed, is discussed in Chapter 16. The verification and validation of the detailed design is explained in Chapter 18. Lastly, Chapter 19 conclude the findings of the final design and the recommendations for further analysis.

[1] https://www.sciencedaily.com/releases/2020/05/200518154941.htm [cited 29-5-2020]
[2] https://climatechange.lta.org/climate-impacts/increasing-wildfires/ [cited 29-05-2020]
[3] https://insideclimatenews.org/news/23082018/extreme-wildfires-climate-change-global-warming-air-pollution-fire-management-black-carbon-co2#:~:text=Wildfires%20emit%20carbon%20dioxide%20and,effects%20on%20warming%20and%20cooling. [cited:22-6-2020]
[4] https://fireaviation.com/2017/05/21/coulson-to-convert-737s-into-air-tankers/ [cited 29-5-2020]
[5] https://modernairliners.com/boeing-737/boeing-737-history/ [cited 29-5-2020]
[6] https://www.naval-technology.com/projects/berievbe200multipurp/ [cited 29-5-2020]

2
Market Analysis

This chapter is a follow-up on the market analysis in the baseline report. It starts with a description of wildfires and where they occur in Section 2.1, followed by a section on fighting these fires and how aircraft are used in Section 2.2. An overview of the direct competitors is given in Section 2.3.

2.1. Wildfires

In order to get a clear view of the use case of the aircraft, background information on wildfires and their evolution over the last years has to be given. First, note that wildfires are not purely a phenomenon caused by human interaction but something that has always existed, with fires being lit by lightning or volcanic eruptions. With the increased human presence all over the world nowadays arson, human carelessness, and sparks (from equipment or powerlines) are among the most common causes of wildfires, leading to more wildfires near populated areas and more fires in general. Another thing leading to more wildfires is climate change. Even without discussing the scope of climate change, parts of the world have become hotter and drier, leading to better circumstances for wildfires and increased fire seasons and fire intensities. Examples of this are the Camp Fire and Swedish wildfires of 2018 which followed season(s) of drought. Another example are the 2020 wildfires in Siberia [1] which are worsened by increased temperatures. An effect of these fires is the release of carbon dioxide in the environment, leading to more climate change (and a viscious circle) [2].

2.1.1. Location of wildfires

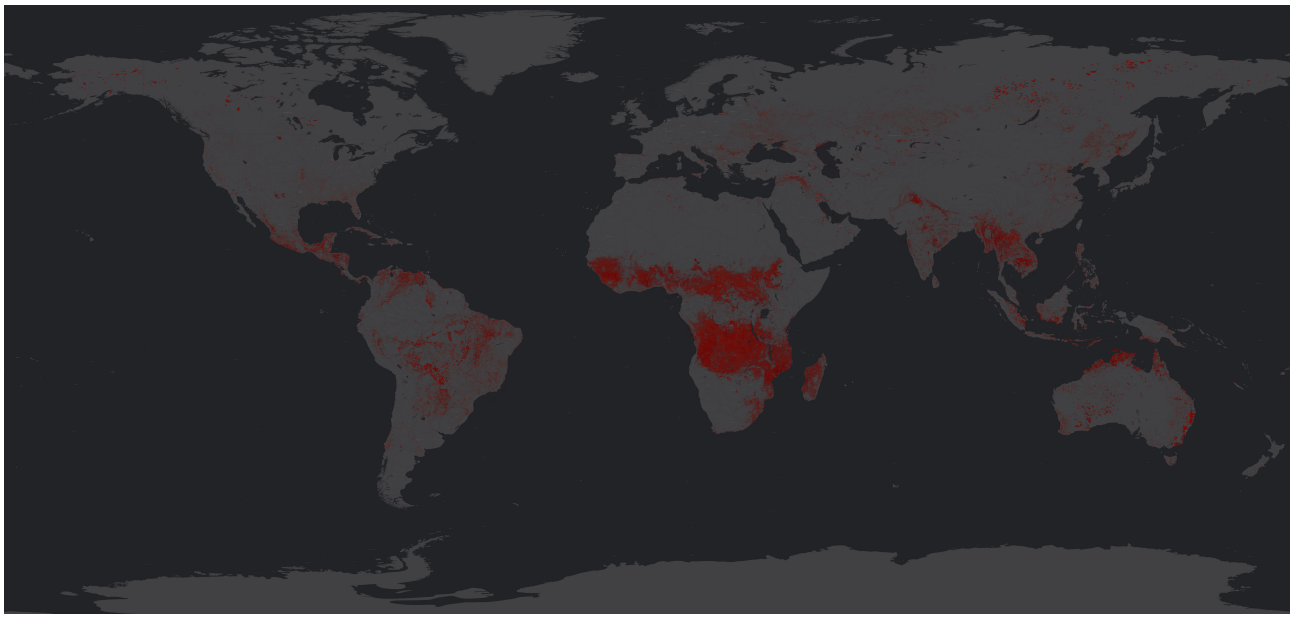

Figure 2.1: Detected fires by MODIS and VIIRS worldwide in 2018

An overview of all the fires detected by MODIS and VIIRS in 2018 can be seen in Figure 2.1. Note that this is not only wildfires but also gas flaring and emissions from oil production and industry. It's visible that the greatest numbers of fires are in South America, Africa and Southeast Asia. These fires are mostly lit by humans in order to clear agricultural land [3]. Areas that are more known for forest fires among the general population like California, Australia, Europe and Siberia seem to be effected a lot less; but these fires are purely wildfires and are close to population centres, leading to a bigger impact on a greater number of people. As can be seen Figure 2.2 and Figure 2.3 most wildfires are close to airports and water sources except for Siberia, which has few airports, and Australia, which has few perennial water sources. These relations are important for firefighting tactics, which will be discussed next.

[1] https://news.mongabay.com/2020/05/siberia-experiences-hottest-spring-on-record-fueling-wildfires/
[2] https://blog.ucsusa.org/carly-phillips/alaska-wildfires-climate-change
[3] https://earthobservatory.nasa.gov/images/12693/fires-in-southeast-asia

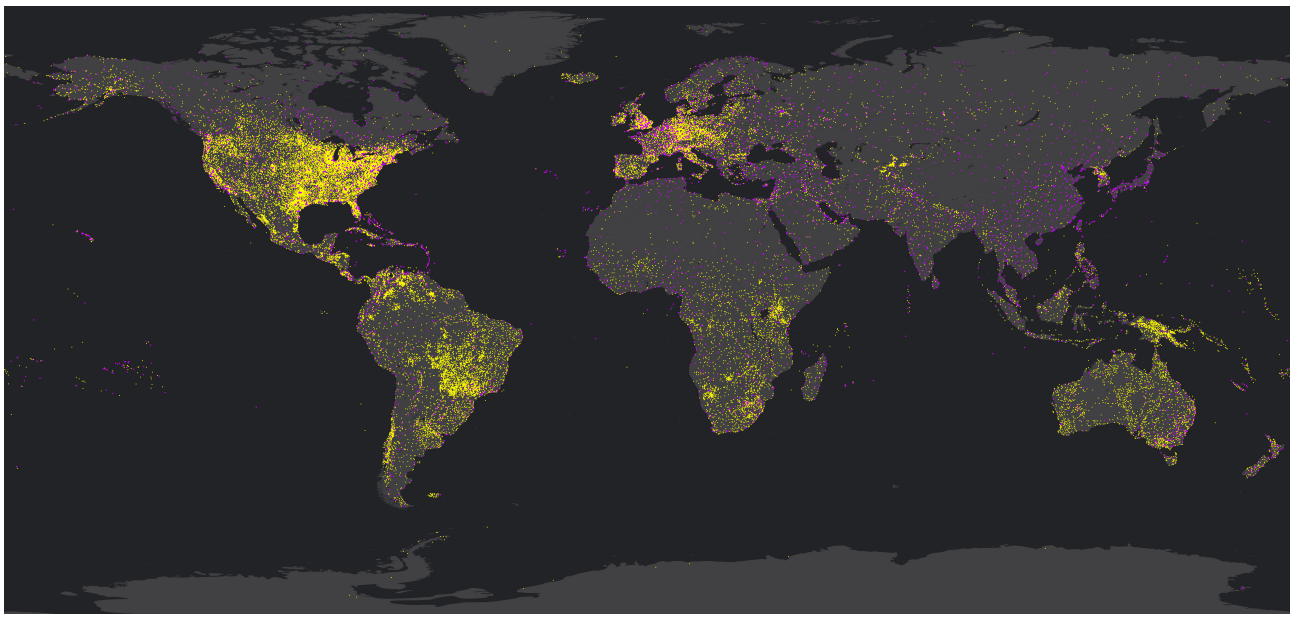

Figure 2.2: Airports of the world; large airports in purple, small airports in yellow

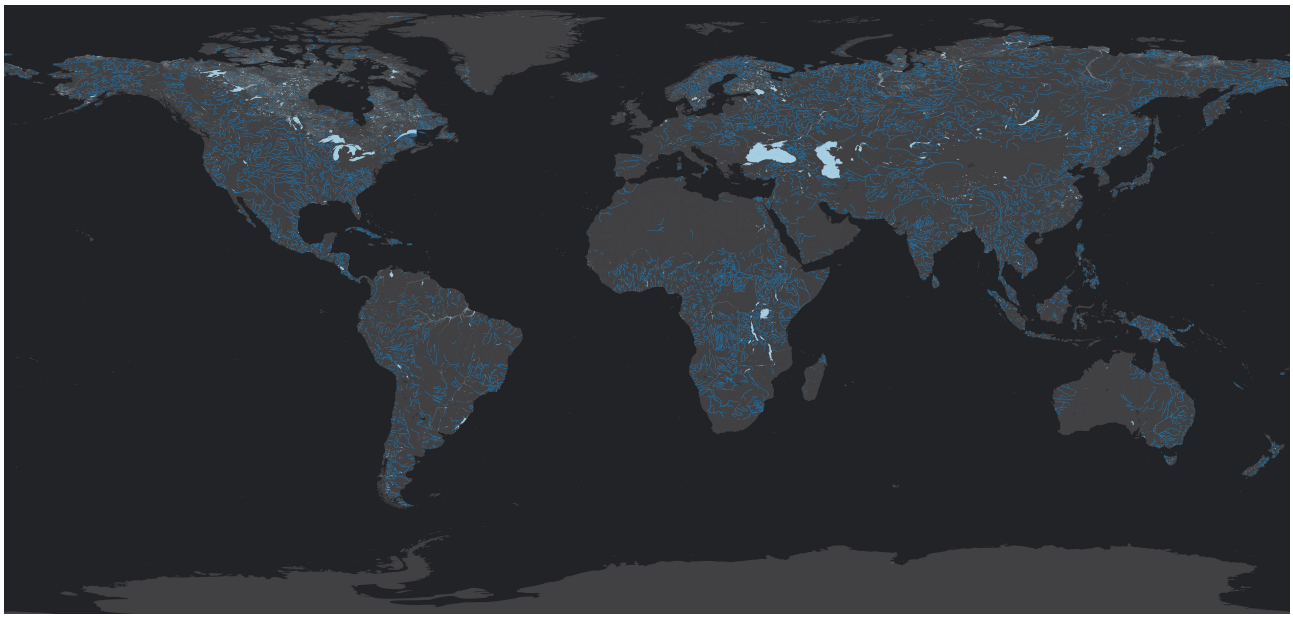

Figure 2.3: Inland water sources of the world

2.2. Fighting Forest Fires

Fire fighting strategies have changed over the years. While the previous idea was that putting out all wildfires helped the most it turned out this was detrimental in the long run as flammable materials were left to build up over the years which led to heavier wildfires. A more modern strategy is to let fires burn controllable; only intervening when the fire reaches urban areas. While this does not prevent any emissions it is the most cost effective approach for firefighting agencies.

2.2.1. Workflow

The first step in fighting fires is currently getting firefighters and equipment on the ground. This can be done by driving them to the site of the fire or by dropping them from an aircraft (so called smokejumpers). The reason for using on-ground personnel instead of directly using aircraft is to create firelines, areas cleared of flammable material. These firelines are needed to stop the spreading of the fire when it is too big to be directly extinguished, which is often already the case when it is detected. Because of this, in the current doctrine, aircraft are purely seen as support [2]. However, there is evidence that a direct attack by aircraft early on may have a better effect than is currently thought [3].

2.2.2. Aerial firefighting

As mentioned before, firefighting aircraft are mostly used in support roles. There are multiple tactics, but in general it can be brought back to 2 actions; direct and indirect attack. Direct attack is where water or fire retardants are dropped on the fire itself in order to lower the intensity. Indirect attack is where an aircraft drops water or retardant ahead of the fire in order to establish or strengthen a control line. The initial attack discussed above is a direct attack method applied early on, when the fire is still small. The goal of this is to put the fire out entirely instead of only decreasing intensity.

All of these tasks can be performed by either retardants or water. Retardants are salts mixed in the dropped water that stay effective even after the water has evaporated. Water, and added substances that turn it into a foam or gel, are at their most effective directly after being dropped as they evaporate and lose their effectiveness. This is explored in further detail in Chapter 8.

2.3. Current Firefighting Aircraft

The current fleet of firefighting aircraft consists of 2 types; Land-based airtankers that operate from an airfield and have to return to refill, and amphibious aircraft and helicopters that can refill nearby a fire from a water source. The fleets of different regions have a mix of these types, depending on conditions (e.g. airfield and water distance) and possible regulations.

2.3.1. Current Market

An overview of current firefighting aircraft and their performance is shown in Figure 2.4. The red line is the minimum amount of water the aircraft should be able to deliver according to the user requirements. The aircraft that make this requirement are shown in Figure 2.5, where their performance is plotted against their cost. The red line is the minimum performance-to-cost that the aircraft needs to have according to the User Requirements. Aircraft that are to the left and above of this line make the requirement. It is clearly visible that amphibious aircraft and rotorcraft are more cost effective than land-based aircraft. However, rotorcraft have a limited range and are therefore only just meeting the 15,000 L/h requirement. In addition to the land-based aircraft being less cost effective, it should be noted that these are also all conversions. Because of this the aircraft are older and already have a large number of flight cycles performed. An effect of this is limited use and a higher operating cost coupled with higher emissions as older aircraft are inherently less efficient than newer designs. In addition to this the designs of the rotorcraft and amphibious aircraft that are currently used are also very old. All of this leads to a clear market gap for a modern amphibious aircraft with a new design that is purposebuilt for firefighting.

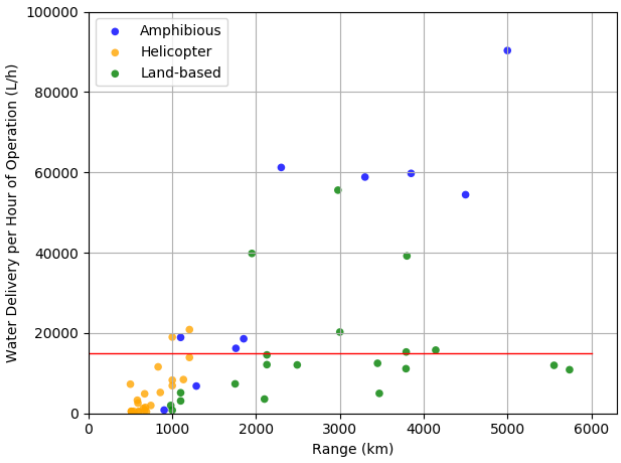

Figure 2.4: Aircraft performance with airfield at 250km, water at 30km. The red line represents performance of 15,000L/h.

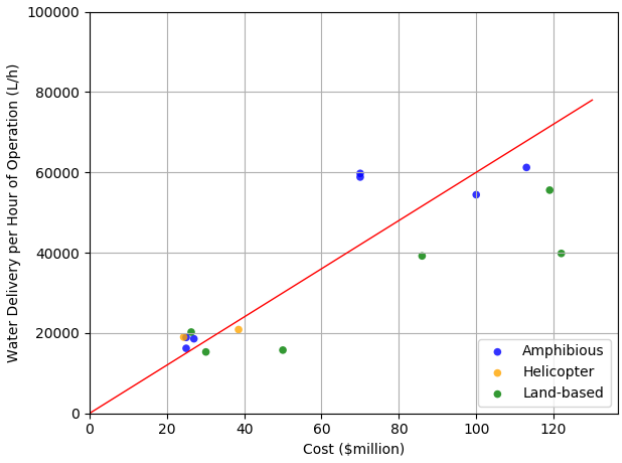

Figure 2.5: Aircraft performance plotted against cost. The red line represents the minimum performance-to-cost relation.

2.3.2. Direct competitors

It can be clearly seen in Figure 2.5 that the best performing aircraft are amphibious aircraft like the design presented in this report. The direct competitors will thus be the Canadair CL-415, the Beriev Be-200 and the ShinMaywa US-2. These aircraft can be seen in Figure 2.6, Figure 2.7 and Figure 2.8. The general characteristics of these aircraft can be seen in Table 2.1.

Figure 2.6: Canadair CL-415

Figure 2.7: Beriev Be-200

Figure 2.8: Shinmaywa US-2

	Canadair CL-415	Beriev Be-200	Shinmaywa US-2
Capacity (L)	6,136	12,000	15,000
Cruise Speed (m/s)	93	167	134
Firefighting Range (km)	1,850	2,100	2,300
MTOW (kN)	195	400	540
Configuration	Propeller, 2 engines	Jet, 2 engines	Propeller, 2 engines
Cost (million $)	27	70	103

Table 2.1: Characteristics of competitor aircraft

Performance per unit cost with varying distance to the airfield and water can be seen in Figure 2.9 and Figure 2.10 respectively. Figure 2.9 varies the airfield distance with a constant water source distance of 30 km, the distance from the design mission. Likewise, Figure 2.10 varies the water source distance with a constant airfield distance of 250 km. These graphs have been made with code that was previously verified in [4] and [5] and is therefore considered verified. It is visible that the performance of current aircraft per cost unit is relatively equal, with the Beriev outperforming the Canadair and the Shinmaywa because of its low acquisition cost.

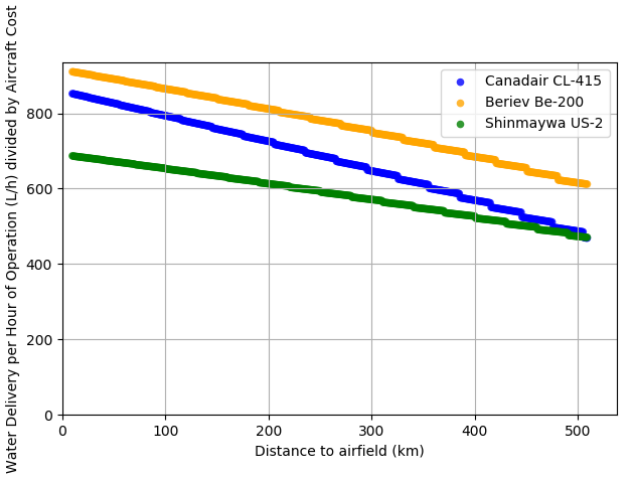

Figure 2.9: Aircraft performance per unit cost for varying distance to the airfield and 30 km distance to a water source.

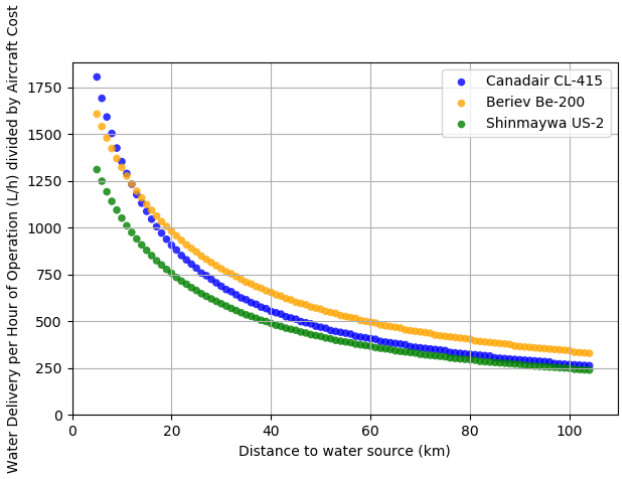

Figure 2.10: Aircraft performance per unit cost for varying distance to water and a 250 km distance to the airfield.

As previously discussed, wildfires can be caused by natural phenomena or humans. They have been happening for a long time, bringing a balance to the vegetation and environment. However, due to the increasing global temperatures, wildfires have become more frequent and are a threat to wildlife, human life and increase the risk of further degradation of nature. For this reason, the constant development and improvement of preventive and contingency measures of wildfires is vital to ensure an environment that remains sustainable for future generations. There are many approaches and methods being used by current firefighting agencies. The most fundamental component is the aerial support via aircraft. Given the ageing fleet of these aircraft, new designs are needed that can perform better in this increasingly important situation. The MANTÆ is an attempt of meeting this need, as the mission need statement describes.

As is shown later in the report, the MANTÆ provides the current market of firefighting aircraft with a combination of high water delivery performance, the best cost effectiveness up to a 400 km distance from the airfield to the fire, a sustainable approach, and a modern configuration which leads to its high performance features. All of these outperforming attributes are achieved through different design characteristics, which are discussed in further detail through the report.

3
Project Overview

This chapter describes the general project overview to ensure a clear view of the project as a whole. Firstly, Section 3.1 explains the functional flow and breakdown of the aircraft system and subsystems. Moreover, Section 3.2 gives a detailed description of the continuation of the project after the DSE. Additionally, this chapter explains the requirements and constraints of this design in Section 3.3. Finally, a short recap is on the trade-off is given in Section 3.4 to show how the final design was established.

3.1. Project Organisation

Firstly, this section describes the Functional Flow Diagram (FFD) in Section 3.1.1. Secondly, the Functional Breakdown Structure (FBS) is elaborated upon in Section 3.1.2. Finally, the Gantt chart is explained in Section 3.2.

3.1.1. Functional Flow Diagram

The Functional Flow Diagrams (FFD) are shown in Figure 3.1 and Figure 3.2. To make sure a that there is a consistent structure within the diagram, the same items are used throughout the flow. The yellow, orange and pink coloured boxes in the FFD are the first, second and third level functions respectively. Moreover, the functions defined are as specified in the legend for clarity. To make efficient use of space, parts of the flow that proved to be repetitive have been assigned a letter and put in a 'function box' shown in Figure 3.2. The functions that feature these letters on the top left of their boxes refer to these function boxes. Finally, different junction types are used in the diagrams to improve the flow. As this grouping of functions may be unclear in the diagram, the group set up the following convention: For example, if the HLD's (high lift devices) are deployed during takeoff (`F C.1.2`) to takeoff from the base during a waterbombing mission (`F M1.3`), then the function number `F C.1.2` becomes `F M1.3.C.1.2` to designate the specific function.
To create a complete picture of the operation of the aircraft, the pre-mission functions such as maintenance and post-mission functions such as travelling to a mission area are included in the diagrams. In this case, travelling to a mission area could entail (inter)continental transportation of the aircraft before the start of the fire season.

3.1.2. Functional Breakdown Structure

This section describes the Funtional Breakdown Structure (FBS), which can be found in Figure 3.3. As can be seen in the diagram, the aircrafts' functions are broken down to the top, first, second and third levels. The top level describes the various stages of the aircraft, namely design, production, pre-mission, mission and post-mission. The first level describes the functions that are to be performed. Finally, the second and third level elaborate more on those functions. Please note that the functions under pre-mission are not elaborated upon. This is because the functions present under this level have already been broken down under mission, and no new requirements were obtained by breaking them down. Moreover, the labelling of the functions is consistent with the functional flow diagram explained in Section 3.1.1. Therefore, the labels might appear somewhat chaotic. In the end, one should note the labelling for loading, prepare for take-off, take-off, landing and unloading in the functional flow diagram. Each mission has their own label assigned to these tasks, whereas in the breakdown these are assigned to a letter. This is explained in more detail in Section 3.1.1.
Finally, it should be noted that cruise is labelled under M1, which is the primary mission, whereas multiple missions have a cruising phase. This is done because only the primary mission has a series of specific functions attached to the cruising phase, whereas the pre-mission and secondary missions have no specific set of functions to do during cruise.

3.2. Project Design & Development Logic

As the DSE has come to an end, the project planning needs to be updated for the coming years up to the delivery of the first MANTÆ in 2015. As can be seen in Figure 3.4, there are top level planning blocks in blue, individually broken down to the right. Before any actual production can be carried out, the design has to be optimised, validated and certified. Optimisation of the design consists of the application of custom airfoils, research the applicability of turbofan engines, etc. Then, a $1:10$ scale model will be built to perform various tests and validate the design. After the results from the scale testing look promising, a prototype will be built and certified in conjunction with EASA. Once the certificate is issued, production can start. Completed aircraft can be delivered via delivery or pickup, depending on the wishes of the customer. The Gantt chart of this process can be seen in Figure 3.5.

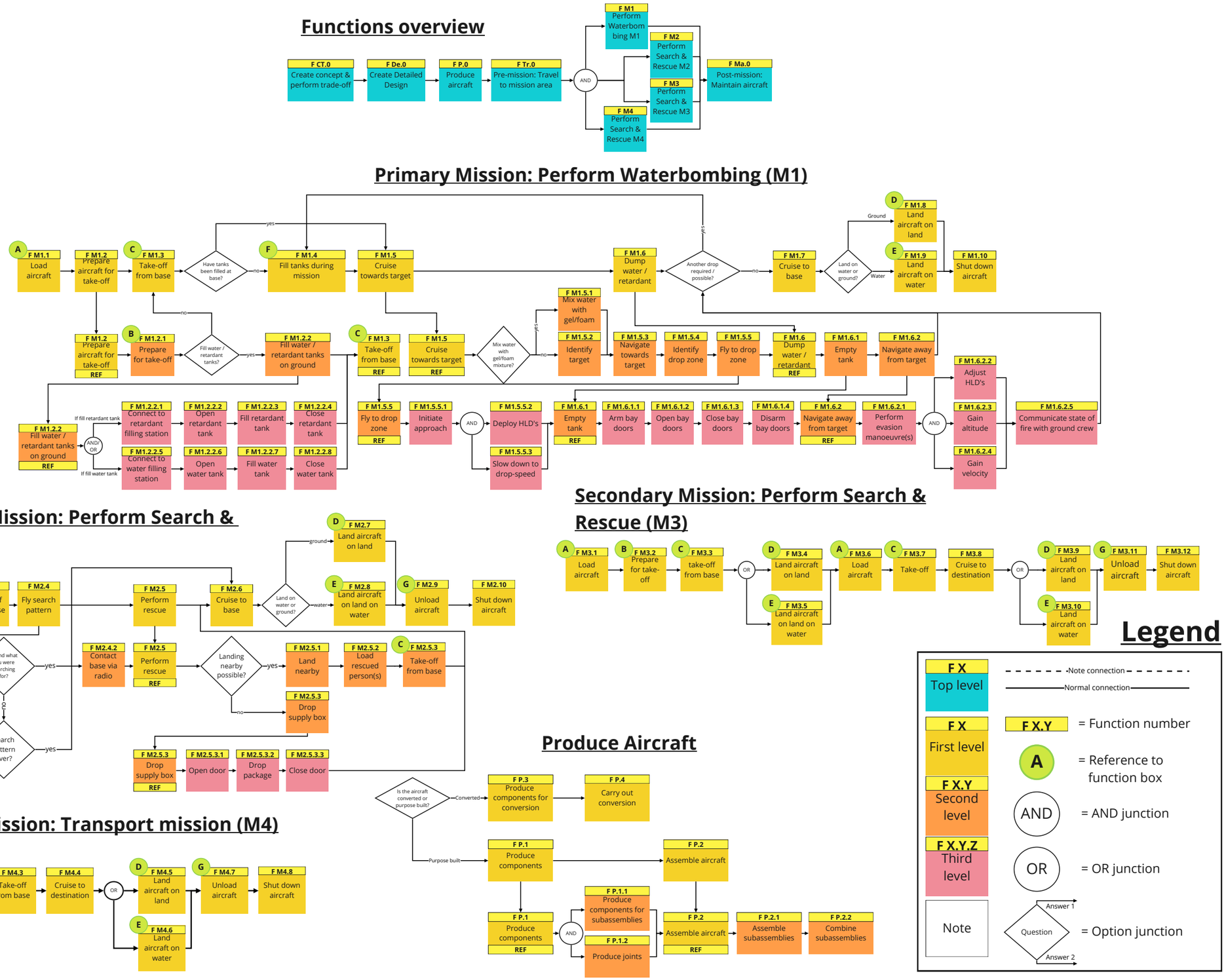

Figure 3.1: Functional flow diagram showing the functions the aircraft should be able to carry out [Part 1]

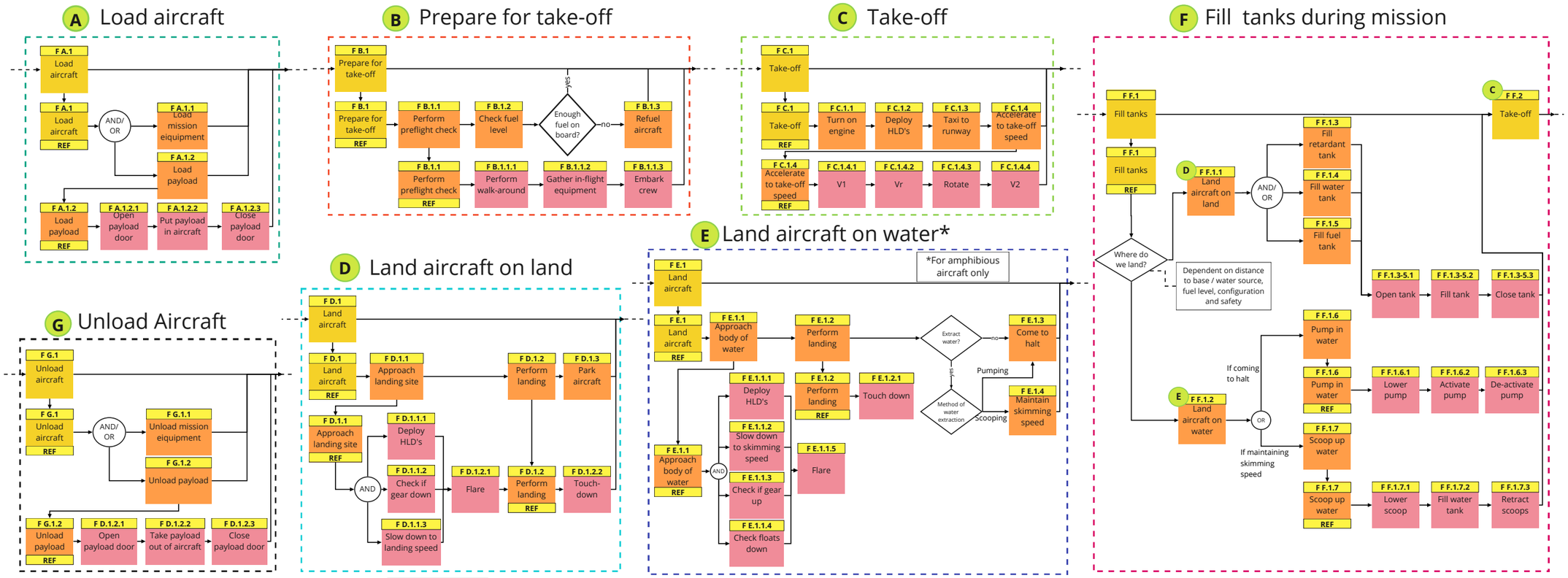

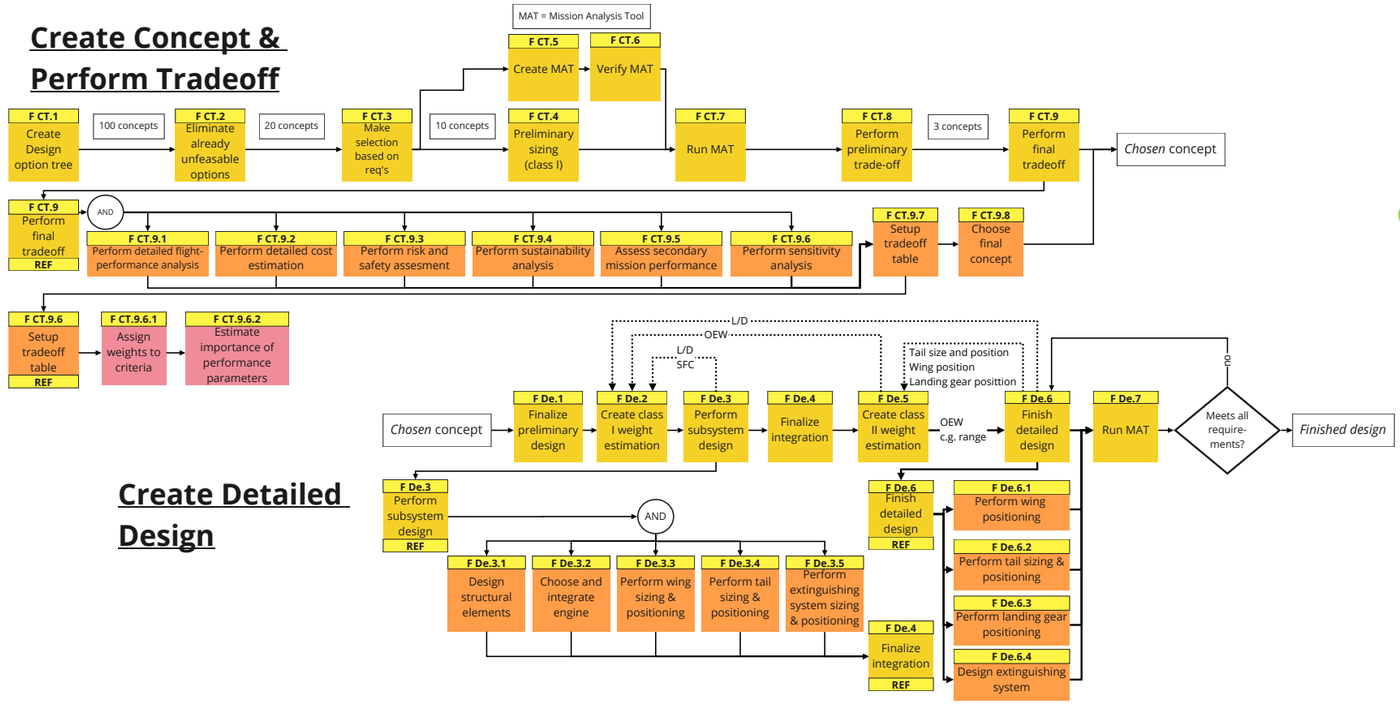

Figure 3.2: Functional flow diagram showing the functions the aircraft should be able to carry out [Part 2]

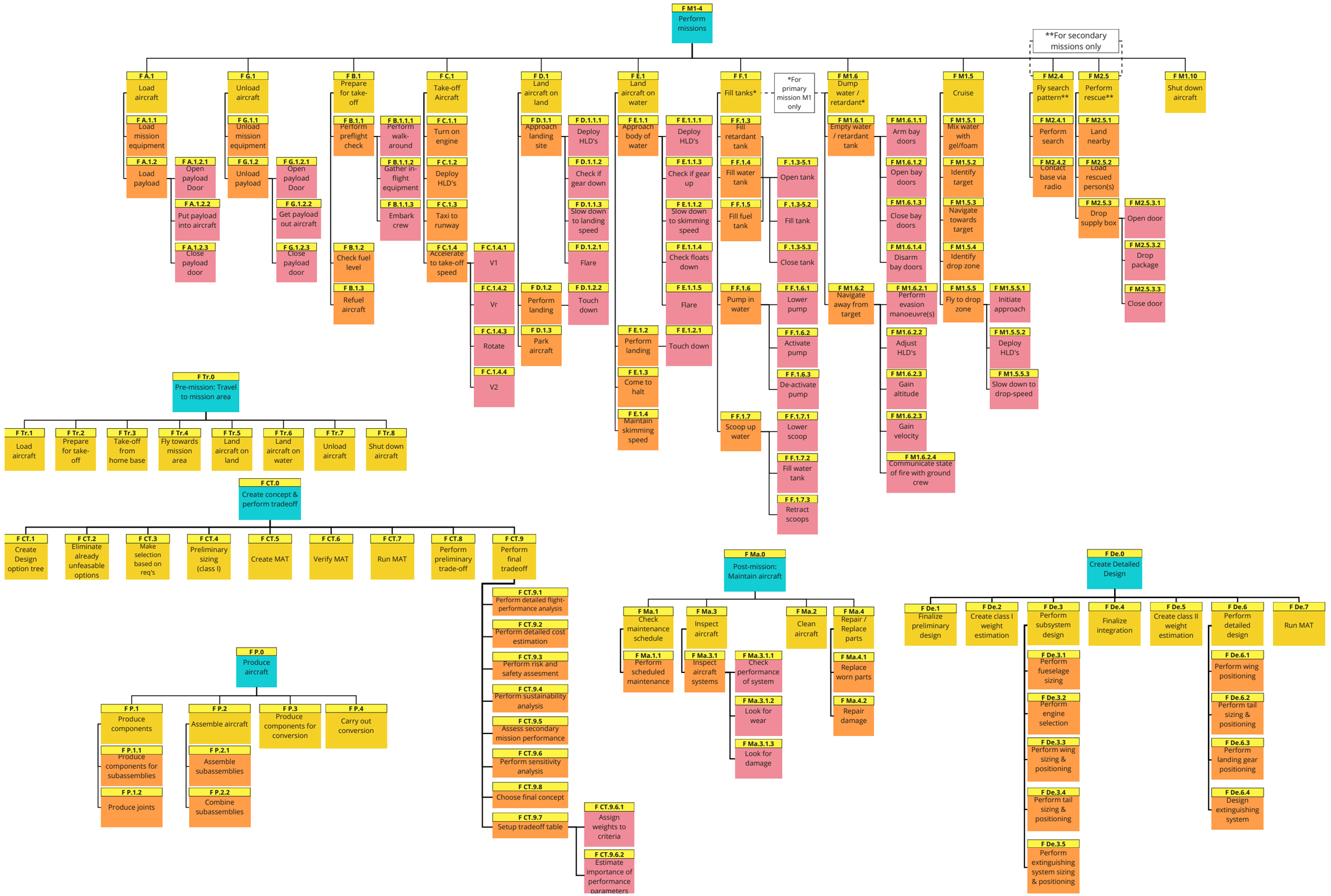

Figure 3.3: Functional Breakdown Structure showing all functions in a categorised manner

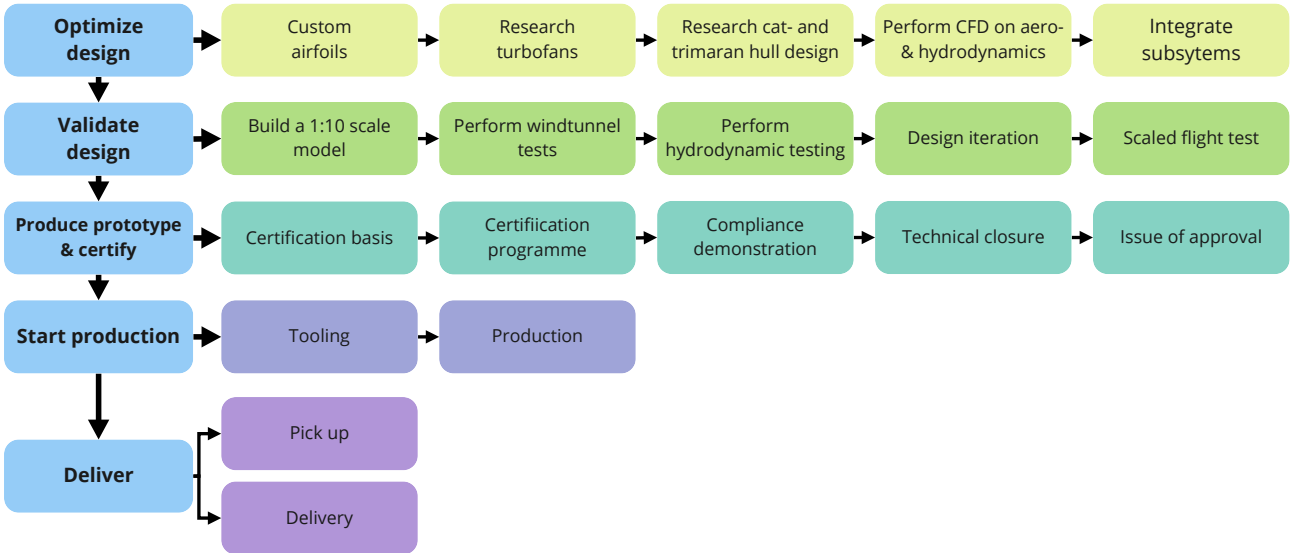

Figure 3.4: Project design and development logic

ID	WBS	Task Name	Start	Finish
1	**1**	**Optimise Design**	**Fri 26/06/20**	**Mon 02/11/20**
2	1.1	Investigate Custom Airfoils	Fri 26/06/20	Wed 26/08/20
3	1.2	Investigate Use of Turbofans	Fri 26/06/20	Wed 26/08/20
4	1.3	Investigate Multihull Configuration	Fri 26/06/20	Wed 26/08/20
5	1.4	Perform CFD for Aero- and Hydrodynamics	Fri 26/06/20	Wed 26/08/20
6	1.5	Integrate Design	Wed 26/08/20	Mon 02/11/20
7	**2**	**Validation**	**Mon 02/11/20**	**Mon 01/03/21**
8	2.1	Build Scale Model	Mon 02/11/20	Tue 01/12/20
9	2.2	Windtunnel Testing	Tue 01/12/20	Fri 11/12/20
10	2.3	Hydrodynamic Testing	Tue 01/12/20	Fri 11/12/20
11	2.4	Design Iteration	Fri 11/12/20	Mon 01/02/21
12	2.5	Scaled Flight Test	Tue 02/02/21	Mon 01/03/21
13	**3**	**Certification**	**Tue 02/03/21**	**Fri 01/03/24**
14	3.1	Certification Basis	Tue 02/03/21	Mon 05/04/21
15	3.2	Certification Programme	Mon 05/04/21	Mon 31/05/21
16	3.3	Compliance Demonstration	Mon 31/05/21	Mon 08/01/24
17	3.4	Technical Closure	Mon 08/01/24	Mon 12/02/24
18	3.5	Issue of Approval	Mon 12/02/24	Fri 01/03/24
19	**4**	**Production**	**Tue 05/03/24**	**Tue 01/04/25**
20	4.1	Create Tooling	Tue 05/03/24	Mon 01/07/24
21	4.2	Start Production	Thu 04/07/24	Tue 01/04/25
22	5	First Delivery	Tue 01/04/25	Tue 01/04/25

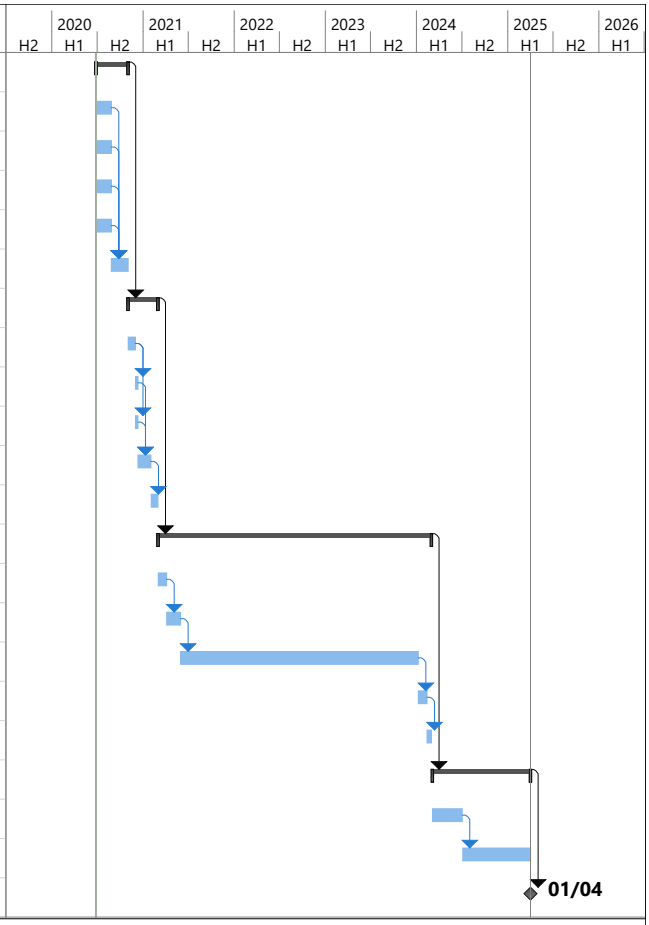

Project: After DSE
Date: Fri 26/06/20

Task
Summary
Manual Summary
Milestone
Manual Summary Rollup

Page 1

Figure 3.5: Project Gantt chart showing the post-DSE planning

3.3. Requirements and Constraints

The MANTÆ aircraft has to follow certain requirements which are listed in the compliance matrix in Chapter 18. These requirements constraint in such a way that the costumer gets a product that 1) Fulfils their needs, and 2) Is legal. In other words, fulfils regulation requirements. These requirements all regard different disciplines, and will be discussed in their respective sections throughout the report.

3.4. Recap of Design Options

During the previous phases of the project, a lot of concepts were considered and discussed. Therefore, this section provides a small summary of the final five concepts that were considered in the last trade-off.

3.4.1. Five Concepts

After disregarding a lot of concepts, five design options proceeded into the final trade-off. These five options can be found in Table 3.1. These five design options differ in being amphibious or land-based, having a propeller or jet engine and having a conventional or unconventional wing.

Table 3.1: The five design options considered in the final trade-off

Concept	**Design configuration**
Concept 1	Amphibious multi jet engine conventional fixed wing
Concept 2	Amphibious multi jet engine unconventional fixed wing
Concept 3	Amphibious multi propeller engine conventional fixed wing
Concept 4	Amphibious multi propeller engine unconventional fixed wing
Concept 5	Land-based multi jet engine conventional fixed wing

3.4.2. Trade-Off summary

For the final design selection, a performance analysis, a RAMS characteristics, a trade-off and a sensitivity analysis were all taken into account. These methods lead to two well performing designs, namely: the amphibious propeller conventional purpose built aircraft, and the amphibious propeller unconventional purpose-built aircraft. As can be seen in Table 3.2, both designs score above a 3.5. While the conventional design scores higher, it only does so by a margin of 0.02. As the sensitivity analysis showed, this was highly dependant on the weight given to the technology readiness level of the configuration [5]. Therefore, the difference is sufficiently small and dependant on a single criteria that choosing the unconventional design is still feasible. Furthermore, when taking into account the uncertainties within the data used for the trade-off, the margin of error generated is likely to surpass this 0.02. Further considerations not included in the trade-off as they were impossible to quantify are also expected to favour the unconventional design, like the layout of the blended wing body and the lack of a need for a pressurised interior during firefighting.

Conventional wing configuration is typical of a current generation firefighting aircraft, but since the mission need statement of this project is to design a next generation firefighting aircraft, the choice for the final concept is the **amphibious propeller unconventional** design, a blended wing body. This is the design that will be worked out further in this report.

Table 3.2: Trade-off summary table including all concepts

Summary	**Weight (%)**	**Amphibious**				**Land basedConversion**
		Propeller		Jet		Jet
		Conventional	Unconventional	Conventional	Unconventional	Conventional
Mission performance	40%	3.0	3.0	2.8	2.8	2.2
Propulsion performance	30%	4.3	4.3	3.4	3.4	3.7
Configuration performance	30%	3.8	3.8	4.3	3.8	3.3
Total		3.65	3.63	3.45	3.27	2.98

4
Wing & Fuselage

The wing and fuselage of a blended wing body are more often referred to as the outer wing and inner wing. Together they make up the weight of the airframe mass. As calculating the structural thicknesses and spacing are highly iterative, Figure 4.1 is a flowchart to give an overview of the process.

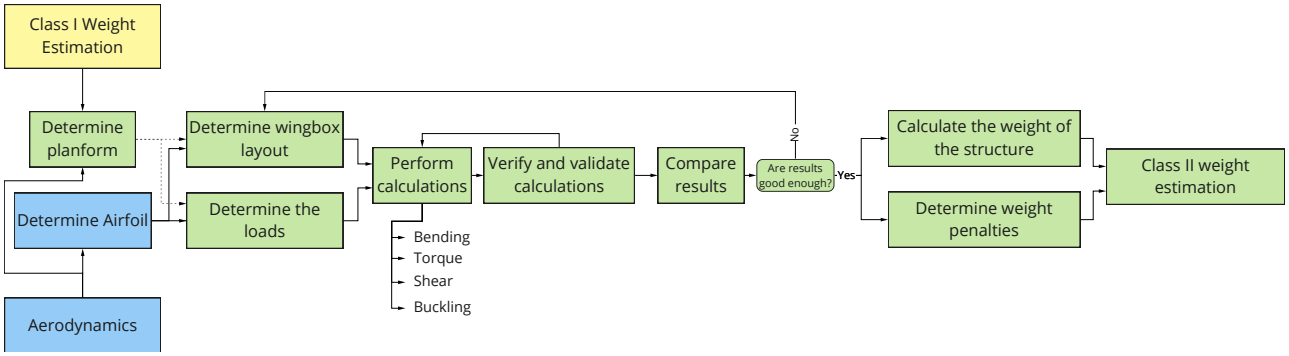

Figure 4.1: The flowchart of the process of determining the structural part of the MANTÆ

First a Class I weight estimation is performed, solely based on statistical data in Section 4.1. With the estimated weight a preliminary planform can be determined. This process is described in Section 4.2. From the airfoil determined by the aerodynamics which is explained in Chapter 6, a wingbox approximation can be established in Section 4.3. From the planform determination and the airfoil selection, the loads which the aircraft endures is determined in Section 4.4. Combining the loads with the wingbox approximation, calculations regarding bending, shear and torque can be performed and are described in Section 4.5 as well as the determination of the weight penalties. All calculations used in this chapter come from the Aerospace Engineering course Structural Analysis & Design at TU Delft.

4.1. Class I mass estimation

The first estimation for the operational empty weight W_{OE} is done with a Class I estimation. This is a more refined estimation than the one performed in the Midterm report. All land-based aircraft and helicopters were deleted from the statistical data. This updated also the Maximum Take-off Weight W_{MTO} and water capacity linear relation to $W_{MTO} = 2.7956 \cdot capacity + 7210.2$ and resulted in a preliminary W_{MTO} estimation of $46349kg$ with a water capacity of $14000L$. Blended wing-body aircraft are added to the statistical data leading to a new statistical relation between the operational empty weight W_{OE} and the W_{MTO}: $W_{OE} = 0.4279 \cdot W_{MTO} + 5275.6$, which resulted in a W_{OE} of $25108kg$. The statistical data used to compute these relations can be found in Appendix A. A more accurate estimation of the weight of the payload W_{PAY} can be seen in Table 4.1 including the different missions, from where it can be seen the total payload has a mass of $16270kg$.

Table 4.1: The division of the payload weight.

Weight	**Value**	**Units**
Water capacity	14000	dm^3
Water density	1	kg/dm^3
Weight of rescue rib	1650	kg
Weight of bed	90	kg
Number of beds	4	-
Weight of medical equipment	100	kg
Weight of the pilots	160	kg
Total payload weight	16270	kg

The major difference in comparison with the Midterm approach is the fuel weight W_f. Two different approaches are taken to get a range instead of one value as it is still an estimation. The first method is dependent only on statistical data and a power relation was used due to the snowball effect and having zero fuel weight when there is no take-off weight. This resulted in a W_f of $9875kg$. The other approach is looking at fuel fractions. To determine the fuel

fractions, first the different mission stages should be defined. The following three main missions are evaluated and the maximum fuel consumption is taken for a conservative calculation:

1. Firefighting mission
2. Search and rescue
3. Ferry

The fuel fraction is dependent on the mission, payload, cruise speed, drop speed, loiter speed, the distance to the fire, distance to the water, loiter time, number of drops and a correction factor that accounts for unknown effect at skimming.

For a firefighting mission the mission profile is very different from normal aircraft, so the following mission profile is assumed:

1. Start-up
2. Taxi
3. Take-off
4. Climb
5. Cruise for X amount of km
6. Descent to water body
7. Land on body of water
8. Scoop up water
9. Take-off from body of water
10. Cruise to fire Y amount of km
11. Descent to fire
12. Drop water (assumed to be a loiter of 1 minute) at drop speed
13. Climb
14. Cruise to water body Y amount of km
15. Repeat from 6 an X amount of dumps and continue with 16
16. Cruise for X amount of km back to base
17. Descend
18. Land

From the three different mission profiles, the firefighting mission is the most fuel intensive mission with a fuel fraction of 0.7275. The fuel fraction method came to a higher fuel weight of $13264kg$. The fuel fraction method is a more accurate way of calculating the fuel weight compared to a statistical relationship and is therefore taken as the new fuel weight. The new W_{MTO} can be calculated by summing W_{OE}, W_f and W_{PAY}. This changed came to a second estimation for W_{MTO}, now being $52372kg$.

The Class I weight estimation is not only dependent on the capacity, but also on some design choices. One of the design choices made after the first estimation is that the capacity of the water tanks will be dependent on the shape of the aircraft and the available space within the hull. As shown in chap: firefighting system later in the report, the size of the tanks actually allows for a larger water capacity of $15020L$. Since the different mission profiles of the aircraft are most likely not performed simultaneously, the payload weight is therefore only based on the water capacity and weight of the pilots and not the secondary mission equipment. From updating the water capacity, a new fuel weight also follows. Now weighing $14080kg$, the weight of the fuel as well as the payload weight are summed together with an updated OEW of $26328kg$ to come to a new W_{MTO} of $55428kg$.

4.2. Surface definition

A simple definition of the surfaces is needed before any further calculation can be performed on the aircraft. It is important for this planform to be set up with parameters that strike a balance between ease of use and flexibility for easy iteration. One of the requirements is that the parametrization can easily be picked up by the aerodynamics and structures departments. Especially for the aerodynamic analysis, which is carried out using MIT AVL (Athena Vortex Lattice), it is important to be able to quickly switch geometrical input. Therefore, a python library of different planforms and vertical stabilisers is created. This library then fed it's parameters to a geometry generating script using the Python interface 'avlwrapper' by Reno Elmendorp[1]. The following subsections will elaborate on the definition of the planform and vertical stabilisers.

4.2.1. Planform Definition

The aircraft planform has been parametrized as can be seen in Figure 4.2 and features sections 0 to 6, with section being the centre chord and section 6 being the tip chord. Note that only the right side of the aircraft is defined due to symmetry. Moreover, section 4 is the root chord of the outboard wing and defines the border between the in- and outboard wing of the aircraft. Lastly, the list of all 19 parameters used is shown in Table 4.2.

[1] `https://gitlab.com/relmendorp/avlwrapper` [cited 9-6-2020]

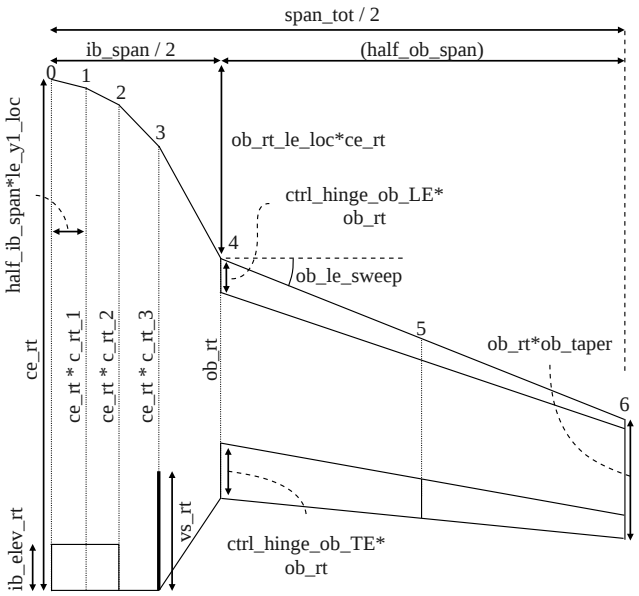

Figure 4.2: Definition of the planform geometry.

Setting values for the parameters creates the geometry in the following way. Defining the total span and inboard wing span results in measurements such as the half outboard wingspan, which is the reason for it being featured in between brackets in Figure 4.2. Note that the total span of the aircraft is limited to $33.5m$ due to the aircraft being required to land on small airports. This span was determined using extensive analysis using Google maps.
The shape of the inboard wing is defined by sections 0-4 and is mainly driven by the cabin space required. For the design to have satisfactory cabin space, an inboard span of $10m$ is initially chosen. The spanwise location of sections 1-3 are defined using percentages of the half inboard span. In addition, the root lengths of sections 1-3 are also defined using percentages of the centre root chord length. This way, scaling the inboard wing can be swiftly carried out by changing only the centre root length and inboard wingspan. As the trailing edge of sections 0-3 is assumed to be straight, leading edge locations of these sections follows from the previously mentioned parameters. The inboard elevator hinge is also assumed to be straight, setting its root chord length determines the size. From a first sight, having this many sections for the inboard wing might seem unnecessary. However, due to the implementation of a hull, having multiple sections where you can define the cross section is thought to improve the results of aerodynamic analysis with AVL.
In contrast to the inboard wing, the parameters for the outboard wing are set up in a more familiar way. The shape of the outboard wing is determined using the outboard wing span, the outboard LE sweep angle and taper ratio. The spanwise location of the root of the outboard wing is determined by the inboard wingspan, whereas the lengthwise location of the LE of the root chord of the outboard wing is a percentage of the centre root chord of the aircraft. Section 5 has been implemented into the outboard wing to serve as a border between the outboard elevator and aileron, it does not alter the planform of the outboard wing, as that is defined by section 4 and 6. Eventually, a classic design of winglets, as defined by R. Whitcomb and found in Raymer, was implemented at the wingtips [6].
Finally, the parameter values for the initial and final planform are featured in Table 4.2. Figure 4.3 and Figure 4.4 show the planforms that these parameters generate.

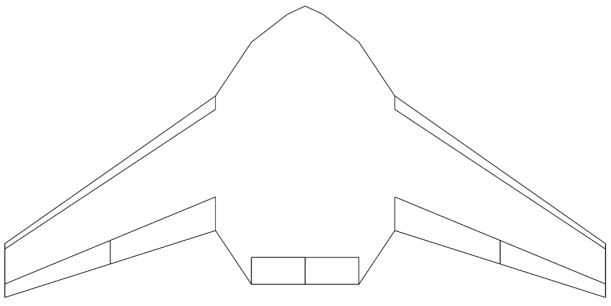

Figure 4.3: Initial planform

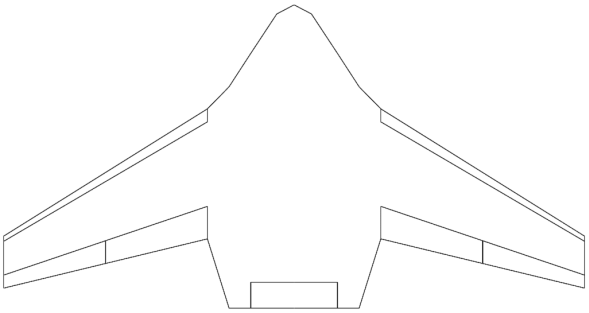

Figure 4.4: Final planform

4.2.2. Vertical stabiliser definition

The vertical stabiliser is positioned on the planform such that its root coincides with the trailing end of section 3, as this will provide the larges moment arm from the c.g. This position is marked by the thick line in Figure 4.2. The

Table 4.2: Parameters and their description used for generating the planform geometry

Parameter	Description	Unit	Initial	Final
span_tot	Total span width	[m]	33.5	33.5
ce_rt	centre root length	[m]	15.5	**17.5**
ib_span	Inboard span width	[m]	10	10
ob_rt	Outboard wing root length	[m]	7.5	7.5
ob_rt_le_loc	Outboard wing root LE location (percentage of ce_rt)	[-]	0.323	**0.343**
ob_taper	Outboard wing taper ratio	[-]	0.4	0.4
ob_le_sweep	Outboard wing LE sweep angle	[deg]	38	**32**
ib_dih	Inboard wing dihedral	[deg]	0	0
ob_dih	Outboard wing dihedral	[deg]	0	0
c_rt_1	Section 1 root length (percentage of ce_rt)	[-]	0.97	0.97
c_rt_2	Section 2 root length (percentage of ce_rt)	[-]	0.92	**0.84**
c_rt_3	Section 3 root length (percentage of ce_rt)	[-]	0.87	**0.73**
le_y1_loc	Section 1 spanwise location (percentage of ib_span/2)	[-]	0.2	0.2
le_y2_loc	Section 2 spanwise location (percentage of ib_span/2)	[-]	0.4	**0.5**
le_y3_loc	Section 3 spanwise location (percentage of ib_span/2)	[-]	0.6	**0.75**
rt_5_loc	Section 5 spanwise location (percentage of half_ob_span)	[-]	0.5	0.5
ib_elev_rt	Inboard elevator root length	[m]	1.5	1.5
ctrl_hinge_ob_LE	Outboard LE control surface hinge chordwise location	[-]	0.1	0.1
ctrl_hinge_ob_TE	Outboard TE control surface hinge chordwise location	[-]	0.75	0.75

vertical stabiliser definition has a lot of resemblance to that of the outboard wing, as can be seen in Table 4.3. The dimensions of the vertical stabiliser are mainly driven by the fact that the two centre turboprop engines are situated on the tip.

Table 4.3: Parameters and their description used for generating the vertical stabiliser geometry

Parameter	Description	Unit	Initial	Final
vs_span	Vertical stabiliser span (height)	[m]	2.5	**3**
vs_rt	Vertical stabiliser root chord length	[m]	3.5	**4**
vs_taper	Vertical stabiliser taper ratio	[-]	0.6	**0.7**
vs_le_sweep	Vertical stabiliser LE sweep angle	[deg]	40	**25**
vs_dih	Vertical stabiliser dihedral (outward positive)	[deg]	10	10

4.3. Wingbox approximation

To start the calculations the wingbox layout should be described. In this section the layout of the inboard and outboard wing is described. Also the centre of gravity and the idealisation calculations are explained.

4.3.1. Outboard wing

For the calculations of the outboard wing the following characteristics are used as can be seen in Table 4.4.

Table 4.4: Characteristics of the outboard wing

Characteristic	information
Airfoil	MH78
Max thickness	0.1447c
First spar placement	0.15c
Second spar placement	0.45c
Third spar placement	0.75c

The wingbox was modelled using the exterior geometry of the airfoil as the upper and lower skin, with the first spar forming the front edge, while the third, rearmost spar formed the the back edge. The first spar and third spar are placed because of the leading and trailing edge devices on 15% and 75% of the chord. This resulted in a a box, which in turn consisted of two cells, with the second, centrally located spar creating the wall shared by both cells. From the coordinates given from `Airfoiltools.com` an accurate placement of the spars with their height can be found which can be seen in Figure 4.5.[2] For the thickness calculations, the idealisation method of boom areas is used. This method assumes that the stress over the skin between two point is equally divided. To make this decision two assumptions were made which make the method valid. First, the assumption is made that the thickness of the skin or spars are constant. This means that the thicknesses are designed for the highest load they encounter and will be over designed. For this stage of the design this is a valid reason as the loads on the wingbox are preliminary. When using a Finite Element Method to determine the loads at every point of the aircraft, the previous two assumption should be eliminated. The boom area idealisation method creates booms at every intersection of the wingbox. The boom area placement can be seen in Figure 4.6.

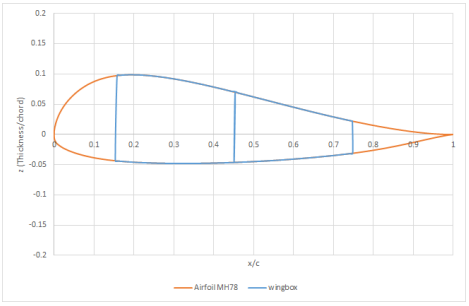

Figure 4.5: Visualisation of the wingbox placement in the airfoil of the outboard wing.

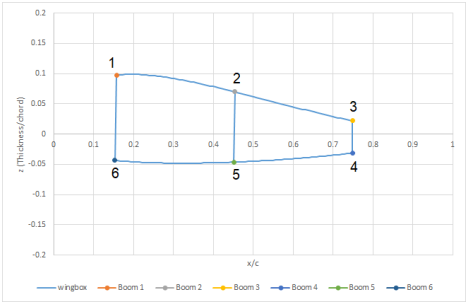

Figure 4.6: The idealisation of the wingbox of the outboard wing.

4.3.2. Inboard wing

For the inboard wing, a different airfoil was chosen,Wortmann FX69 with a different maximum thickness. The spar placement is the same as the outboard wing. The characteristics of the outboard wing can be found in Table 4.5.

Table 4.5: Characteristics of the outboard wing

Characteristic	information
Airfoil	Wortmann FX69
Max thickness	0.274c
First spar placement	0.15c
Second spar placement	0.45c
Third spar placement	0.75c

For the winbox placement, the same method of the outboard wing with the coordinates from `airfoiltool.com` was used which results in Figure 4.7 and Figure 4.8.[3]

[2] `http://airfoiltools.com/airfoil/details?airfoil=mh78-il`[Cited: 25-6-2020]
[3] http://airfoiltools.com/airfoil/details?airfoil=fx69274-il

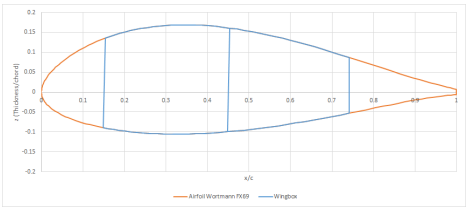

Figure 4.7: Visualisation of the wingbox placement in the airfoil of the inboard wing.

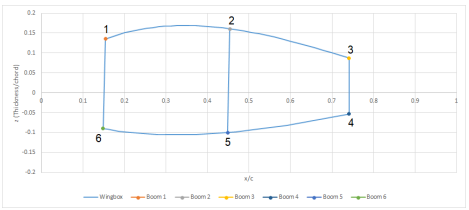

Figure 4.8: The idealisation of the wingbox of the inboard wing.

4.3.3. Center of gravity

The centre of gravity is important for further calculations. However, as the calculations are only focused on the wingbox. The equations to calculate the centre of gravity can be found in Equation (4.1).

$$cg_x = \sum \frac{A \cdot dx}{A} \quad \text{and} \quad cg_z = \sum \frac{A \cdot dz}{A} \tag{4.1}$$

From the Figure 4.7 and Figure 4.5, the axis system is defined on the leading edge of the airfoils on the beginning of the camber-line. The deviation in x- and z-direction for the skin is determined by using the data set from `airfoiltool.com` for the airfoils. Between each data point the average height(dz) and x-position (dx) was used and the length of between two data points is calculated with Pythagoras. [4] For the spars, the dx is simply the location of the spar from the leading edge and the dz is the height is divided by two as the thickness is constant over the spar. The area(A) is calculated by factoring the length of the section with its thickness.

4.3.4. Idealisation

The boom area Idealisation method, each boom is dependent of four different components: the attachment area between the skin and the spar, the length between booms, the stress in each boom and the thickness. This relation can be seen in Equation (4.2).

$$B_i = A_{attachment} + \sum \frac{t_i b}{6}\left(2 + \frac{\sigma_{i+1}}{\sigma_i}\right) \tag{4.2}$$

The attachments($A_{attachment}$ between the skin and spar are only present at the booms and are assumed to be $600mm^2$. The thicknesses(t_i) are assumed and are evaluated after the bending, torque and shear calculations to iterate to the required thicknesses. The thicknesses assumed for the first iteration can be found in Table 4.6.

Table 4.6: The assumed thicknesses for the first iteration

Component	thickness for inboard wing[mm]	thickness for the outboard wing[mm]
Skin	4	1.5
Spars	6	3
Ribs	3	6

In Equation (4.2)can be seen that the booms are dependent on tress(σ). However, for simplicity the stress is only dependent on the height from the camber-line as can be seen in Equation (4.3). When a finite element method is used, the local stress can also be calculated, however, this is not evaluated in this report. The lengths(b) and heights between each booms are easily calculated from the data of the airfoil.

$$\sigma_z = \frac{M_x \cdot z}{I_{xx}} \tag{4.3}$$

The moment of inertia are calculated by using Equation (4.4) and as the deviation in z-direction is taken from the camberline to improver approximation and therefore the $I_{xz} = 0$.

$$I_{xx} = \sum_{i=1}^{n} (dz_i)^2 B_i \quad \text{and} \quad I_{zz} = \sum_{i=1}^{n} (dx_i)^2 B_i \tag{4.4}$$

4.3.5. Materials

As far as materials are concerned, the fire-fighting mission is leading. During this mission, the aircraft will have to deal with three different crucial circumstances. The first condition is extreme manoeuvring. Therefore it is important that the materials can withstand them and have high strength properties. Secondly, because the aircraft is amphibious, it will also have to deal with water during the mission. It is important that it is resistant to corrosion. However, this can easily be tackled with a layer of paint and with inspection of the surfaces that come into contact with water. And

[4] `https://www.calculator.net/pythagorean-theorem-calculator.html`[Cited:25-6-2020]

the most important circumstance is that the aircraft flies close to and above the wild fires and therefore encounters heat and embers from the fire. These embers not only damage the engines, but can also damage the structure of the aircraft. Aluminium alloys were chosen, due of the high thermal conductivity, high strength properties and the relatively low cost. The aluminium alloys used can be seen in Table 4.7.

Table 4.7: The materials used during designing of the wingbox of the outboard and inboard wing

Material	Where used
Aluminium 7075	Spars
Aluminium 7050	Skin, ribs

4.4. Loads

The loads the aircraft experience during firefighting missions are gust and manoeuvre loads. The load spectrum can be calculated analytically with the use of statistics to obtain the maximum and minimum manoeuvre loads. A flight envelope is generated by plotting the load factor experienced by the aircraft versus the velocity relative to the air. After illustrating and analysing the flight envelope, the statistical figures on cumulative exceedence of the loads can be used to validate the flight envelope and assess the reliability of the estimated maximum loads.

Firstly, the manoeuvre loading diagram is made by considering the maximum and minimum manoeuvre loads that the aircraft should be able to perform. Hall performed an extensive study into statistical data of the loads of different firefighting during mission [7]. The load factors are highly dependent of the Maximum Take off weight of the aircraft. The lighter the aircraft, the higher the ultimate structural loads. Hall divides the weigh in three different Categories: Light-, Medium and Heavyweight aircraft. From the design tools it was determined that the Maximum Take-off Weight will be around $55,000kg$ and therefore falls in the Heavy weight class. Two aircraft can be taken as reference aircraft: aircraft 19 or 20. The W_{TO} of aircraft 19 is $126000lbs$ ($57200kg$) and has 166 hours of recorded data. Aircraft 20 has a W_{TO} of $106000lbs$($48100kg$) and has 613 hours of recorded data. As said, the lighter the aircraft, the higher the load the aircraft has to withstand. Since the W_TO of aircraft 20 is closer and lower than the estimated W_{TO} of the design aircraft and due to the fact that it had more recorded data, aircraft 20 is chosen as the reference aircraft. For this aircraft, the largest loads measured were between $+3.75g$ and $-1g$, including both gust and manoeuvre loads, and occurred at a cumulative exceedence of 10^{-3}. Data gathered on the CL415 reveals a total flight time of 3392.8 hours over a period of 10 years before being written off due to a major crash, equivalent to 339 hours per year [8]. For a design life of 30 years, this is equal to 10178 hours of operation in total. If a limit load occurs once in this lifetime, that is equal to a cumulative exceedence of 10^{-4}. Even though this lower cumulative exceedence would result in larger loads than $+3.75g$ and $-1g$, the aircraft analysed to obtain these values weighed approximately $7000kg$ less, hence the limit loads remain a good estimate for the BWB design.

Apart from these maximum manoeuvre loads, other values must also be incorporated into the flight envelope. The stall speed V_S is the lowest airspeed to be considered, whereas the dive speed V_D is the limiting speed of the graph, and is equal to $1.25V_{cruise}$. The stall curve of the aircraft is proportional to V^2 and limits the maximum manoeuvre loads that can be obtained. This curve is obtained using Equation (4.5) [9].

$$n = \frac{C_{L_{max}} \frac{1}{2} \rho V^2 S}{MTOW} \tag{4.5}$$

Two manoeuvre envelopes are created, one for the configuration with HLD deployed and one in clean configuration. These configurations also have different stall speeds V_S and maximum speeds, as the HLD configuration is limited by the maximum speed of the aircraft with flaps deployed. For these calculations, the Class I weight estimation method from Section 4.1 is used for the load calculations, and the maximum structural loads obtained in the flight envelope will be used to size the aircraft structure and will be incorporated in the Class II weight estimation.

The gust loading diagram is generated by considering several specific gust speeds dictated by airworthiness authorities. Although these gust speeds are used for regulations regarding civilian aircraft, aerial firefighting aircraft are designed with these same loads in mind [10]. At V_D, the aircraft must be able to withstand a gust speed of $7.62m/s$. At V_{cruise} the maximum tolerable gust speed increases to $15.24m/s$. Finally, a rough gust of $20.12m/s$ must be endured by the aircraft without stalling, at a velocity V_B smaller than V_{cruise}. A linear change in gust loads can be assumed between these points. The resulting load as a consequence of these gusts is calculated as follows:

$$n = 1 \pm C_{L\alpha} \frac{\frac{1}{2} \rho_0 U_e V_e}{W/S} \tag{4.6}$$

In this equation, $C_{L\alpha}$ is the lift rate coefficient of the entire aircraft, ρ_0 is the air density at sea level, U_e is the gust speed, V_e is the equivalent aircraft velocity and W/S is the aircraft wing loading. The true airspeed of the aircraft is linked to the equivalent velocity through:

$$\frac{1}{2} \rho V^2 = \frac{1}{2} \rho_0 V_e^2 \tag{4.7}$$

ρ is the air density at cruise conditions, equal to $1.007 kg/m^3$ at $2000m$, and ρ_0 is an air density at sea level of $1.225 kg/m^3$. The complete flight envelope of the aircraft is illustrated in Figure 4.9.

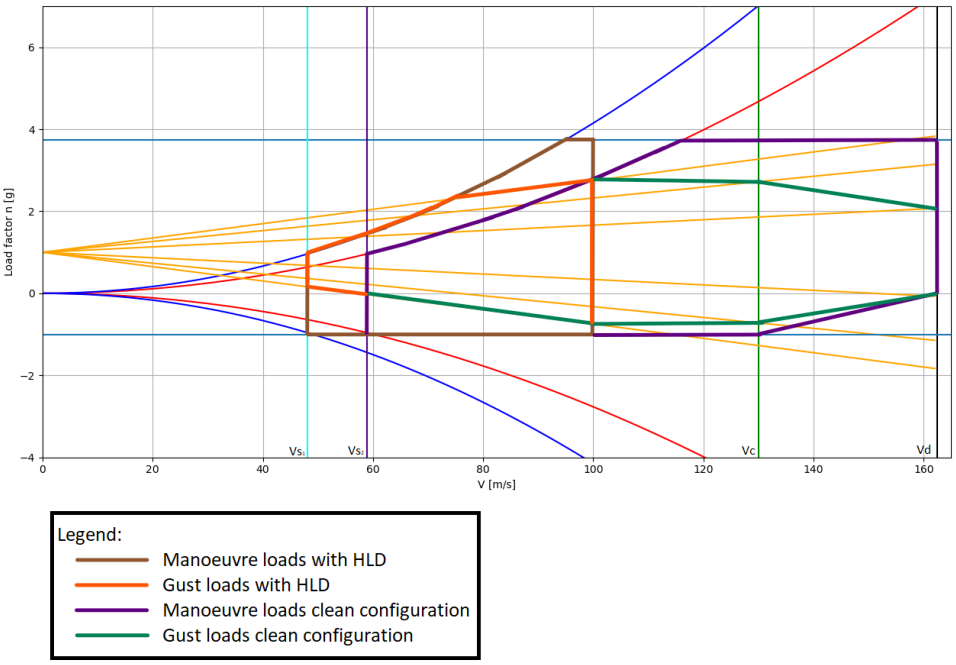

Figure 4.9: Flight envelope with combined gust loads and manoeuvre loads

The cyan and purple vertical lines on the left of the graph represent the stall speeds V_{S1} and V_{S2} with HLD deployed and in clean configuration respectively. The thin green and black vertical lines on the right are V_{cruise} and V_d respectively. The thin second order polynomial red lines indicate the stall limit of the aircraft in clean configuration, whereas the blue second order curves represent the stall limit with HLD deployed. The thin orange lines are the loads caused by the varying gust speeds, with the strongest gust of $20.12 m/s$ being the steepest line and the gust of $7.62 m/s$ the shallowest line. From all of these lines, the manoeuvre load and gust load envelopes are created and labelled in the legend. From the plot, it is evident that the gust load envelopes are positioned within the manoeuvre load envelopes, illustrating that if the aircraft is sized solely for manoeuvres then all gust load requirements will also be met. The limit loads are outlined in Figure 4.10 by joining together the outermost envelopes of Figure 4.9. Hall concludes from statistics that the load spectrum is predominantly manoeuvre-dominated [7]. This concurs with the results found in the flight envelope and increases the reliability of the load estimations.

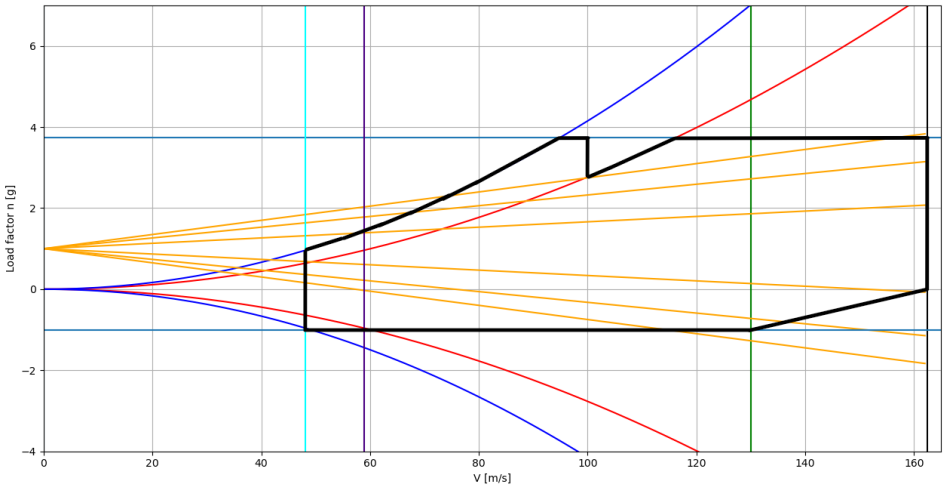

Figure 4.10: Overall flight envelope

4.4.1. Structural Design

As with conventional aircraft, wing loading is generally supported by a wingbox. This wingbox is effectively a closed structure, with spars inside resulting in multiple cells. The larger the wingbox, the more efficient it is at withstanding loads. This is because the enclosed area, as well as the distance of the outer skin from the centreline are the primary factors with regards to load bearing efficiency. In order to keep such a large structure from buckling however, stiffeners are required.

This wingbox was subjected to three primary loads. Each load had to be considered, with careful attention paid to ensure all contributing forces and moments are taken into account.

1. M_y Torsion about the y axis, which is pointing in the direction of the span. This was defined as being positive if it rotated the wing such that the angle of attack increased, according to the right hand rule. The primary contributions to this force are the aerodynamic moment, dependant on the aerofoil, and the lift force. The lift force produces a moment about this axis due to the backwards sweep of the wing, resulting in a negative moment, which varies with the flight condition.

$$M_y = 0.5 \cdot C_{m_{c/4}} \cdot \rho \cdot V^2 \cdot S \cdot c + 0.5 \cdot C_l \cdot \rho \cdot V^2 \cdot S \cdot d \tag{4.8}$$

   The surface area S and chord length c are both dependent on the section being analysed, with in particular the surface area being the multiplication of the chord length of that section and the spanwise width of that section. The parameter d depends on the section being analysed, but also the location at which the moment is being calculated, as it is the distance between the locations of the quarter chords of the location where the moment is being analysed and the section. The contribution of each section from the location being analysed to the wingtip are summed to find the total moment at that location.
2. M_x Bending about the x axis, which is pointing along the central axis of the aircraft, from the nose towards the tail. The positive direction was once more defined according to the right hand rule. The primary contribution to this force is the lift generated by the wing, causing a moment due to the spanwise distance of the lift force.

$$M_x = 0.5 \cdot C_l \cdot \rho \cdot V^2 \cdot S \cdot \Delta(y) \tag{4.9}$$

   The moment about the x axis is calculated in a similar manner to the moment about the y axis. Once again, each section is analysed independently, with the results summed together. The only new parameter is therefore the $\Delta(y)$, which is the spanwise distance between the location of the section being analysed and the spanwise location where the moment is being calculated.
3. V_z Shear force in the z axis, pointing upwards. This force was generated by the lift of the wing, acting in the positive direction, and the weight, acting in the negative direction. The shear force at a point in the spanwise direction is the cumulative sum of forces in the z axis acting along the rest of the wing to the wingtip.

$$V_z = 0.5 \cdot C_l \cdot \rho \cdot V^2 \cdot S \tag{4.10}$$

   The shear in the z direction at a spanwise location is the simplest to calculate. It is simply the sum of the lift force of each section between the spanwise location and the wingtip.

To analyse the loads, and size the required thicknesses of the wingbox sections, data was taken from AVL, which had split each half of the aircraft into 22 sections. These sections were each analysed by the program, with values returned, including the lift coefficient, spanwise location, local chord length, quarter chord moment coefficient. As it is necessary to size for the worst case scenario, these sections were analysed at cruise speed, where the highest loads could be expected. Furthermore, the analysis was repeated under two different conditions; at 0 angle of attack, which is where the aerodynamic moment coefficient peaked, and at 14 degrees. This 14 degrees was chosen after careful consideration of the factors involved. While lift and drag increase with angle of attack, eventually, the wing will stall, at which point the lift begins to generate less lift, and so the loads on the wing decrease, despite increasing the angle of attack. This means, that as long as we size for theoretical loads beyond the stall condition should the aircraft not stall, the aircraft will always stall prior to reaching the design load. This is the so called stall before load design that has been used in other firefighting aircraft [10]. While AVL has the limitation that it cannot predict flow separation, as well as modelling stall conditions, it is reasonable to assume that by the time the airfoil has reached the angle of attack of 14 degrees, especially in the clean configuration, the airfoil will have stalled. Hence this was taken as the angle of attack to analyse and size for.

Figure 4.11 Shows the lift distribution across the span of the wing. A spanwise location of 0 is the centreline of the aircaft, so the lift distribution to the other wingtip is the mirror of this plot. The values are based on the local lift generated per meter span. This was calculated by changing the surface area in the lift formula, by removing the widt of each section, and only including the chord length. This allows for a better overview of the lift generated by a spanwise location, as the width of each of the 22 sections varies, which would skew the results.Figure 4.12 shows the spanwise moment distribution generated by the lift. This is the moment about the x axis, and is purely due to the moment arm and magnitude of the lift, resulting in the steep curve. The steps are still present, however, the change in spanwise

distance is prevalent for the result, hence the steps are difficult to distinguish, and mostly at a high spanwise location, where the moment arm is smaller.

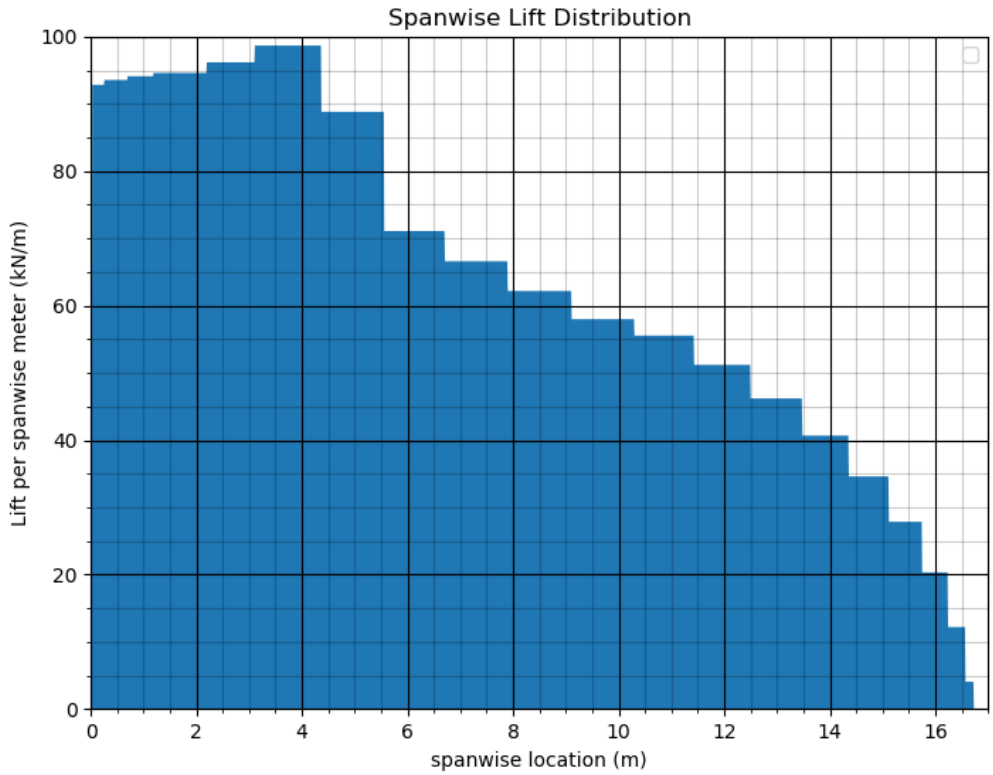

Figure 4.11: Spanwise lift distribution, note the jumps caused by the 22 sections

The values returned by AVL was, as previously discussed, for 22 discrete sections along one side of the aircraft. In order to use this in the analysis, it was interpolated for the chord length and location from the nose of the aircraft. This was not performed on the coefficients, as these did not vary linearly. The data converted into functions which gave the three primary loads as a function of the spanwise location. This also required the input of the geometry of the design to find the exact chord length and location of each section of the wing, such that all the loads could be accurately calculated.

To ease calculations, no cut outs and their required reinforcements were considered for the outboard wing. These will be necessary for maintenance purposes, but due to time constraints, are not designed in detail, with a estimated weight factor of 1.05 added to the final wing mass estimation instead, based on the size of the wing and limited areas that need to be accessed. As no engines are mounted far out on the wing, and the fuel tank is limited to a small spanwise section, only a small amount of cutouts for control surface actuators will be needed. .

For the centre section, the same general method was used. However, as the centre section includes the cabin, this needs to be accounted for. This was done by treating it as a large cutout in the vertical spars. This cutout would have a significant impact on the structure, depending on it's size relative to the size of the surrounding wingbox. For this reason, it was decided to limit the cutout to being two meters tall, and three meters wide. The idea is that the rest of the spar will form a bulkhead, with this cutout potentially being a door. This door would also provide some load bearing capacity, but for the analysis it was considered to be a hole. The aircraft will need to be able to ferry both cargo and medical evacuees, hence, this cutout was sized such that both of these could easily pass through it. For this reason, the cutout was assumed to be 2 meters tall, and 3 meters wide.

As can be seen in Figure 4.13, the cutout dimensions define the variables L2 and H2, leaving L1, L3, H1, H3 and sheaf flow q. Using the dimensions of the centre section, evenly distributed across L1 and L2, the shear flows to the left and right of the cutout can be calculated. For the H1 and H3, it was assumed that the centre of the cutout was exactly at the chord position of the airfoil, and that 1m was cut out above and below that chord line. This method gave an H1 and H3 value dependent on which spar was being analysed. Furthermore, it also ensured that the floor of the cutout

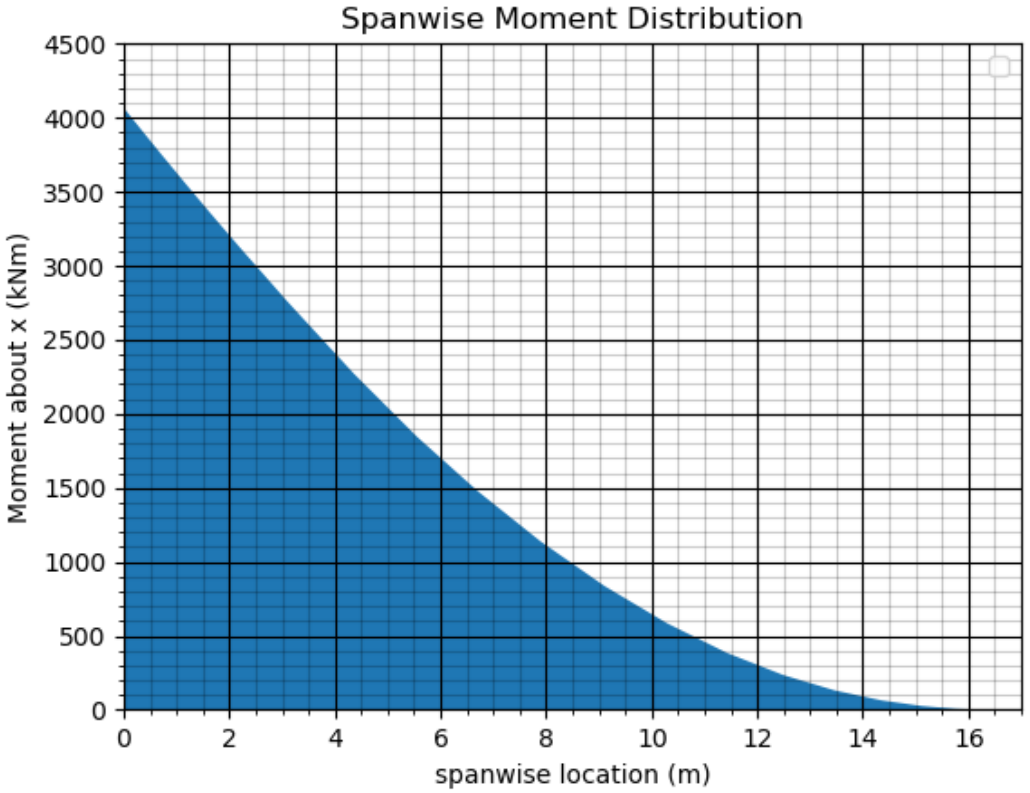

Figure 4.12: Spanwise moment about the x axis distribution

was at a constant height throughout the centre section. These values for H1 and H3 allow the shear flows above the cutout to be calculated using the shear flows that ignore the cutout.

Using these parameters, the shear flow variations as shown in Figure 4.14 can be calculated. Note that, as it is assumed the spar has a constant thickness throughout, the value of shear flow q_C is not important, as it decreases the shear flow, and is therefore not going to be the critical condition. The following equations were used to find shear flows q_H and q_S.

$$q_H = q \cdot \frac{H_2}{H_1 + H_3} \tag{4.11}$$

$$q_S = q \cdot \frac{L_2}{L_1 + L_3} \tag{4.12}$$

The final shear flows around the cutout in each spar was calculated. To simplify calculations and manufacturing, the spars are each assumed to have the same thickness, hence the worst case shear flows in any section of any of the spars drive the spar thickness of the entire centre section.
The final results are tabled in Table 4.8 and are measured at the centre line of the aircraft, so at a spanwise location of 0.

M_y	4253075.8	Nm
M_x	7241242.4	Nm
V_z	1021330.7	N

Table 4.8: Final results at the aircraft centre line

4.4.2. Bending

For bending Equation (4.13) was used:

$$\sigma = \frac{M_x \cdot z}{I_{xx}} \cdot SF \tag{4.13}$$

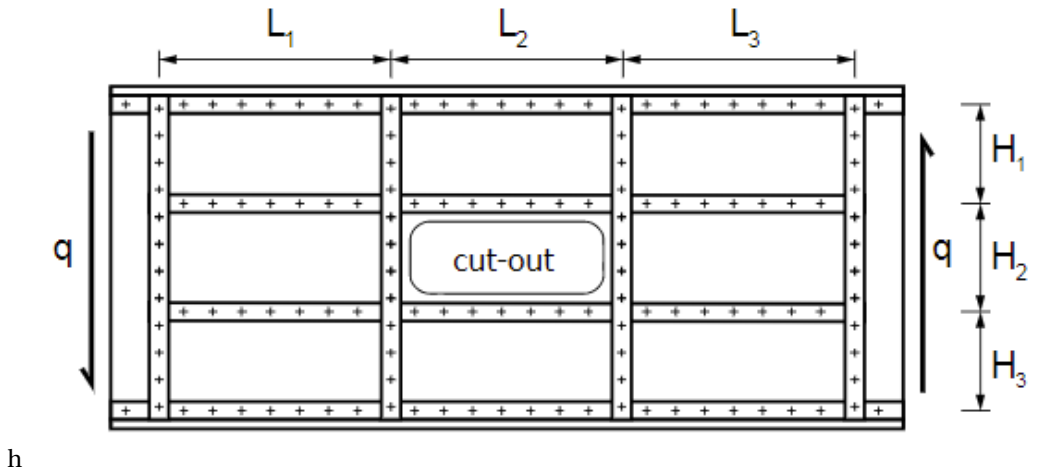

Figure 4.13: Parameters of the centre section cut-out [11], the horizontal axis points in the Y axis, and the vertical axis points in the Z axis of the body axis system

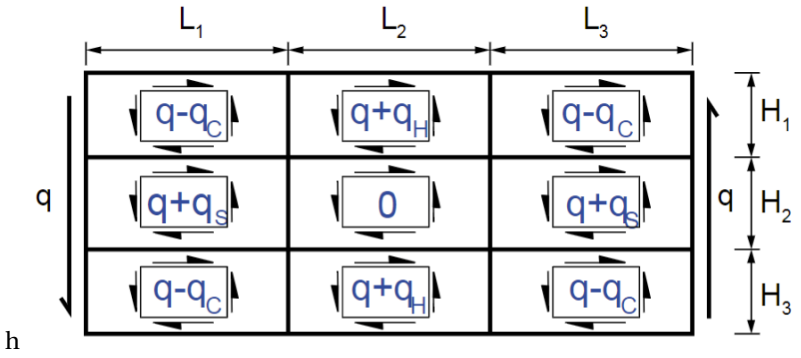

Figure 4.14: Shear flow around the centre section cut-out[11]

With the moment(M_x) calculated in Section 4.4.1, the bending stress can be calculated at every point along the wingbox with a safety factor(SF) of 1.5. The bending stress should always be below the ultimate stress (σ_{ult}) of the material which can be found in Table 4.9. If the bending stress is exceeding the σ_{ult}, the thickness should be increased.

Table 4.9: The material properties

Material	units	AL7075-T6[1] (spars)	Al 7050-T7451[1] (skin and ribs)
Physical properties			
Density [ρ]	g/cm^3	2.81	2.83
Mechanical Properties			
Ultimate tensile strength [σ_{ult}]	MPa	572	524
Tensile yield strength [σ_y]	MPa	503	469
Max strain	-	0.11	0.11
Youngs Modulus [E]	GPa	71.7	71.7
Poission's Ratio [υ]	-	0.33	0.33
Shear modulus [G]	GPa	26.9	26.9
Shear strength [τ]	MPa	331	303

However, the thickness of the spars and skin is not only dependent on the bending. Therefore, the torque and shear force is evaluated before determining the thickness.

4.4.3. Torque

With a known torque force(T) determined in Section 4.4.1, the local shear flows due to torque can be calculated. First wingbox is divided in two cells by the middle spar. The enclosed area(A_i) of the both cells is calculated by integrating between data points of the airfoil. The total torque can be divided over the two cells using Equation (4.14).

$$T = \sum 2 \cdot A_i \cdot q_{T_i} \tag{4.14}$$

[1] http://asm.matweb.com/search/SpecificMaterial.asp?bassnum=MA7075T6[cited: 21-6-2020]
[2] http://asm.matweb.com/search/SpecificMaterial.asp?bassnum=MA7050T745[cited: 21-6-2020]

Also the Equation (4.15) describes the angle of twist($\frac{d\theta}{dz}$) with ds being the length between two booms of a cell.

$$\left(\frac{d\theta}{dz}\right)_i = \frac{1}{2A_i}\oint \frac{q_{T_i} ds}{tG} \tag{4.15}$$

By combining Equation (4.14) and Equation (4.15), the shear flow(q_{T_i}) in each cell can be calculated as there are 3 equations with three unknowns(shear flow in the first cell(q_{T_I}) and the second cell($q_{T_{II}}$) and the angle of twist($\frac{d\theta}{dz}$)). The total shear flow in the cells is also dependent on the lift force and therefore the shear force results needs to be evaluated before calculating the thicknesses.

4.4.4. Shear

After calculating the shear flows(q_{T_i}) due to torque, a correction with the shear flows(q_{s_i}) due to the lift force(V_z) should be taken into account. First, the shear flow as an open section is considered with making a cut in the skin between boom 1 and 2 for the first cell and between boom 2 and 3 for the second cell, as can be seen in Figure 4.15.

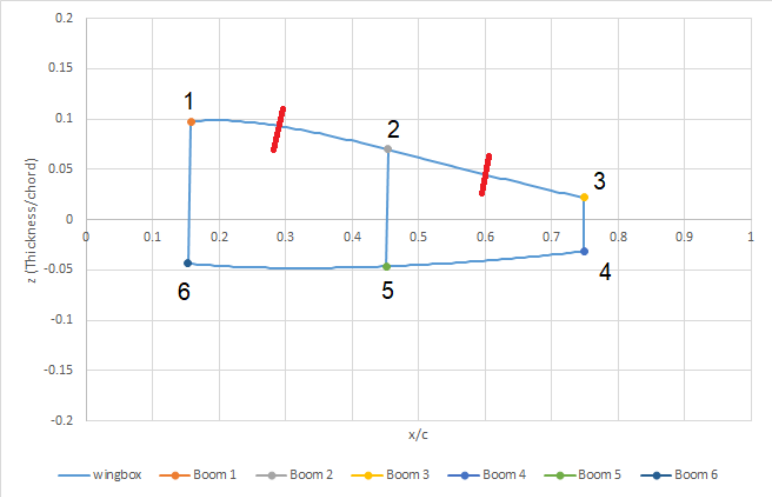

Figure 4.15: The wingbox with red lines as indicated cuts for shear calculations

The shear flows(q_b) for an open section are calculated with the use of Equation (4.16).

$$q_b = -\frac{V_z}{I_{xx}}\sum_{r=1}^{n} B_r z_r \tag{4.16}$$

This equations only works for symmetric multi-cell beams around the x-axis. Therefore, the average length between the upper skin between two booms is taken instead of the actual length for the boom calculations. This will result in a slight lower boom area for the upper boom and a slight higher boom area for lower booms, so this will compensate each other. To calculate the shear flows(q_s) in the spar and skins, Equation (4.17) was used for the two cells of the wingbox.

$$\frac{d\theta}{dz} = \frac{1}{2A}\oint \frac{q_s ds}{tG} \quad \text{where} \quad q_s = q_b + q_{s_0} \tag{4.17}$$

However, there is still one unknown to solve this system. To solve this, the moment around mid height of the second spar is taken, which results in Equation (4.18).

$$V_z \cdot dx = q_{b_{16}} ds_{16} dx + q_{b_{43}} ds_{43} dx + 2A_I q_{s_{0_I}} + 2A_I I q_{s_{0_{II}}} \tag{4.18}$$

Now the shear flowsQq_s) due to torque and shear are calculated and the actual required thicknesses can be calculated.

4.4.5. Result of Bending, torque and shear calculations

In this section the results of the previous calculations is showed. First the shear flows due to torque and lift force are combined and multiplied by 1.5 as a safety factor to find the actual needed thickness with Equation (4.19).

$$t = \frac{1.5q}{\tau} \tag{4.19}$$

After taken the shear flows and the bending moment into account, the thicknesses of Table 4.10 are found.

Table 4.10: The resulted thicknesses

Component	thickness for inboard wing[mm]	thickness for the outboard wing[mm]
Skin	0.5	1.9
Spars	2.6	2.5
Ribs	4	1

4.4.6. Rib spacing

In this section the rib spacing calculations are explained by the method of Ajaj et al.[12]. To calculate the rib spacing(l_{rib}) Equation (4.20) is used.

$$l_{rib} = \frac{SF \cdot L \cdot E_{sk} \cdot F^2}{\sigma^2_{comp}} \tag{4.20}$$

For the safety factor(SF), 1.5 is taken. The lift(L) is taken from the shear calculations. The young's modulus(E_{sk}) can be found in Table 4.9. F is dependent on which stringer is used in the design. In our design hat-stringers are assumed to be used and therefore F is equal to 0.9. Lastly, σ_{comp} is also taken to be σ_{ult} from the skin, which can also be found in Table 4.9. This results in a final rib spacing of $113mm$ for the outboard wing. For the inboard wing, the different sections are taken to be the ribs.

4.4.7. Buckling

The buckling was not taken into account of the design due to the time constraint. However, the suggested method will be explained to evaluate the stinger spacing. First, Euler buckling is formed during bending when the upper skin will experience compression. Therefore the initial buckling stress of the skin with an assumed stringer spacing should be evaluated with Equation (4.21). For Equation (4.21), the skin and spars should be evaluated separately as a panel each.

$$\sigma_{cr} = C\frac{\pi^2 E}{12(1-\nu^2}\left(\frac{t}{b}\right)^2 \tag{4.21}$$

The young's modulus E and the poison ratio (ν) needed for these calculation are dependent on the materials and can be found in Table 4.9. This critical stress(σ_{cr}) is the amount of stress which the panel can resist before buckling. This critical stress is also dependent on the thickness(t) of the panel and the length of the panel(b).This can be met with changing the effective length(L_e) and therefore the stringer spacing. However, first the panel should be evaluated with the effective width($2w_e$) of the stringers. After calculating the initial buckling stress, the crippling stress of the stiffener should be calculated with using Equation (4.22) and Equation (4.23).

$$\sigma^i_{cc} = \left(C\frac{\pi^2 E}{12(1-\nu^2)}\left(\frac{t}{b}^2\right)\right) \tag{4.22}$$

$$\sigma_{cc} = \frac{\sum \sigma^i_{cc} A_i}{\sum A_i} \tag{4.23}$$

In Equation (4.22), C is the buckling coefficient. For sections with one free edge, C is 0.425 and for a fully supported section the C is 4. In this calculation, the corners of the stringer not taken into account, because they act as supports to the thin plates. After calculating the crippling stress of the stringers, the effective width of the stringer can be evaluated with Equation (4.24).

$$w_e = \frac{t}{2}\sqrt{\frac{C\pi^2}{12(1-\nu^2}}\sqrt{\frac{E}{\sigma_{cc_{stiffener}}}} \tag{4.24}$$

The effective width ($2w_e$) is the effect of the stringer stiffening the skin. After knowing the effective width the buckling stress stress of the total panel can be recalculated with using Equation (4.23). This will give a increase of the critical stress(σ_{cr}) of the panel and should be higher than the yield stress (σ_y) to prevent buckling failure.

4.4.8. Verification and Validation

To verify the method used for calculating the thicknesses, different data sets are used from the course structural analysis & design of the TU Delft The results were equal to the results from the course and therefore this calculation was verified. Regarding validation, The best way to validate the structure is simulation of the loads on the aircraft or tests. As neither of these method were performed, the thicknesses could not be validated. Therefore it is recommended to use a Finite Element Method for the load simulation and after that test can be performed to validate the structure of the design.

4.5. Class II Weight estimation

Now the final weight of the inboard and outboard structure can be calculated. The weight of the airframe mass so far can be found in Table 4.11.

Component	Weight[kg]
Inboard wing	10953.84
outboard wing	3760.96

Table 4.11: The weight estimation of the inboard and outboard wing of only the skin, ribs and spars.

The weight of the airframe is not the entire operational empty weight. Since the aircraft is a blended wing-body, some penalties are awarded as described by Howe[13], which are explained in Section 4.5.1. Furthermore, the weight of the operational equipment also adds to the W_{OE}, as will be explained in Section 4.5.2.

4.5.1. Weight penalties

After the outer and inner mass are calculated, some weight penalties still have to added. These weight penalties are related to the nose section mass, the payload and any cutouts in the airframe structure and all given in kg.

Nose section mass

The nose section mass comprises of multiple sections, being the outer shell, leading edge extensions (LE), nose landing gear attachment and bay, windscreen (WS), crew floor (CF) and an extra allowance for doors (near the cockpit) and miscellaneous items. Since the final design is a non-pressurised aircraft, the calculations for the outer shell and windscreen are not used even though they belong to the nose section mass, since the pressurisation difference is zero. The weight are dependent on the pressurisation difference however, setting the weight penalties to zero as well. There are also no leading edge devices on the inner wing, hence the penalty for that section is zero. The equation that is used to calculate the crew floor is given Equation (4.25). The penalty for the doors and miscellaneous has a fixed value of $0.002 \cdot M_{MTO}$ and the penalty for the nose landing gear $0.003 \cdot M_{MTO}$. All section penalties are added together to form the nose section mass penalty, ΔF_{NOSE}

$$\Delta F_{CF} = (7 + 1.2B)S_{CF} \tag{4.25}$$

Here, S_{CF} is the surface area of the crew floor.

Payload volume

The payload volume penalty ΔF_{PAY} comprises only of the freight floors. In Howe's method, there are more weight penalties for other payload related sections, but they all relate to a pressurised aircraft and are therefore not taken into account for the same reason as mentioned for the nose section mass. The penalty for the freight floors, and so of the entire payload volume, is described by Equation (4.26). The equation has to be multiplied by 1.3 to account for the non-pressurisation.

$$\Delta F_{PAY} = \Delta F_{FRF} = 1.3 \cdot 2.6(1 + 0.6B_F)S_{FRF}\rho \tag{4.26}$$

Secondary structure

The secondary structure penalties comprise of the apertures (APT) and a ramp-type freight door (FD). The total secondary structure penalty ΔF_{FSS} is then the sum of both section penalties, whose functions are described by Equation (4.27) and Equation (4.28). Again, pressurisation equations were neglected.

$$\Delta F_{APT} = 60 \cdot S_{APT} \tag{4.27}$$

The area of the apertures differs from the doors and miscellaneous items. This value only accounts for one entrance door leading to the cockpit, so other doors and hatches are included in the apertures instead. In the final design, there is one cargo door in the front of the aircraft near the cockpit from which large equipment can be loaded or unloaded while on the water. There is also a hatch in the rear of the aircraft on the ceiling, from which the roof of the aircraft can be reached.

$$\Delta F_{FD} = 10 \cdot (1 + 0.75B_F)S_{DOOR} \tag{4.28}$$

In the final design, there is a ramp-type freight door in the back that allows for heavy gear loading when the aircraft is on the ground.

All the weight penalties can be found in Table 4.12 as well as a total weight penalty. The total weight penalty is added to the airframe mass of the inner wing since those calculations don't account for additional cut-outs in the airframe structure.

Table 4.12: Weight penalties of the nose section, payload volume and secondary structures for the inner wing

Weight component	Weight penalty [kg]
Nose landing gear	166.28
Crew floor	133.00
Allowance	110.85
Freight floor	1756.52
Apertures	363.00
Ramp-type freight door	302.25
Total	2831.90

4.5.2. Operational equipment

Next to the airframe mass the OEW also comprises of removable and non-removable operational equipment, that add to the weight of the inner wing for the BWB design. In commercial airliners this can weigh up to 50% of the airframe mass, so it can have a large impact on the OEW. There are multiple Class II weight estimation methods to calculate the weight of the operational items, but none are specified for a blended wing-body. Therefore a method needs to be chosen that represents the final design best. The chosen Class II estimate is specified for a commercial transport aircraft, since this seems to be the best approximate fit for the final design. Within this choice of aircraft, there is a choice between the Torenbeek method or the GD method. The Torenbeek method has the most equations regarding the operational equipment needed, so this method is chosen.

Equation (4.29) calculates the weights of the flight control system W_{fc}. The 1.2 is a penalty factor for leading edge devices. With this equation, the weight of the associated hydraulics system is already incorporated, but the weight of the electric system is combined with the hydraulic system as well. To obtain the weight for the flight control system, the weight for the hydraulics is subtracted for this weight.

$$W_{fc} = 0.64 W_{MTO}^{2/3} \cdot 1.2 \tag{4.29}$$

Equation (4.30) is used to calculate the weight of the hydraulic system W_{hps} and the electrical system W_{els}. W_E is the basic empty weight of the aircraft. To aid the calculation for the flight control system, it is assumed that the hydraulics take up 80% of the weight.

$$W_{hps} + W_{els} = 0.325 W_E^{0.8} \tag{4.30}$$

Equation (4.31) concearns the weight of the oxigen system W_{ox}, where N_{pax} is the number of passengers. Since there are two pilots, the aircraft needs an oxygen system designed for at least two people, but in case another passengers boards (for example a medic for a rescue mission) the number of passengers was set to one. The Torenbeek method actually provides three different equations: flight below $25,000 ft$, flight above $25,000 ft$ and extended flight. The latter is chosen because the oxygen system should provide for a mission flight as well as a ferry flight.

$$W_{ox} = 40 + 2.4 N_{pax} \tag{4.31}$$

Equation (4.32) calculates the weight of the internal furnishing W_{fur}, where N_{cr} denotes the number of crew members. The weight calculated with the method from Torenbeek was higher than $3000 kg$, which is to be far to high for an aircraft with only two seats. The Torenbeek method is used for commercial aircraft where the weight for the furnishing of all passengers is included as well, which is not applicable to the final design. The GD method is used to calculate W_{fur} instead. There were originally extra terms involved for the weight of passenger and cabin crew furnishing. Since the main mission of the aircraft does not include any passengers or cabin crew, setting the terms to zero results in the equation as it is now.

$$W_{fur} = 55 N_{cr} + 0.771 \left(\frac{W_{MTO}}{1000} \right) \tag{4.32}$$

The weight of the auxiliary gear W_{aux} can be calculated with Equation (4.33). W_{aux} is only determined by a statistical relation to W_E. Auxiliary gear is defined by Torenbeek as fire axes, sextants, unaccounted items and manufacturers variation.

$$W_{aux} = 0.01 W_E \tag{4.33}$$

The paint weight W_{pt} is dependent on the maximum take-off weight and can be calculated with Equation (4.34). The value usually ranges between $0.3 - 0.6\%$ of the MTOW and was set here to 0.5%. This is because the BWB configuration has a high wetted area compared to conventional aircraft. Also, the aircraft will most likely not be painted white, which is the lightest paint colour

$$W_{pt} = 0.005 W_{MTO} \tag{4.34}$$

Regarding the weight of the air-conditioning and anti-icing systems W_{api}, there is no equation for an unpressurized commercial transport aircraft so instead Torenbeek's method for multi-engine unpressurized general aviation planes is used, which is Equation (4.35).

$$W_{api} = 0.018 W_e \tag{4.35}$$

Lastly, the weight of the nacelles (or in the case of the final design pylons) can be calculated with Equation (4.36). The weight calculated here is associated with the external ducts and the engine mounting trusses. P_{TO} is the maximum thrust produced by all engines, which is at maximum take-off weight and specified in Chapter 7 Section 7.4.6.

$$W_n = 0.14 P_{TO} \tag{4.36}$$

The weight of all the different component can be found in Table 4.13. The weights are based on the MTOW of the Class I weight estimation as mentioned in Section 4.1.

Table 4.13: Weights for the operational equipment

Weight components	**Mass [kg]**
Flight control system	431.90
Hydraulics and electric system	532.40
Oxygen system	21.41
Furnishing	92.63
Auxiliary gear	279.97
Paint weight	125.71
Air-conditioning and anti-icing system	51.62
Pylons	1287.94

An overview of the total aircraft weight, which includes the airframe mass, weight penalties and operational items can be found in Chapter 16.

5
Hull Design

The hull of the aircraft is primarily responsible for ensuring sufficient buoyancy for the aircraft to stay afloat while on the water. Furthermore, the area inside the hull can also be used to house the extinguishing tanks and the nose landing gear. The design of the hull must take into account both the aerodynamic and hydrodynamic performance of the aircraft in order to optimise the geometry. Furthermore, the hull must be integrated with the main BWB structure to ensure stability on water and ground clearance on land.

5.1. Hull Sizing

First of all, the choice exists between a monohull and a multihull configuration. A monohull provides a more optimal use of space inside the aircraft as the fire extinguishing tanks can be easily placed inside the hull. Furthermore, due to this being the standard design of amphibious aircraft, there is substantially more data on sizing such a hull compared to a multihull. On the other hand, the stability of monohull designs on water is less than for multihull designs as the aircraft will tend to rock more with turbulent waters. Additionally, a multihull results in a smaller wetted surface area and thus reduced drag, allowing the aircraft to take off in shorter distances.
Ultimately, the choice is made to design a monohull for the BWB aircraft. The ability to rely on data gathered from other amphibious aircraft allows for a more reliable hull design with sufficient buoyancy. Furthermore, the stability of the monohull design is improved by designing flat sections on the underside of the aircraft which can provide an additional buoyant force when the aircraft rocks on the water. It is in these sections that the belly flaps will be placed.

As a first step of the hull design, the volume of water that must be displaced is calculated as this provides the buoyancy force. The apparent weight of the aircraft on water is calculated using eq. (5.1).

$$W_a = W_{object} - F_{df} \tag{5.1}$$

In this equation, W_a is the apparent weight of the aircraft in water, W_{object} is the actual weight of the aircraft, and F_{df} is the weight of the fluid that is displaced. For our design, this is assumed to be fresh water as it is less dense than sea water and will therefore lead to a bigger volume. The resulting buoyant force is equal to:

$$F_{buoy} = \rho_W g V \tag{5.2}$$

In the above equation, ρ_W is the density of fresh water, g is the gravitational constant and V is the volume of the submerged section of the aircraft.

According to regulation 14 CFR §25.751, the volume of water that can be displaced by the aircraft must account for 1.8 times the weight of the aircraft, as this would allow a part of the float to stay above water. For a MTOW of $59000kg$, this is equivalent to $106200L$ or $106.2m^3$ of displaced water. Not all of this volume must be displaced by the hull, as the underside of the BWB fuselage can displace some water volume as well and increase the stability of the design on water. Thus, the hull design can be designed to carry approximately 100% of the aircraft weight, equal to $59m^3$ of water, and will thus be completely submerged when the aircraft is stationary. The underside of the BWB can displace the remaining 80% of water as dictated per regulations, but will not be submerged during normal operating conditions. The sketch in Figure 5.1 illustrates this. The underside of the BWB fuselage section is parallel with respect to the water surface, minimizing the water drag during takeoff, landing and skimming operations. Furthermore, this section does not experience any large load factors directly, as the impact of the water is absorbed by the hull. Thus, little structural reinforcement needs to be added to this section of the BWB as the maximum aerodynamic loads experienced during flight of +3.75g is expected to be similar to those experienced due to contact with water. [14]

With an initial volume of $59m^2$ in mind, the basic dimensions of the hull can be calculated, after which a CATIA model will provide a more accurate value for the total volume of the hull. In Figure 5.2 The total length L has been set at $16m$, as this allows the hull to stretch from the nose of the aircraft until just before the elevator control surfaces. The width b of the hull is constrained by the addition of belly flaps to the underside of the inner wing. Since the total width of the inner wing is $10m$ and two belly flaps must also be positioned with a width of $3m$ each, the width of the hull is constrained at a maximum of $4m$. Another constraint is the location of the step in the hull, which must be positioned behind the aircraft c.g. dictated by the step angle. According to literature, this angle should be between 10° and 15° to allow the aircraft to rotate easily during takeoff on water. The location of the step, as well as the step height and step

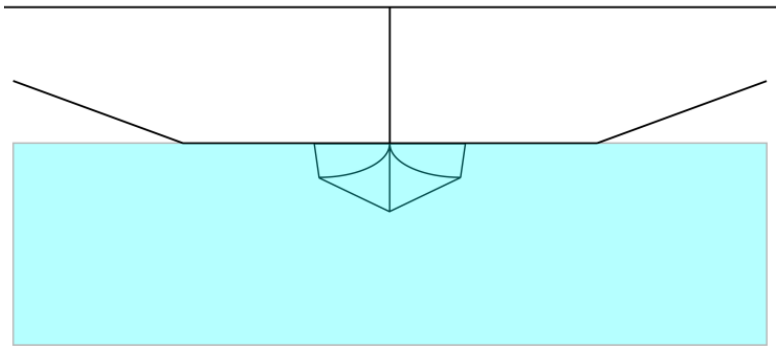

Figure 5.1: Location of water line with respect to the BWB inner wing and hull

incline, determine the sternpost angle α and afterbody length L_a. The step height should be approximately equivalent to $0.08b$, and the step can be inclined to reduce skin friction drag [15].

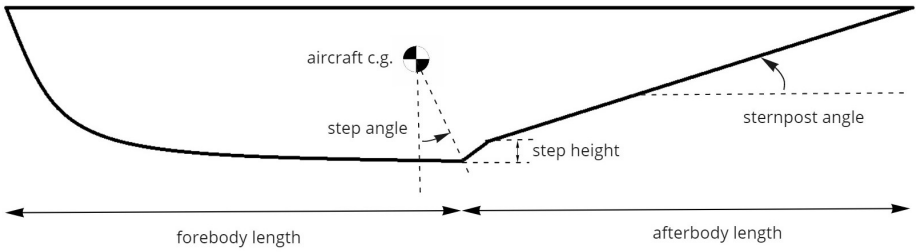

Figure 5.2: Definition of hull parameters

Next to the exterior shape of the hull, the structural reinforcement of the hull must also be designed with the impact loads of the water in mind. Data gathered during seaplane operations yields the following empirical relation:

$$n_{w_s} = \frac{0.012V_s^2}{\sqrt[3]{(tan^2(\beta)W}} \tag{5.3}$$

In this equation, n_{w_s} is the load due to water impact, V_s is the stall velocity, W is the aircraft weight and β is the deadrise angle on the bottom of the hull. This angle should be equal to 25° for heavy amphibious aircraft [15], and the angle should increase towards the nose to 40° to better cut through the waves when taking off and landing on water. The stall speed is calculated in Table 10.2 and the weight in Section 4.5. Overall, this results in a maximum load factor n_{w_s} of $3.86g$. This is relatively close to the $3.75g$ load factor endured in the maximum manoeuvring load case, however extra structural support and skin thickness must be added to ensure that the structure can withstand the water loads without the material yielding due to impact or fatigue loads.

5.2. Final Geometry

The final geometry was based on the combination of formulas and integration parameters. As such, the total length of the hull is 16 meters, which allows the hull to start right below the cockpit and end just before the elevator. In order to achieve the require volume, the final width at the top of the hull where it touches the fuselage is 4 meters. The depth required for the volume was 2 meters, which was the maximum that was considered to ensure the aircraft could still scoop and land in the majority of lakes. Due to the presence of the water tanks within the confines of the hull, the width prior to the beginning of the deadrise angle was fixed at 3.6 meters. The forebody length ended up at 8.44 meters, which includes the frontal curved section, and end just before the step. The step length was fixed at 0.9 meters, which is included in the afterbody length of 7.56 meters. The deadrise angle was set at 25 degrees at the start of the step, rising along the forebody to 35 degrees before the forebody begins to curve upwards, 2.5 meters from the nose of the aircraft. The tail of the hull narrows down to a point at the rear for optimal aerodynamics, while the slope of the afterbody is higher than the step to ensure it meets the rear of the hull, and prevent tail strike during take-off.

5.3. Hull Integration

Integrating the hull into the fuselage requires careful consideration of the impact of the integration method. The final geometry of the hull needs to be attached to the fuselage in such a way that it does not compromise the aerodynamics, or the hydrodynamics. Due to the buoyancy requirement, no geometry can be sunk into the fuselage

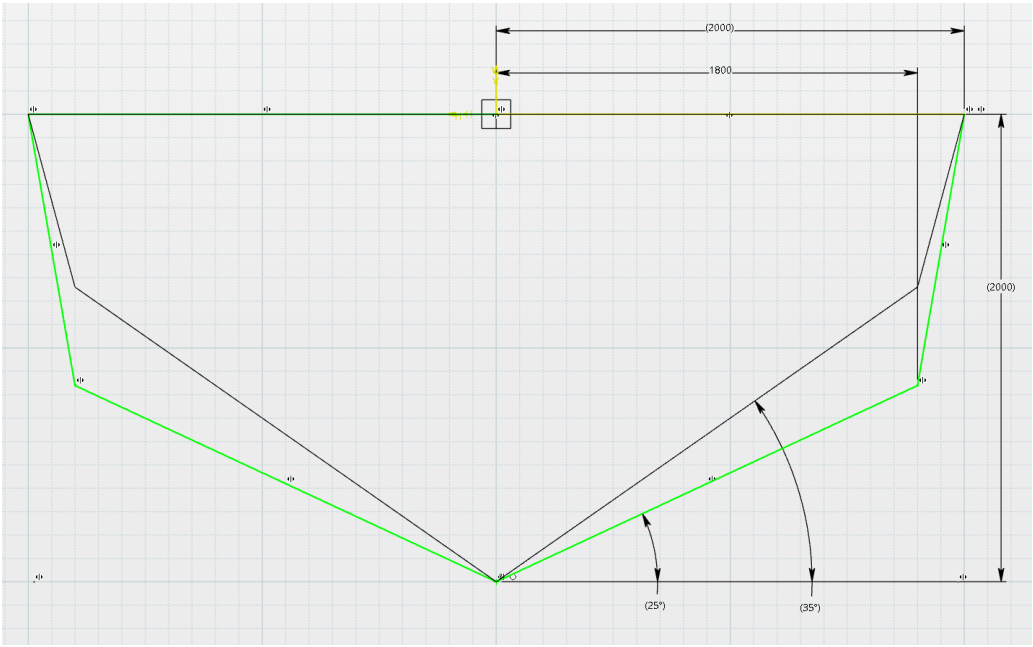

Figure 5.3: Cross sectional view of the hull, with the green lines showing the cross section prior to the step, and the black lines showing the cross section 2.5m from the nose

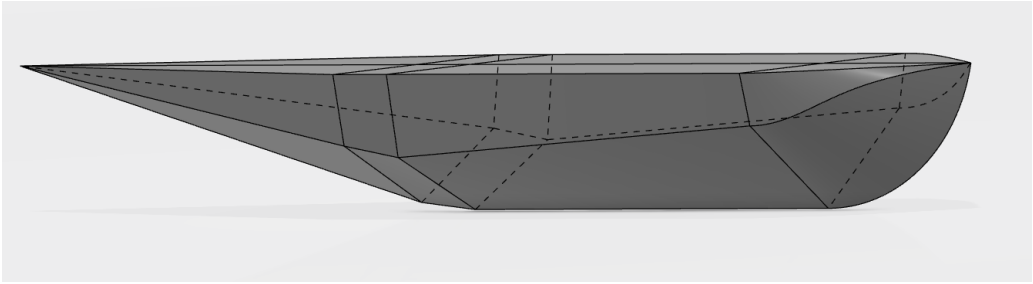

Figure 5.4: Overview of the hull geometry, with black lines showing sharp geometry

without significant adverse affect on take-off performance due the the added resistance and difficulty in taking off while a large part of the fuselage is in direct contact with the water. Conversely, a mounting that is distant from the fuselage will adversely affect aerodynamics, and can critically affect the overall stability of the aircraft during flight. Another consideration is that the hull needs to be mounted in such a way to avoid ground strike while taking off from a runway.

The hull was integrated by placing it centrally in the fuselage, with the nose curving up to the cockpit, while the rear end stopped just short of the elevators, which have to be kept free to function. The flat top of the hull posed a problem for the curved underbelly of the fuselage. The flat top was placed such that it was in contact with the lowest part of the curved underbelly, while a fairing was installed between the front and back ends of the hull and the fuselage. This fairing is curved specifically to minimise the disturbance of the flow of air due to the hull. The front of the hull requires only a minimal amount of fairing, as the distance between the hull and the fuselage at this location is small. However, the rear end of the fuselage curves up significantly, and therefore requires significantly more fairing. Due to the narrowing of the hull to a point towards the rear, it is possible to have this fairing be vertical for a significant stretch, before curving into the fuselage. The point will prevent pressure drag, while the flat surface allows for easy manufacturing, and simplifies the the underlying structure, the design of which is beyond the scope of this document.

This integration means that the fuselage structure is minimally impacted by the hull. Additional structure is likely necessary to provide a load path from the hull into the fuselage, and this can be placed within the fairing, and can make use of the fairing itself. The cargo floor incorporated within the fuselage of the aircraft will make transferring the loads from the hull easier, reducing the weight and volume of structure needed. Detailed design of this structure is outside the scope of this document.

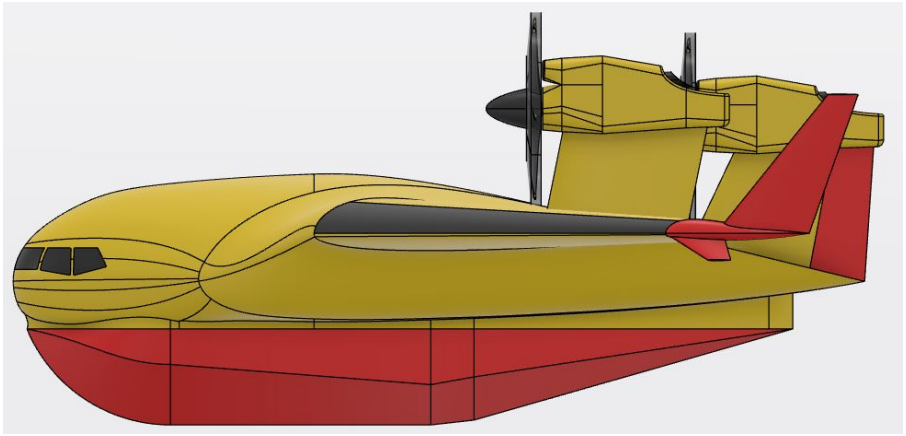

Figure 5.5: Side view of the integrated hull

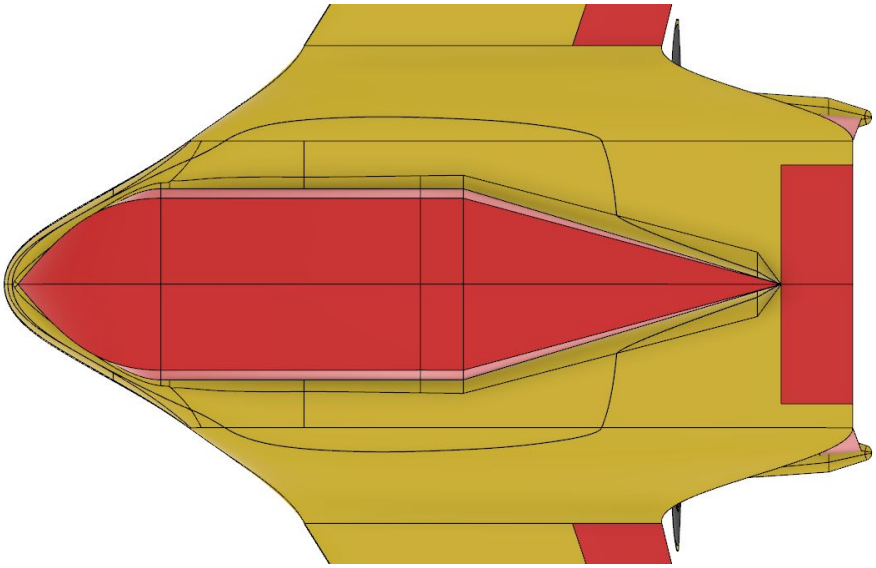

Figure 5.6: Bottom view of the integrated hull

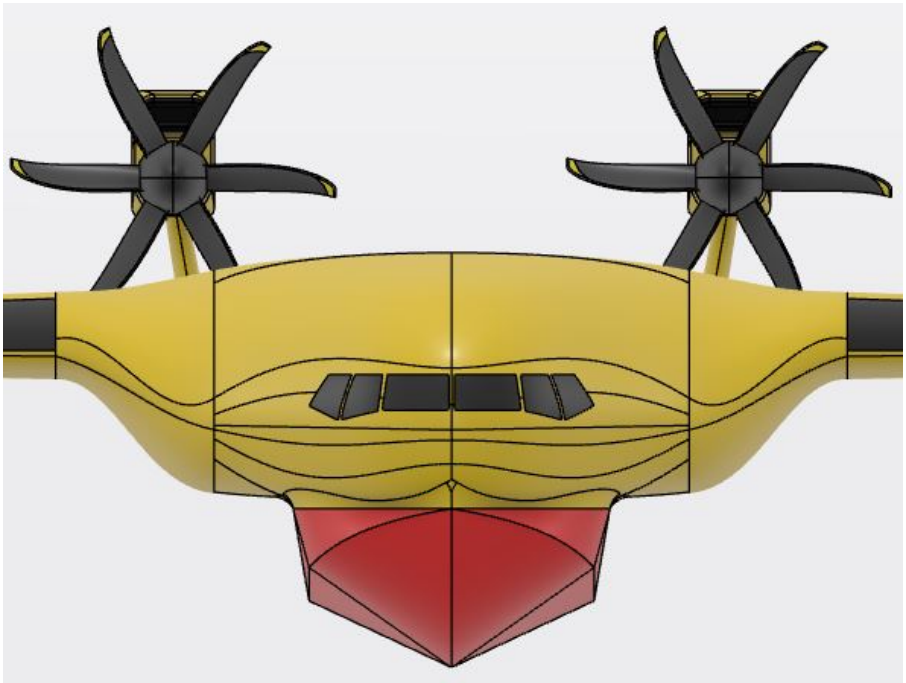

Figure 5.7: Front view of the integrated hull

6
Aerodynamics

Due to the unconventional design of the aircraft, a careful analysis of the aerodynamic properties of the design is required. In this chapter, a detailed description of the analysis method and process and the constraints of the method are given in Section 6.2. Secondly, the planform selection is discussed in Section 6.3. Afterwards, the airfoil selection is discussed in Section 6.4. High lift devices are discussed afterwards in Section 6.5. Moreover, various flight cases are analysed for their performance, loadings and case parameters in Section 6.6.

6.1. Requirements and Constraints

In earlier phases of the project, of which the planning can be found in Section 3.1, requirements and constraints were set regarding various parts of the aircraft design. As the aerodynamic plan form of the design is a widely integral part of the aircraft, it has an influence on quite some subsystem requirements. However, as there are no specific requirements or constraints set for the aerodynamic characteristics of the design, those requirements are not listed here as they are discussed in their own respective parts.

6.2. Analysis Method

Firstly, this section will elaborate upon the analysis process in Section 6.2.1. Secondly, the analysis method used to analyse the aerodynamic characteristics of the design is given in Section 6.2.2. Thirdly, the constraints and method assumptions of this analysis method are outlined in Section 6.2.3.

6.2.1. Analysis process

In this section, the analysis process of the aerodynamic characteristics is outlined. The process, as a graph, is given in Figure 6.1. Firstly, the general planform and airfoil are selected based on their performance and characteristics. Then, the control surfaces and wingtips are optimised according to the chosen planform. Afterwards, the stability and control is assessed. If these values are acceptable, a preliminary final geometry is determined. Finally, if the final parameters are calculated, verified and validated, it concludes into the final aerodynamic design.

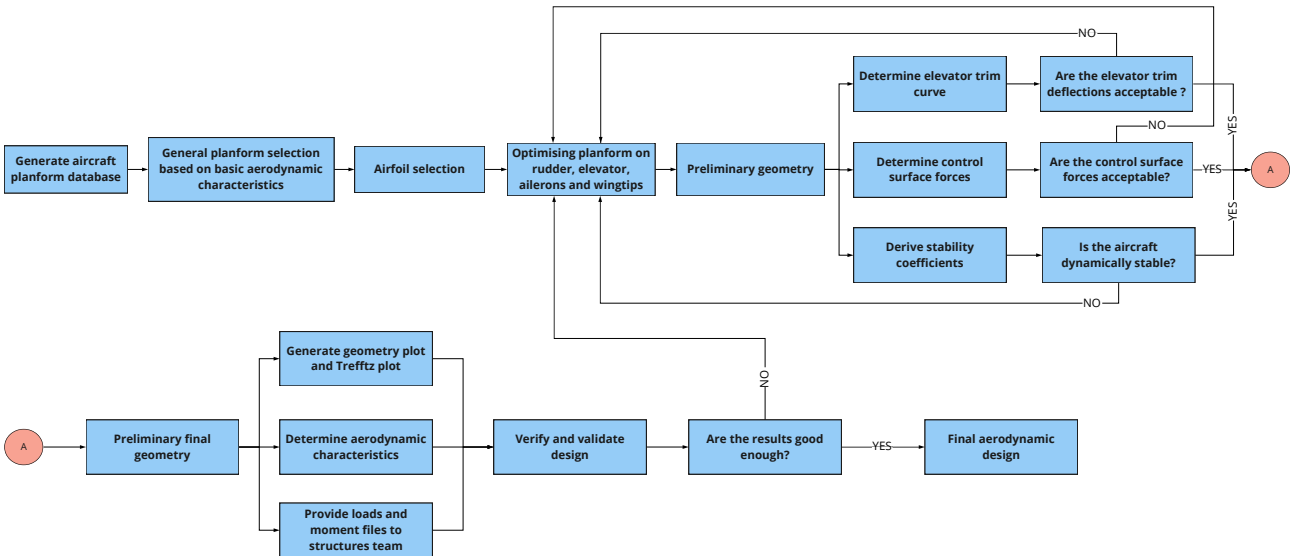

Figure 6.1: Planning of the aerodynamic design.

6.2.2. Athena Vortex Lattice

For the aerodynamic analysis of the designed aircraft, the software Athena Vortex Lattice (AVL) was chosen to be the used tool. Due to the time and resource constraints within this project, it is not possible to analyse using for example Computational Fluid Dynamics (CFD) methods. Therefore, the easily accessible method of AVL was chosen as analysis method for the final design.

Theoretical Background of AVL As the name of the software suggests, the programme uses the Vortex Lattice Method (VLM) as theoretical analysis method. The VLM models the aircraft's wing and body as a camber, hence neglecting

airfoil thickness. This camber is modelled using horseshoe vortexes, which are distributed along the modelled camber and across the wing span. The mesh of these vortexes can be altered. Hence, for preliminary analysis a small mesh can be used and when finalising the analysis the mesh size is increased for improved accuracy. These horseshoe vortexes are lift producing elements and therefore the aircraft geometry within AVL can be modelled and analysed.

Automatisation of the Analysis Designing an aircraft from scratch requires a lot of analysis on various geometry planforms, wing design, airfoil design, rudder design, elevator design and aileron design. Although AVL allows for a quick learning curve and is therefore quickly implemented in the design process, analysing all the aforementioned design choices is labour intensive and therefore it is unfeasible to do these by hand within the time constraint. Therefore, a small research was done to search for an option to automate the analysis process, which concluded in the use of AVLWrapper, which is written by Reno Elmendorp [1]. This code produces a geometry file and a case file as required by the inputs for AVL. Afterwards, the code automatically starts AVL and runs these cases. Moreover, the programme allows for automatising the analysis of trim cases of the aircraft for a range of angle of attacks, quick changes in geometry and the plotting of the geometry and the Trefftz plot. With making slight changes in the programme, the analysis of different airfoils and different planforms but also control surface forces and stability analysis were automatised as well. I

6.2.3. Method Constraints and Assumptions

Although AVL provides a sufficient preliminary, aerodynamic analysis, it also has some drawbacks regarding the assumptions it makes and the constraints the programme poses to the aircraft geometry one can implement in the programme.

Assumptions The first and most noticeable assumption that AVL makes is the thin surface approximation. Therefore, the fuselage and wing are approximated by their respective airfoil camber. As the centre section airfoil of the Blended Wing Body (BWB) is far from thin, the data gotten from these airfoil sections need to be analysed carefully in order to prevent large perturbations in the resulting data.

Secondly, AVL makes the small angle approximation. This means that the data is most accurate for small angles of attack and sideslip. Hence, when analysing the BWB for large angles of attack and sideslip, these data need to be handled carefully and with some margin.

Finally, AVL assumes irrotationality and linearisation about the freestream. The linearisation assumes small perturbations (thin surfaces), which is not completely valid when free-stream velocity perturbations become large [2]

Constraints Firstly, AVL does not allow for engines to be implemented into the geometry. Therefore, the added moments of the engine thrust and weight are not implemented. However, the weight can be implemented by adding it to the total weight and moment of inertia's.

Secondly, AVL is designed for aircraft's with low Reynolds numbers. However, due to the large chord at the centre section of the aircraft, the Reynolds numbers encountered for the BWB are relatively large and hence data might be offset.

Finally, as determined in Section 6.5, the final design of the aircraft makes use of belly-flaps. However, it is not possible to model these flaps in AVL.

6.3. Planform Selection

The first thing for the aerodynamic characteristic determination was to choose a planform. As the this analysis was automatised, a lot of planforms could be analysed. To give an idea of what sort of planforms analysed, some general planforms are given in Figure 6.2 up to Figure 6.7. It should be noted that the two pylons of the remaining two engines were not added in the geometry as the choice of the engine placement was made too late in the design process, hence there was too little time to add them. Moreover, these general planforms were altered in sweep, taper ratio, etc. in order to see if they were not altered too much by there planforms. These planforms were then analysed for their lift, drag, moment and stability coefficients.

[1] https://gitlab.com/relmendorp/avlwrapper
[2] http://web.mit.edu/drela/Public/web/avl/avl_doc.txt

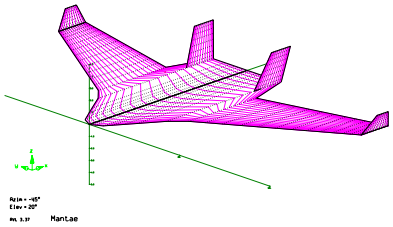

Figure 6.2: Final design with the conventional wing roughly midway through the reference chord.

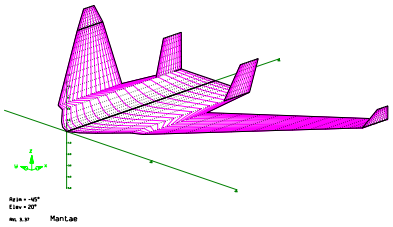

Figure 6.3: Design option with the conventional wing at two meters from the front and large sweep.

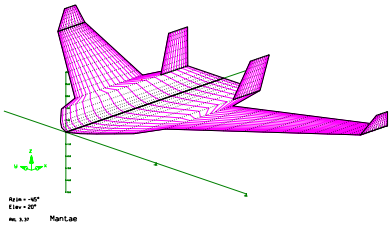

Figure 6.4: Planform option with the conventional wing midway through the reference chord with an alteration in sweep.

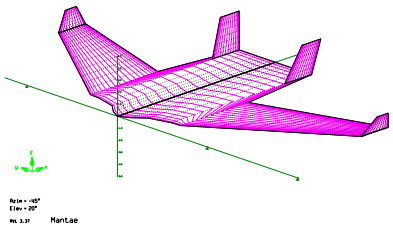

Figure 6.5: Planform option with the conventional wing completely at the front.

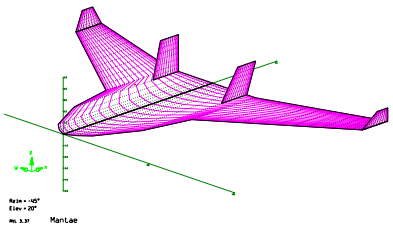

Figure 6.6: Planform option with the conventional wing at the back of the aircraft.

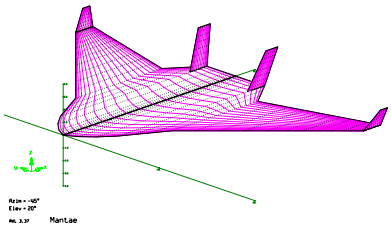

Figure 6.7: Planform option with an alteration in taper ratio

After thorough analyses, the planform in Figure 6.2 was chosen to be our final design planform.

6.4. Airfoil Selection

Secondly, for the aerodynamic characteristic determination, two different airfoils were chosen; one for the inner wing and one for the outer wing section of the aircraft. Due to the automatisation of the AVL analysis, a large amount of airfoils are analysed for their aerodynamic performance.

6.4.1. Inner Wing Airfoil

For the centre section it was chosen to pick an existing, rather thick airfoil as reference point for simplicity. Moreover, due to time constraints it was chosen not to design an airfoil specifically optimised for the integration of the hull. From the AVL analysis, it was found that the Wortmann FX 69-274 was best fit for the centre section, based on aerodynamic characteristics such as lift, drag and moment coefficients.[3] The Wortmann FX 69-274 airfoil is depicted in Figure 6.9. Due to its rather thick centre section, it fits the characteristics needed for the fuselage section of the aircraft. After the selection of this airfoil, the hull was added to this airfoil in CAD in order to come up with the airfoil with the hull integrated in order to analyse the implementation of the hull. This hull-integrated airfoil is used for the inner $4m$ of the aircraft and is shown in Figure 6.8. For the remaining part of the centre body section the Wortmann FX69-274 airfoil is used.

6.4.2. Outer Wing Airfoil

For the outer wing section, various airfoils were analysed of which the Martin Hepperle MH78 airfoil was found to be the best performing airfoil aerodynamically. [4]

[3] http://airfoiltools.com/airfoil/details?airfoil=fx69274-il
[4] http://airfoiltools.com/airfoil/details?airfoil=mh78-il

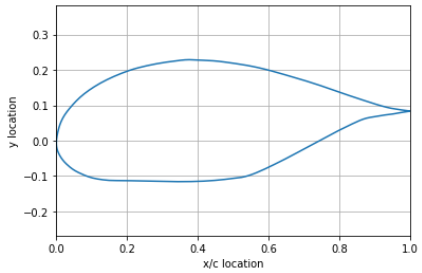

Figure 6.8: Center body airfoil with hull integration

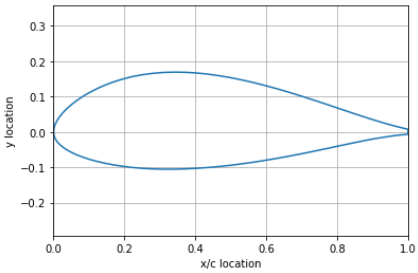

Figure 6.9: Center body airfoil without the hull integration

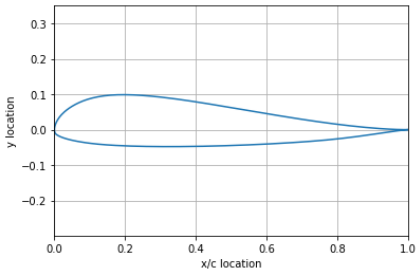

Figure 6.10: Outer wing airfoil starting for the whole conventional wing part

6.5. High Lift Devices

In order to achieve the takeoff, landing and skimming requirements, high lift devices must be added to the aircraft to improve low speed performance. Adding wing flaps is a design challenge for BWB aircraft, as the negative pitching coefficient caused by the flaps cannot be countered by a horizontal stabiliser like with conventional aircraft. Thus, other methods must be explored to increase C_L values at low speed.

Firstly, leading edge slats can be added to the aircraft without a detrimental effect to the pitching moment of the aircraft. The primary function of slats is to extend the $C_L - \alpha$ curve, thereby increasing the angle of attack α at which the aircraft stalls and the value of C_{Lmax}. According to Brown, slats would increase C_{Lmax} by 0.2 for a land-based BWB aircraft. However, the presence of the hull on the bottom side of the aircraft substantially reduces the lift rate coefficient $C_{L\alpha}$ of the aircraft with respect to other BWB designs. Consequently, an increase in C_L of 0.1 has been assumed as a preliminary estimate.

Even though trailing edge flaps are not a viable option, flaps positioned on the underside of the aircraft are a possibility, as they can generate a positive pitching moment. These are called belly flaps and their effect on lift can be rather substantial when positioned correctly. Staelens performed experiments and CFD calculations on different types of belly flaps and found two designs that produce the largest benefit to aircraft performance [16]. The flat plate used for the flap can be designed with and without circular holes drilled into it. The flat plate without holes has a greater positive influence on pitching moment coefficient with respect to the flat plate with holes, which is beneficial for stability purposes. The flat plate with holes on the other hand has a larger increase in C_L and a smaller increase in C_D which results in an aerodynamically better performance. Ultimately, the decision was made to implement the belly flaps with holes since the aerodynamic effects will provide greater benefits for low speed performance.

According to Staelens, the total length of the belly flaps should be 20% of the total wingspan of the aircraft, and should deploy to an angle of 90° for the greatest lift increase. For a wingspan of $33.5m$ this is equal to a total length of $6.7m$. Due to the presence of the hull on the underside of the aircraft, this length can be split in two and placed on either side of the hull to obtain similar aerodynamic results [16]. For this length, the height of the belly flap should ideally be equal to $1.1m$. The plate thickness should be equal to $3.4cm$, scaled according to the model used by Staelens [16]. The configuration of the belly flaps is illustrated in Figure 6.11. Proper design of the belly flap mechanism is essential for avoiding corrosion damage due to frequent contact with water, hence the flaps should be watertight when in the undeployed position. The belly flaps cannot be used when on water as they would drag through the water surface, generating strong forces on the hinge mechanisms and causing a substantial increase in drag to the aircraft when taking off.

Overall, the belly flaps generate a 35% increase in lift and a 30% increase in drag at takeoff and landing speed [16]. These values are obtained for a BWB scale model without hull, but the presence of a hull speeds redirects the airflow and speeds it up along the sides, theoretically creating a larger increase in lift. However, since this effect cannot be accounted for within the scope of this project, the effect of the redirected airflow has been neglected.

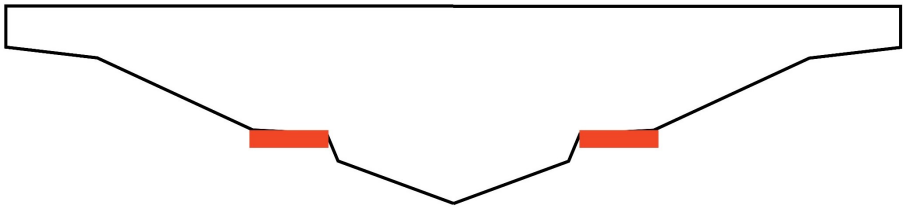

Figure 6.11: Location of the belly flaps, highlighted in red

6.6. Flight Cases

In this section, several flight parameters of the cruise and drop (before and after) flight cases are given. For every analysed case, the required lift coefficient CL was calculated in AVL, after which the angle of attack was set to this lift coefficient in order to generate the lift required. After setting the pitching moment to zero by trimming the elevators, the flight case is analysed in AVL. In Table 6.1, a short overview of the angle of attack, lift coefficient and elevator deflection for every flight case is given. The CD is not given, as AVL does not give accurate values for the CD as it underestimates them.

Table 6.1: Shows the required parameters for different flight cases.

Flight Case	α **[deg]**	**CL [-]**	δ_e **[deg]**
Cruise	4.01	0.18	-2.44
Before drop	11.01	0.86	-4.17
After drop	8.49	0.56	-3.92

6.7. Verification of the Aerodynamics Tool

In order to ensure righteousness of the code of the aerodynamics tool, a verification is performed. Th verification of the tool consists of verifying the used code, identifying and solving bugs in it.

6.7.1. Verification of the Code

As mentioned before, the verification of the code consists of identifying and debugging of errors the code produces. It should be noted that the software behind AVL is assumed to be correct. Hence, the verification (and also validation) of the aerodynamics tool is about the link between the used code and the AVL software. In order to verify the code, firstly the code was checked thoroughly, with checking small parts of the code for its correctness by doing tests with it. As mentioned before in Section 6.2.2, AVL requires a geometry and case file as input before the analysis are made. Hence, the final step in verification of the code was to produce a hand made geometry and case file in order to see if the geometry plotted by AVL and the result values were coherent.

6.7.2. Calculation Verification

For the verification of the calculation, it was chosen to set the geometry in the AVL analysis to before drop conditions for which a certain angle of attack and CL value rolled out, namely an angle of attack of 11.01 deg and a CL value of 0.86. Then, using AVL, it was found that the centre section of the aircraft including the hull produces 40.0% of the total lift of the aircraft. Moreover, the remaining part of the fuselage provides 24.0% of the total lift and the outer wing produces the remaining 36% of the total lift in before drop conditions. Then, using XFLR, it was found that, at an angle of attack of 11.01, the center hull section produces a CL of 0.55, the remaining fuselage produces a CL of 1 and the outer wing produces a CL of 1.1 for drop conditions. After multiplying the percentages with their respective CL values, one comes to a value of CL is 0.856. Hence, as can be seen, the aircraft produces the values as given by AVL and therefore it can be concluded that the aircraft is verified.

6.8. Validation of the Aerodynamics Tool

For the validation of the aerodynamics tool, one would compare the aerodynamic characteristics, for example lift and drag, of the tool with existing blended wing body aircraft. Unfortunately, as currently there is no amphibious, blended wing body aircraft in use which nears our firefighting purposes, the validation of the aerodynamics tool could not be performed.

6.9. Sustainability Approach

Regarding sustainability, the aerodynamic characteristics of the aircraft mainly have an influence on the aerodynamic noise MANTÆ produces. During landing, this noise is most apparent and with increasing noise reduction demands around airports, it is of importance to address this factor of noise generation. Airframe noise is mostly generated by the flaps, slats and the landing gear [17].

Flaps

Flaps introduce noise due to the existence of strong vortexes between the flapped surface of the aircraft and the non-flapped surface of the aircraft's body due to the change in local produced lift [17]. Hence, controlling these flap edge vortexes results in a lower noise level for the flapped surfaces. This can be done by brushing the flap edges or by adding an flap edge fence [18]. Moreover, the use of the Continuous Mold-line Link (CML) is a possibility in the further design of the aircraft, which essentially blends in the edge of the flap with the aircraft body part. The actual effect of these design options can be further estimated by the use of Computational Fluid Dynamics (CFD) [19].

Slats

For slats, the most noise is generated by the cavity between the slat itself and the main wing. This cavity mainly

contributes to having the turbulent boundary layer transform into sound waves. Adding porous or brushed edges at the trailing edge of the slat significantly reduces the noise generation for the slats [17].

Landing Gear
The landing gear mostly produces noise because of the bluntness of its body, which introduces airflow separation. In order to reduce landing gear noise generation, the landing gear should be placed behind a fairing in order to reduce its bluntness relative to the airflow and make it appear as a more streamlined body to the airflow. To remain easily retractable landing gears, the components of the landing gear should have an individual fairing [18].

6.10. Final Remarks

The values of the aerodynamics presented in this section are preliminary assessed. Hence, these values should be taken with care and further designing should be done if conclusive values are to be found. As the design of the aircraft is far from finished, the following recommendations regarding aerodynamics are made.

Centre Body Airfoil
In the aerodynamic analysis presented in this chapter, an already existing airfoil was chosen for the centre body section of the aircraft. This was done due to time constraints within this project and for simplicity's sake. However, a custom made airfoil for the centre body should introduce better hull integration and improved aerodynamic characteristics for the airfoil.

Wing Twist
Currently, the design and especially the aerodynamic analysis has been assessed without introducing wing twist. As wing twist greatly influences local angle of attack and delays stall near the wing tips, this could influence the aerodynamic characteristics positively. Due to the time constraints within this project, the design for MANTÆ could not be optimised for wing twist, but this is something that should be analysed in the future.

Computational Fluid Dynamics
The aerodynamic analysis presented in this chapter made use of the Athena Vortex Lattice software by Mark Drela. This software uses the thin-wing assumption. However, as the aircraft is relatively thick because of its hull and general thick centre body section, more realistic data should be provided by Computational Fluid Dynamics (CFD) as this allows for proper 3D modelling of the entire aircraft. Moreover, CFD allows for analysing the local airflows at for example the slats, flaps and landing gear. This allows to analyse local noise generation and hence introduces opportunity to reduce local noise levels to increase the sustainability of the aircraft.

Adding engines to aerodynamic analysis
As of now, only two pylons are added within the AVL geometry. In further analysis, not only the remaining two pylons should be added to the design, but also the engines itself and their added thrust and weight forces. As stability is quite challenging for the blended wing body, the thrust vectors of the engines might have a large negative influence. Therefore, they should be added in further analysis together with their pylons.

7
Propulsion

In this section the propulsion system design, selection and characteristics are discussed. As has already been determined in the midterm report , the system consists of a set of turboprop engines[5]. First, an overview of the requirements that drive the power plant selection is performed in Section 7.1. This comprises of a set of user, system and certification requirements. Next, given the required performance of the aircraft, a series of important relations used to determine the power that the engine must provide are developed and shown in Section 7.2. With these, the results of the tool developed for estimating the power requirements are shown, verified and validated in Section 7.3. After this turboprop engine options that can be obtained for the development of an aircraft are explained. Then the engine selection is performed by trading-off different characteristics, arriving to a final decision in Section 7.4. After this the selection of the propeller system is discussed in Section 7.5. With the power plant selected, a fuel performance analysis is performed, verified, and validated to determine that the amount of fuel is enough to meet the requirements. This is done in Section 7.6. Finally, a sustainability approach, consisting of noise and pollution is discussed in Section 7.7 and a risk analysis based on possible malfunctions is performed in Section 7.8.

7.1. Requirements

To determine the required size of the power plant it is important to determine the requirements which drive it. These requirements can be split into two main categories. The first one is the user and system requirements, which are set by the stakeholder and the design team in order to develop the required aircraft. The second category are requirements which the aircraft must be able to achieve in order to be certified to fly. These are imposed by regulation authorities.

7.1.1. User and System Requirements

The following requirements, which were set by the stakeholders and design team, have an influence and impact on the design of the propulsion system of the aircraft.

FFA-Per-003 The aircraft shall be able to take-off from a $2,000m$ runway at sea-level and standard atmosphere conditions.[1]

FFA-Sus-003 Propulsion using bio-fuel shall be used if possible.

FFA-Oth-001 The platform shall be equipped with a well-known power plant model to ease maintenance work in remote locations where spare parts may be scarce.

FFA-Per-006 The aircraft shall have a rate of climb of at least $12m/s$.

FFA-Per-007 The aircraft shall have an operational range of $1,250.0km$.

FFA-FOp-001 The aircraft shall have a ferry range of $2,700.0km$.

FFA-S&R-007 The propulsion shall have single redundancy.

7.1.2. Other Requirements and Regulations

For the aircraft to be certified to fly it must abide by the CS25 regulations[20]. These regulations state the following requirements regarding the climb gradients that the aircraft must achieve at five different configurations. The five configurations are the following:

1. Landing configuration at minimum landing speed, or 1.15 times the landing stall speed.
2. Take-off configuration at minimum take-off speed, or 1.1 times the take-off stall speed.
3. Take-off configuration at minimum climb speed, or 1.13 times the take-off stall speed.
4. Clean configuration at minimum climb speed, or 1.13 times the take-off stall speed.
5. Landing configuration at minimum approach speed, or 1.3 times the landing stall speed.

Taking the numbering of these configurations into account, the specific requirements are shown in Table 7.1.[2] From these minimum climb gradients that the aircraft must be able to reach, the minimum rates of climb can be obtained. The value of these, however, depends on the stall speeds of the aircraft. Their calculation is shown in Table 7.2.

[1] This is a stakeholder requirement, however, it was decided to develop an aircraft capable of taking off from a $1,000m$ runway to be operational in small airfields. This goes in line with the mission need of a widely deployable aircraft design.

[2] Table used previously in Midterm Report[5]

Table 7.1: Climb gradient requirements specified by CS25.119 and CS25.121 [20]

Climb gradient	2 Engines	3 Engines	4 Engines
CGR_1	0.032	0.032	0.032
CGR_2	0.001	0.003	0.005
CGR_3	0.024	0.027	0.030
CGR_4	0.012	0.015	0.017
CGR_5	0.021	0.024	0.027

Table 7.2: Rate of climb requirements by gradients as specified by CS25.119 and CS25.121 [20]

Climb rate	Calculation
ROC_1	$V_{landing}(CGR_1)$
ROC_2	$V_{take-off}(CGR_2)$
ROC_3	$V_2(CGR_3)$
ROC_4	$V_2(CGR_4)$
ROC_5	$V_{approach}(CGR_5)$

Lastly, an additional requirement imposed by the CS25 regulations that affect the sizing of the engine, **CS 25.115 Take-off flight path** states that an altitude of 35 ft must be reached within the take-off platform.

7.2. Relations for the Sizing of the Turboprop Engine

To determine the necessary power that the power plant must have available given the stated requirements it is important to determine their mathematical expressions and relations. Firstly, some general relations for a turboprop engine are shown. After this, relations to performance in cruise are explained. Later, relations for take-off performance, climb performance and finally manoeuvrability expressions are shown.
It is an important remark that not all of the size determining factors are encompassed by the requirements. The most important of these factors are reaching a cruise speed of $130 m/s$, a manoeuvring load factor of $2g$ at the drop speed and a take-off distance of $1000m$ instead of the $2000m$ stated in **FFA-Per-003**. Another important remark is that not all of the requirements on the propulsion system provide a limit on the engine's size, some of them, such as **FFA-Per-007**, provide a requirement on the fuel required. Other requirements such as **FFA-S&R-007** state a requirement on the intrinsic reliability of the design rather than on the size of the engine. These requirements will be discussed in further detail after the engine sizing is determined.

7.2.1. General Relations

The most determining factor for the required engine capabilities is the power available it must provide. The power available P_a is determined as shown in Equation 7.1.

$$P_a = \eta_j P_{br} + T_j V_0 \tag{7.1}$$

Where:

- η_j: Propulsive efficiency of the propeller. For turboprop engines $\eta_j \approx 0.8$
- P_{br}: Shaft power of the engine.
- T_j: Jet thrust of the engine. Usually accounts for $10-20\%$ of the total engine's thrust[9].
- V_0: Freestream velocity under which the engine is being operated.

From this relations another parameter can be derived. The definition of the so-called equivalent shaft power, P_{eq}, includes the contribution of the jet thrust. Its relation is given by Equation 7.2.

$$P_{eq} = \frac{P_a}{\eta_j} = P_{br} + \frac{T_j V_0}{\eta_j} \tag{7.2}$$

The relation of the equivalent power output of the engine to the altitude is related by the air density. In this was the power which the engine must provide at sea-level can be obtained by taken into account the altitude. The relation is as seen in Equation 7.3.

$$\frac{P_{eq}}{(P_{eq})_0} = \left[\frac{\rho}{\rho_O}\right]^n \tag{7.3}$$

Where the subscript 0 designates sea-level condition and the power n in the troposphere is equal to 0.75. Additionally, a relation that is useful for the calculation of rate of climb, and angle of climb (also mentioned as climb gradient) is shown in Equation 7.4. Where γ is the angle of climb and ROC is the rate of climb .

$$ROC = V \sin\gamma = \frac{P_a - P_r}{W} \tag{7.4}$$

An important final remark is that given the dependence on velocity of the jet thrust and the low contribution of it to the total power available of the engine, only the shaft power that the aircraft can provide will be taken into account for the sizing. This will end up slightly overstating the required available shaft power of the engine. This is a safe and conservative approximation and it gives a margin for the engine on its performance.

7.2.2. Cruise

For the aircraft to maintain cruise, the power provided by the power plant for the thrust must match the power required to counteract the drag. The power required is related to the drag by $P_r = DV$. From this relation the power required can be expressed as shown in Equation 7.5.

$$P_r = C_D \frac{1}{2}\rho V^3 S = C_{D0}\frac{1}{2}\rho V^3 s + \frac{{W_{MTO}}^2}{\pi A e \frac{1}{2}\rho V S} \tag{7.5}$$

Where:

- C_D: Drag coefficient at cruise conditions.
- C_{D0}: Zero-lift drag coefficient.
- W_{MTO}: The maximum take-off weight of the aircraft[3].
- A: Aspect ratio of the aircraft.
- e: Oswald efficiency factor.

7.2.3. Take-off

There are two main take-off related performance parameters that the engine must be able to make the aircraft reach. These are the take-off ground run and airborne phase distance stated by **FFA-Per-003**, although, as previously mentioned, a take-off distance of $1,000m$ is ultimately required. Therefore the ground take-off distance plus the airborne take-off distance must be less or equal than $1,000m$, meaning $s_g + s_a \leqslant 1,000m$.

Take-off Ground Run The ground run distance can be analytically or numerically found by the integration shown in Equation 7.6. However, this can be simplified as shown in Equation 7.7, where $\bar{a}$ is the average acceleration and it can be taken at a speed $\frac{V_{LOF}}{\sqrt{2}}$ [9]. Where V_{LOF} is 1.1 times the speed which makes the lift of the aircraft equal its weight or $L = W$.

$$s_g = \int_0^{V_{LOF}} \frac{V dV}{a} \tag{7.6}$$

$$s_g = \frac{V_{LOF}^2}{2\bar{a}} \tag{7.7}$$

The acceleration can be obtained by a formulation of Newton's second law $F = ma$, as shown in Equation 7.8. Where T is the aircraft's thrust force, D is the aerodynamic drag force and D_g is the ground friction drag. The ground friction drag is obtained as shown in Equation 7.9 where μ_r is the friction coefficient and it can be taken as 0.02 for a concrete or asphalt airfield and as 0.05 for a rougher surface[9]. Since the aircraft is to be widely deployable a $\mu_r = 0.05$ is assumed because the airfield's might be of a rough surface in certain locations.

$$\frac{W_{MTO}}{g} a = T - D - D_g \tag{7.8}$$

$$D_g = \mu_r (W_{MTO} - L) \tag{7.9}$$

With these relations in mind the power that the engine must have available is obtained. This is shown in Equation 7.10.

$$P_a = \left(\frac{{V_{LOF}}^2}{2 s_g} + \frac{D + D_g}{W_{MTO}/g} \right) \frac{\sqrt{2} V_{LOF}}{2} \frac{W_{MTO}}{g} \tag{7.10}$$

Take-off Airborne Phase After the ground take-off run the aircraft must reach a minimum *screen height* of $35ft$ or $10.7m$ within the take-off runway distance of $1,000m$, according to regulation **CS 25.115**. The screen height is given by the relation shown in Equation 7.11 and the horizontal distance that the aircraft covers to reach that height is given by the relation shown in Equation 7.12.

$$h_s = R\left(1 - \cos\gamma_s\right) \tag{7.11}$$

$$s_a = R\gamma_s \tag{7.12}$$

The value of the radius of climb R is obtained through the expression shown in Equation 7.14. The angle of climb when reaching the screen height γ_s is calculated through the expression previously mentioned in Equation 7.4. This is shown specific for this case in Equation 7.13. To calculate the load factor the simple expression of $n_{LOF} = \frac{L}{W_{MTO}}$ is used.

$$\gamma_s = \frac{P_a - P_r}{V_{LOF} W_{MTO}} \tag{7.13}$$

$$R = \frac{V_{LOF}^2}{g\,(n_{LOF} - 1)} \tag{7.14}$$

[3] Although the aircraft will not be operating at maximum take-off weight during cruise, it will not have burnt much fuel at the beginning of cruise. This is a conservative estimation and can therefore be used safely.

The power required P_r is computed by multiplying the drag force by the aircraft's take-off speed. From these relations the power available the engine must have can be obtained. This expression derives directly from Equation 7.13 and is shown explicit in Equation 7.15.

$$P_a = \gamma_s V_{LOF} W_{MTO} + D_{TO} V_{LOF} \tag{7.15}$$

7.2.4. Climb

As described in Section 7.1.2, there are several requirements by the CS 25 regulations on the rates of climb and climb gradients that must be reached. The relations used for any of the five configurations previously discussed about are essentially the same, the difference being the lift coefficients and velocities used as input. The relations for calculating the power available that the engine must have are further discussed in the following paragraphs.

Rate of Climb The main relation for the rate of climb was previously shown in Equation 7.4. From this equation the power available can be obtained by the relation shown in Equation 7.16. The second term on the right side of the equation represents the power required by the drag force on the aircraft.

$$P_a = (ROC)W + \frac{D}{L}WV \tag{7.16}$$

Climb Gradient The angle of climb, or climb gradient, is obtained by the equation shown in Equation 7.17. From this relation the power available is obtained by using Equation 7.18, where the power required P_r can be obtained in the same way it was for the rate of climb calculation.

$$\gamma = \sin^{-1}\left(\frac{RC}{V}\right) = \sin^{-1}\left(\frac{P_a - P_r}{WV}\right) \tag{7.17}$$

$$P_a = V \sin\gamma W + P_r \tag{7.18}$$

An important remark is that, in the case of the CS 25 regulations, since the climb rates are derived from the climb gradients the power which the power plant must provide for the requirement is the same. For this reason sizing for the climb gradient will make the aircraft be able of reaching the rate of climb and vice versa.

7.2.5. Manoeuvring

Finally, the engine must be able to provide the power to perform manoeuvres during flight. As previously mentioned, at the beginning of this section, the aircraft should be able to perform a $2g$ manoeuvre at its drop speed V_{drop}. The power required for such manoeuvre is obtained through the relation shown in Equation 7.19. Since the lift generated by the aircraft is given by $L = n_{man} W_{MTO}$, this results in Equation 7.20.

$$P_r = DV = \left(C_D \frac{1}{2}\rho V^2 S\right) V \tag{7.19}$$

$$P_r = C_D \frac{1}{2}\rho V^3 S = C_{DO} \frac{1}{2}\rho V^3 s + \frac{(W_{MTO} n_{man})^2}{\pi A e \frac{1}{2}\rho V S} \tag{7.20}$$

7.3. Propulsion Sizing Tool

Taking into account the requirements explained in Section 7.1 and the relations in Section 7.2, a tool in python is developed. This tool takes as inputs all the relevant parameters which have been previously discussed and calculates the remaining through the relations. The power available that the engine must have is determined for a range of different weights of the aircraft, which have been determined as preliminary values for the design. In this section the results of the sizing tool developed are shown and discussed. Lastly, the verification and validation procedures taken to determine the usefulness of the tool are described.

7.3.1. Results from the Tool

From the relations developed, each of the values of power available required by in the different phases were obtained. This was performed for a range of a range of different maximum take-off weights. The results of this calculations are shown illustratively in Figure 7.1. The range of the maximum take-off mass was obtained to be between $49,198.93 kg$ to $55,426.91 kg$, which results in a maximum take-off weight ranges represented by the two red vertical lines in the figure.

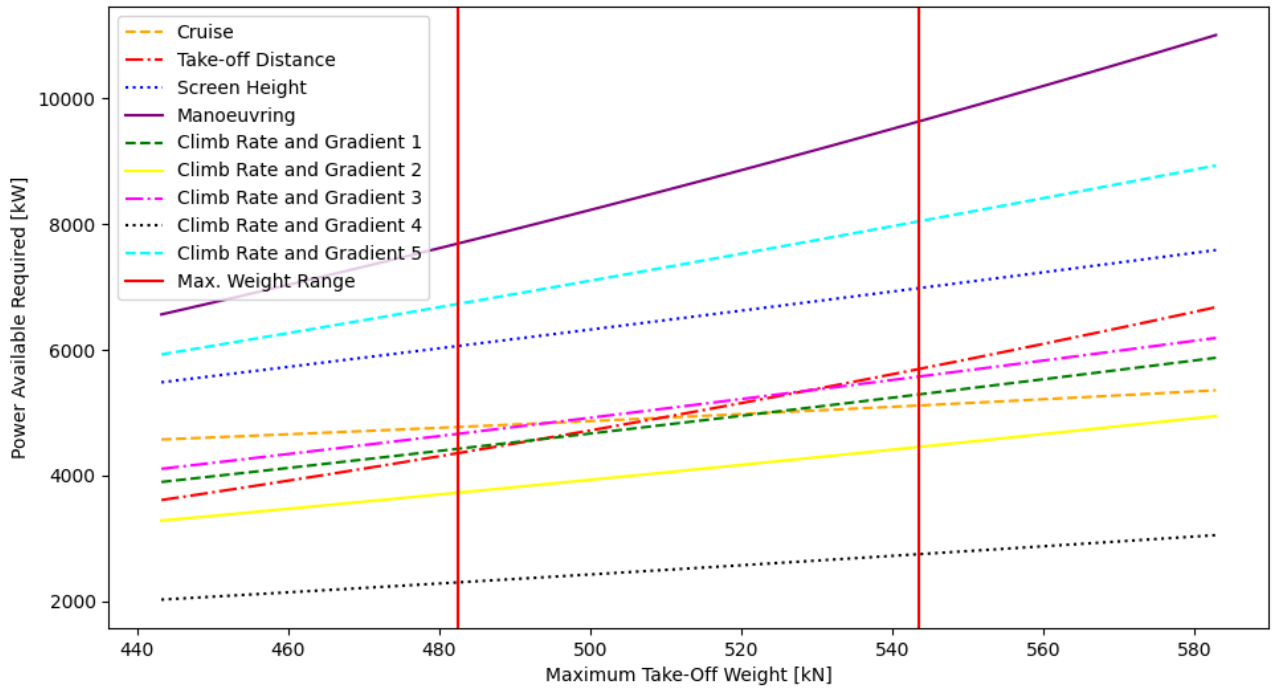

Figure 7.1: Power available required of the power plant for the different requirements.

From the values obtained, the highest required power for each of the performance requirements is shown in Table 7.3. From the power available P_a that the engine must provide it is possible to obtain the shaft power P_{br} it must have from the relation shown previously in Equation 7.1. Note that, as previously mentioned, the power provided by the jet thrust is not taken into account for the sizing of the engine. The shaft power estimated by the tool for the different requirements is shown in Table 7.4. In this table the minimum shaft power for which the engines must be sized is also shown. The power plant shall be able to provide at least $12,048.14 kW$

Table 7.3: Power available that the power plant must provide by different requirements.

Power available requirement	Value	Unit
Cruise (at h=2000m):	4,304.16	kW
Cruise (at sea level):	4,985.61	kW
Ground take-off distance	6,598.36	kW
Airborne take-off screen height	7,139.26	kW
Manoeuvring	9,638.51	kW
Climb rate and angle 1	5,452.15	kW
Climb rate and angle 2	4,568.30	kW
Climb rate and angle 3	5,741.12	kW
Climb rate and angle 4	4,056.70	kW
Climb rate and angle 5	8,275.41	kW

Table 7.4: Shaft power that the power plant must provide by different requirements ($\eta_j = 0.8$).

Shaft power requirement	Value	Unit
Cruise (at h=2000m):	5,380.19	kW
Cruise (at sea level):	6,232.01	kW
Ground take-off distance	8,247.97	kW
Airborne take-off screen height	8,924.07	kW
Manoeuvring	12,048.14	kW
Climb rate and angle 1	6,815.18	kW
Climb rate and angle 2	5,710.38	kW
Climb rate and angle 3	7,176.57	kW
Climb rate and angle 4	5,070.86	kW
Climb rate and angle 5	10,344.26	kW
Min. shaft power required	**12,048.14**	kW

7.3.2. Verification of the Tool

To ensure that the propulsion design tool is developed in the right way, a set of verification procedures is performed. Firstly, a code verification is performed in various progressive steps. After this, a calculation verification is performed to determine that the final values obtained are the ones according to the relations developed in Section 7.2.

Code Verification As it was previously discussed in the midterm report[5], a code verification of a tool consists on the identification and debugging of mistakes in a progressively larger part of the code. This is performed through a set of unit tests, subsystem tests and finally a system test. The code verification is structured in the following way:

- After a set of functions is developed for the power calculation of one of the performance parameters, each of the functions is independently tested to make sure no errors are obtained. The specific verification of a single function is considered the unit test.
- When each of the functions out of the set is found to work correctly, a test is performed to check that the power value and plotting of the performance requirement works without errors. This is considered the subsystem test.

- Finally, when all the sets of functions and plotting have been checked, the final plotting and run of the entire code is performed. Since a graph is plotted and a value is obtained for each of the performance requirements the code is considered verified through this last system test.

Calculation Verification After the code has been properly verified a calculation verification is required. This determines whether the values obtained through the tool provide the same value that they are supposed to according to the relations developed. For this two main procedures are taken. The first is to perform a hand solution for the higher weight in the range. Since the equations are relatively short this is possible. Additionally, the same equations are input to an excel sheet. This makes the calculations verified again.

7.3.3. Validation of the Tool

Finally, for the validation of the tool, a comparison to other aircraft was performed. As previously mentioned, the shaft power that the aircraft's power plant must provide is of $12,048.14kW$. To validate this result a list of aircraft with similar missions and layout were selected. Seven turboprop aircraft, most of which have performed as firefighting aircraft, are chosen. The shaft power of their power plants is plotted against their maximum take-off weight. The values of take-off weight and shaft power are shown in Table 7.5. The plot of their values is observed in Figure 7.2. With the relation of the regression line shown in the figure an estimated shaft power required is obtained for the aircraft in design. For the W_{MTO} = 543.55kN a shaft power of $11,929.45kW$ was obtained. This presents a difference of 0.985% from the calculated value with the design tool. Since the difference is relatively small and shows a conservative estimation from part of the tool it can be considered that the output of the tool makes sense in relation to existing aircraft. From the observation that the tool outputs a value for the power requirement which goes in accordance to what is expected from real-life data the tool can be considered to be validated.

Table 7.5: Validation data for the propulsion sizing tool.

Aircraft Name	**Max. Take-Off Weight** (kN)	**Shaft Power** (kW)
Canadair CL-415	195.05	3,550.00
Beriev Be-12P	353.05	7,928.00
ShinMaywa US-2	540.82	13,696.00
Harbin SH-5	441.45	9,400.00
Airbus A400M Atlas	1,383.21	32,800.00
Lockheed Martin C-130J	689.71	13,832.00
Lockheed C-130H/Q	673.79	13,680.00

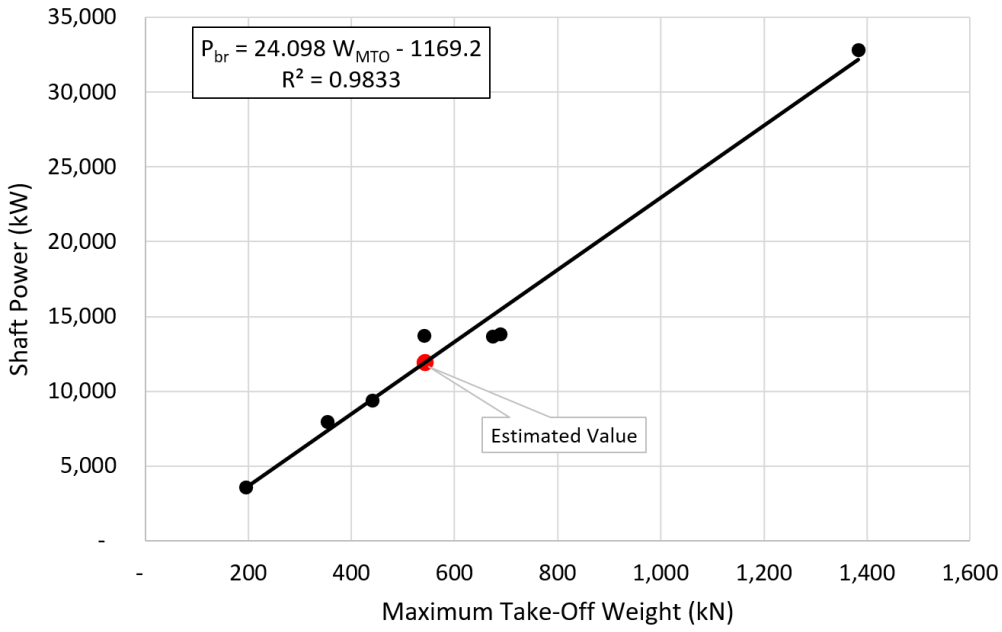

Figure 7.2: Validation for the obtained minimum shaft power required.

7.4. Engine Selection

After the shaft power that the aircraft's power plant power plant must provide, it is possible to select a suitable engine. In this section first the engine options are explored. With the main capabilities of the engines it is possible to perform

an initial screening of the suitable engines. After this an engine performance comparison between the engines is done to later perform a trade-off and select the engine to be used.

7.4.1. Available Turboprop Engines

It is first necessary to determine which are all the available turboprop engine options. For this it is first necessary to have an overview of the available turboprop engine manufacturers. The considered manufacturers are the following:

- Pratt & Whitney [21][22]
- Honeywell Garret [23]
- Rolls Royce [24][25]
- General Electric [26] [27]
- Europrop [28]
- Ichvenko - Progress [29][30][31]

From each of this manufacturers all of their turboprop engine families are taken into account, out of which the shaft power of the engines in those families is important to determine if the engine's power can be used for the aircraft. The number of engines that would be required to meet the power requirements can be obtained by dividing the total power needed over the power that a single engine provides. A decision has been taken of limiting the maximum number of engines to four and the minimum number of engines to two. This reduces the probability of an engine failure and in the case it happens there is redundancy in the propulsion so that the aircraft can land safely, as it is stated in **FFA-S&R-007**. Therefore any engine which would require more than 4 engines to meet the power requirements is discarded. The results of this process can be observed in Appendix B in Table B.1.

7.4.2. Possible Turboprop Engines

As seen in Table B.1 in Appendix B, there are twelve turboprop engines which are powerful enough to provide with the required shaft power. These engines are considered the possible turboprop engines for the design. Of each of this engines a more extensive list of characteristics is obtained for a more detailed comparison of their performance. These specifications can be seen in Table 7.6 and Table 7.7.

Table 7.6: First specifications of possible turboprop engines for the aircraft.

Engine Name	**Maximum Shaft Power Take-Off** (kW)	**Continuous Shaft Power** (kW)	**Number of Engines Required**	**Total Maximum Shaft Power** (kW)	**Total Continuous Shaft Power** (kW)	**Dry Mass** (kg)	**Total Dry Mass** (kg)
PW150A	3,781.00	3,415.00	4	15,124.00	13,660.00	716.90	2,867.60
AE 2100D2	3,458.00	3,458.00	4	13,832.00	13,832.00	805.49	3,221.96
AE2100 D3	3,458.00	3,458.00	4	13,832.00	13,832.00	805.49	3,221.96
AE 2100J	3,423.00	3,423.00	4	13,692.00	13,692.00	880.00	3,520.00
T56-A-14	3,433.00	3,433.00	4	13,732.00	13,732.00	880.00	3,520.00
T56-A-15	3,425.00	3,425.00	4	13,700.00	13,700.00	880.00	3,520.00
T56-A-425	3,433.00	3,433.00	4	13,732.00	13,732.00	880.00	3,520.00
T56-A-427	3,920.00	3,920.00	4	15,680.00	15,680.00	880.00	3,520.00
T56-A-427A	3,806.00	3,806.00	4	15,224.00	15,224.00	880.00	3,520.00
TP-400-D6	8,251.00	7,971.00	2	16,502.00	15,942.00	1,986.90	3,973.80
AI-20D series 4	2,900.00	2,600.00	4	11,600.00	10,400.00	1,040.00	4,160.00
AI-20D series 5	2,900.00	2,600.00	4	11,600.00	10,400.00	1,040.00	4,160.00

Table 7.7: Second specifications of possible turboprop engines for the aircraft.

Engine Name	**Cost** (M\$)	**Length** (mm)	**Width** (mm)	**Overall Height** (mm)	**Volume** (m^3)	**Current Platform**	**Propeller Diameter** (m)
PW150A	1.30	2,420.00	790.00	1,100.00	2.10	Bombardier Aerospace Q400	4.11
AE 2100D2	3.10	2,970.00	729.00	1,330.00	2.88	C-27J Spartan	4.15
AE 2100 D3	3.10	2,970.00	729.00	1,330.00	2.88	C-130J Hercules	4.11
AE 2100J	3.10	2,890.00	729.00	1,330.00	2.80	ShinMaywa US-2	4.12
T56-A-14	1.60	3,710.00	685.00	685.00	1.74	Lockheed P-3/EP-3/WP-3	4.10
T56-A-15	1.60	3,710.00	685.00	685.00	1.74	Lockheed C-130H Hercules	4.11
T56-A-425	2.40	3,710.00	685.00	685.00	1.74	Grumman C-2A Greyhound	4.11
T56-A-427	2.40	3,710.00	685.00	685.00	1.74	Northrop Grumman E-2D	4.11
T56-A-427A	2.40	3,710.00	685.00	685.00	1.74	Northrop Grumman E-2D Advanced Hawkeye	4.11
TP-400-D6	N/A	4,180.00	1,218.00	1,218.00	6.20	Airbus A400M-Atlas	5.30
AI-20D series 4	N/A	3,096.00	842.00	1,080.00	2.82	Beriev Be-12	5.06
AI-20D series 5	N/A	3,096.00	842.00	1,080.00	2.82	Antonov An-32	4.70

7.4.3. Engine Performance Comparison

To select the correct engine it is first important to establish certain performance parameters for comparison. These parameters are to be used for the trade-off of the engines. To evaluate the performance the following parameters are

chosen:

- **Shaft power to mass performance.** This parameter is essential since it is always necessary to decrease the total mass of the aircraft as much as possible. A power to mass parameter ensures that the weight remains a fundamental factor for the decision on the engine.
- **Power to cost performance.** Given the requirement **FFA-Cos-001** on the total cost of the aircraft, it is necessary to keep the cost of the engines as low as possible. That is the reason for this parameter to be a part of the decision on the engine.[4]
- **Power to volume performance.** Finally, a bulky engine is not beneficial for an aircraft. An engine increases the total wetted area of an aircraft which influences the drag. For this reason it is beneficial if an engine has a lower volume.

The evaluation of these performance parameters for each of the engines that can be possibly used in the design is shown in Table 7.8.

Table 7.8: Performance parameters of the engines.

Engine Name	**Power to Mass Performance** (kW/kg)	**Power to Cost Performance** ($kW/M\$$)	**Power to Volume Performance** (kW/m^3)
PW150A	4.76	2,626.92	1,623.89
AE 2100D2	4.29	1,115.48	1,200.85
AE 2100 D3	4.29	1,115.48	1,200.85
AE 2100J	3.89	1,104.19	1,221.60
T56-A-14	3.90	2,145.63	1,972.05
T56-A-15	3.89	2,140.63	1,967.46
T56-A-425	3.90	1,430.42	1,972.05
T56-A-427	4.45	1,633.33	2,251.81
T56-A-427A	4.33	1,585.83	2,186.32
TP-400-D6	4.01	NA	1,285.41
AI-20D series 4	2.50	NA	923.50
AI-20D series 5	2.50	NA	923.50

7.4.4. Engine Trade-Off

To perform a trade-off based on the previously mentioned parameters it is necessary to do the following:

- Assign weights to each of the performance parameters based on their importance and relevance for the engine selection.
- Give a score to each of the engine options for each of the parameters based on their comparison to the other engines.
- Obtain the total score for each of the options by multipying their scores and weights and adding them up.

To assign the weights to the parameters, first a score from one to ten based on their relevance is assigned. From this the weight of each of the parameters is obtained. For the initial trade-off an equal weight is assigned to each of the performance parameters.

- **Power to Mass Performance:** Score of 10, weight of 33%.
- **Power to Cost Performance:** Score of 10, weight of 33%.
- **Power to Volume Performance:** Score of 10, weight of 33%.

To give a score to each of the parameters the maximum and minimum performance values for each parameter are obtained. The score for the option is obtained through the relation shown in Equation 7.21. The score can therefore have a value between 0-1. The total score of each option, as previously mentioned, is calculated by multiplying the score with the weight of each performance and adding them up. The result of this process is shown Table 7.9. From this trade-off the best option appears to be the Pratt & Whitney PW150A engine. This engine is the best performing one in terms of power to mass and power to cost. However, it is still necessary to perform a sensitivity analysis to ensure that it is the best option.

$$Score = \frac{Per_{option} - Per_{\min}}{Per_{\max} - Per_{\min}} \tag{7.21}$$

[4]There is no information found regarding the price of the TP-400-D6 and the Ichvenko engines.

Table 7.9: Trade-off of engine options.[5]

Engine Name	Power to Mass Performance Weight = 33%	Power to Cost Performance Weight = 33%	Power to Volume Performance Weight = 33%	Total Score
PW150A	1.0000	1.0000	0.5273	0.8424
AE 2100D2	0.7921	0.0074	0.2088	0.3361
AE 2100 D3	0.7921	0.0074	0.2088	0.3361
AE 2100J	0.6140	0.0000	0.2244	0.2795
T56-A-14	0.6190	0.6839	0.7894	0.6974
T56-A-15	0.6150	0.6806	0.7859	0.6939
T56-A-425	0.6190	0.2142	0.7894	0.5409
T56-A-427	0.8635	0.3475	1.0000	0.7370
T56-A-427A	0.8063	0.3163	0.9507	0.6911
TP-400-D6	0.6679	N/A	0.2725	N/A
Al-20D series 4	0.0000	N/A	0.0000	N/A
Al-20D series 5	0.0000	N/A	0.0000	N/A

7.4.5. Sensitivity Analysis

As it was previously mentioned, the engine that appears to be the best option so far, the PW150A, is the best performing one in terms of the first two parameters. Therefore increasing these weights would only result in the same engine outperforming the other. So the approach taken is to increase the weight of the third performance parameter relative to the others until this engine is no longer the best option. After testing this approach it is found that this happens when the scores are the following:

- **Power to Mass Performance:** Score of 5, weight of 25%.
- **Power to Cost Performance:** Score of 5, weight of 25%.
- **Power to Volume Performance:** Score of 10, weight of 50%.

The results from assigning these weights to the parameters are shown in Table 7.10. In this case, the best option is the Rolls Royce T56-A-427 engine. However, this engine has a low power to cost performance. Additionally, it does not seem that the power to volume performance is more relevant than the other performance parameters. For this reason it can be concluded from the sensitivity analysis that the best engine option is indeed the Pratt & Whitney PW150A.

Table 7.10: Sensitivity analysis trade-off of engine options.

Engine Name	Power to Mass Performance Weight = 25%	Power to Cost Performance Weight = 25%	Power to Volume Performance Weight = 50%	Total Score
PW150A	1.0000	1.0000	0.5273	0.7636
AE 2100D2	0.7921	0.0074	0.2088	0.3043
AE2100 D3	0.7921	0.0074	0.2088	0.3043
AE 2100J	0.6140	0.0000	0.2244	0.2657
T56-A-14	0.6190	0.6839	0.7894	0.7204
T56-A-15	0.6150	0.6806	0.7859	0.7169
T56-A-425	0.6190	0.2142	0.7894	0.6030
T56-A-427	0.8635	0.3475	1.0000	0.8027
T56-A-427A	0.8063	0.3163	0.9507	0.7560
TP-400-D6	0.6679	N/A	0.2725	N/A
AI-20D series 4	0.0000	N/A	0.0000	N/A
AI-20D series 5	0.0000	N/A	0.0000	N/A

7.4.6. Final Engine Choice

Finally, based on the trade-off and the sensitivity analysis performed, the selected engine is the Pratt & Whitney PW150A. It has proven to be the best performing engine on the power to mass and power to cost criteria and is the best performing engine overall. The engine is shown in Figure 7.3 and its most important specifications are in Table 7.11.

[5] Since there is no information on the price of the TP-400-D6 and Ichvenko engines it is not possible to find the total score, however, they can be seen to perform poorly in the other two criteria.

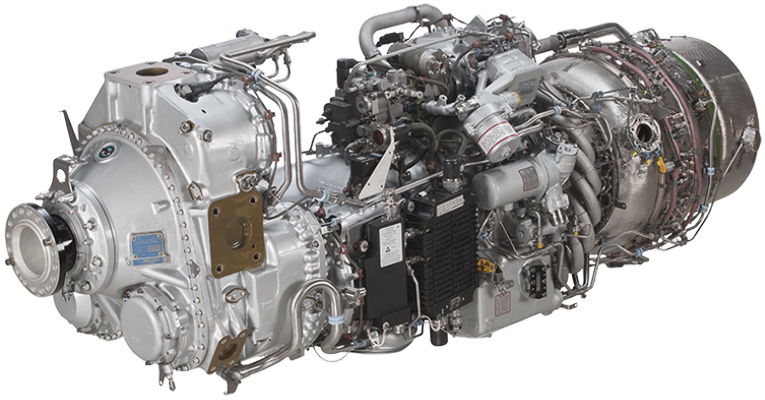

Figure 7.3: The Pratt & Whitney PW150 engine[32].

Table 7.11: Information of the selected engine[33].

Technical Characersitics		**Value**	**Units**
Maximum Take-Off Power	Shaft Power	3,781.0	kW
	Jet Thrust	3,750.0	N
Continuos Power	Shaft Power	3,415.0	kW
	Jet Thrust	3,412.0	N
Length		2,420.0	mm
Width		790.0	mm
Overall Height		1,100.0	mm
Dry Mass		716.9	kg
Air Bleed Extraction	Max HP	10.0	%
	Max LP	6.0	%
Fuel Type		Kerosene Jet A, A-1 JP8	
		Wide Cut Jet B JP4	
		High Flash JP5 JP1	
Equivalent Specific Fuel Consumption[34]		0.255	$kg/(kWh)$
Cost[35]		1.3	M\$
Operatonal Limits			
Max Inter Turbine Temperature	Max Take-Off	880.0	$^{\circ}C$
	Max Continuous	880.0	$^{\circ}C$
	Transient (20s)	920.0	$^{\circ}C$
Max Output Shaft Speed	Max Take-Off	1,020.0	rpm
	Max Continuous	1,020.0	rpm
	Transient (20s)	1,173.0	rpm

7.5. Propeller Blade Selection

Once the engine is selected, propeller blades to go with it are chosen. For this the propeller blades that are used on the turboprop engines that were considered are researched in tandem with all the main aircraft propeller manufacturers. The propellers used and their diameters are shown in Table 7.12. The main propeller manufacturers which are currently supplying big aircraft with propeller blades are:

- *Dowty Propellers*, which works jointly with *General Electric* and *Rolls Royce*.
- *Collins Aerospace*, which used to be *Hamilton Propellers* and is also known as *UTC Aerospace*.

Table 7.12: Propellers used in engines of similar aircraft.

Engine Name	Current Platform	Propeller of aircraft	Propeller diameter (m)
PW150A	Bombardier Aerospace Q400	6-bladed Dowty Propellers R408	4.11
AE 2100D2	C-27J Spartan	6-bladed Dowty Propeller 391/6-132-F/10	4.15
AE2100 D3	C-130J Hercules	6-bladed Dowty Propeller R391	4.11
AE 2100J	ShinMaywa US-2	6-bladed Dowty Propeller R414	4.12
T56-A-14	Lockheed P-3/EP-3/WP-3	4-bladed Hamilton Standard 54H60-77	4.10
T56-A-15	Lockheed C-130H Hercules	4-bladed Hamilton Standard 54H60	4.11
T56-A-425	Grumman C-2A Greyhound	8-bladed UTC Aerospace Systems NP2000	4.11

A very important characteristic that the propeller system must have is a control on the pitch of the blades. This allows the system to have the following characteristics:

- **Variable Pitch:** this allows the propeller to increase its efficiency. Opposite to the fixed pitch propellers, this capacity allows the engines to perform as efficiently as possible at different points during their operation[9]. The benefits of a variable pitch propeller are illustrated in Figure 7.4.
- **Constant Speed:** this allows the pilot to fix the rotational speed of the propellers at a value through the *governor*[36].
- **Feathering:** in the case of an engine failure a full feathering of the blades prevents the occurrence of high wind-milling drag[9], allowing a more efficient flight.
- **Reverse Thrust:** this capability can support the aircraft during landing, generating a negative thrust.

All of these described characteristics can be seen in Figure 7.5.

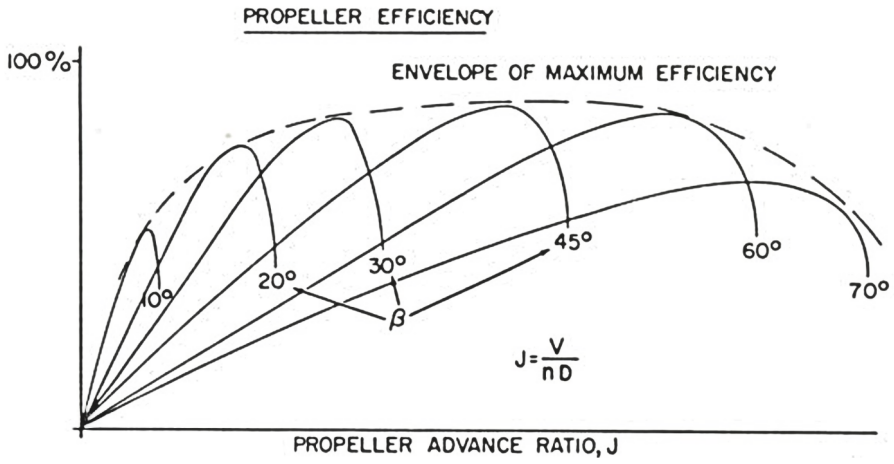

Figure 7.4: Propeller efficiency at different advance ratios for different pitch angles of the blades[37].

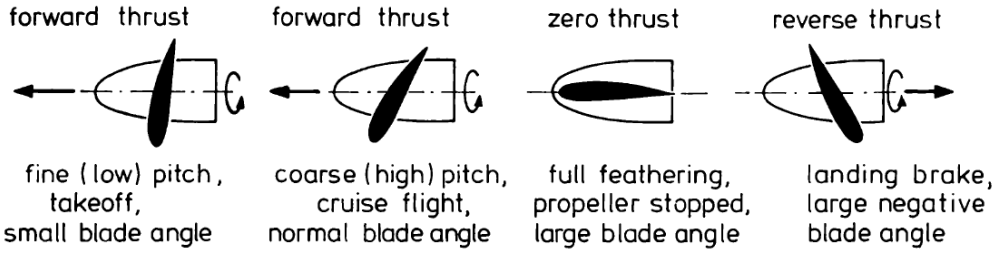

Figure 7.5: Propeller pitch angle settings[9].

As previously mentioned, the engines used in the Bombardier Q400, also known as the Dash 8, are the same as selected for this design. The propeller system that this aircraft uses is the Dowty R408 series. This propeller systems operates within the same limits of the selected engine since it was developed for this purpose and has proven a very reliable and high performing propeller for the aircraft[38]. The Antonov A-132, a multipurpose turboprop aircraft, uses the same power plant and the same propeller blades. For this reason it is decided to select the same propeller system as the one used in the Q400 aircraft. The information on the propeller selected and its specifications are shown in Table 7.13 and Table 7.14 respectively. The propellers mounted on the PW150A engines on the Q400 are shown in Figure 7.6.

Figure 7.6: Dowty R408 propellers on the Bombardier Q400[38].

Table 7.13: Information of the selected propeller[39]

Manufacturer	Dowty Propellers
Type	R408 series
Model	R408/6-123-F/17
Material	Aluminum
Capabilities	Variable Pitch
	Constant Speed
	Feathering
	Reverse Type

Table 7.14: Dowty R408 propeller specifications[39]

Parameter	**Value**	**Units**
Dry Weight	295	kg
Take-off speed	1020	rpm
Transient over-speed	1173	rpm
Max Take-Off Power	3782	kW
Continuous Power	3782	kW
Max Reverse Power	1119	kW
Feather Angle	86	°
Reverse Angle	-17.75	°
Idle Angle	17.55	°

7.6. Fuel Performance

Through the mass estimations a maximum fuel capacity is estimated for operations. A fuel mass $M_{fuel} = 14,079.5kg$ can be carried. Now, given the specifications from the engine and propeller selected, it is possible to determine what the fuel required is for the different stages of the operation. To determine the fuel used it is first necessary to have a better understanding of the drivers for fuel consumption. This explanation is given in Section 7.6.1. Following this, the procedures for obtaining the fuel used for the different stages of the operation of the aircraft are explained in Section 7.6.2 and Section 7.6.3. Finally, with an understanding of the fuel used it is important to determine if the fuel tank size is sufficient to meet the requirements. The amount of drops, water delivery and other performance parameters are briefly discussed, since they are related to the fuel consumption of the engines, in Section 7.6.6.

7.6.1. Specific Fuel Consumption and Fuel Flow

The fuel flow of the aircraft is defined and determined as shown in Equation 7.22. The specific fuel consumption c_P is the amount of fuel consumed per unit of time and per unit of power. The unit of this parameter for the calculations is in $\frac{kg}{Ws}$, but it is usually presented in $\frac{kg}{kWh}$. At the same time however, the value of the specific fuel consumption itself is dependant on the power rating at which the engine is being used. Therefore, it is first necessary to determine the specific fuel consumption of the engines at different power ratings, based on the equivalent specific fuel consumption of the engine at 100% rating ($c_{P_{eq}} = 0.255$), shown previously in Table 7.11.

$$\dot{M}_{fuel} = \frac{dM_{fuel}}{dt} = c_P P_{br} \tag{7.22}$$

As mentioned, the specific fuel consumption is a function of the power rating of the engine. This function is obtained from a set of specific fuel consumption values given for a Pratt & Whitney engine at different power ratings[40]. The factor by which the equivalent specific fuel consumption must be multiplied to obtain the specific fuel consumption at an specific rating is shown in Figure 7.7.

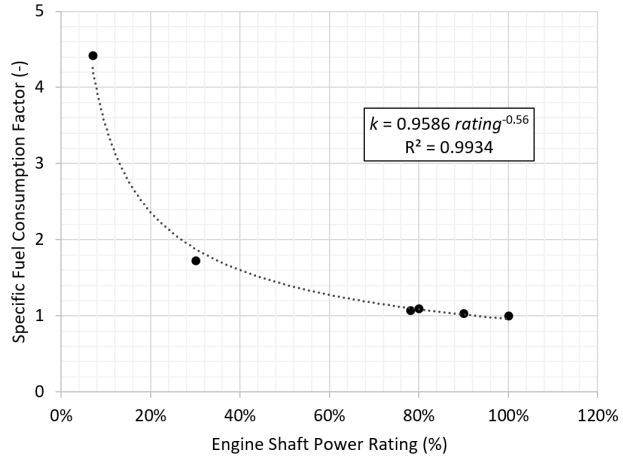

Figure 7.7: Specific Fuel consumption factor as a function of the engine shaft power rating [40]

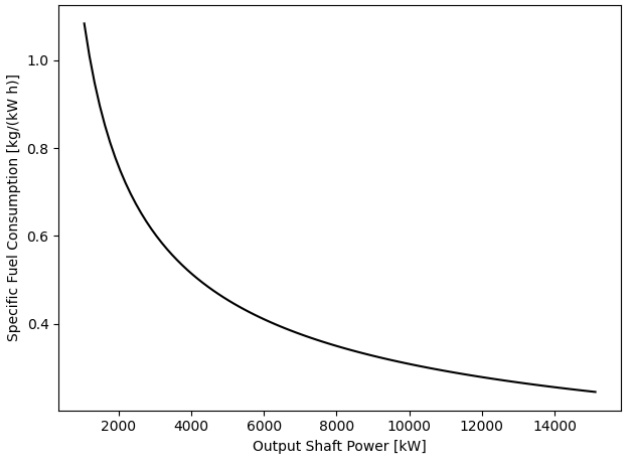

Figure 7.8: Specific fuel consumption from idle (7%) to maximum take-off power (100%).

The specific fuel consumption is therefore given as shown in Equation 7.23. $P_{br_{TO}} = 15,124.0kW$ is the maximum take-off shaft power that the four engines can deliver. From this it is possible to obtain the fuel flow, as shown previously in Equation 7.22.

$$c_P = kc_{P_{eq}} = 0.9856\left(\frac{P_{br}}{P_{br_{TO}}}\right)^{-0.56} c_{P_{eq}} \tag{7.23}$$

7.6.2. Ground, Climb and Descent Operation

These operations encompass aspects that the engine is going to encounter nominally besides cruising. As previously shown, in Section 7.3, there are certain minimum power requirements that the aircraft must meet during some of these operations, such as take-off and climb. For operations which do not have a power or performance requirement which determines the shaft power, a statistical approach is used to determine the fuel required[6].

Warm up, Startup, Taxiing, Descent, Approach and Landing. These operations do not present a power requirement on the engines. For this reason the computation of the fuel requirement on these phases of the operation was performed through statistical data, as mentioned earlier. The results on the amount of fuel which is estimated to be required for each of the phases is shown in Table 7.15.

Table 7.15: Fuel requirements for some operational phases, based on statistical data[6].

Parameter	Value	Units
Fuel Required for Warm up and Startup	112.64	kg
Fuel Required for Taxiing	70.40	kg
Fuel Required for Descent	254.27	kg
Fuel Required for Approach and Landing	70.40	kg

Take-off The minimum shaft power for take-off and its computation was previously explained in Section 7.3. Additionally, the maximum take-off shaft power is limited by the power plant capabilities, shown in Table 7.11. Therefore, the aircraft can take-off with any power setting between these two values and would still meet the take-off distance requirement. From the shaft power provided by the engine the specific fuel consumption is computed as shown in Equation 7.23. It is then possible to compute the average acceleration, taking into account the aerodynamic drag and ground drag. The mathematical representation of these relations is shown in Section 7.2. It is then possible to compute the distance and time it takes for the take-off at the different power settings. It is also possible to compute the fuel flow, as previously mentioned, and hence the fuel required can be obtained. The fuel flow and time to take off for the different shaft power settings is shown in Table 7.9. An overview of some important parameters obtained from the take-off simulation can be seen in Table 7.16. For the following computations the maximum fuel required for take-off is used.

Table 7.16: Parameters regarding the take-off of the aircraft at the maximum take-off weight.

Take-Off Parameters	Value	Units
Min Shaft Power	7,139.26	kW
Max Shaft Power	15,124.00	kW
Min Time	12.01	s
Max Time	23.66	s
Min Distance (ground)	338.34	m
Max Distance (ground)	666.52	m
Average Fuel Flow	0.92	kg/s
Min Fuel Required	24.68	kg
Max Fuel Required	38.21	kg

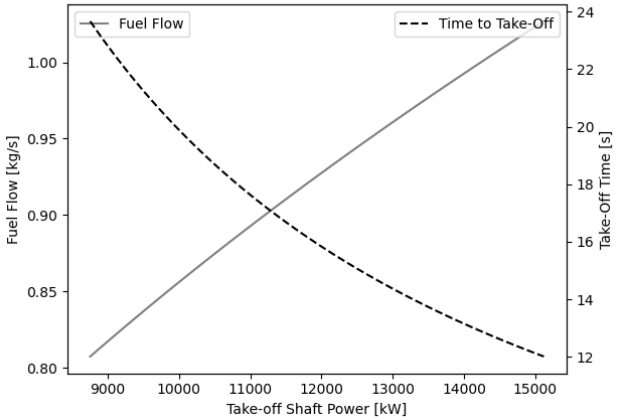

Figure 7.9: Fuel flow and take-off time for the minimum and maximum shaft powers possible.

Climb Similarly to the take-off calculations, there is a minimum shaft power and a maximum shaft power for the climb operation. The minimum shaft power is obtained from the **CS25** requirements, as mentioned before. The maximum shaft power is limited by the engine's performance. Since the cruise altitude is set as $2,000m$ above sea level, it can be assumed that it must climb that distance. For different power settings it is possible to calculate the excess power, and therefore the rate of climb. With this the time to climb can be obtained, $t_{climb} = h_{cruise}/ROC$. Since the fuel flow can be obtained for the different power setting it is possible to obtain the fuel required for a climb to the cruise altitude. The fuel flow and rate of climb with respect to the shaft power relation is shown in Table 7.10. Some important values are shown in Table 7.17. As it can be seen by the maximum rate of climb value, the rate of climb required by **FFA-Per-006** can be met. For the rest of the calculations the average fuel required is assumed for the fuel used during climb.

Table 7.17: Parameters regarding the climb of the aircraft at the maximum take-off weight.

Climb Parameters	Value	Units
Min Shaft Power	5,070.87	kW
Max Shaft Power	13,660.00	kW
Average Time to Climb	420.55	s
Average Rate of Climb	7.83	m/s
Max Rate of Climb	13.64	m/s
Average Fuel Required	315.99	kg

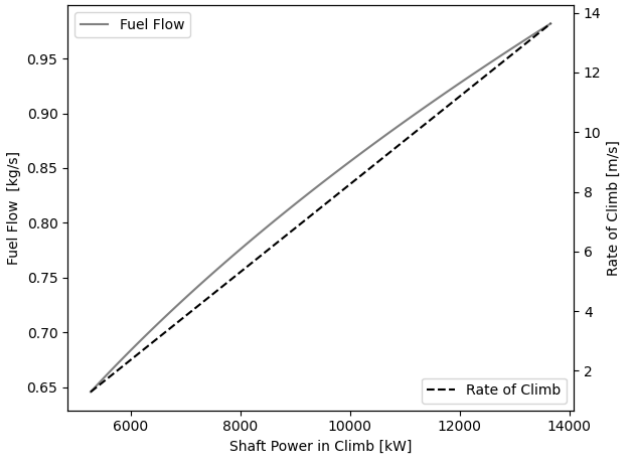

Figure 7.10: Fuel flow and rate of climb for the range of shaft powers possible in climb.

Fuel reserve An additional requirement on the aircraft is to carry fuel reserves, enough for a 30 minute loiter during the day and a 45 minute loiter during the night[41]. Using the minimum power required for a steady horizontal flight, calculated in Section 7.3, the required reserve fuel to be carried on the aircraft is of $1,251.40kg$ during a daytime flight and of $1,877.11kg$ during a night time flight. These fuel reserves are not used during any of the operations explained as they are to be used only in special circumstances. For this reason, when estimating the total fuel available this value will be the maximum fuel capacity minus the reserve fuel. It is assumed that the reserve fuel is always the value for night time flying. Therefore, the aircraft is assumed to be constantly carrying $1,877.11kg$ of fuel which are not used and stored in the fuel tanks in special circumstances.

7.6.3. Cruise Operations

Once the aircraft reaches the cruise altitude the cruise phase starts. It was previously mentioned in Section 7.3 what the minimum shaft power is required for a cruise at $2000m$ altitude. The maximum shaft power is the given by the continuous shaft power that the engines can provide. By performing a simulation of the cruise of the aircraft it can

be seen in Figure 7.12 that the maximum cruise distance is of $2,184.39 km$. This is using all the fuel available in the tanks, excluding the fuel reserve. As the aircraft cruises, its weight decreases. This is shown in Figure 7.12, where the difference between the values represented by the horizontal lines is the weight of the fuel used during cruise. As the weight decreases, also the power required for the cruise decreases, this is shown in Figure 7.11. The fuel required, only for cruise, for different distances covered is illustrated in Figure 7.11 as well. A brief summary of some important values of the cruise operation are shown in Table 7.18. As can be seen, it is possible to meet the requirement **FFA-Per-007** with the current fuel tank size.

Table 7.18: Parameters regarding cruise operations of the aircraft.

Cruise Parameters	Value	Units
Min Shaft Power	6,232.01	kW
Max Shaft Power	13,660.00	kW
Total Fuel Required for 1250 km	9,351.94	kg
Max Operational Range	2,184.39	km

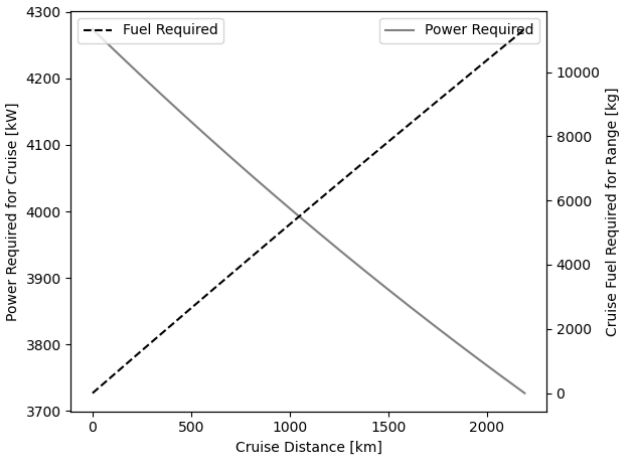

Figure 7.11: Power required and cruise fuel required for cruise distances.

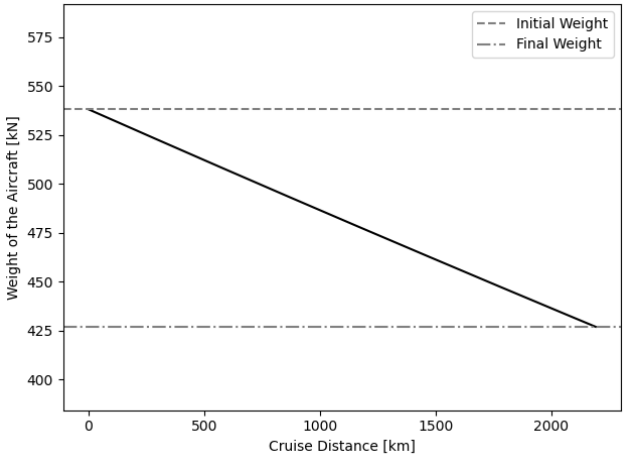

Figure 7.12: Decrease of the weight of the aircraft through the cruise phase.

Ferry The engine must also meet a ferry requirement in order to be able to be moved from one location to another prior to its operation. This is reflected in requirement **FFA-FOp-001**, which states that a ferry range of at 2,700.0 km must be reached. The ferrying of the aircraft is done without any of the payload. This decreases the aircraft's weight, which is beneficial for fuel consumption. The aircraft can also be o with ferry tanks, which are removable tanks of fuel that are used solely for ferrying purposes. This increases the aircraft's available fuel and hence its range. The aircraft can basically carry the same amount of weight of payload in ferry tanks and extra fuel. In Table 7.19 the fuel available with and without ferry tanks is shown (excluding the reserve fuel). Additionally, the take-off weight and range of a ferrying with and without ferry tanks is shown. As it can be seen, also in Table 7.13, the ferry range almost doubles when the aircraft carries ferry tanks. It can also be noted that for the aircraft to meet the ferry range requirement it must carry additional ferry tanks.

Table 7.19: Parameters regarding the ferry operation of the aircraft.

Ferry Parameters	Value	Units
Fuel Available (no ferry tanks)	12,202.39	kg
Take-Off Weight (no ferry tanks)	390.53	kN
Range (no ferry tanks)	2,350.53	km
Fuel Available with ferry tanks	26,940.76	kg
Take-Off Weight with ferry tanks	537.82	kN
Range with ferry tanks	5,224.31	km

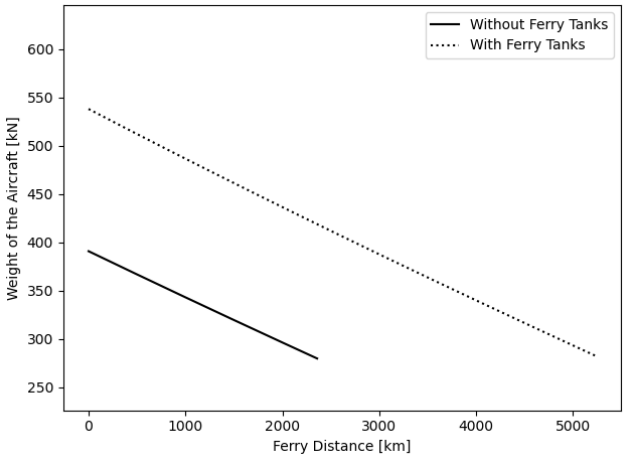

Figure 7.13: Decrease in weight of the aircraft for ferrying distances with and without ferry tanks.

7.6.4. Verification of the Fuel Estimating Tool

The verification of the tool which estimates the fuel consumption at the different stages of the design is done in a similar way to the one that estimates the power requirements. The verification consists of a code verification and a calculation verification.

Code Verification As previously discussed, this process consists on identifying and debugging errors in the code. For this process the following steps were taken:

- Firstly, unit verification was performed in each of the calculated parameters. These are the for instance fuel flow, specific fuel consumption and other computations.
- After this the subsystem test can be done for the computation of fuel used for each of the phases of the aircraft.
- Once each of the fuel requirements for the different phases work the system test verification is performed. This entails the computation of the total range and total fuel consumed calculations. If all the values are printed out then that concludes the code verification and error debugging.

Calculation Verification In order to determine that the values obtained are according to what is expected from the mathematical model some other verification is required. This is done in the form of hand calculations for simpler relations, such as the specific fuel consumption and fuel flow calculations for the different power ratings. For other more involved simulations, such as the cruise, it is useful to verify through the plots obtained. This is done by checking that the decrease in weight of the aircraft in fact corresponds to the total fuel available for cruise for instance. Additionally, the response of the fuel consumption to a change in one of the parameters is performed. This is, for example, increasing the fuel tank size and examining that indeed the range increases, or decreasing the equivalent specific fuel consumption and checking that the performance decreases.

7.6.5. Validation of the Fuel Estimating Tool

Once the tool is thoroughly verified it is necessary to validate it with real data of current aircraft. For this the information on fuel used during the different phases of an aircraft is searched. The ATR 72-500 aircraft has two PW127 turboprop engines. Although the aircraft is a different one from the design, the fuel consumption tool can be validated with it, as it counts with the information regarding fuel consumption necessary[40]. For this reason, this aircraft is used to validate the tool. Firstly the parameters of the aircraft that are inputs for the tool are changed, such as maximum take-off weight, range required, wing surface area, continuous power, maximum take-off power, aspect ratio, cruise altitude, etc. After changing all the relevant parameters, the fuel required for the different phases can be obtained in a similar manner that they were obtained for the main design. A comparison between the values obtained from the tool and the ones available from the aircraft are shown in Table 7.20. The difference of the total fuel used is $44.72kg$, or 6.9%. It can be seen that the main discrepancy is in the fuel used for climb. However, as previously mentioned, this value is the average of the fuel required for climb at different power ratings. The median value for the different power settings is actually of $212.7kg$, much more similar to the one obtained from the data. It can be seen that the tool provides accurate values on fuel consumption. If the median value was used for the climb fuel consumption the difference would reduce to 2.8%. From this comparison the tool can be considered validated.

Table 7.20: Validation results from the developed tool and available data[40].

Parameter	Value from tool (kg)	Value from data (kg)
Fuel used in Taxiing	15.50	18.00
Fuel used in Take-Off	44.20	35.00
Fuel used in Climb	239.52	218.00
Fuel used in Cruise	229.00	228.00
Fuel used in Descent	100.00	81.00
Fuel used in Approach & Landing	15.50	19.00
Total Fuel used	**643.72**	**599.00**

7.6.6. Mission Fuel Achievement

Finally, it is important to determine that the amount of fuel carried in the aircraft allows it to perform the necessary water delivery per hour. To evaluate this performance it is important to determine the number of drops that can be done taking into account the fuel that is being consumed at each stage. The procedure to obtain the number of drops and water delivery performance with a full fuel tank is the following:

1. First a number of drops is assumed.
2. Given the number of drops the total distance that must be covered can be calculated. The distances from the water to the fire and from the airfield to the fire are obtained from requirement **FFA-Per-001**. The aircraft must cover the $250km$ twice, at the beginning of the mission and at the end. The aircraft must also cover the $30km$ distance to the water body the same amount of times that the water is dropped.
3. From the number of drops also the number of landings and take-offs can be found, since the aircraft is performing these every time it fills up with water. The same goes for descent and climbing.
4. With the fuel used for each phase found in Section 7.6.2 and Section 7.6.3 the total fuel required is found and the total time that it takes for the whole mission. For this, other time parameters, such as time to load water ($12s$ as seen in Chapter 8), time to refuel of 45 minutes and other parameters are used.
5. Given the water capacity of 15,019.58 litres the total water delivered can be obtained and from there the water delivery capacity per hour.
6. This procedure should be repeated, increasing the number of drops until the total fuel required is just below the maximum fuel capacity. Once again, the reserve fuel is already considered as part of the fuel but it is not used during the mission.

Following the mentioned approach, the values shown in Table 7.21 were obtained. As it can be seen, a maximum number of 10 drops can be made and still be within the limits of the fuel tanks capacity. It can also be observed that this number of drops allows the aircraft to meet the water delivery performance. Therefore, the fuel weight estimated for the fuel can be considered to be sufficient for the design.

Table 7.21: Mission parameters and performance of the aircraft with the available storage capacity.

Mission Parameters	Value	Units
Distance to Water	30.00	km
Distance to Airfield	250.00	km
Cruising Distance covered	1,100.00	km
Max Number of Drops	10	-
Fuel Storage Available	14,079.50	kg
Total Fuel Required	13,449.20	kg
Water Delivery Performance	31,499.29	L/h

7.7. Sustainability Approach

There are two main components from the aviation industry regarding sustainability. These are noise and emissions. One of the main components for the noise pollution from the aircraft is generated by the engines. From the emissions component, the fundamental driver is the type of fuel used and the fuel consumption.

7.7.1. Noise

Turboprop engine aircraft are generally known as noisy. This is one of the reasons why they are often not preferred for short haul flight when they actually more fuel efficient than jet engine aircraft[42]. However, the PW150A engine has proved to be remarkably quiet on the Bombardier Q-400 aircraft - where Q stands for 'Quiet'[43]. The noise generated, in terms of effective perceived noise level, is comparable and even lower than some very frequently used aircraft, such as the A320. The lateral, flyover and approach EPNLs of the Q400 are of 84, 78 and 93 dB[44]. The A320, in comparison has values of 94, 84 and 96 dB[45]. The low levels of noise of the Q400 is a characteristic that has made it particularly popular and a well received aircraft for the fleet of many airlines[42]. Since the design of the aircraft being developed

uses the same engines and propeller system, it can be assumed that the noise levels will also be relatively low.

7.7.2. Emissions

As previously mentioned, the fuel used and fuel consumption in the aircraft has a significant impact on its emissions. In terms of fuel consumption, the turboprop aircraft usually perform better than jet aircraft for short haul flights with up to 50% lower CO2 emissions[32]. With the engine selected, the fuel required for different phases of the operation was already shown in Section 7.6.
The fuels that are nominally used in the PW150A engine were mentioned in Table 7.11. These are civil aviation fuels Jet A, Jet A-1, Jet B and military grade fuels with additives JP1, JP4, JP5 and JP8. All of these are fossil fuels and are therefore part of a production process that constantly increases the emissions into the environment. However, the PW150A engines are bio fuel compatible [32]. Indeed, some airlines have already flown the Q400 aircraft - partly - on bio fuels. It started with a joint bio fuel test program ran by *Bombardier Aerospace*, *Porter Airlines*, *Pratt & Whitney Canada* and *Targeted Growth* and funded by *GARDN*[46]. On the 12 of April of 2012 the bombardier Q400 aircraft, with two PW150A engines, flew from Toronto to Ottawa with a 50/50 blend of bio fuel and Jet A1 on one of its engines. The bio fuel used is the Camelina HRJ, which derives from the *Camelina Sativa* oilseed crop and *Brassica Carinata*. The test was successful, becoming the first revenue flight on bio-fuels in Canada. Since then other airlines using the Q400 and PW150A engines have ran on bio fuels, such as the Indian airline *SpiceJet*[47].
Since aircraft using the same power plant of the PW150A engines have successfully tested the use of bio fuels, it is safe to assume that the same can be done for the firefighting aircraft.

7.8. Risk Analysis

There are many important risks that derive from the turboprop engine. These are generally in the forms of malfunctions due to different causes. In this section these malfunctions with their consequences and appropriate responses are discussed[48][49].

Compressor Surge This is a rare event. It results from an instability of the engine's cycle. It corresponds - as the name suggests - to the compression phase of the air. When for any reason the air that should be compressed by the engine stalls the passage of air is unstable and the air finally exits through the inlet of the engine. After an initial surge, noticed by a largely audible bang, the engine can take different directions. It can self-recover immediately, self-recover after more surges, recover with the action of the pilot, or be unrecoverable. In the case that the surge does not recover the engine ends up in a severe malfunction, making the engine inoperable for the rest of the flight. The surge can be caused by ingestion of birds, ice or engine deterioration.
In order to minimise the risk of an engine failure due to a compressor surge, the crew must be adequately trained for such a situation. The power level should be lowered and then slowly increased. The engine and propeller system must also be equipped with auto feathering to minimise the damage on the engine once the compressor surges and lights to let the crew know about the surge. Although an engine failure does not occur often after a surge, it is possible that the compressor blades and other components of the engine must be changed after the event.

Flameout, Engine Shutdown or Severe Failure In this situation the engine completely stops providing shaft power, there is a drop in the torque and engine pressure ratio. This can result from a depletion of the fuel tank, unstable engine, or foreign object ingestion. It is important for the engine to count auto-feathering or negative torque sensing features to avoid windmilling drag which can drive the aircraft to instability.

Engine Fire By engine fire it is usually referred to the fire that occurs at the nacelle of the engine. It is almost unnoticeable for the crew flying the aircraft at first, for this reason it is important there are sensors on the engine for such situations. Once the existence of an engine fire is acknowledged the engine must be totally shut off by closing the fuel flow and feathering the propeller blades. Additionally, any other systems connected to the engine must be disconnected immediately, such as any bleed air extraction.

Tailpipe Fire This is a different situation from the common engine fire. It can result from a fuel accumulation in turbine casing and exhaust, which then ignites. Different procedures are set for this situations and they can reach to the evacuation of the aircraft.The expected outcome is for the fuel in the crevices ends up being consumed.

Bird strike or Foreign Object Damage These situations occur usually at low altitudes, during take-off or landing. It can result on a surge, vibrations, propeller blade damage, etc. Although the strike of birds is a hard parameter to minimise, it is always important to not have the engines very low to minimise the debris ingestion during take-off or landing in the runway.

Fuel System Problems There are some problems regarding the fuel system that can also lead to an engine malfunction. These are:

- Fuel leaks, these may result on an engine fire or flameout. This can be managed and a high impact prevented through proper instrumentation such as flow meters in the fuel tanks.
- Inability to shutdown engine, this problem can have a high impact in the case that an engine must be shutdown due to an engine fire, tailpipe fire etc. For this reason there should be two valves closing the fuel feed system to the engine.
- Fuel filter clogging, this can occur by debris or other forms of contamination in the fuel line. If the filter clogs up and the contaminated fuel reaches the engine system it can result on flameout of the engine.

Oil System Problems The oil system can, similarly to the fuel system, arise malfunctions in the engine. The most common ones are:

- Oil leaks
- Oil pump failure
- Oil system Contamination

A common and efficient way of mitigating the risk that arises from the problems of the oil system is the use of an auxiliary oil pump system. This system can at least provide the oil required for a feathering of the propellers in case the engine must be shutdown.

Propeller System Malfunctions Additionally from the engine malfunctions the propeller system also has certain inherent problems. The possible propeller system malfunctions are the following[48]:

- Loss of reverse function
- Overspeed governor activation
- Overspeed above the overspeed governor setting
- Overtorque
- Uncommanded feather
- Inability to change pitch
- Vibration
- Sudden high vibration
- RPM and torque fluctuation
- Loss of de-icing
- Electronic propeller control failure indication
- Loss of synchronising/synchrophasing
- Lightning strike
- Blade/propeller separation

In order to reduce the probability or minimise the impact of these possible malfunctions the propeller system must count with some safety features. Redundancy for the feathering control was already mentioned, as part of the redundancy in the oil system. Pitchlock prevents the propeller blades to go lower than a certain pitch angle at which they were with the governor. This reduces the possibility of overspeed occurring and damaging the engine. An overspeed governor is already a redundancy for the propeller system, and while it can also malfunction, it reduces the probability of many malfunctions from occurring.

8
Extinguishing System

This chapter will contain the analysis and the design of the extinguishing system. Starting of with a general layout in Section 8.1 and requirement overview in Section 8.2. In Section 8.3 the tank dimensions are given. Next, the retardant types are investigated in detail in Section 8.4. After that, Section 8.5 gives an overview of the tank design model and in Section 8.6 the weight and moment of Inertia of the system is presented. Finally, in Section 8.7 and Section 8.8, a sustainability approach and risk analysis is done.

8.1. General Extinguishing System Layout

The general idea of the extinguishing system is based on water scooping (also called water skimming) which can be seen in Figure 8.1. By extending probes down from the bottom of the aircraft water can be redirected upwards into the water tanks, while the thrust provides a forward velocity. When the tank are full the pilot retracts the probes and the aircraft takes off. By use of an indication in the cockpit the pilot can obtain the status of the tanks. Next, at the drop region the pilot releases the actuators that hold the doors at the bottom of the tanks. This can be done in several ways depending on the type of attack. Section 8.5.3 will contain more information about the different drop possibilities. The effectiveness of the drop is dependent on multiple factors such as:

- Drop capacity
- Drop flow rate
- Drop velocity
- Drop altitude
- Retardant burn-through time
- Type of fuels (fuels such as eucalipt, grass, pine etc)
- Wind speed
- Terrain elevation

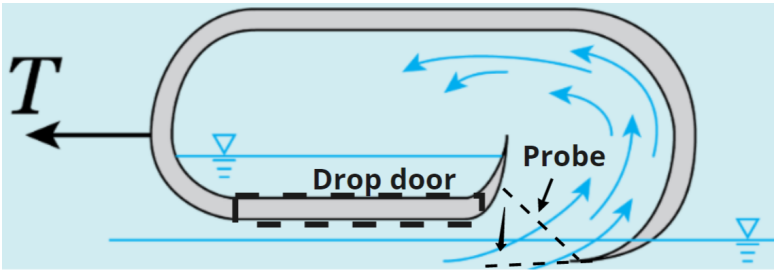

Figure 8.1: overview of water scooping principle

8.2. Requirements and Design Considerations

For the extinguishing system design, the requirements made in mid-term report are revised and adjusted [5]. These are also present in the compliance matrix in Chapter 18. The adjustments are indicated within brackets. The abbreviation can be obtained in the nomenclature. Bellow one can find the most significant requirements that effect the extinguishing system design.

- **FFA-Per-001** The aircraft shall be capable of delivering an average of 15 tonnes of water per hour of operation on a fire taking place 250 km away from the airfield and 30 km away from the nearest usable body of water.
- **FFA-ExS-001** The aircraft shall have a retardant tank.
- **FFA-ExS-003** The aircraft shall have a retardant mixing system. [The aircraft shall have a possibility to add retardant concentrate]
- **FFA-ExS-004** The retardant tanks shall be able to refill on the airport.
- **FFA-ExS-005** The retardant tank shall store commercially available liquid fire retardant.
- **FFA-GrO-006** Refilling retardant tanks shall take at a rate of 2000 L/min.
- **FFA-GrO-007** Refilling concentrate tanks shall take at a rate of 500 L/min.

Next to the above mentioned requirements, regulation and operations result in several additional requirements and design considerations. Additionally, existing firefighting aircraft protocols are reviewed and implemented in new requirements. Bellow one can find a list of those requirements;

- **FFA-ExS-007** The tanks shall be empty within 3 seconds at all times[50].
- **FFA-ExS-009** The aircraft's minimum drop height is 75 meter above the ground or canopy cover whichever is higher.[50]

- **FFA-ExS-010** Water sources shall be a minimum 2 meter deep[51].

With the knowledge gained from the mission analysis tool from the mid-term report, requirement **FFA-Per-001** resulted in an minimum tank capacity of 14,000 litre of water/retardant[5].

8.3. Tank Dimensions

The tanks are designed such that their placement will be underneath the cabin floor, possibly as close to the centre as possible as this optimises the drop effectiveness. Further analyse on the optimal drop sizing will be done in Section 8.5.3. The extinguishing system contains four tanks number similar to engine numbering standards. Tank dimensions and drop door placement are designed simultaneously with the hull design to obtain an optimal design. For specific hull dimensions and design choice refer to Chapter 4. In Figure 8.2 the tank layout can be found. The tanks are numbered from most port to most starboard, which is consistent with the engine numbering. The general dimensions of the extinguishing system are; a length of 4 m (3.5 m for the tanks and 0.5 m for two hydraulics and electronic bays), a width of 3.5 m, minimum height of 1 m and maximum height of 1.5 m.

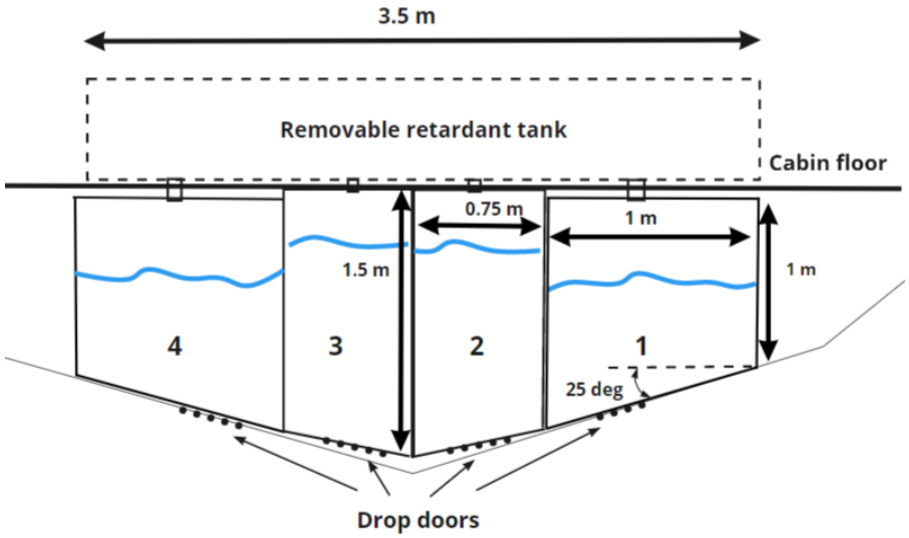

Figure 8.2: Front view tank layout

8.4. Retardant Selection

The use of retardant is beneficial for the effectiveness of fire extinguishing, however the chemicals used can cause harm to its environment (i.e. sealife and forest health). The use of retardant is restricted by the fire management plan (FMP). This section will elaborate on the effectiveness and consequences of the use of retardant such as cost, environmental impact and the weight penalty.

8.4.1. Retardant Effectiveness

Next to water, it is possible to use other retardants. Retardants can be broken down into three categories; long-term retardants, foams and water enhancing gels. In short, long-term retardants act as a retardant to fire whereas foams and water enhancing gels work as a suppressant.

Long-term Retardants From past models it can be seen that water scoopers play a significant role in an initial attack [2]. However, their effectiveness is half of that of a retardant drop as can be seen in Figure 8.3.
Note that for medium wild fires the fire intensity is $5000 MW/m$ [52]. So, the graph clearly shows a that over the range of fire intensities the long-term retardant is performing twice as good as water. The key virtue of scoopers is that they can drop more water per hour on most fires than airtankers can drop retardant. In the time land-based airtankers have returned to the fire, scoopers have already applied three more water loads [52]. For a complete comparison cost per drop and total drop capacity should be taken into account since retardant cost are significant. From the US Forest Service a list with qualified retardant is presented [53]. Retardants present in that list have been thoroughly tested on environmental impact. The candidates for long-term retardant 'MVP-FX Fire Retardant' and 'LC95 Fire Retardant' from PHOS-CheK Australia.[1]

Foams

Foams are a fire suppressant that is a mixture of water and air, such that a layer of bubbles is created. The main benefit

[1] https://www.phos-chek.com.au/retardant[Cited on 14-06-2020]

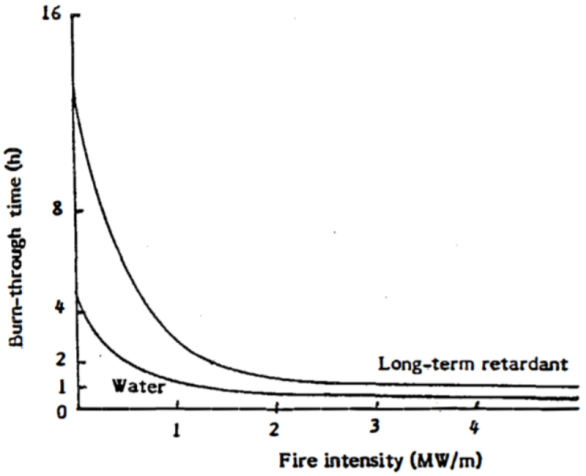

Figure 8.3: Retardant Burn-through time [52]

of foams is reduced drainage with respect to water. The drainage is dependent on the foam mix ratio, which can be seen in Figure 8.4. For missions where no tree canopy and rocky hills are present the use of dry foams can provide an advantage because foams will more likely not drain down. However, for region with a closed tree canopy fluid foams are better options because the goal is to get the foams through the canopy layer and to the surface fuels. The fluid foams reduce the burn-though time w.r.t. water and result in minimal added weight. The tank and pump will not weight more than 30 kg. Additionally, for every 100 L water 5 L foam concentrate will be needed [54]. Note that the foam will not be effective anymore when it the water has vaporised due to the fire. The candidate that are currently used are Phos-Chek WD881 and FireFoam 103B

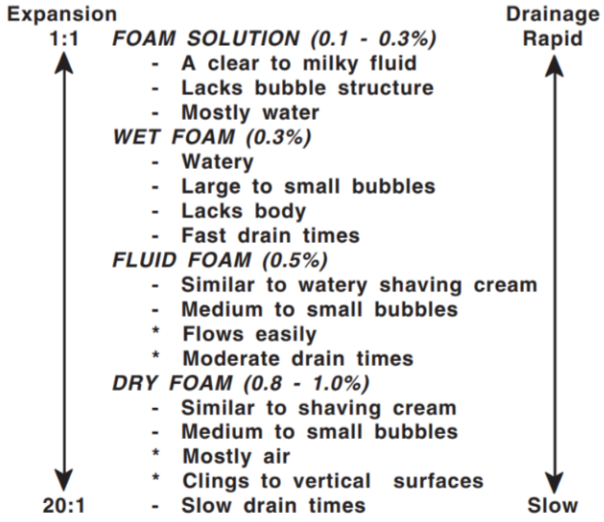

Figure 8.4: Drainage of foams as a function of mix ratio [55]

Water enhancers Water enhancers rely primarily on water with an addition of polymers or other thickeners to improve their fire fighting capabilities. The advantages of water enhancers is the ability to adhere to fuels, build up thick wet layer and keeping the aerial drift minimal. The dry coloured water enhancers that are on the market nowadays are FireIce 561 Cool Blue-F and FireIce HVB-Fx, where the FireIce HVB-Fx water enhancer is already certified for the seaplanes like the CL-415 [53]. However, before using this enhancer more research has to be done into the risks when exceeding the allowed the amount of enhancer since the water tanks will be scaled to almost twice the capacity of the Cl-415, which can be obtained in Section 8.5.

To bring focus back to the tradeoff, let us now look at how different retardants compare to the effectiveness of water. From analysis based upon data provided by US Forest Service, ICL Performance Products LP and Phos-chek Table 8.1

was created. [2] [3] [4]

Table 8.1: Retardant drop effectiveness [55]

For every liter dropped	Long-term retardant	Water enhancer	Foam	Water
Water content (%)	0.9	0.98 to 0.99	0.990.999	1.0
Dropped liquid that reaches the tree canopy (%)	0.7-0.9	0.7 - 0.8	0.35- 0.65	0.35- 0.65
Water on the fire (%)	0.65-0.8	0.7-0.8	0.35-0.65	0.35-0.65

From Table 8.1 a few things can be obtained. First, the efficiency of water dropping can be as inefficient as 35 percent. This will be analysed in Section 8.5.3 drop optimisation. Second, water on fire for long-term retardants is decrease with around 10 percent with respect to the dropped amount. This is due to low vaporisation temperatures of the water in the long-term retardants. Lastly, long-term retardants have an additional benefit together with fuel and heat water is generated from retardants [55]. When combining Table 8.1 with different mission tactics, Table 8.2 is created. In Table 8.2 the effectiveness of the retardants and water are compared for different mission tactics and scaled from 0 to 4, with 0 is not showing any effect on the fire and 4 is completely distinguishing or controlling the fire.

Table 8.2: Retardant mission effectiveness

	Long-term retardant	Water enhancer	Foam	Water
Indirect attack	4	2	1	0
Direct and parallel attack	4	3	2	1
Interior structure attack	0	2	4	1
Structure protection - indirect	4	3	2	1
Structure protection - direct	0	4	3	1
Mop-up of smoldering fire	2	2	4	1
Prescribe burn control	4	3	2	1

From Table 8.2 the mission is of significant importance for effectiveness of the retardants. Previous water scoopers were only designed to drop water which is not efficient for an indirect attack (e.g making firelines). Other retardants tends to perform better overall w.r.t. water. Therefore, the water tank will be coated such that premixed retardants can be loaded at the airbase. However, the benefit of amphibious aircraft is the ability to quickly return to the fire. So, retardant concentrate/powder is an option when the mission specifically asks for fire-line construction. In the design of the tanks four access holes placed at the upper parts of the tanks. The reason doing so it that the water tanks can be converted to retardant tank by applying retardant concentrate, stored in the cabin, through the holes into the tanks. So, when the tanks are empty retardant concentrate will be pumped in. Then, when turbulent water rushes in through the probes the water get mixed with the retardant. Using this principle no difficult changes are necessary to convert for retardant drops.

8.4.2. Drop Cost

When trading off retardants versus water, cost is of major importance. The addition cost per drop is highly dependent on the type of retardant, differing between 100 and 9000 euro. Yet water scooping has been free. Nevertheless organisation want to introduce a law that imply cost penalties for scooped water. To make an efficient extinguishing design, cost is analysed for long-term retardants, foams and water enhancing gels. The US Forest Service provides a qualified list of retardants in accordance with forest service specification [55]. The cost of the products stated in Table 8.3 are taken from the manufacture websites. When looking at Phos-Chek-MVP-FX it can be seen that fire retarding chemicals come at high cost and weight. It should be noted that added weight of 1680 kg is obtained by taking the water capacity of the tank and applying the retardant concentrate, which means that the actual volume of the mix will be 20 percent higher than the water capacity. To conclude the cost investigation, retardant will add to additional cost and more weight if the water capacity is retained. Nevertheless, the effectiveness of retardants balances with cost.

Table 8.3: Cost breakdown of retardants

Chemical	Mix ratio (kg per L water)	Cost (euro per kg)	Cost for 1 drop (euro)	Added weight per drop (kg)	Type
Phos-Chek MVP-FX	0.12	5.03	8450.4	1680	Long-term retardant
Phos-Chek WD881	0.01	0.6265	87.71	140	Foam (Class A)
Thermo-Gel 200L	0.02	0.4	112	280	Water enhancing gels

[2] https://www.fs.fed.us/rm/fire/wfcs/index.htm[Cited on 11-08-2020]
[3] https://www.icl-group.com/[Cited on 11-08-2020]
[4] https://www.phos-chek.com.au/[Cited on 11-08-2020]

8.4.3. Environmental Impact

As the toxicity levels of the retardant can influence the flora and fauna life, it is important that the use of retardants is no severe effects on wildlife, while preserving their effectiveness. Designing a fire retardant is out of the scope of this project. However, choosing the right retardant is of major importance to minimise effects on the local environment. The most commonly used fire retardants are Phos-Chek, Fire-Trol and Termo-gel. The only disadvantage of this inhibitor is that it affects aquatic life. However, the wildfire itself also affects aquatic life and it has been shown that heating up the water and ash of the fire is several times more harmful than the flame retardant. Nevertheless, measures are taken to avoid direct contact between aquatic life and the fire retardant during the mission as much as possible.

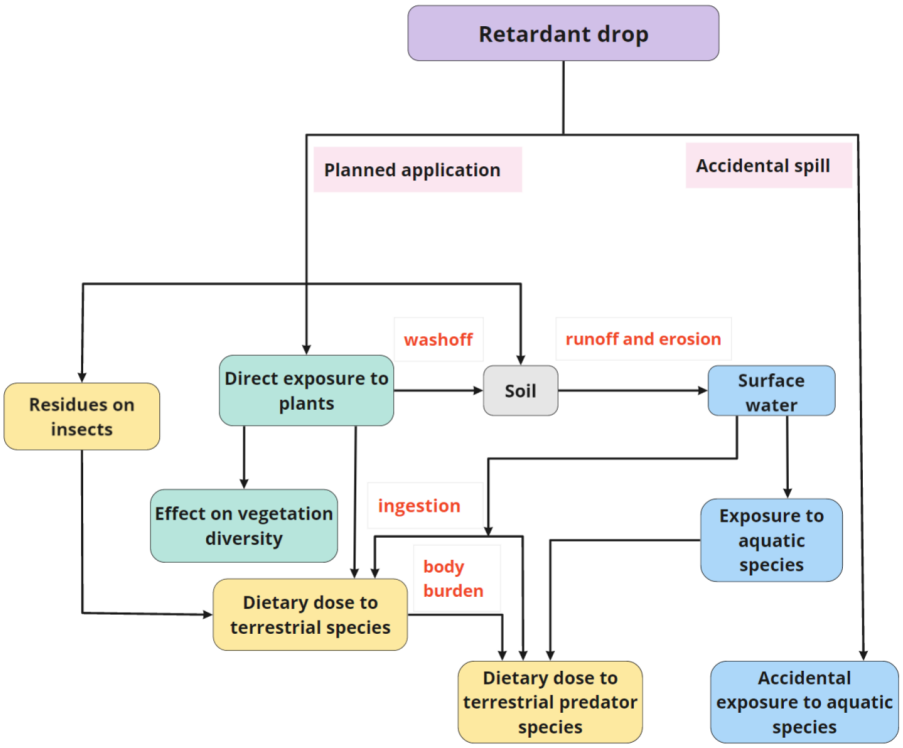

Figure 8.5: Over of retardant impact on terrestrial and aquatic wildlife

PhosChek MVP-FX All data about PhosChek MPV-FX was found using an investigation by the Fire and Aviation Management US Forest Service.[5] The use of MPV-FX is found not to cause much harm to humans, other than eye and skin irritation when exposed to high concentration for long time. However, some fish species were sensitive to MPV-FX at 6 gpc gallons per hundred square feet. Only for mussels contact with the foam can lead to mortality. Next, the MVP-FX could have phytotoxic effect to individual plants, but no severe widespread is expected. The effect of the foams will not be more harmful than the effect of the fire.

Phos-Chek WD881 The impact of Phos-chek WD881 is obtained by the information given by Phos-Chek.[6] From single contact or ingestion, tests have found Phos-Chek WD881 not to be causing any damage to human health. However eye and irritation can be experienced if not washed off. Next, Phos-Chek WD 881 contains biodegradable organic compounds that after use are converted by bacteria to carbon dioxide. As for plant harmfulness, the foam has been widely used for the past eleven year without any report of vegetative mortality. It is found that this foam can be toxic to fish when applied in large amounts. Unless a drop door failure occurs over a lake, it is not likely to cause any issues. At last, a study from National Biological Service no effect was found on wildlife or farm animals.[7].

Thermo-Gel 200L Thermo-Gel 200L has been previously tested and approved in accordance with the Environmental Protection Agency (EPA) and the United States Forest Service (USFS).[8] From this research it is found that when applied is less than 28 mg/L no harm will be done to fish. So far no severe effect were found on plants, other than that some leave can dry out because the gel absorbs water. Thermo-gel 200L is benefitial for recovery of the soil after the fire and doing so it is biodegradable.

Uncertainties The use of chemical with firefighting has been wide accepted, yet uncertainties exist. Every brand does its own investigation which could be in favour of their product by leaving out certain investigation. On the other hand the US Forest Service is bringing those investigation together to generate limits and regulations. But the long term

[5] `https://www.fs.fed.us/rm/fire/wfcs/documents/EcoRA-Retardants-PUBLIC-Dec2013-rev3_080614.pdf` [Cite on 18-06-2020]
[6] `http://www.phos-chek.com.au/pdf/wd881/enviro_q_a.pdf` [Cited on 18-06-2020]
[7] `https://www.federalregister.gov/agencies/national-biological-service` [Cited on 18-08-2020]
[8] `http://www.thermogel.com.au/images/docs/ForestryReport.pdf` [Cited on 18-06-2020]

damage is hard to conclude when investigation are not taking into account retardant that were used over 40 years. Also, current well-validated model assume a uniform drop such that so it underestimates the residue level on food and water. So, these uncertainties should be taken into account with the choice of a retardant.

8.4.4. Concluding remarks

After going over the effectiveness, cost and environmental impact it is good to combine these aspect and make some remarks. The extinguishing system is design with the main purpose of dropping water. Water is effective for direct attacks at low cost and environmental impact. But to make efficient fire lines retardants are more effective. However this increase cost and impact on the environment. Since this choice for water or retardant is dependent on the mission and operative region the tank design is adapted for retardant addition. This asks for non-corrosive coatings and a fail safe drop door mechanism. The implementation of retardant addition can be found in Section 8.5

8.5. Tank Sizing and Integration

For the tank sizing the tank layout from Section 8.3 is used. The material used for the tanks is Al 2024 T4 for its high strength and low weight properties. To give an overview of the tank sizing tools, it starts from constrains such as the hull design and the cabin floor. Then, multiple tank configuration are designed while keeping the drop doors near the centre of the aircraft. For each tanks configuration the capacity is calculated. If need tank dimensions are adjusted to comply with the 15,000 litre capacity. Note that the design tool takes into account that only 90 percent of the tank is filled. After sizing, the structural weight of the tanks is calculated. Added with the mass of hydraulic actuators and drop doors this result in the total structural weight of the extinguishing system. This was gathered into the extinguishing system tool whose outputs can be obtained in Table 8.4.

Table 8.4: Tank sizing results

	Value	Unit	Comments
Capacity inboard tanks per tank	7087.5	L	Taken into account 90% of capacity
Capacity outboard tanks per tank	7932.1	L	Taken into account 90% of capacity
Total capacity	15019.6	L	-
Tank thickness	0.006	m	-
Inboard weight per tank	300.2	kg	-
Outboard weight per tank	266.9	kg	-
Structural weight[a]	520	kg	Hydraulic system, adhesives/rivet, drop doors and probes excluding tank weight
Extinguishing system empty weight	1798.8	kg	Total system weight excluding water
Total extinguishing system weight	17193.9	kg	Total system weight including water

[a] The structural weight is based on an estimation that takes into account material reinforcements high load components.

8.5.1. Features

To increase effectiveness of a salvo and trail drop the total capacity is divided into four compartments, each containing its own drop door and probe inlet. Trail drop is a sequence of drops resulting in a line whereas a salvo droop release all water in one go. The drop doors will be moved by hydraulics actuators that are controllable and electrically unlatched such that when necessary the door can move to the most open position in 0.7 seconds. The hydraulic bay is located on both outer sides of the tanks to reduced malfunctions due to chemical retardants. Four probe inlets are located at the backside of the tank near the step of the hull since the main point on contact during skimming is located at the step. Next, the tanks will have two access hole each, so eight in total. These access hole will penetrate the cabin floor to transfer fluid or powder from the cabin to the tanks underneath. The tank options are retardant concentrate tanks, additional water tanks (when water scooping is not possible), water sanitiser and colour addition (for fire-line recognition). Additionally, the tank will contain an overflow vents located on the top of the tanks for potential overflow, however their main function is to increase inlet speed of from the probes by pushing the air out through these outlet vent. With the same reason water can be dropped faster since air is taken in via the overflow vent. The last feature of the tank design is the ability to fill up the tanks at an airbase. A non-corrosive pipe will run through the tanks from left to right. In each tank the pipe will have two throughput holes to fill the tanks. From both side of the aircraft the tanks can be filled to be able to have a flow-rate of 35 L/s. Lastly, the tank design is done such that flow rate are optimised while keeping additional weight low and preventing water baffling. Structural plates are installed such that water baffling is decreased. Circular hole are cut in these plates to keep additional weight minimal. For better understanding of the internal structure see Figure 8.8

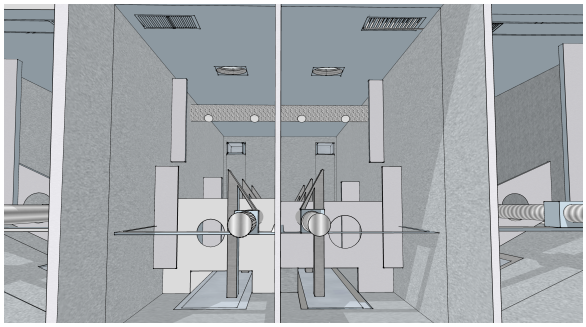

Figure 8.6: Front view of 3D design extinguishing system

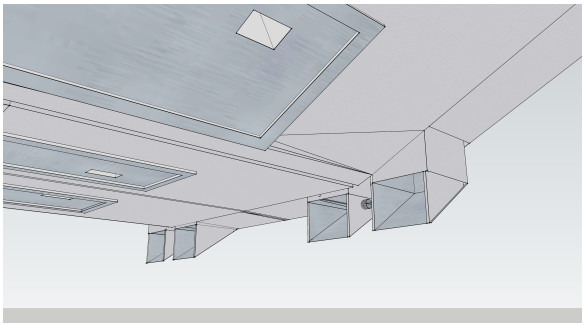

Figure 8.7: Probe view of 3D design extinguishing system

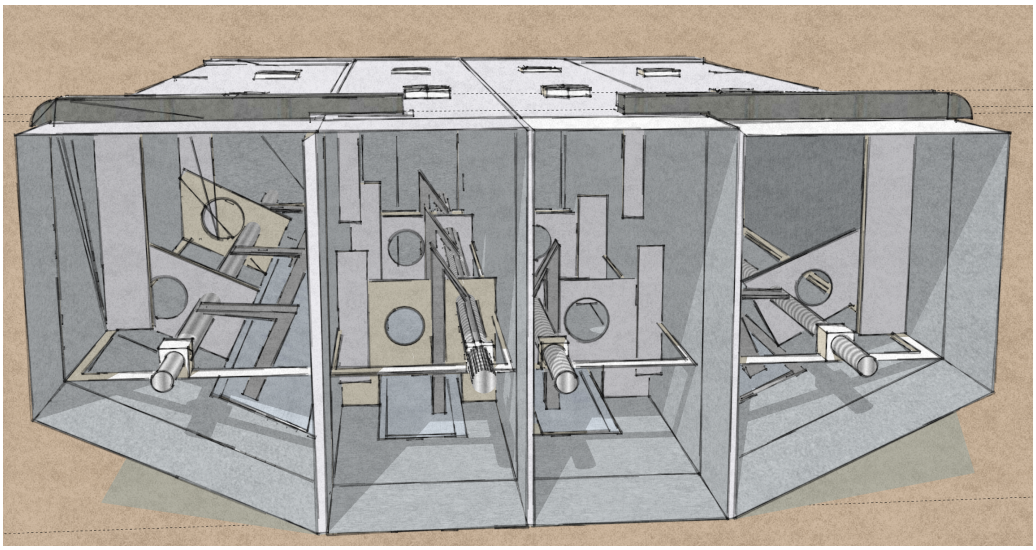

Figure 8.8: 3D perspective of the extinguishing system

8.5.2. Probe Design

For optimal scooping performance the probe have to be sizes accordingly. The probe inlet size must large enough to attain the skim speed without effecting performance and structural loads significantly. In Figure 8.9 one can obtain the illustration of skimming water into the fuselage tanks. The aircraft is designed to fill its water tanks in 12 seconds to 90 percent of their capacity. Assuming that the flow is incompressible and the aircraft will retain its speed, the mass flow is calculated by using Equation (8.1).

$$\dot{M}\,[kg/s] = \frac{capacity\,[L]\cdot\rho}{skim\ time\,[s]} \tag{8.1}$$

By using a capacity of 15019.58 L, a water density of 1.025 kg/s and skim time of 12 seconds the mass flow results to be 610.5519026 kg/s. To be able to integrate the retractable probes the inlet area is calculated using Equation (8.2).

$$A_e[m^2] = \frac{\dot{M}\,[kg/s]}{\rho\cdot V_{skim}\,[m/s]} \tag{8.2}$$

By using a water density of 1.025 kg/L, Equation (8.2) results to $A_e = 0.106m^2$. So the final dimensions of the probe result into a width of 12 cm and height of 8.5 cm. The probes will be retractable in pairs, outboard probe together and inboard probe together. The main advantage of being able to only fill the inner of outer tanks is the range. If the waterway is further away than the range of four tank operative than the choice can be made of only extending the inboard probes.

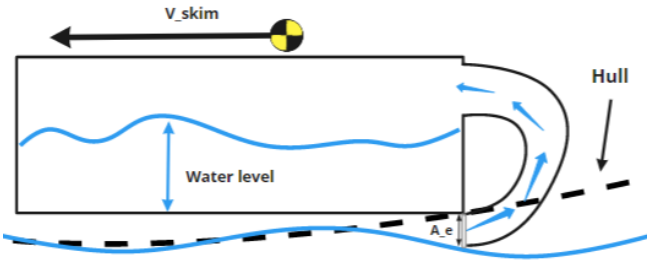

Figure 8.9: Illustration of a probe directing water in the tank

8.5.3. Drop Optimisation

The dropped water/retardant does not necessarily mean the water/retardant measured on the ground. Due to evaporation of water, fire suppressants get less effective. Main factors influencing water evaporation are: flow rate, drop speed and drop altitude. For an effective drop a certain amount of depth of water/retardant is required. This section will provide an overview of optimal drop factors and the resulting design choices.

Drop type Drop can be categorised into two categories. A drop that releases four tanks simultaneously known as a 4T x 1R salvo and a drop consisting of four releases, each of one tanks, 0.7 seconds apart known as a 1 T x 4R trail sequence. Other drop sequences will be optional such as a salvo drop split into two. The drop sequence defines the flow rate of water/retardant which strongly related to its effectiveness. Different missions will ask for different drop sequences. For a direct attack of a public property a salvo drop may be necessary and for protection of ground forces a water line is needed to give them more time to evacuate.

Flow Rate As already mentioned above, drop flow rate are important for drop effectiveness. The drop flow rate is dependent on drop door location, outlet area, evaporation of water. Evaporation is unfavourable since water is extracted from the mixture which leads to less volume or a retardant not being useful when it reaches the surface. High flow rate drops have as benefit that penetration through the tree canopy is easier. The flow rate is not constant for a conventional drop, where the drop door are fully opened in one go. In fact, the flow rate slow increases from the tank toward the peak and then decreases again, as modelled in Figure 8.10. From the patter simulation done by Swanson it was noted that controlled drop doors give signification improvement because it allows for a constant flow rate [56]. For controlling the flow rate, the door mechanics will be equipped with door actuators that allows three door angles to provide a choice of flow rate, since different flow rate can be favourable for different fuels as can be seen in Figure 8.11. To conclude, the door will be optimised for constant flow rate by automated door opening and different doors position can be set from the cockpit to allow better drop efficiency.

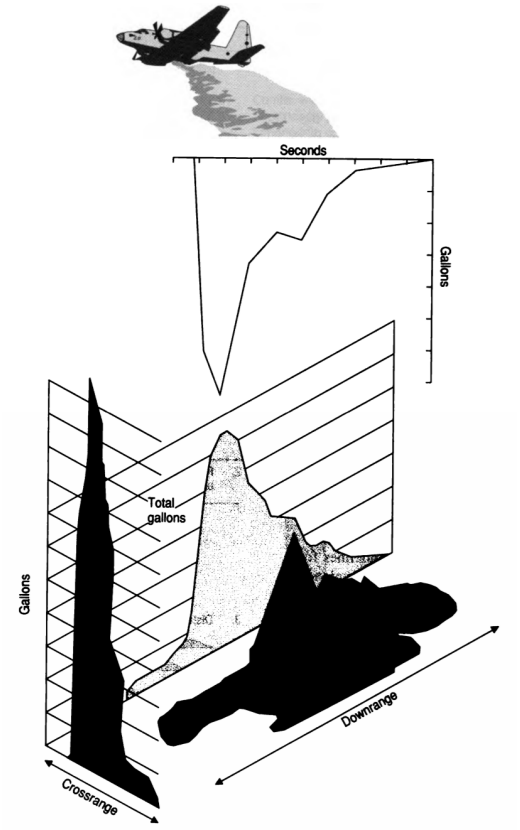

Figure 8.10: Relationship between ground distribution patterns and characteristics of water/retardant flow from tank system

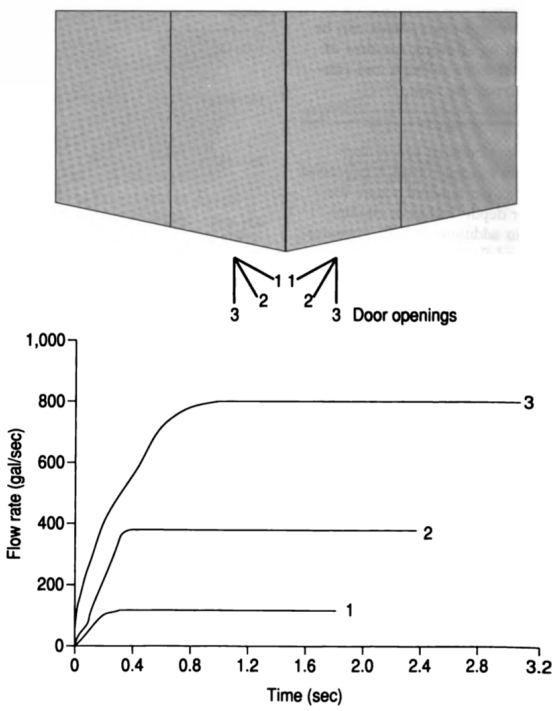

Figure 8.11: Flow-rate as function of time for three door positions

Skim speed For loads on the probe it would be favourable to have a low skim speed. However, too low skim speeds would result in improper water flow into the water/retardant tanks. A lower limit on the skim speeds result from the stall speed in landing configuration. When landing in turbulent weather with turbulent water including waves it is desired to have a margin such that the aircraft does not stall while skimming. So, to have optimal skimming characteristic the skim speed is set to be around 50 m/s, for more specifics on the skim speed look at Section 10.2.2.

Drop altitude The altitude at which the drop is performance is often limited by aircraft performance characteristics. From effectively perspective drops would be performance at zero velocity. This can not be achieved for aircraft (excluding VTOL) so the aircraft's drop speed is set to be a low as performance limits permits. From a drop modelling from Satoh it is found that efficiency decreases with increasing airspeed and altitude [57]. The data can be obtained in Table 8.5. Here one can see that drop efficiency decreases significantly when drop speed and altitude are increased. So for an optimal design stall speeds should decreased and drop altitude should a low as possibility without generating unsafe flight conditions.

Table 8.5: The ratio of the amount of water reaching the ground against the total water amount dropped from the tank.

speed (km/h)	At height of 60 m	At height of 120 m
138-185	75%	65%
204-222	60%	55%

8.6. Weight Envelop for Extinguishing System

Firefighting mission are known for their intense weight shift due to retardant/water dropping. This section lists the main items in the extinguishing system with relevant parameters. The weight of the extinguishing system can be broken up into steady weight (such as structural weight and extinguishing equipment) and dynamic weight (such as water weight and retardant weight). Dynamic weight is referred to as weight that can drastically change during flight such as water skimming or dropping. With dividing up the tanks in the weight tool, it can be used to obtain an accurate representation of the weight shift in case of the trail drop when only two tanks are simultaneously opened. The specification on weight and mass moment of inertia can be obtained in Table 8.6.

Table 8.6: Retardant tank design parameters

C.G. Range	Mass (kg)	X_cg (m)	Y_cg (m)	Z_cg (m)	Ixx	Iyy	Izz
Water Tank1	350.92	5.50	0.35	1.50	0.06	0.06	0.00
Water Tank2	343.24	5.50	-0.38	1.73	0.06	0.04	0.00
Water Tank3	343.24	5.50	0.38	1.73	0.06	0.04	0.00
Water Tank4	350.92	5.50	0.35	1.50	0.06	0.06	0.00
Concentrate tank	68.65	5.50	0.00	2.20	0.00	0.00	0.00
Extinguishing equipment	520.00	7.00	0.00	1.33	0.06	0.06	0.00
Water in Tank1	3,966.04	5.50	-0.60	1.50	661.01	4,524.59	6,160.58
Water in Tank2	3,543.75	5.50	-0.50	1.73	830.57	4,282.03	3,783.69
Water in Tank3	3,543.75	5.50	0.50	1.73	830.57	4,282.03	3,783.69
Water in Tank4	3,966.04	5.50	2.60	1.50	661.01	4,524.59	6,160.58
Retardant concentrate	140.00	5.50	0.00	2.20	0.00	0.00	0.00

8.7. Sustainability Approach

Components that effect sustainability are mainly the tank materials and the choice for retardant. The tank material that is chosen is Al 2024 T4 which is a strong and light weight aluminium alloy. The choice for metal was made for easy production and recyclability. Next, the choice of using retardant makes the design less sustainable than using water. The environmental and cost aspect have already been investigated in Section 8.4. So a proper choice can be made taking those aspects into account. But other than tank materials and retardant, production and maintenance should not cause problems during the aircraft's lifespan. The use of a easy to manufacture geometry of the tank will decrease production cost and time. The tank design has implemented 8 access holes for retardant addition, but their secondary purpose is for inspection and maintenance. Lastly, since the tank can be will be water or retardant changes of corrosion will be likely so the material used for the tanks has already been proven to retardant tanks in helicopter and fixed wing aircraft[9].

8.8. Risk Analysis

The extinguishing system imposed some additional risks in comparison with passenger aircraft due to water dropping and skimming operation. In this section, the main risks involved with the extinguishing system will be defined and rated on likelihood of occurrence and impact. Then, the risk is calculated, which is the multiplication. Finally, mitigation strategies will mitigation the amount of risk for each identified item. The main risks factor are the retardant drops, probes and skimming. The risk assessment of the extinguishing system can be found in Table 8.7. For a more general and mission related risk assessment continue to the risk assessment chapter Chapter 14.

[9] https://www.fs.fed.us/rm/fire/wfcs/documents/5100-304d_LTR_Final%20Draft_010720.pdf [Cited on 18-06-2020]

Table 8.7: Risk identification and mitigation for the extinguishing system

Extinguishing System Risk Assessment									
			Before Mitigation				**After Mitigation**		
Category	**ID**	**Description**	**Likelihood**	**Impact**	**Risk**	**Mitigation strategy**	**Likelihood**	**Impact**	**Risk**
Retardant Drop	RD1	Unwanted drop deviation	Low	Moderate	Moderate	Specific training on drop techniques including possible delays of the system.	Very low	Moderate	Moderate
	RD2	Spilling of retardant	Low	Moderate	High	The drop doors will be equipped will anti-leak strips. Additionally, the overflow vents are adjusted such that retardant cannot easily pass through.	Very low	Moderate	Moderate
	RD3	Retardant type not allow in region and not notified about the change	Moderate	High	High	Pre-flight checks will include review the latest update about the qualified retardant of the region.	Low	Moderate	Moderate
	RD4	Drop doors not functioning	Low	High	Moderate	Next to well known hydraulics actuators and manual release mechanism is installed in cause of an emergency.			
Probe	Pr1	Exceeding loads on the probe while extended	Moderate	High	High	Define skim velocity limit for probe extension.	Very low	Moderate	Moderate
	Pr2	Probes transferring fish into the water/retardant tank	Moderate	Moderate	Moderate	The probe inlet will design such that structural connections will act as a filter to larger fish.	Very low	Low	Low
Skimming	Sk1	Excessive skimming resulting into slow takeoff performance.	Moderate	Moderate	Moderate	Water capacity meters will be closely monitored by the person responsible for retardant drops. Overflow vents will act as throughput for retardant if overflow occurs.	Low	Low	Low
	Sk2	Excessive skimming resulting in damage to the water tank structure.	Moderate	High	High	The structural plate installed in the tanks will be placed such that high speed skimming does not harm the strength.	Low	Low	Low

9
Stability and Control

The stability analysis of MANTÆ will be performed in this chapter. This will be done, by first assessing the ground stability of the aircraft in Section 9.1. Here, the process of determining centre of gravity (cg) position as well as the positioning of the landing gear will be discussed. In Section 9.2, the static stability analysis is done. After that, the dynamic stability is discussed in Section 9.3. This is followed by a preliminary actuator sizing in Section 9.4. Finally, some remarks will be given regarding the stability of the aircraft in Section 9.5.

9.1. Ground stability

The ground stability of the aircraft is presented in this section. This is done in order to determine the required position of the landing gear. This section is laid out as follows: First, the cg-range of the aircraft is discussed in Section 9.1.1. This cg-range will then drive the positioning of the landing gear discussed in Section 9.1.2. Then, a weight and size estimation of the landing gear system is performed in Section 9.1.3. Finally, the storage of the landing gear system will be elaborated upon in Section 9.1.4.

9.1.1. cg-range

Determining the centre of gravity of the aircraft is rather straight forward. By taking the average of the cg-positions of the individual components of the aircraft, the cg-position follows. During the mission however, the cg-position shifts due to the consumption of fuel and the acquisition/dropping of the payload. This movement of the cg-position is visualised by construction of a loading diagram. This diagram starts at the cg-position of the W_{OE} and shows the shift of the cg depending on the loading of the aircraft. This diagram is shown in Figure 9.1. Note that the cg-position is measured as a function of the mean aerodynamic chord (MAC). One of the observations that can be made from this figure, is that the cg-range is rather small. The reason for this is that the location of the water and fuel tanks is chosen specifically for a small cg-range. Especially the placement of the water tanks was chosen rather close to the cg-position of the M_{OEM}, which is also visible in Figure 9.1. The general idea behind this is that having only a small shift of the cg when emptying the tanks over a fire would only cause minor disturbance to the stability of the aircraft. Also, by having a small cg-range, the trim drag created by the trimming of the elevator would stay roughly constant during flight. It should also be noted that there are two red lines in Figure 9.1 labelled limit. This is a 2% safety margin on the most forward and most aft cg-position. Those two lines represent 25.2% and 32.0% of the MAC. This is equal to a cg-range of $7.94 - 8.68m$ measured from the nose of the aircraft. Furthermore, the Z-coordinate of the cg-position is estimated to be roughly $2.4m$ of the ground and the Y-coordinate of the cg-position is estimated to be $0m$ (the centre-line of the aircraft) due to the symmetry of the aircraft.

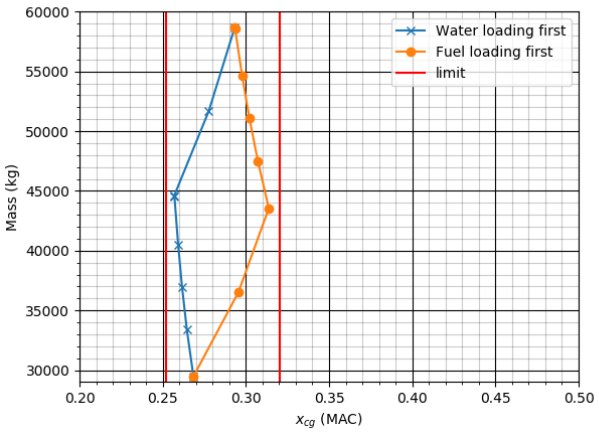

Figure 9.1: Loading diagram for MANTÆ aircraft

9.1.2. Landing gear position

According to Raymer[6], the landing gear has to follow the following criteria with the most aft cg-position and the landing gear in its compressed state:

- The aircraft must have a a longitudinal tip-over clearance of at least 15°.

- The aircraft must have a a lateral turn-over angle of at most 63°.
- The aircraft must have a an aft ground clearance of at least 15°.
- The aircraft must have a a wingtip ground clearance of at least 5°.
- The nose gear must have a load smaller than 20% of the M_{MTO} and larger than 5% of the M_{MTO}.

Additionally, requirement **FFA-GRO-001** requires that the aircraft shall have a turning radius of a maximum of 20.0m. In order to determine the most forward allowable longitudinal position of the main landing gear that fulfils the tip-over clearance, Equation (9.1) is used. Note that in this equation, variable H is taken to be the Z-coordinate of the aft cg-position. $X_{min_{main}}$ is the most forward x-position of the main landing gear, measured from the nose of the aircraft. To determine the most inward allowable location of the landing gear, equation Equation (9.2) is used. Here, H is also taken to be the Z-coordinate of the aft cg-position. For clarification on the definition of H, see Figure 9.4.

$$X_{min_{main}} = H \cdot \arctan(15°) \tag{9.1}$$

$$Y_{min_{main}} = \frac{H}{\arctan(63°)} \tag{9.2}$$

Fixing the landing gear position, enables the determination of the position of the nose landing gear. As mentioned before, the nose gear shall have a loading of $0.05 \leq P_{nose} \leq 0.2$ times the maximum take-off weight. This means that for a given main gear position, there is a forward limit and a backward limit of where the nose gear can be located. In order to find this range, the distance from the main gear towards the nose gear is computed using Equation (9.3) and Equation (9.4) from Raymer [6], where variables M_a and M_f represent the distance of the main landing gear with respect to the most forward and most aft centre of gravity position. For clarification on the variables M_a and M_f, see Figure 9.4 is provided showing the nomenclature regarding the variables used. It should be noted that in Equation (9.3), the aft cg-position is taken, whereas in Equation (9.4) the forward cg-position is taken. This is done since the load on the nose gear is maximum under the condition for the most forward cg-position and minimum for the aft cg-position respectively.

$$B_{min} = \frac{M_a}{0.05} \tag{9.3}$$

$$B_{max} = \frac{M_f}{0.2} \tag{9.4}$$

With the distance range between the nose gear and the main gear determined, the nose landing gear can be placed within that range. After iteration, it is found that the nose gear can be positioned between $0 - 2.50m$ measured from the nose. For this stage of the design, the middle of this range is chosen and the nose gear is placed at $1.25m$. The main landing gear will be placed at $9.3m$ measured from the nose using Equation (9.1). According to Raymer[6], the optimal position would be there where the nose gear carries 8% of the load with the aft cg-position and 15% with the forward cg-position. This is for steering purposes. With the current layout of the landing gear, the nose landing gear will carry between 8% and 17% which is roughly the optimum position Raymer[6] mentions. The lateral displacement required for the main landing gear is equal to $1.22m$ using Equation (9.2). The lateral displacement will, however, be larger than this. This is due to the fact that the hull has a width of $4m$, meaning that the lateral position of the landing gear is at least $2.76m$, when taking the width of the tires and the spacing between them into account. These dimensions are discussed in Section 9.1.3. See figure Figure 9.2 and Figure 9.3 for the final landing gear placement. Note that the landing gear is coloured in green. Furthermore, note that the current landing gear position pass the required clearance angles, which are also present in these figures. Additionally, It should be noted that the aircraft has a ground clearance of $0.5m$. This height is chosen to ease work done during ground operations. Especially since the water tanks are located in the hull section of the aircraft. Finally, the turn radius requirement is assessed. If no nose wheel slip occurs, the turn radius of the aircraft is calculated using Equation (9.5)[1] with $R_{turn_{ground}}$ being the turn radius, B the track width (8.04m under current landing gear positioning) and $\angle_{rotate}$ the rotation angle of the nose gear. Filling in the required turn radius of $20m$ yields a required rotation angle of the nose wheel of at least 23.70°. This is manageable, considering aircraft sometimes have rotation angles of 78°[2]. This means that the turning radius requirements can be fulfilled.

$$R_{turn_{ground}} = \frac{B}{\sin(\angle_{rotate})} \tag{9.5}$$

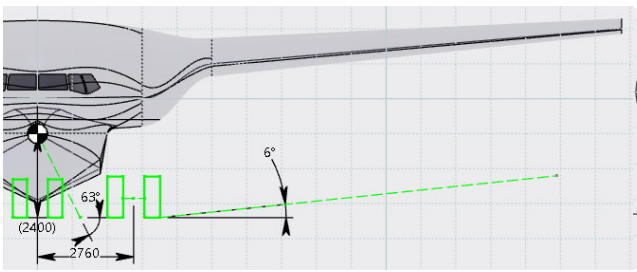

Figure 9.2: Landing gear placement front view.

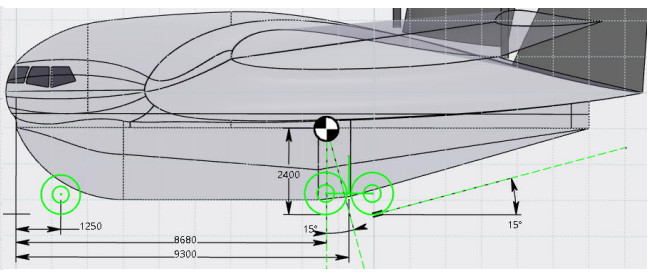

Figure 9.3: Landing gear placement side view.

[1] http://www.davdata.nl/math/turning_radius.html [cited: 22-06-2020]

[2] The Boeing 737 has a nose wheel turning angle of 78 degrees. https://www.jvejournals.com/article/17977 [cited: 22-06-2020]

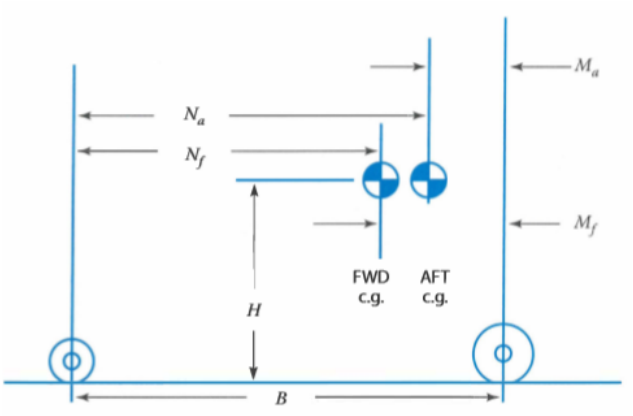

Figure 9.4: Nomenclature for landing gear positioning[6]

9.1.3. Weight Estimation Landing gear

With a location of the landing gear, the loading per tire can be determined by dividing the load on the gear by the amount of tires present on that gear. For the main landing gear, a number of 8 tires was chosen divided over two bogeys having a $2x2$ layout. This is shown in Figure 9.2 and Figure 9.3. The nose gear will use 2 tires side by side. Given the loading per landing gear, explained in Section 9.1.2, and knowing that the M_{MTO} is equal to $58712.3kg$, the load per tire on the nose and main landing gear is equal to $5304kg$ and $6527kg$ respectively.

From the global aviation tires data sheet[58], tires have been selected to assess what type of tires the MANTÆ aircraft will use. The biggest constraint in this regard is the ground pressure exerted by the tires on the runway. The allowable tire pressures are presented in Table 9.1 obtained from Raymer [6]. Since the aircraft will likely operate in remote areas, it must be capable of landing on runways that have low maximum tire pressure requirements. This could include hard packed sand runways, or even dry grass runways. Therefore, the tires are selected to operate on such runways and the aim is to have tires with a ground pressure of around $50psi$.

In order to determine the tire pressure of a certain tire, the load per tire is divided by the contact area the tire makes with the runway. The contact area of a tire is determined using Equation (9.6) from Raymer [6]. Note that the tire width w, the tire diameter d and the rim radius R_r are available in the aviation tires data sheet [58]. For illustration, figure Figure 9.5 shows the dimensions for a tire.

$$A_p = 2.3\sqrt{w \cdot d}\left(\frac{d}{2} - R_r\right) \tag{9.6}$$

After iteration, the following tires have been selected: The nose wheel will use tires of the type $43x16.0-20$ [58]. These tires have a width of $0.41m$, a diameter of $1.09m$ and a rim radius of $0.46m$. The contact area computed using Equation (9.6) is equal to $0.14m^2$ giving the tire a pressure of 55 psi. This was deemed sufficient. The weight of such a tire is equal to $72kg$. The main landing gear will use tires of the type $H46x18.0-20$ [58]. These tires have a width of $0.46m$ a diameter of $1.17m$ and a rim radius of $0.48m$. The contact area computed using Equation (9.6) is equal to $0.18m^2$ giving the tire a pressure of 53 psi. This was deemed sufficient. The weight of such a tire is equal to $88.86kg$.

The tires mentioned above have been selected for their tire pressure. Having a tire pressure of roughly $55psi$ enables the aircraft to land on hard sand and dry grass runways. The only runway types the aircraft would not be capable of operating on would be wet grass runways and soft sand runways. This is, however, not a problem since the aircraft does not need to land at such airports.

Given the amount of tires and their respective weight, a more detailed estimation of the landing gear weight can be made. The combined weight of the tires is equal to $854.9kg$. Applying a weight factor of 2, to account for the attachments of the landing gear, and its components yields an estimated landing gear weight of $1709.9kg$. It must be noted that the safety factor of 2 is a rough estimate and not based on literature. Therefore, the true weight of the individual component shall be analysed in a later design phase.

Table 9.1: Tire pressure recommended per runway surface[6].

Surface	Maximum Pressure psi	kPa
Aircraft carrier	200+	1380+
Major military airfield	200	1380
Major civil airfield	120	828
Tarmac runway, good foundation	70-90	480-620
Tarmac runway, poor foundation	50-70	345-480
Temporary metal runway	50-70	345-480
Dry grass on hard soil	45-60	310-415
Wet grass on soft soil	30-45	210-310
Hard packed sand	40-60	275-415
Soft sand	25-35	170-240

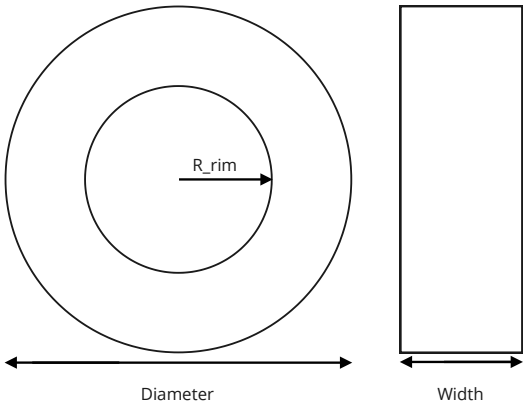

Figure 9.5: Tire nomenclature

9.1.4. Storage of Landing gear

Due to the pressure requirements on the landing gear, the tires used for the landing gear are rather large. Therefore, answering the question of how to store the landing gear is of great importance. The nose gear can be stored inside the hull as shown in Figure 9.6. The main landing gear will be stored in the fuselage section of the aircraft next to the hull of the aircraft. This is shown in Figure 9.7. Both the nose and the main landing gear shall be folded up during flight and can be folded back down for landing and take-off. It must, however, be noted that the exact folding mechanism used to fold up the landing gear will be further investigated in the future.

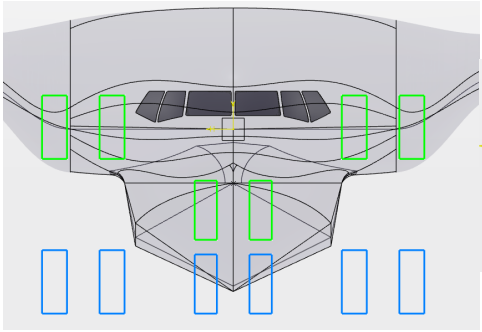

Figure 9.6: Landing gear stowage front view.

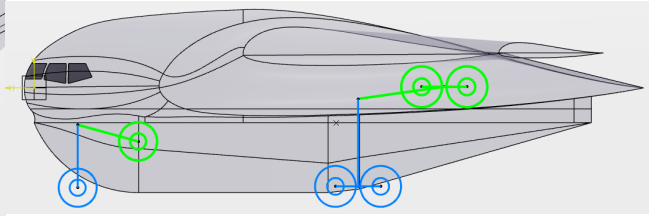

Figure 9.7: Landing gear stowage side view.

9.2. Static Stability

In this section, the static stability of the MANTÆ aircraft will be assessed. This is done by first assessing the location of the neutral point with respect to the centre of gravity in Section 9.2.1. Then, in Section 9.2.2, the elevator trim curve of the aircraft will be presented to assess the effectiveness of the elevator. Finally, an analysis is done on the required force needed to operate the elevators in Section 9.2.3.

9.2.1. Location neutral point

The neutral point is a geometric point on the wing of the aircraft on which, if the aircraft's cg-position were to be located there, the aircraft is neutrally stable. This is caused by the fact that the change in lift due a change in angle of attack acts through that point creating no moments if the cg were to be located there. In reality, the aircraft's centre of gravity shifts during the whole flight, and can never be located exactly at this point. Therefore, there will always be a moment caused by the change in lift due to a change in angle of attack. For an aircraft to be statically stable, the moment caused by a changed lift due to a changed angle of attack should be negative. This way, the aircraft naturally produces a moment that counters the change in angle of attack and brings the aircraft back to its original position, see Figure 9.8 and Figure 9.9. In other words, the derivative of the moment coefficient of the aircraft with respect to the angle of attack or C_{m_α} must be negative for static stability. This can be achieved by having the aircraft's centre of gravity in front of the neutral point. The more in front it is, the larger the moment arm of a changed lift, the more negative (or positive if the cg is behind the neutral point) C_{m_α} becomes.

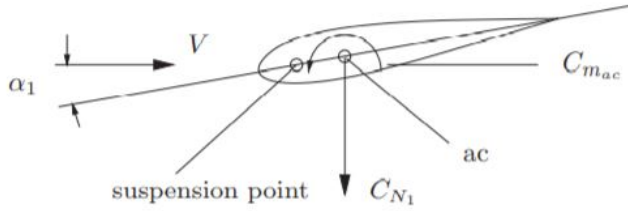

Figure 9.8: Statically stable configuration with the suspension point (or centre of gravity) in front of the neutral point [59]

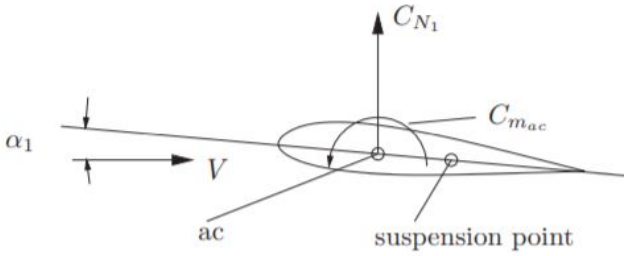

Figure 9.9: Statically unstable configuration with the suspension point (or centre of gravity) aft of the neutral point [59]

The neutral point as well as the C_{m_α} can be found using AVL. Therefore, the static stability of the aircraft can be assessed rather straight forward. Furthermore, knowing the location of the neutral point allows for careful placement of the centre of gravity to get the aircraft statically stable. In general, the centre of gravity is placed by moving the water tanks, fuel tanks and equipment forwards and backwards, whereas the neutral point is shifted by using sweep angles of the outboard wing to control the neutral point position. The neutral point is found to be located at $8.55m$ measured from the nose. With the cg-range explained in Section 9.1.1, C_{m_α} is found to be -0.29 for the most forward, and -0.045 for the most aft cg-location. The C_{m_α} being negative means that the aircraft is statically stable. Note that C_{m_α} is more negative for the most forward cg-location meaning that the aircraft is most stable under that condition.

9.2.2. Elevator trim curve

The elevator trim curve shows the required elevator deflection for static flight as a function of the angle of attack. With this curve, one can determine whether the required deflections to fly at a certain angle of attack are acceptable. It also provides insight on how easy the aircraft is to control. This is done since large elevator deflections produce rather much trim drag, and should therefore be avoided if possible. Large elevator deflections also require a larger actuator force, meaning that more actuators are required, making the control system heavier. The elevator trim curve is presented in Figure 9.10. It represents two cases: The case of the most forward cg-position and the most aft cg-position.

One thing that immediately catches attention is the fact that both curves are non-linear. This is not surprising, since a changed elevator deflection also brings a change in the shape of the lifting body. Another observation made is that the elevator deflections required for static flight are larger for the most forward cg-position and smaller for most aft cg-position. This difference is caused by the fact that the most forward cg-position is located further away from the neutral point of the aircraft. This means that the elevator has to balance out a larger moment caused by the centre of gravity. For angles of attack above $9.3°$, the required deflection angle becomes positive. This is caused by the effect shown in Figure 9.11. Here, the aircraft's mass produces a negative moment around the neutral point, rather than a positive moment. This means that the elevators must counter that moment with a positive elevator deflection. The impact of this shift in elevator deflections is not known as of now. Due to the fact that in body reference, C_{m_α} is still negative, the aircraft is still statically stable, however is would be rather confusing for pilots to push on the controls to keep the nose up. Especially, since the aircraft will be flying in this regime during the dropping phase where the aircraft flies at low altitudes, and the margin for errors is rather small. This can be countered by either moving the centre of gravity further forward, switching to a fully automated control system or by very good pilot training. The two latter options being rather expensive and therefore undesirable. Therefore, a revision of the aircraft lay-out is required in later design stages.

To conclude, Figure 9.10 shows that for trimmed flight, the required elevator deflection is between $(-)2.1° - (-)0.4°$ for cruise and $(-)7.66° - (+)1.09°$ for dropping, depending on the cg-location of the aircraft. These deflection angles will be revised in Section 9.4.

9.2.3. Control Forces

In this section, the forces required to operate the controls is elaborated upon. This is done by constructing a control force curve shown in Figure 9.12 and Figure 9.13 for both the cruise and dropping condition. The aerodynamic forces on the controls are measured by keeping the aircraft at a constant angle of attack of $0°$ and varying the control surface deflection between $(-)25° - (+)25°$. This yields a a pressure coefficient difference over the surface of the controls. By taking the average pressure coefficient over the control surface, multiplying it with the dynamic pressure ($\frac{1}{2}\rho V_0^2$) and the area of the control surface, the aerodynamic force on the control surface is computed. The areas of the control surfaces are $3.75m^2$, $1.59m^2$, $1.03m^2$ and $3.06m^2$ for the inboard elevator, outboard elevator, aileron and rudder respectively.

In Figure 9.12 and Figure 9.13, the aerodynamic force on both the outboard and the inboard elevators, the ailerons and rudder during cruise is shown. Given that under the cruise condition, the aircraft flies roughly twice as fast under this condition than the dropping phase, the required forces on the control surfaces are roughly four times as large due

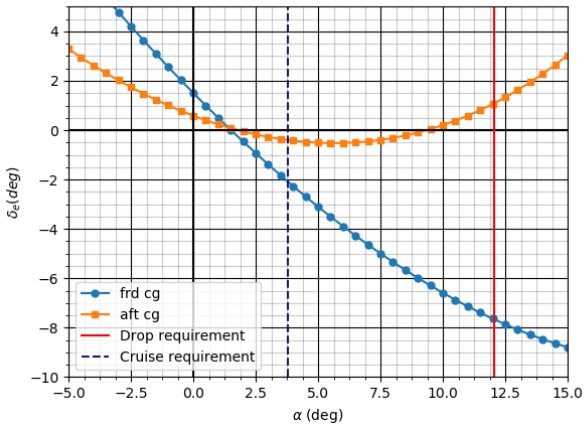

Figure 9.10: Elevator trim curve for most forward (frd) and most aft cg-position. The required angles of attack required for the cruise and drop phase are also marked.

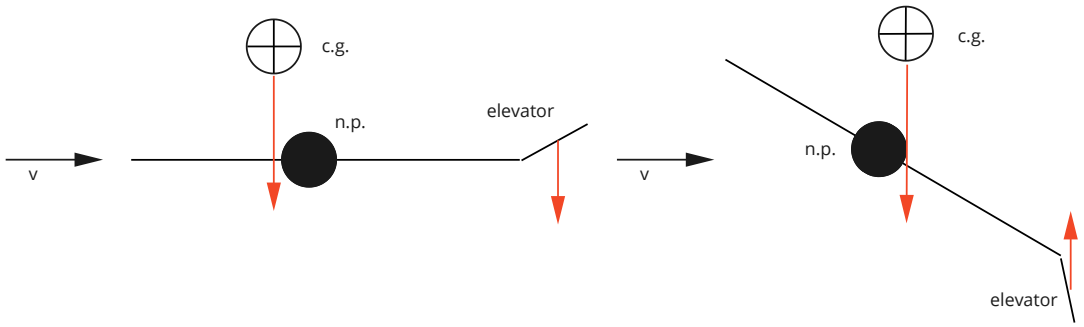

Figure 9.11: Diagram showing effect of high angles of attack on the required elevator deflection.

to the fact that the dynamic pressure scales with velocity squared.
Additionally, it can be observed that the forces on the outboard elevator are much smaller than those on the inboard elevator. This makes sense, considering that the inboard elevator is located on the centre section of the aircraft that produces the most lift. This means that the pressure gradient is highest on that elevator. These two figures will be used to estimate the amount of actuators required for the control surfaces in Section 9.4.

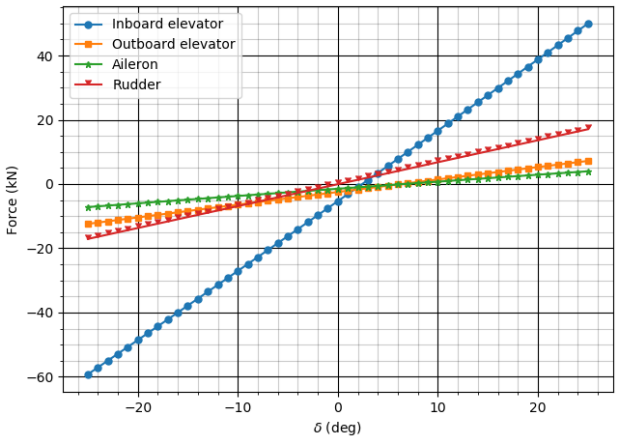

Figure 9.12: Aerodynamic force on inboard elevator, outboard elevator, ailerons and rudder, given a deflection angle δ at an angle of attack of 0° in cruise condition.

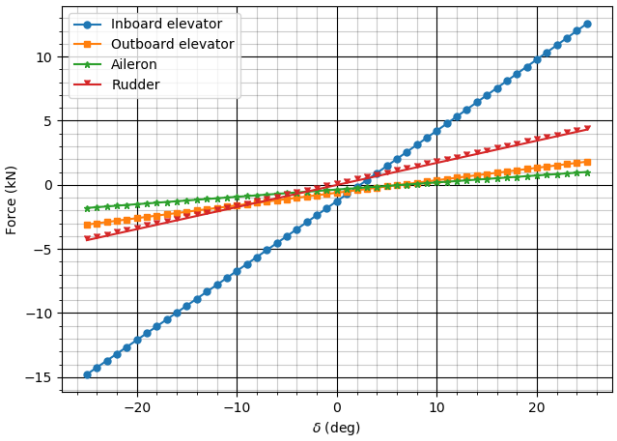

Figure 9.13: Aerodynamic force on inboard elevator, outboard elevator, ailerons and rudder, given a deflection angle δ at an angle of attack of 0° in dropping condition.

9.3. Dynamic Stability

Dynamic stability concerns itself with the eigenmotions of the aircraft. Also, it is important to realise that, although an aircraft is statically stable, the aircraft can be dynamically unstable. Therefore, an analysis is performed on the

dynamic stability of the aircraft. This is done by first showing the equations of motions used for this analysis described in Section 9.3.1. Then, a state-space system is constructed using those equations of motion. This is discussed in Section 9.3.2. After that follows a short explanation on the use of full state feedback to make the aircraft respond as intended in Section 9.3.4. After that, the dynamic response of the aircraft for different situation will be discussed is Section 9.3.3. Note that in this stage of the design, only two situations are assessed. These are the cruising and the dropping phase. Other flight phases shall be investigated in a later stage of the design.

9.3.1. Equations of Motion Steady Straight Symmetric Flight

In order to assess the dynamic stability of the aircraft, equations are necessary to evaluate the forces and moments created by the aircraft and the aerodynamic effects. For this, the equations of motion for steady straight symmetric flight shown in Equation (9.7) and Equation (9.8) are used. These are taken from the Flight Dynamics Course reader [59]. Note that there are two sets of equations. Equation (9.7) shows the aircraft's symmetric response, whereas Equation (9.8) shows the aircraft's asymmetric response. Note that since the aircraft's response is split up into symmetric and asymmetric responses, no coupling is simulated. In reality, this does take place which means that this needs to be assessed in a later design stage. The equations of motions have the following assumptions:

1. The vehicle is a rigid body.
2. The vehicle's mass is constant.
3. The earth is non-rotating.
4. The earth is flat, curvature not taken into account.
5. The earth has a constant gravity field.
6. The aircraft has a symmetry axis.
7. The effect of rotating masses is neglected.
8. The resultant thrust vector acts through the symmetry line and only affects the aerodynamic forces in X- and Z-direction and the aerodynamic moment M.
9. Gliding flight. The forces and moments caused by the engines are neglected.

The following should be noted about assumption 2: The mass of the system can only be assumed constant for short period simulations (in the order of minutes). Furthermore, when dropping water, the mass of the aircraft changes significantly over a very short period. Therefore, these equations are not suited for the bombing phase of the mission. Therefore, the effect of bombing is simulated by assessing the aircraft's response just after dumping the water as explained down below. The equations of motion are useful for the analysis of the cruise phase of the mission, in which the mass of the aircraft does not change very quickly. Also, assumption 9 implies that the effect of the engines is not taken into account in these equations of motion. Due to the engines being on top of the fuselage, and therefore being placed rather far away from the centre of gravity, the moments created by the engines should be investigated at a later design phase.

$$\begin{bmatrix} C_{X_u}-2\mu_c D_c & C_{X_\alpha} & C_{Z_0} & C_{X_q} \\ C_{Z_u} & C_{Z_\alpha}+\left(C_{Z_{\dot\alpha}}-2\mu_c\right)D_c & -C_{X_0} & C_{Z_q}+2\mu_c \\ 0 & 0 & -D_c & 1 \\ C_{m_u} & C_{m_\alpha}+C_{m_{\dot\alpha}}D_c & 0 & C_{m_q}-2\mu_c K_Y^2 D_c \end{bmatrix} \begin{bmatrix} \frac{u}{V} \\ \alpha \\ \theta \\ \frac{q\bar{c}}{V} \end{bmatrix} = \begin{bmatrix} -C_{X_{\delta_e}} \\ -C_{Z_{\delta_e}} \\ 0 \\ -C_{m_{\delta_e}} \end{bmatrix} \begin{bmatrix} \delta_e \end{bmatrix} \tag{9.7}$$

$$\begin{bmatrix} C_{Y_\beta}+\left(C_{Y_{\dot\beta}}-2\mu_b\right)D_b & C_L & C_{Y_p} & C_{Y_r}-4\mu_b \\ 0 & -\frac{1}{2}D_b & 1 & 0 \\ C_{\ell_\beta} & 0 & C_{\ell_p}-4\mu_b K_X^2 D_b & C_{\ell_r}+4\mu_b K_{XZ} D_b \\ C_{n_\beta}+C_{n_{\dot\beta}}D_b & 0 & C_{n_p}+4\mu_b K_{XZ} D_b & C_{n_r}-4\mu_b K_Z^2 D_b \end{bmatrix} \begin{bmatrix} \beta \\ \varphi \\ \frac{pb}{2V} \\ \frac{rb}{2V} \end{bmatrix} = \begin{bmatrix} -C_{Y_{\delta_a}} & -C_{Y_{\delta_r}} \\ 0 & 0 \\ -C_{\ell_{\delta_a}} & -C_{\ell_{\delta_r}} \\ -C_{n_{\delta_a}} & -C_{n_{\delta_r}} \end{bmatrix} \begin{bmatrix} \delta_a \\ \delta_r \end{bmatrix} \tag{9.8}$$

Simulation water bombing phase

Due to the fact that the mass is changing quickly during water bombing, assumption 2 is not valid, and the change in mass must be incorporated. For simulating the dropping of water, additional assumptions are made:

- The dropping of water happens instantaneous.
- The wings of the aircraft are level. This means that the load created by the dropping of water only acts through the symmetry line of the aircraft.

These assumptions have as effect that the mass change happens in an instant. This also means that the cg-position changes in an instant, changing the stability coefficients. To simulate the response of the aircraft during this event, the stability coefficients will be taken from the aircraft without payload (directly after dropping) and an acceleration upwards in earth-fixed reference frame will be added as an impulse input. The value of this acceleration is given by Equation (9.9) with M_1 being the mass before dropping, M_2 the mass after dropping and g the gravitational acceleration. The effect of this acceleration on the velocity components is shown in Equation (9.10) and Equation (9.11) and is dependent on the initial pitch angle θ.

$$a = \frac{M_1 - M_2}{M_2} g \tag{9.9}$$

$$\dot{u} = a\sin(\theta) \tag{9.10}$$

$$\dot{w} = a\cos(\theta) \tag{9.11}$$

It should also be noted that the angle of attack α is equal to $\frac{w}{V}$, and therefore:

$$\dot{\alpha} = \frac{\dot{w}}{V} \tag{9.12}$$

With $\dot{u}$ and $\dot{\alpha}$ being the derivatives of the states in the state space system presented in Section 9.3.2.

9.3.2. State-Space Representation

Analysing the response of the aircraft given a disturbance is done by converting the equations of motion into a state-space system. This system is able to compute the new state of the aircraft, given an old state and an input. In this case, the elevator is the input for the symmetric motion, and the ailerons and rudder the inputs for the asymmetric motion. In general, a state space system has the form shown in Equation (9.13). With $\bar{x}$ being the state vector, $\bar{u}$ the input vector and $\bar{y}$ the output vector. Matrices A,B,C and D are the state matrix, input matrix, output matrix and feedtrough matrix of the system respectively. For this simulation, however, the output matrix is set to the identity matrix, and the feedtrough matrix is set to a zero matrix. This is done, since the output of the state space system is the new state of the system.

$$\begin{aligned} \dot{\bar{x}} &= \bar{A}\bar{x} + \bar{B}\bar{u} \\ \bar{y} &= \bar{C}\bar{x} + \bar{D}\bar{u} \end{aligned} \tag{9.13}$$

Converting Equation (9.7) and Equation (9.8) to state space is shown in Equation (9.15) and Equation (9.16)[59]. Here, the system has the form shown in Equation (9.14), meaning that matrices A and B are equal to $C_1^{-1} \cdot C_2$ and $C_1^{-1} \cdot C_3$ respectively.

$$\begin{aligned} C_1\dot{\bar{x}} &= C_2\bar{x} + C_3\bar{u} \\ \bar{y} &= \bar{C}\bar{x} + \bar{D}\bar{u} \end{aligned} \tag{9.14}$$

$$\begin{bmatrix} 2\mu_c\frac{\bar{c}}{V^2} & 0 & 0 & 0 \\ 0 & \left(2\mu_c - C_{Z_{\dot{\alpha}}}\right)\frac{\bar{c}}{V} & 0 & 0 \\ 0 & 0 & \frac{\bar{c}}{V} & 0 \\ 0 & -C_{m_{\dot{\alpha}}}\frac{\bar{c}}{V} & 0 & 2\mu_c K_Y^2\frac{\bar{c}^2}{V^2} \end{bmatrix} \begin{bmatrix} \dot{u} \\ \dot{\alpha} \\ \dot{\theta} \\ \dot{q} \end{bmatrix} = \begin{bmatrix} \frac{C_{X_u}}{V} & C_{X_\alpha} & C_{Z_0} & \frac{C_{X_q}c}{V_s} \\ \frac{C_{Z_u}}{V} & C_{Z_\alpha} & -C_{X_0} & \frac{\left(C_{Z_q}+2\mu_c\right)\bar{c}}{V} \\ 0 & 0 & 0 & \frac{c}{V} \\ \frac{C_{m_u}}{V} & C_{m_\alpha} & 0 & \frac{C_{m_q}\bar{c}}{V} \end{bmatrix} \begin{bmatrix} u \\ \alpha \\ \theta \\ q \end{bmatrix} + \begin{bmatrix} C_{X_{\delta_e}} \\ C_{Z_{\delta_e}} \\ 0 \\ C_{m_{\delta e}} \end{bmatrix} \delta_e \tag{9.15}$$

$$\begin{bmatrix} \left(C_{Y_{\dot{\beta}}}-2\mu_b\right)\frac{b}{V} & 0 & 0 & 0 \\ 0 & -\frac{1}{2}\frac{b}{V} & 0 & 0 \\ 0 & 0 & -2\mu_b K_X^2\frac{b^2}{V^2} & 2\mu_b K_{XZ}^2\frac{b^2}{V^2} \\ C_{n_{\dot{\beta}}}\frac{b}{V} & 0 & 2\mu_b K_{XZ}^2\frac{b^2}{V^2} & -2\mu_b K_Z^2\frac{b^2}{V^2} \end{bmatrix} \begin{bmatrix} \dot{\beta} \\ \dot{\varphi} \\ \dot{p} \\ \dot{r} \end{bmatrix} = \begin{bmatrix} -C_{Y_\beta} & -C_L & -C_{Y_p}\frac{b}{2V} & -\left(C_{Y_r}-4\mu_b\right)\frac{b}{2V} \\ 0 & 0 & -\frac{b}{2V} & 0 \\ -C_{\ell_\beta} & 0 & -C_{\ell_p}\frac{b}{2V} & -C_{\ell_r}\frac{b}{2V} \\ -C_{n_\beta} & 0 & -C_{n_p}\frac{b}{2V} & -C_{n_r}\frac{b}{2V} \end{bmatrix} \begin{bmatrix} \beta \\ \varphi \\ p \\ r \end{bmatrix} + \begin{bmatrix} -C_{y_{\delta a}} & -C_{y_{\delta_r}} \\ 0 & 0 \\ -C_{\ell_{\delta a}} & -C_{\ell_{\delta_r}} \\ -C_{n_{\delta_a}} & -C_{n_{\delta_r}} \end{bmatrix} \begin{bmatrix} \delta_a \\ \delta_r \end{bmatrix} \tag{9.16}$$

The Stability coefficients in Equation (9.15) and Equation (9.16) are found using AVL and presented in Appendix C. Assessing the poles, or eigenvalues, of the system it is possible to deduce whether the system is stable or not. These poles are either real or complex. Real poles, only have a damping (if negative) or resonance (if positive) effect, whereas a complex poles also have an oscillatory effect. Furthermore, a system can only be stable if all poles have a negative real component. The poles to the aircraft's system in steady, straight and symmetric flight are shown in Table 9.2 and Table 9.3. From this table, one can see that the system is dynamically unstable for symmetric motion under cruise condition, and completely unstable for both symmetric and asymmetric flight during the dropping phase. This instability is caused by the poles with a positive real component present in those flight conditions. This will be further discussed in Section 9.3.3.

Table 9.2: The poles of the MANTÆ aircraft in cruise condition at a velocity of $130 m/s$ and at an altitude of $2,000 m$.

Poles cruise	Real part	Complex part
Symmetric	(-)39.72	-
	(-)0.38	-
	(+)0.13	-
	(-)1.69	-
Asymmetric	(-)2.22	-
	(-)0.02	(+)1.18j
	(-)0.02	(-)1.18j
	(-)0.0015	-

Table 9.3: The poles of the MANTÆ aircraft in dropping condition at a velocity of $60 m/s$ and at sea level.

Poles dropping	Real part	Complex part
Symmetric	(-)19.28	-
	(-)0.03	(+)0.16j
	(-)0.03	(-)0.16j
	(+)0.48	-
Asymmetric	(-)1.82	-
	(+)0.008	(+)0.90j
	(+)0.008	(-)0.90j
	(+)0.001	-

9.3.3. Dynamic Response

In this section, the dynamic response of the aircraft will be analysed given a disturbance to its initial condition. These disturbances will typically be gusts, which could come from any direction. For simulation, two types of gusts are applied to the symmetric system: One coming from the front increasing the velocity and one coming from below creating an updraft, increasing the angle of attack. Updrafts are especially interesting during the dropping phase of the aircraft, since it will be flying over rather turbulent rising air when flying over fires. For the asymmetric system, only one type of gust from the side is applied creating a side-slip angle. Due to the altitude difference between cruise and dropping, different gust speeds need to be taken into account. For cruise, a gust speed of $66 fps$ is taken and for dropping a gust speed of $25 fps$ [10].
Simulation of disturbances is done by using an initial response of the aircraft given a disturbance vector $X0$ as shown in Equation (9.17) where Δu is the gust speed if it is a head gust, $\Delta\alpha$ is $\frac{V_{gust}}{V_0}$ if it is a gust upwards and $\Delta\beta$ is $\frac{V_{gust}}{V_0}$ if it is a side gust. V_0 is the speed at which the aircraft flies and is equal to $130 m/s$ in cruise and $60 m/s$ during dropping.

$$X0 = \begin{bmatrix} \Delta u \\ 0 \\ 0 \\ 0 \end{bmatrix} or \begin{bmatrix} 0 \\ \Delta\alpha \\ 0 \\ 0 \end{bmatrix} or \begin{bmatrix} \Delta\beta \\ 0 \\ 0 \\ 0 \end{bmatrix} \tag{9.17}$$

If the aircraft is in the dropping phase, an extra column is added to the input matrix B. In this column, the accelerations explained in Section 9.3.1 are placed. Simulation is then done by simulating a forced response and having the input vector u equal to a zero vector with two rows, with a 1 in the second row, first column to simulate an impulse acceleration. The disturbance vector $X0$ remains unchanged.
The system's response to those gusts is shown in Figure 9.14 - Figure 9.19. Note that there is only one stable condition, shown in Figure 9.18. This is also visible from Table 9.2, where the asymmetric poles all have negative real components. Furthermore, note that the aircraft's response to disturbances is very aggressive. Either by quick divergence due to the unstable nature of the aircraft, or by having a very short period if the motion is oscillatory, or a combination of those. Especially the dropping condition is very unstable. The aggressive response of the aircraft is corrected by implementing a fly-by-wire system having a feedback loop with a certain gain. This will be explained in Section 9.3.4.

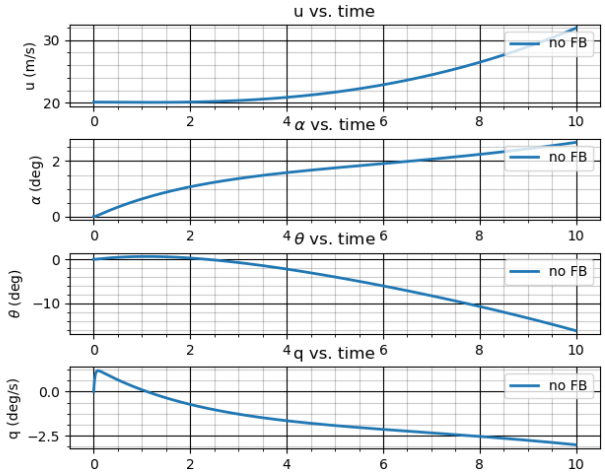

Figure 9.14: Aircraft's response to a head gust in cruise condition.

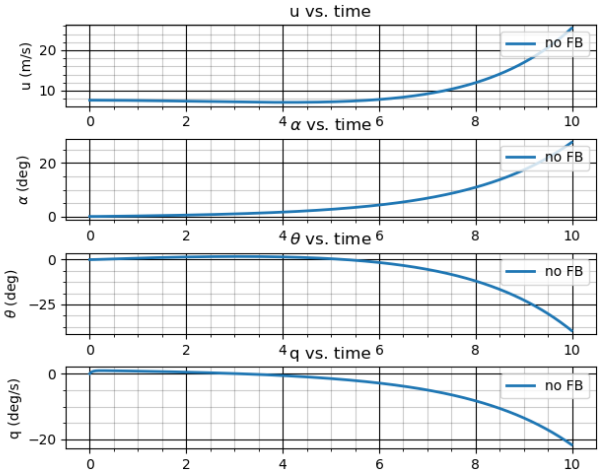

Figure 9.15: Aircraft's response to a head gust in dropping condition.

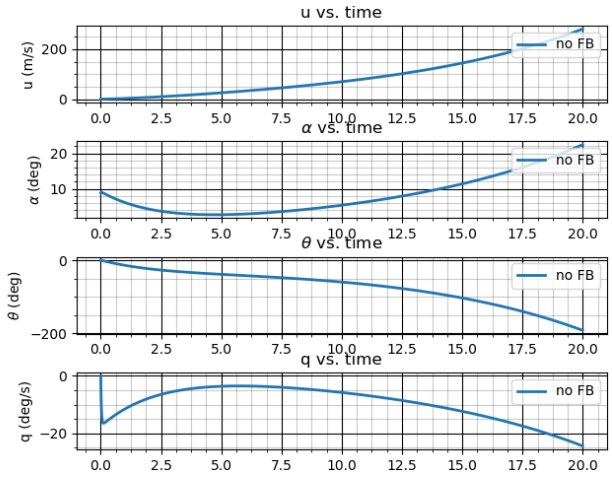

Figure 9.16: Aircraft's response to an updraft in cruise condition.

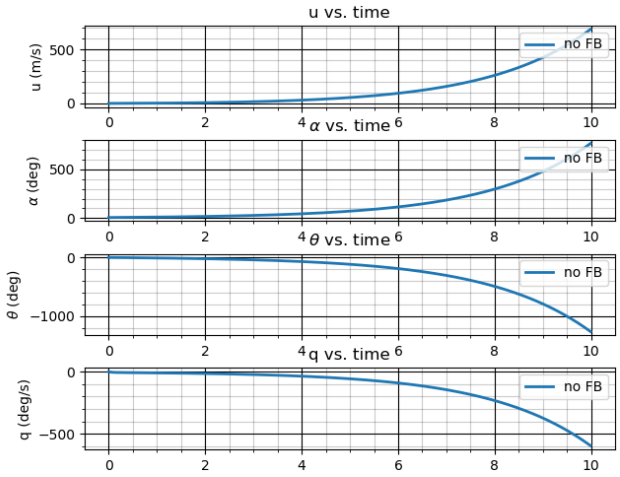

Figure 9.17: Aircraft's response to an updraft in dropping condition.

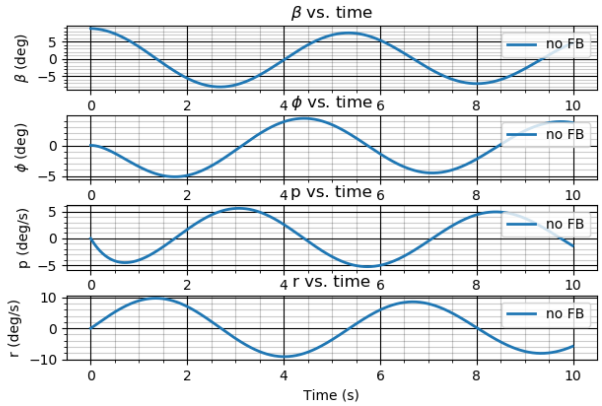

Figure 9.18: aircraft's response to a side gust in cruise condition

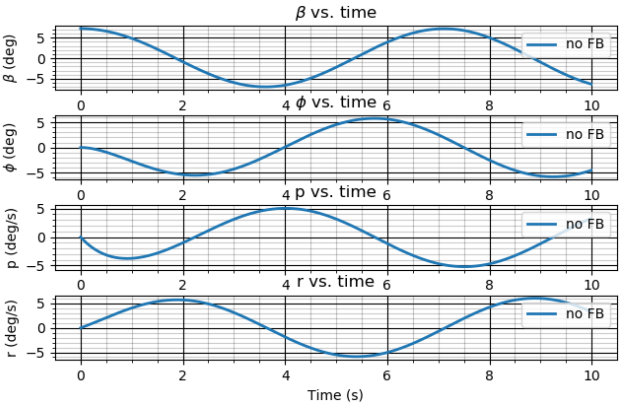

Figure 9.19: aircraft's response to a side gust in dropping condition

9.3.4. Full State Feedback

From Section 9.3.3, it is clear that the aircraft is dynamically unstable and that the aircraft's motion is very aggressive. Countering this can be done by implementing a feedback loop shown in Figure 9.20. This feedback loop takes the current state of the system, multiplies it with a certain gain matrix K, and uses that as an input vector in the system. This simulates the control surfaces on the aircraft deflecting to counter the motion of the aircraft caused by the disturbance.

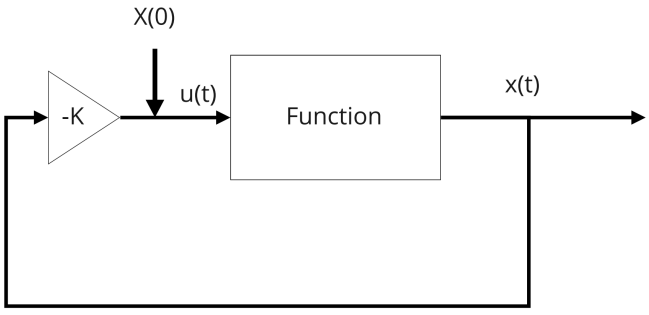

Figure 9.20: Block diagram showing the addition of a feedback loop.

From Figure 9.20, one can gather that:

$$\bar{u}(t) = -K\bar{x}(t) \tag{9.18}$$

This means that:

$$\dot{\bar{x}} = A\bar{x}(t) + B\bar{u}(t) = [A - BK]\,\bar{x}(t) = A_{CL}\bar{x}(t) \tag{9.19}$$

From this, one could see that the derivative of the state, is purely a function of the current state, if the gain matrix K is known. The poles of the A_{CL} matrix are dependent on the the gain matrix K . Therefore, one could choose a set of

poles for the system, which would then determine the gain matrix K. A full explanation can be found in reference [60]. Using the method of full state feedback, the poles of the system can be chosen to have the exact desired response of the aircraft.
The new poles for the system are presented in Table 9.4 and Table 9.5. The gain matrices are shown in Equation (9.20) - Equation (9.23). Note that all poles now have a negative real part. This means that the aircraft with feedback loop is dynamically stable. The new response of the aircraft as well as the response without feedback given a disturbance is shown in Figure 9.21 - Figure 9.26. Furthermore, the required control surface deflections are presented. δ_e being the required elevator deflection, δ_a being the aileron and δ_r the rudder deflection respectively. Judging by the required control surface deflections, the elevator, aileron and rudder require a maximum deflection of $-2.6°$ $-2.6°$ and $-18°$ during cruise and $-32.8°$ $-3.6°$ and $11.2°$ during dropping.

Table 9.4: The poles of the MANTÆ aircraft in cruise condition at a velocity of $130 m/s$ and at an altitude of $2,000 m$ with feedback loop.

	Real component		Complex component	
Poles	Old	New	Old	New
Symmetric	(-)39.72	(-)40	-	-
	(-)0.38	(-)1.6	(+)0.16j	(+)0.2j
	(+)0.13	(-)0.1	(-)0.16j	(-)0.2j
	(-)1.69	(-)0.08	-	-
Asymmetric	(-)2.22	(-)2.3	-	-
	(-)0.02	(-)1.5	(+)1.18j	(+)0.3
	(-)0.02	(-)1.5	(-)1.18j	(-)0.3
	(+)0.0015	(-)0.1	-	-

Table 9.5: The poles of the MANTÆ aircraft in dropping condition at a velocity of $60 m/s$ and at sea level with feedback loop.

	Real component		Complex component	
Poles	Old	New	Old	New
Symmetric	(-)19.27	(-)20	-	-
	(-)0.03	(-)1.3	(+)0.16j	(+)0.2j
	(-)0.03	(-)1.3	(-)0.16j	(-)0.2j
	(+)0.48	(-)1.0	-	-
Asymmetric	(-)1.82	(-)1.9	-	-
	(+)0.008	(-)0.4	(+)0.90j	(+)0.5
	(+)0.008	(-)0.4	(-)0.90j	(-)0.5
	(+)0.001	(-)0.2	-	-

$$K_{symmetric_{cruise}} = \begin{pmatrix} 0.4894583 & 5.46018142 & -3.52132918 & 1.09486089 \end{pmatrix} \tag{9.20}$$

$$K_{asymmetric_{cruise}} = \begin{pmatrix} 0.48392724 & -0.16090772 & 0.06145989 & 0.14853873 \\ -0.52673176 & 0.65273715 & 4.65024002 & -5.44423732 \end{pmatrix} \tag{9.21}$$

$$K_{symmetric_{dropping}} = \begin{pmatrix} 0.4894583 & 5.46018142 & -3.52132918 & 1.09486089 \end{pmatrix} \tag{9.22}$$

$$K_{asymmetric_{dropping}} = \begin{pmatrix} 0.48392724 & -0.16090772 & 0.06145989 & 0.14853873 \\ -0.52673176 & 0.65273715 & 4.65024002 & -5.44423732 \end{pmatrix} \tag{9.23}$$

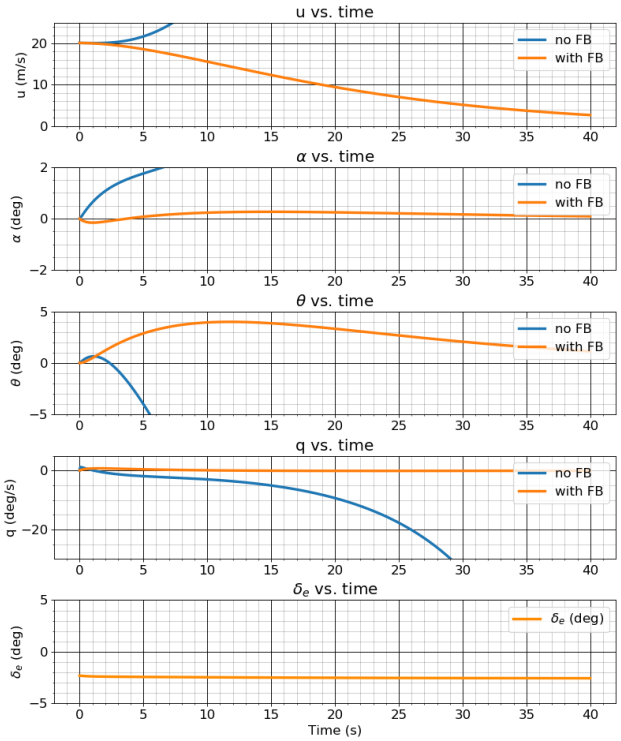

Figure 9.21: Aircraft's response to a head gust in cruise condition with and without feedback loop.

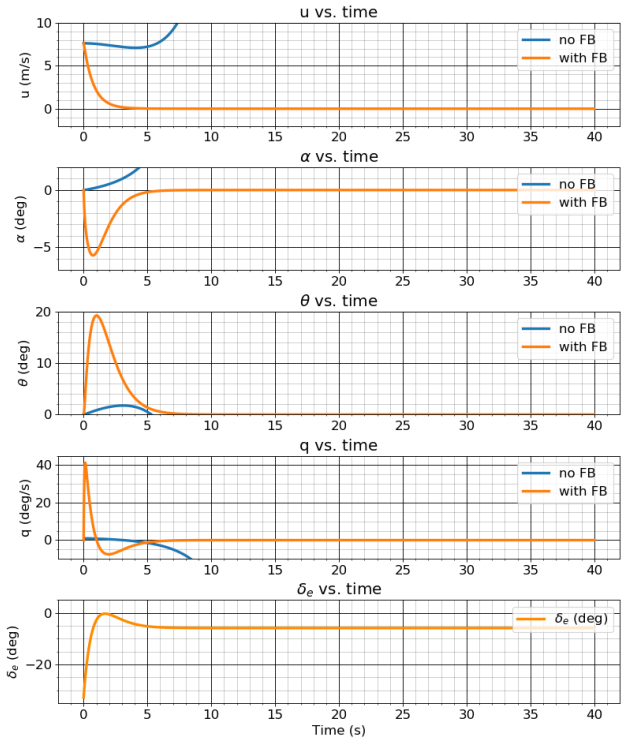

Figure 9.22: Aircraft's response to a head gust in dropping condition with and without feedback loop.

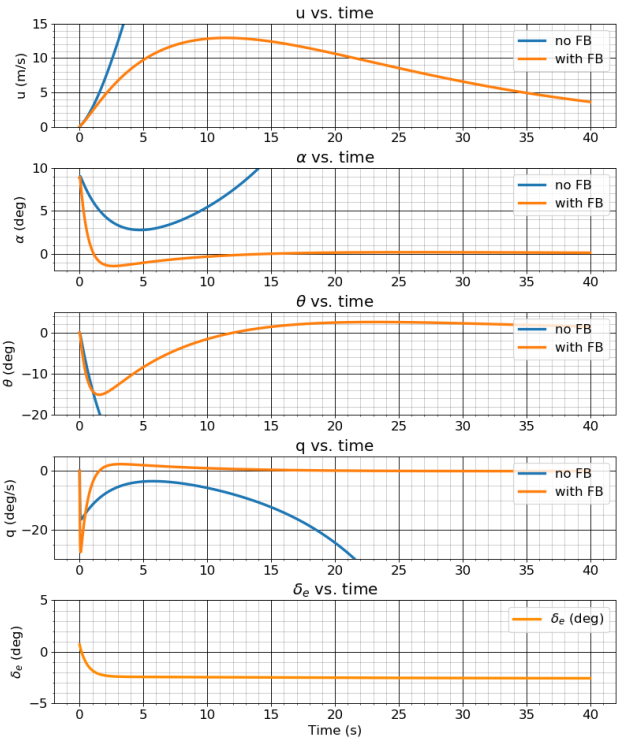

Figure 9.23: Aircraft's response to an updraft in cruise condition with and without feedback loop.

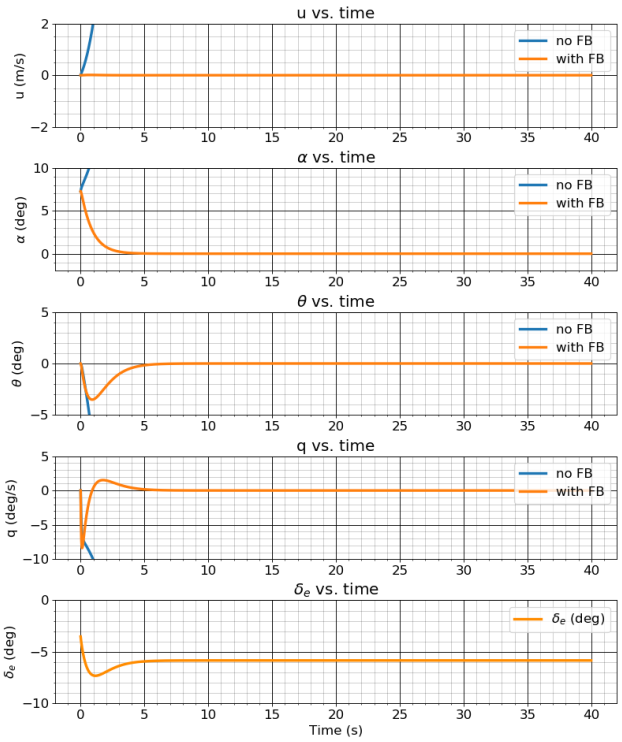

Figure 9.24: Aircraft's response to an updraft in dropping condition with and without feedback loop.

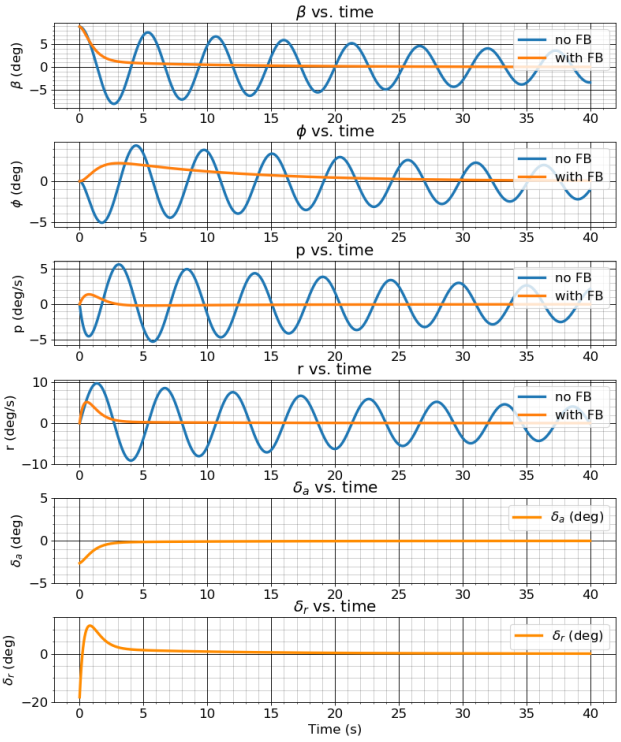

Figure 9.25: Aircraft's response to a side gust in cruise condition with and without feedback loop.

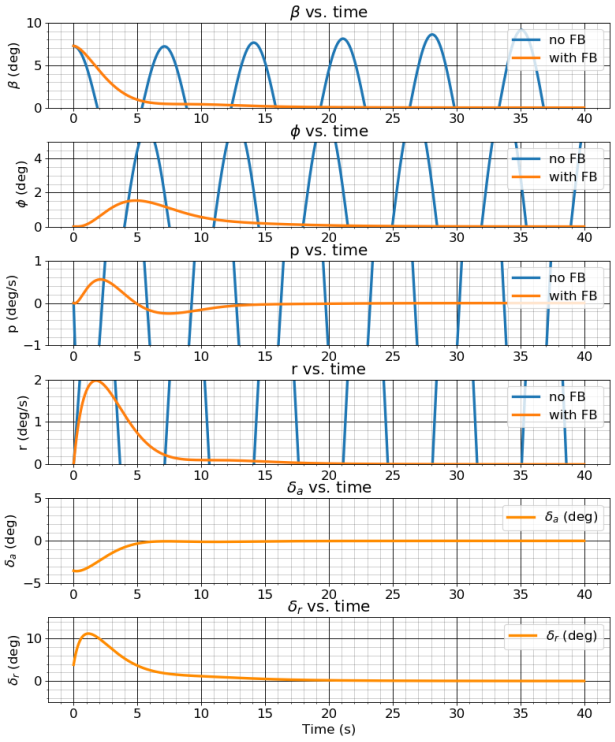

Figure 9.26: Aircraft's response to a side gust in dropping condition with and without feedback loop.

9.4. Actuator sizing

In this section, some preliminary actuator sizing is performed. This is done by combining the observed required controls surface deflection of trimmed flight, the dynamic response to disturbances and the control force curve shown in Section 9.2.3. Recall from Section 9.2.2 that the maximum required elevator deflection for trimmed stationary flight is equal to 2.1° for cruise and 7.66° for dropping. From Section 9.3.4, the maximum deflections performed

by the elevator, aileron and rudder are (−)2.5°, (−)2.5° and (−)17.9° for cruise and (−)32.8°, (−)2.5° and (−)11.2° for dropping respectively. Looking at Figure 9.12, Figure 9.13 and taking the largest required elevator deflections the absolute aerodynamic forces on the control surfaces are equal to $3.46kN$, $10.78kN$, $2.03kN$ and $12.30kN$ for for the outboard elevator, inboard elevator, aileron and rudder in cruise and $4.0kN$, $19.0kN$, $0.57kN$ and $1.94kN$ during dropping. In order to determine the required actuator force, the following assumptions are made:

- The actuator system can be idealised as shown in Figure 9.27.
- The aerodynamic force has a moment arm equal to half the average chord of the control surfaces. For the outboard wing and the vertical stabilisers, this is equal to $79.70cm$, $51.56cm$ and $51.0cm$ respectively. The aerodynamic force on the inboard elevator has a moment arm equal to half the inboard elevator's chord, which is equal to $75cm$. See Section 4.2 for clarification on distances.

With the aforementioned distances, it is possible to obtain the required actuator force on the control surfaces. This is shown in Equation (9.24) where F and L represent the force and the moment arm respectively. The moment arm of the actuators is mainly dependent on the required deflection rates of the elevators. From reference [61], it is found that the required deflection rates of the control surfaces are in the order of 25, 45 and 45 degrees per second for the elevator, aileron and rudder respectively.

To investigate the amount of actuators required, the no-load speed of the MOOG actuator model 974 is chosen [62]. This no-load speed (the maximum deflection speed) is equal to 0.87 inches per second[62]. With this information the required actuator arm can be computed using Equation (9.25), where $V_{no-load}$ is the no-load speed and $\dot{\delta}$ the deflection speed. It is found that the required actuator arm for the elevators, aileron and rudder is equal to 4.7, 2.2 and 2.2 cm respectively. This means that, using Equation (9.24), the required actuator force for the outboard elevator, inboard elevator, aileron and rudder is equal to $67.3kN$, $300.7kN$, $47.4kN$ and $283.9kN$. To find the weight penalty of such actuators, the other actuators on the MOOG fact sheet[62] are used as reference. The statistical relation is presented in Figure 9.28. Note that the statistical relation is rather rough, as the R^2 of the linear approximation is only 0.355. However, a first order estimation on the weight of the actuators can still be made. Assuming that each control surface requires 4 actuators, the outboard elevator, inboard elevator, aileron and rudder require actuators with a force of $16.8kN$, $75.2kN$, 11.85 and $71.0kN$. The statistical relation in Figure 9.28 then yields an actuator weight of $16.6kg$, $14.5kg$, $4.1kg$ and $13.8kg$ per actuator. Taking 1 extra actuator per control surface for redundancy and recalling that the aircraft has two outboard elevators, two ailerons and two rudders, the total weight of the actuators can be estimated to be roughly $245kg$. A summary of the values computed above can be found in Table 9.6.

$$F_{actuator} = \frac{L_{aerodynamic}}{L_{actuator}} F_{aerodynamic} \tag{9.24}$$

$$L_{actuator} = \frac{V_{no-load}}{\dot{\delta}} \tag{9.25}$$

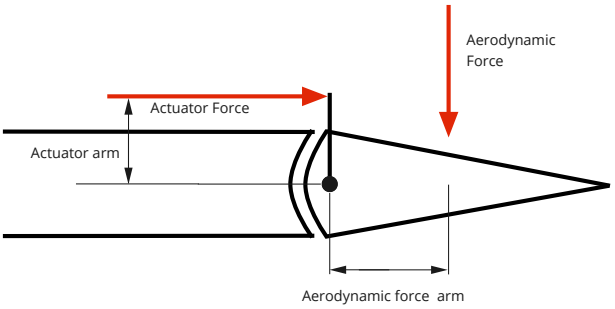

Figure 9.27: Idealised control surface deflection mechanism.

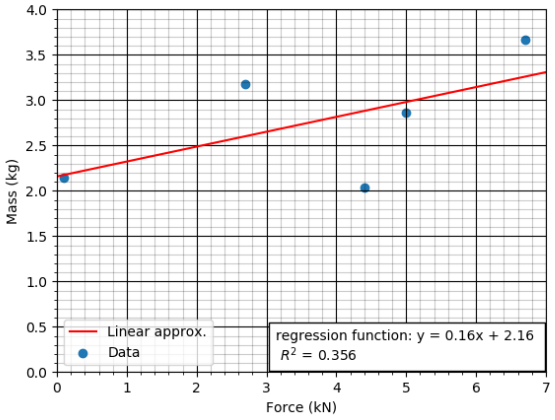

Figure 9.28: Actuator mass as a function of the provided force in kN. The data has been obtained from the MOOG data sheet [62]

. Note that these values assume an actuator no-load speed of 0.87 inches per second.

Table 9.6: Summary of actuator weight estimation. Note that the actuator weight for the control surface takes 1 redundant actuator into account.

	Aerodynamic force (kN)	Aerodynamic arm (cm)	Deflection rate (deg/s)	Actuator arm (cm)	Total actuator force (kN)	Force per actuator (kN)	Weight per actuator (kg)	Actuator weight control surface (kg)
Outboard elevator	4.0	79.7	25	4.7	67.3	16.8	16.6	83.0
Inboard elevator	19.0	75.0	25	4.7	300.7	75.2	14.5	72.5
Aileron	2.0	51.56	45	2.2	47.4	11.85	4.1	20.5
Rudder	12.3	51.0	45	2.2	283.9	71.0	13.8	69.0
Total								245

9.5. Final Remarks

This section is intended to give some remarks regarding the stability analysis. First of all, it is important to realise that this analysis is far from complete. Stability of the aircraft, that is ground stability, static stability and dynamic stability, should be checked at all steps of the design process, which is far from finished. The more detailed the design gets, the clearer the picture becomes regarding stability. The following future recommendations are made:

Ground stability

Regarding ground stability, there are some things that will be designed at a later stage. Especially the landing gear system itself is rather preliminary. A detailed analysis on the landing gear is required to determine the weight, size and cost in a more detailed manner. Also the forces acting on the different components of the system as well as the connections between the aircraft and the landing gear must be further investigated. Finally, a study must be done on how to fold the landing gear inwards and store them. This requires a rather complex system of hinges and actuators which is outside the scope of a design of this scale.

Static and dynamic stability

The lay-out of the cabin and the control surface sizes are not final. In Section 9.2.2, the problems regarding the elevator trim curve are discussed. Large angles of attack require a counter-intuitive input on the flight controls, which could very well lead to dangerous situations. Therefore, the position of the neutral point w.r.t. the aft centre of gravity must be reassessed in a later design phase. From Section 9.4, it became very clear that the aileron could be scaled down, considering the low amount of force it is carrying. Moreover, during the design phase, two particular flight situations are analysed to determine the stability of the aircraft. Of course, there are many situations during a mission that require a detailed investigation. Especially take-off and landing should be a high priority. On top of that, the gains required for dynamic stability are rather preliminary as well. A complete fly-by-wire system is very complex, and would require a lot of testing and certification.

10 Performance

In this chapter, the firefighting performance of the aircraft is evaluated to to determine whether or not the driving requirement of 15000 L/h has been met or not. Additionally, the stall speeds in different aircraft configurations is calculated to determine the skimming speed and drop speed. At this drop speed, the aircraft turn radius and rate of descent are also calculated as these are important indicators of manoeuvrability that have not already been calculated in Chapter 7. This paints a complete picture of the overall performance of the aircraft when fighting fires and can determine which type of terrain the aircraft is able to tackle.

10.1. Water Delivery

In the midterm report, five different mission profiles were outlined, consistent with typical mission scenarios in various parts of the globe. A table summarising these missions is included in Appendix D. For each of these scenarios, the water delivery per hour of operation has been calculated using the mission performance tool mentioned previously in Section 7.6.6. A more in-depth explanation of the tool is given here.

The tool functions by comparing the total fuel carried aboard to the amount of fuel consumed during the mission. For this, the mission time must first be computed. The time taken to complete the mission takes into account the time for the aircraft turnover, refueling, taxiing, acceleration to cruise speed from the runway and climb to cruise altitude. The time to scoop water from a water source and complete n drop manoeuvres is added, as well as the $n-1$ times that the aircraft has to travel in between the fire and the after source to refill the water tanks. Finally, the time taken to cruise back to base and land is also included to complete the calculation.

Next, the fuel used in the mission adds the consumption during each of the phases described for the time calculation, with the addition of fuel used during the engine warm-up procedure. The number of drops n is varied until the fuel used in the mission is slightly below the total fuel carried aboard. For this number of drops, the total water delivery per hour is calculated by multiplying the litres of water in the water tanks by the number of drops, and dividing by the total mission time. The inputs "distance to water" and "distance to the fire" are varied to match each mission profile, and then the number of drops is once again adjusted. The results of the tool are presented in Table 10.1.

Table 10.1: Water delivery per hour of operation for each mission profile and the maximum number of drops that can be made without refueling

Mission Profile	Distance to Fire [km]	Distance to Water [km]	Water Delivery [L/h]	Number of drops
A	100	15	49842	16
B	250	30	31500	10
C	250	45	25523	8
D	350	15	34585	11
E	350	45	21975	8

The values listed above exclude the installation of additional water tanks in the cabin of the aircraft, which was discussed further in Section 8.5.1. Mission A has the higher water delivery performance, as is expected due to the small distances to cover in Southern Europe and North America. Mission B represents the main mission of $250km$ to the base and $30km$ to a water source. The performance to cost ratio of this mission will be evaluated in Section 16.2 to evaluate whether the requirement of performance to cost has been met or not. Mission E has the worst performance due to the large distances that must be covered in Siberia and Africa.

10.2. Speeds

Throughout each mission, the aircraft encounters some critical phases of flight. With these phases come associated speeds. In this section, the stall, skimming and drop speeds will be discussed.

10.2.1. Stall speeds

For the conceptual design tool, the stall speeds in different aircraft configurations had to be estimated in order to generate the power loading and thrust loading diagrams. These estimations were based on statistics of similar aircraft or concepts. During the detailed design phase however, a more accurate weight estimation and wing surface area allows for the stall speeds to be recalculated with greater accuracy. These are calculated as follows [9]:

$$V_s = \sqrt{\frac{W}{S}\frac{2}{\rho}\frac{1}{C_{Lmax}}} \tag{10.1}$$

In this equation, the air density at sea level is used, $\rho = 1.225 kg/m^3$. Additionally, $C_{Lmax} = 0.9$ for the aircraft clean configuration and 1.35 for takeoff and landing configurations, as gathered from AVL analysis and literature-based data on the high lift devices [63] [16]. This yields the following stall speeds:

Table 10.2: Comparison between initial stall speed estimates and recalculated values for different configurations

	Stall Speed		
Configuration	**Initial Assumption [m/s]**	**Recalculated Value [m/s]**	**Discrepancy (%)**
Takeoff	55.00	48.14	14.2
Clean	60.00	58.96	1.77
Landing	55.00	48.14	14.2

The primary explanation for the discrepancy between the initial assumption and recalculated value for takeoff and landing configuration is the addition of belly flaps to the aircraft design, substantially increasing lift at low speeds and reducing stall speeds. The initial design only featured leading edge slats and thus could not achieve a substantial increase in lift with respect to the clean configuration. Furthermore, the discrepancy between the stall speeds in clean configuration stems from two reasons: firstly, the wing surface area is influenced by the constraints of the cabin geometry and consequently the wing is slightly over-sized. In addition, the MTOW has been recalculated using more precise payload and fuel weight estimations as described in Section 4.5.1. These factors also contribute to the discrepancy for the takeoff and landing configurations.

10.2.2. Skimming Speed

While the aircraft is using the scoops to refill the water tanks, the vicinity to the water reduces the size of the wingtip vortices, resulting in a smaller lift-induced drag and greater lift at the same angle of attack. This is known as the ground effect, and can lead to a lower than expected minimum skimming speed.

The formula to calculate the drag coefficient is given in Equation (10.2).

$$C_D = C_{D0} + KC_L^2 \tag{10.2}$$

The coefficient K governing the induced drag term of the equation is given by Equation (10.3).

$$K = \frac{1}{\pi Ae} \tag{10.3}$$

When the aircraft approaches the ground, the downwash gradient is reduced and the value of K changes according to Equation (10.4). [6]

$$\frac{K_{eff}}{K} = \frac{33(h/b)^{1.5}}{1+33(h/b)^{1.5}} \tag{10.4}$$

In this equation, b is the wingspan and h is the height of the wing above the water surface. h can be calculated by considering the average between the height of the fuselage and the height of the wings above the water, both in m. This is a conservative estimate since the fuselage of a BWB produces more lift than the wings, and the fuselage section is closer to the water surface. Taking the average results in a height of $h = 2.50m$. With a wingspan of $b = 33.5m$, the reduction of induced drag is $\frac{K_{eff}}{K} = 0.402$, or 40.2%. During steady, straight symmetric flight, the lift generated equals the weight of the aircraft and consequently, the lift coefficient can be calculated as follows:

$$C_L = \frac{W}{\frac{1}{2}\rho V^2 S} \tag{10.5}$$

Additionally, the value of the induced drag C_{D0} can be found using Equation (10.6). [6]

$$C_{D0} = C_{f_e}\frac{S_{wet}}{S} \tag{10.6}$$

The skin friction drag coefficient C_{f_e} is approximately equal to 0.0065 for propeller seaplanes [6], and the ratio of wetted surface area to wing surface area S_{wet}/S is equivalent to 2 for BWB aircraft. Thus, C_{D0} is equal to 0.013. When belly flaps are deployed, drag increases by approximately 30% as mentioned in Section 6.5, resulting in a C_{D0} of 0.0169.

Using these equations, a reduction in C_D of 31.9% is observed at the beginning of the scooping manoeuvre and this increases to 36.0% by the end of the scooping manoeuvre, once the water tanks are completely filled. Thus, the increase in drag caused by the aircraft contact with water is partially compensated for by the reduced aerodynamic drag, meaning less thrust needs to be applied to maintain a sufficient velocity.

Additionally, the lift rate coefficient $C_{L\alpha}$ increases by approximately 10% when the aircraft is less than 20% of the wingspan from the ground. Hence, at an altitude of less than $6.7m$ from the ground, the combined effects of a lower induced drag and increased lift rate coefficient result in an increase in L/D from 4.81 to 8.90 at the beginning of the scooping manoeuvre and from 6.50 to 10.4 at the end of the manoeuvre.

As a consequence of these effects, the scooping speed can be relatively close to the stall speed without an increased risk of stall. Ground effect increases C_{Lmax} from 1.35 to 1.49, meaning a reduction in the stall speed by 4.65% from $48.1m/s$ to $45.9m/s$. A margin of $1.15V_{stall}$, as used for liftoff speed estimation, results in a minimum skimming speed of $52.7m/s$. This is slightly larger than the value previously assumed in Section 8.5.3, however this should not significantly impact the probe sizing and material selection. In fact, it allows for the water tanks to theoretically be filled in less than 12 seconds, further reducing the distance covered skimming over the water surface.

10.2.3. Drop Speed

The drop speed should be as low as possible to increase the retardant effectiveness, as explained in Chapter 8. However, the drop speed should be sufficiently high to deal with gusts caused by wildfires without a substantial risk of stalling. Looking back at the flight envelope in Figure 4.9, a positive load factor of 2 can be endured without stalling at a speed of $70m/s$, when the HLD are deployed. This also means that the aircraft can withstand vertical gusts of over $15.24m/s$, equivalent to approximately $30kn$. Although gust loads of this magnitude are possible above wildfires, the probability that such a gust acts perfectly vertically on the aircraft is small. Consequently, $70m/s$ is a suitable drop speed for fires causing a substantial amount of strong winds, or in hilly terrain where manoeuvrability is key. Above smaller fires, this drop speed can be reduced to $65m/s$ as this would increase the drop effectiveness. Speeds lower than $65m/s$ result in a substantial increase in risk of stalling the aircraft and give the pilots less freedom for manoeuvrability, and is therefore not advised.

10.3. Manoeuvrability

Although the rate of climb of the aircraft has already been analysed in Chapter 7 in order to size the power plant, the descent rate and turning radius must also be calculated to obtain a sense of the aircraft manoeuvrability. As discussed in Section 7.3.1, a sustained turn of $2g$ was the limiting performance factor in the calculation of required engine power, and thereby the selection of the power plant type. Calculating the turn radius caused by a $2g$ turn can depict the manoeuvrability of the aircraft in hilly terrain. The formula for calculating turn radius in m is given in Equation (10.7) [9].

$$R = \frac{V^2}{g \cdot tan(\phi)} \tag{10.7}$$

In this equation, V is the airspeed in m/s and ϕ is the bank angle. This angle can be calculated using:

$$cos(\phi) = \frac{W}{L} = \frac{1}{n} \tag{10.8}$$

In this equation, W is the weight of the aircraft, L is the lift produced by the aircraft and n is the load factor. For a sustained turn of $2g$, this results in $\phi = 60°$. Assuming the aircraft is flying at the drop speed equal to $70m/s$ when performing the turn, R is equal to $288.5m$. Thus, the aircraft needs a total of $577m$ in width to perform a U turn.

Next, the rate of descent of the aircraft can be calculated at drop speed, to give an indication of the ability of the aircraft to deal with uneven terrain. The rate of descent can be calculating using Equation (10.9).

$$RD = V sin(\gamma) \tag{10.9}$$

In this equation, V is the drop speed and γ is the flight path angle. For standard operations, this angle is limited due to practical reasons: to avoid the water in the water tanks being forced into the overflow vents, the maximum angle γ before performing a drop should be 20°. Using a drop speed of $70m/s$, this results in a rate of descent $RD = 23.94m/s$. This satisfies the performance requirement of at least $20m/s$ at drop speed, as mentioned in Section 7.1. In reality, the pilot could begin the descent manoeuvre with a greater speed in order to achieve a greater rate of descent and then slow down before beginning the water drop. The descent performance of the aircraft is limited by the design dive speed V_d if the aircraft is in clean configuration, or $100m/s$ if the aircraft has HLDs deployed. Thus, once the limit speed is reached, the pilot must pull back on the control stick to reduce airspeed.

Overall, the large aircraft size compared to other firefighting competitors does not reduce manoeuvrability to unacceptable limits. Uneven terrain such as in the Mediterranean can be tackled without the need to deploy smaller aircraft. The aircraft is able to fly through and navigate valleys and make rapid approaches to fires, further contributing to the Project Objective Statement of making the aircraft widely deployable.

11
Communication

The communication during operations of the aircraft is not only between the pilots, but also between the pilots and the air traffic control (ATC) and other aircraft. To provide information to one another, the aircraft needs to be equipped with avionics. These avionics are connected to sensors that output the information to the avionics and then to the pilot. In this chapter, the avionics used for the final design are described in Section 11.1 and the relations between the sensors, avionics and the pilots in Section 11.2.

11.1. Avionics

Aircraft avionics is a collective term for all electrical systems used in the aircraft. The output of the avionics are displayed to the pilot(s) in the cockpit and also provide information to the ATC. This chapter describes the avionics used in the cockpit and for communication with the ATC. The systems are explained in Section 11.1.1, Section 11.1.2, Section 11.1.3, Section 11.1.4, Section 11.1.5 and Section 11.1.6. Due to the time constraint of this project and the lack of experience in aircraft programming regarding avionics of the team, the avionics used are off-the-shelf systems. After researching the avionic systems of several fire fighting aircraft, it is apparent that all aircraft support roughly the same systems (differing in manufacturer). It is taken into account that systems from the same manufacturer often have very good compatibility and therefore most of the avionics are chosen from the same manufacturer.

11.1.1. Voice and data communication

The communication systems in the aircraft can be used for air-to-ground and air-to-air communication. There are two types of systems on board that aid in either voice communication or data communication. There are also visual communication systems, but these are not used for this aircraft.

Voice communication will be used to deliver voice and audio messages to the ATC. The communication system can broadcast messages on ultra high, very high, or high frequencies (UHF/VHF/HF). For the final design, a glass cockpit will be used, that functions as a GPS, navigator and radio.

Data communication will be used to provide the ATC with real-time position parameters, like altitude and heading. Since January 2020, an automatic dependant surveillance-broadcast (ADS-B) system is mandatory in Australia, which is one of the focus regions of this project. Aircraft in Europe will also have to be equipped with an ADS-B from June 7th 2020 onward[1]. This system periodically broadcasts its position tot the ATC via ADS-B 'out' and other aircraft that have an ADS-B 'in' or compatible transponder option. Therefore, the final design is fitted with this system.

11.1.2. Navigation System

The most used navigation systems are GNSS (global navigation satellite system) receivers. There are four main receiver systems: GPS (United States), Galileo (Europe), GlONASS (Russia) and BeiDou (China). The receivers pass information to the pilots regarding the location of the aircraft. The GNSS information is displayed to the pilot via the glass cockpit.

Since this project is developed by students in the Netherlands, the GLONASS and BeiDou receiver options have been ruled out due to incompatibility. While Galileo is the newest and most precise GNSS system, it is not yet fully operational as of right now, so therefore it is chosen to use a GPS receiver for this design. This receiver will be, as mentioned in Section 11.1.1, incorporated in a glass cockpit, with a separate link to an ADS-B system. The combination of the GPS and ADS-B system also provides a flight information service-broadcast (FIS-B), which updates the receiver on the current weather and its changes through weather satellites. The system also has a built-in wide area augmentation system, that augments the GPS. However, this is only possible right now when the aircraft is situated in Northern America.

Another part of navigation is the attitude and heading reference system (AHRS). The AHRS is an inertial measurement unit that provides the aircraft information on the pitch, yaw and roll rates. It consists of gyroscopes, accelerometers and magnetometers. This system is used in every aircraft as an aid for the GPS and is therefor also incorporated in the final design.

[1] `https://www.easa.europa.eu/sites/default/files/dfu/EASA_STC_NEWS_JUNE_2018.pdf` [26-06-2020]

11.1.3. Flight management system
The aircraft is also fitted with a flight management system (FMS). The FMS consists of a flight management computer, an automatic flight guidance system, an electronic flight instruments display and a navigation system consisting of the AHRS and GPS. It's primary function is to guide the aircraft flight plan, but is also able to perform other in-flight tasks that reduce the workload of the pilots. The FMS does not only use the data from the GPS and AHRS, but can also use VHF omnidirectional range (VOR) sensors and distance measuring equipment (DME) to increase the accuracy on its position [64].

11.1.4. Collision Avoidance System
Requirement **FFA-S&R-001** states that the aircraft should be equipped with collision avoidance systems to guaranty flight safety during operations. A collision avoidance system is crucial in aerial operations. There are two types of collision avoidance: mid-air collision avoidance and terrain avoidance. With the introduction of the ADS-B system, most aircraft are able to perceive other aircraft in their surroundings. Even if aircraft are not equipped with an ADS-B system themselves, they can still perceive signals from other aircraft if they have a compatible transponder on board. This decreases the change of having a mid-air collision not only with large airliners, but also with smaller general aviation.

Next to mid-air collision avoidance systems, there are also terrain avoidance and warning systems (TAWS). In case of heavy smoke or thick, low-hanging clouds the pilot might have trouble seeing when flying towards or above a forest fire. There is a built in digital elevation map in the TAWS software, which works with the aircraft's altimeter to determine if the aircraft is too close to the ground. The most recent TAWS is the enhanced ground proximity warning system (EGPWS). Considering a widely deployable fire fighting aircraft will also have to fight fires in mountainous areas, the final design will be fitted with a EGPWS. The EGPWS is compatible with the GPS system in the glass cockpit, to provide a better terrain awareness for the pilot. The TAWS has class A and class B systems. Class A is mandated for an aircraft like the final design. This does require an extra horizontal situation display to be fitted into the instrumentation. With a class A system, the pilots will receive a visual and audio warning if one of the following situations occurs[2]:
- Excessive descend rate
- Excessive terrain closure rate
- Altitude loss after take-off or at a higher power setting
- Flight into terrain when not in landing configuration
- Excessive deviation below glideslope (working with the instrument landing system (ILS))
- Descent below $500\,ft$ above terrain or the nearest runway elevation

To avoid incidents during landing operations, a landing aid is often used to guide the pilots during touchdown. The glass cockpit has a built in landing aid system (ILS), so the final design will be equipped with this. The landing aid system works with a marker beacon (a VHF radio beacon), DME, glideslope and localizer.

11.1.5. Data processing and storage
The air data computer is an indispensable avionic system that is found in all modern aircraft. It is a data processor that calculates the calibrated airspeed, mach number, altitude and altitude trend. The air data computer gathers data from numerous sensors, as explained in Section 11.2. As is common in non-airliner aircraft, two air data computers are used for the data processing in the final design to avoid lags due to insufficient processing speeds.

The communication between the pilot, co-pilot and the ATC, as well as the flight data, is registered in the cockpit voice and data recorder (CVDR). This is a mandatory system for all aircraft that use data link communications. The CVDR works with an emergency locator transmitter, which sends out the location of the aircraft in case of a crash.

11.1.6. Display
All information has to be displayed to the pilot. The glass cockpit incorporates a number of LED displays to output the information gathered by the weather radar, FMS, air data computer, GPS and the collision avoidance systems. The primary flight display shows the basic flight instruments. These include the airspeed-, attitude-, heading- and course deviation indicators and the altimeter. Flight plans can also be entered through this display. Lastly, the primary flight display has a small map displayed in the bottom corner, where traffic information can be seen. There is also a multi-function display, that outputs the engine instrumentation and a moving map. The collision avoidance systems can be accessed through this display as well. Also, the weather information can be view via this display. The buttons next to the displays can be used for the communication transponder. The displays can be set to either the primary flight display or the multi-function display interchangeably. The final design is fitted with one screen directly in front of the pilots and an extra one in the middle so both pilots can view the primary flight display when needed.

[2] `https://skybrary.aero/index.php/Terrain_Avoidance_and_Warning_System_(TAWS)#Information_provided_by_TAWS` [Cited on: 26-06-2020]

11.2. Relations

The input for the avionics comes from a large number of sensors fitted on the inside and outside of the aircraft. Some sensors don't necessarily provide input for the avionics regarding flying, but are used to display other information to the pilot or assist in the external communication. To give a clear overview of the difference between the functions of the sensors and antennas, Section 11.2.1 describes the internal relations and Section 11.2.2 the external relations. Section 11.2.3 regards the software and data handling of the aircraft. Lastly, Section 11.2.4 describes the relation between the electrical systems and their source of power.

11.2.1. Internal communication

The internal aircraft communication comprises of the sensors, antennas, avionics, pilot and subsystems. Table 11.1 provides a overview of the sensors and antennas used as input for the avionics. Since the pitot tube and the angle-of-attack sensors are important inputs for the stability given by the fly-by-wire system, both of them have one extra unit for redundancy and risk reduction after loss of a single unit. This also holds for the fuel level sensors and the force actuator sensors.

Table 11.1: List of internal and external sensors that interact with the avionics, along with their function and the number present

External sensors & antennas	**Function**	**Amount**
Pitot tube	Measure the total and static pressure to provide information on the airspeed, mach number, altitude and altitude trend	4 independent systems
GPS receiver	Gather information on velocity and direction for the flight management system	2
Angle-of-attack sensor	Measure the angle-of-attack of the aircraft	4
VOR antenna	Provide extra information on velocity and direction to the flight management system	2
Internal sensors		
Flow sensors	Measure the flow rate of the fuel and the retardant	4 for the engines, 4 for the retardant tanks
Level sensors	Measure the fuel level	2 per fuel tank
Force & torque sensor	Measure the force applied by the pilot or autopilot on the control surfaces	2 per control surface
Position & displacement sensor	Measure the displacement of the control surfaces	1 per actuator
Proximity sensor	Measure if a metal surface is in proximity	1 for every door, slat, airbrake, landing gear bay and thrust reverser actuator
Temperature sensor	Measure the oil temperature inside the engine	1 per engine

The sensors pass information to the avionics, which in turn provide information to the pilots. The pilots use this information to adjust certain subsystems, after which the input for the sensors changes. An overview of the relation between the hardware components can be seen in Figure 11.1. In this diagram, light blue denotes the sensors and antennas, orange the avionics, magenta the subsystems and green the pilots.

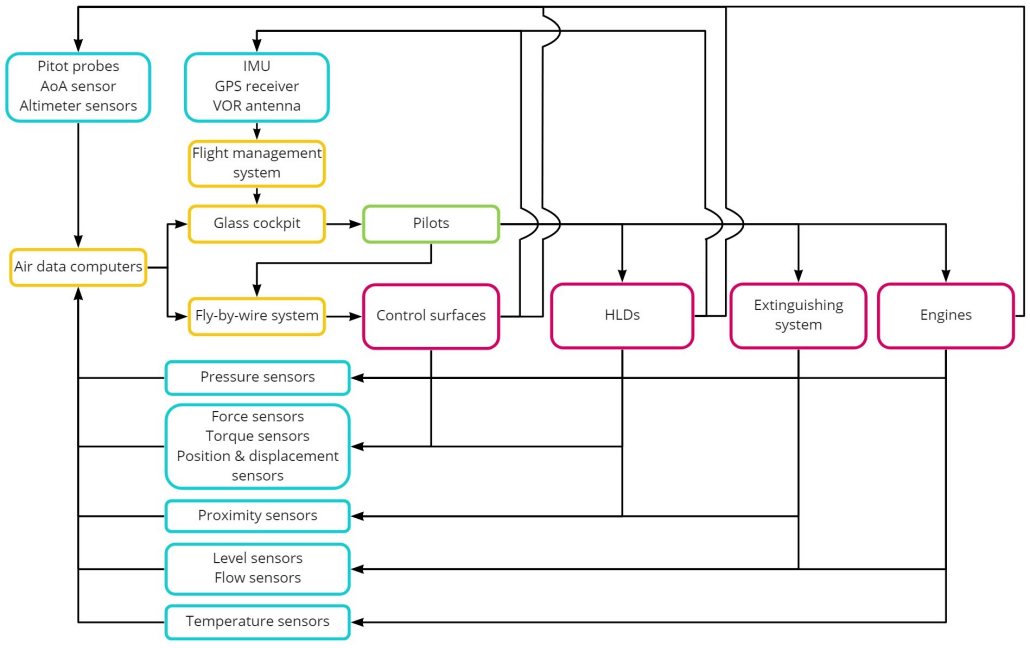

Figure 11.1: The internal hardware and communication diagram

11.2.2. External communication

For a firefighting aircraft, there should be a form of communication between itself and the ATC, ground fire brigade and other aerial fire fighting aircraft. As mentioned in Section 11.1.1, there can be voice and data communication between parties. Since this communication takes place to parties outside of the aircraft, it is called external communication. Table 11.2 shows the transmitters and receivers used for the external communication with again the number and amount.

Table 11.2: Transmitters and receivers used for external communication, including function and amount

Transmitter/receiver	Function	Amount
VHF/HF radio transceiver	Receive and send radio signals for voice communication	4
ADS-B transceiver	Receive and send information regarding aircraft position	1
Marker beacon transmitter	Provide information on position along an established route towards a ground station	1
Distance measuring transponder	Measure the range between the aircraft and the ground station	1
Glideslope transponder	Measure the vertical deviation of the optimal glideslope during approach	1
Localizer transponder	Provide the horizontal location during approach	1
Emergency locator transmitter	Transmit the aircraft's location in case of a crash	1

The communication between the aircraft hardware and relation between the aforementioned parties can be found in Figure 11.2. In this diagram, light blue denotes the transponders, dark blue the external parties, orange the related avionics and green the pilots.

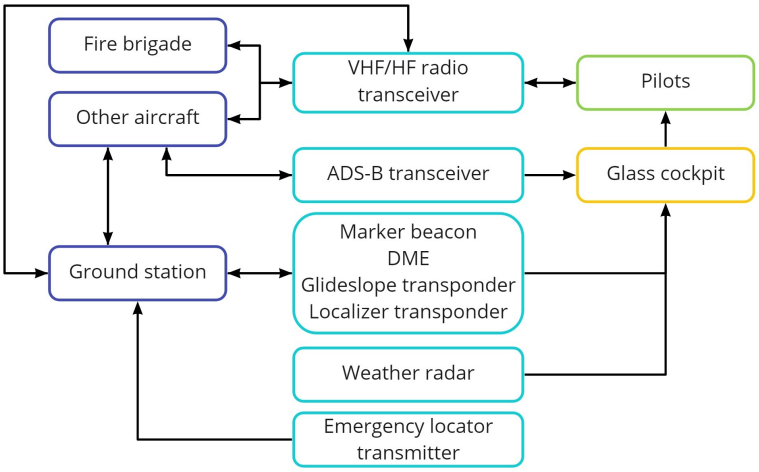

Figure 11.2: The external hardware and communication diagram

11.2.3. Software and data

The relations between the hardware are based on certain software relations. Figure 11.3 shows what parameters certain hardware devices share with one another, to perform continues iterations that provide flight data to increase the situational awareness to the pilot. The software diagram used the same colour scheme as the internal and external hardware diagrams. The data passing through the software is collected and saved in the CVDR. The data handling and subsequent commands are illustrated in Figure 11.4.

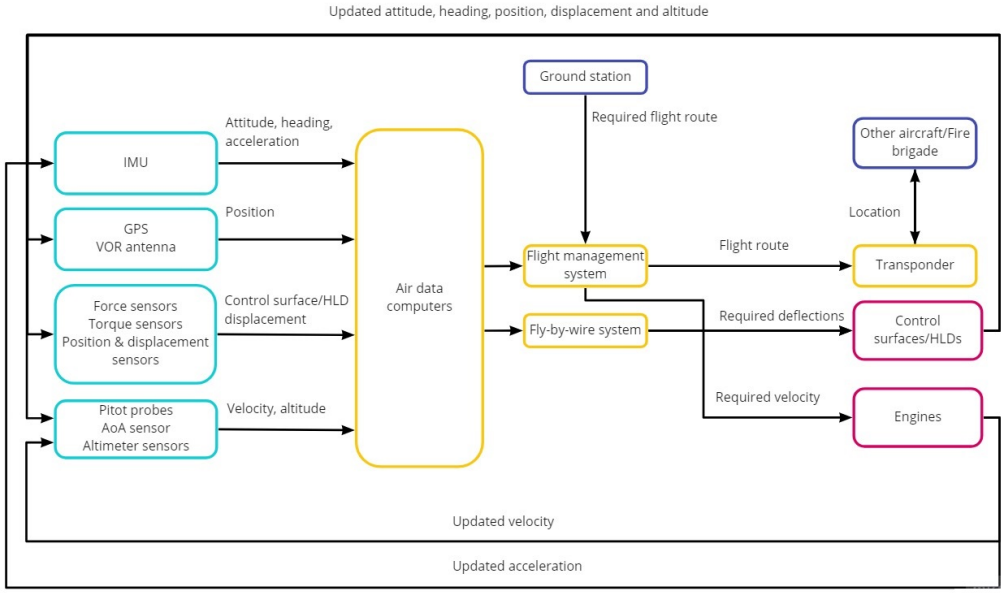

Figure 11.3: The software diagram

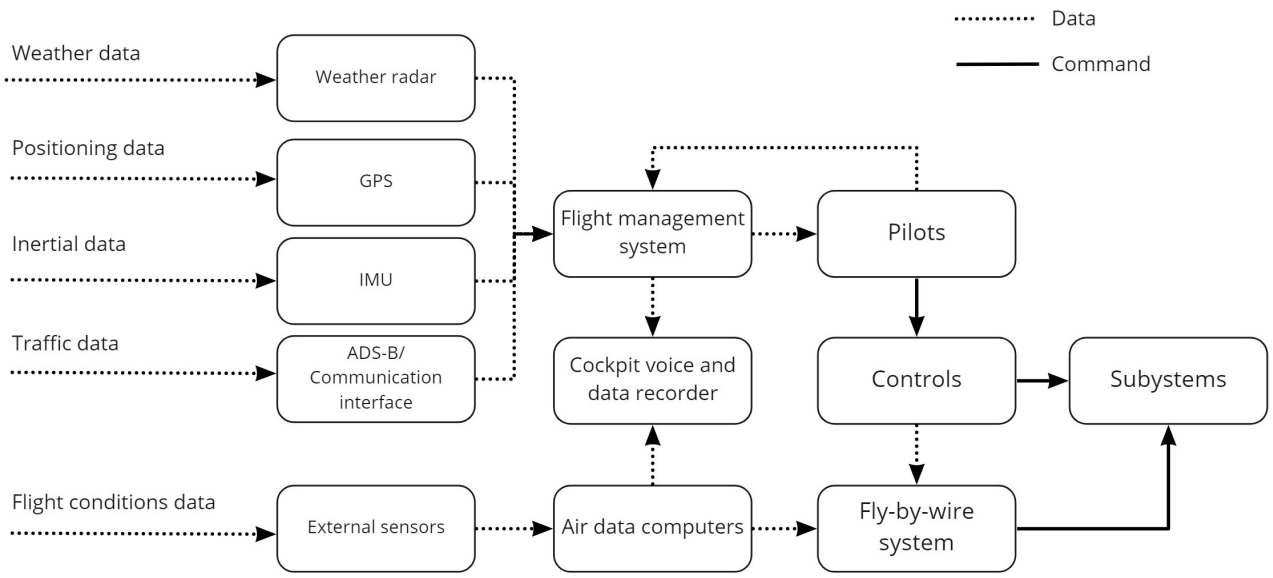

Figure 11.4: Command and data handling block diagram

11.2.4. Electrical configuration

The electric systems in the aircraft are powered by a generator, which gets its power from the engines. The generator powers all the electrical systems through a series of power distribution units. There are two generators in case one fails. Also, the generators are only linked to two engines to decrease the risk of a power deficit when one or more engines fail. Figure 11.5 shows the relations between the engines, generators, power distributors and power receiving systems.

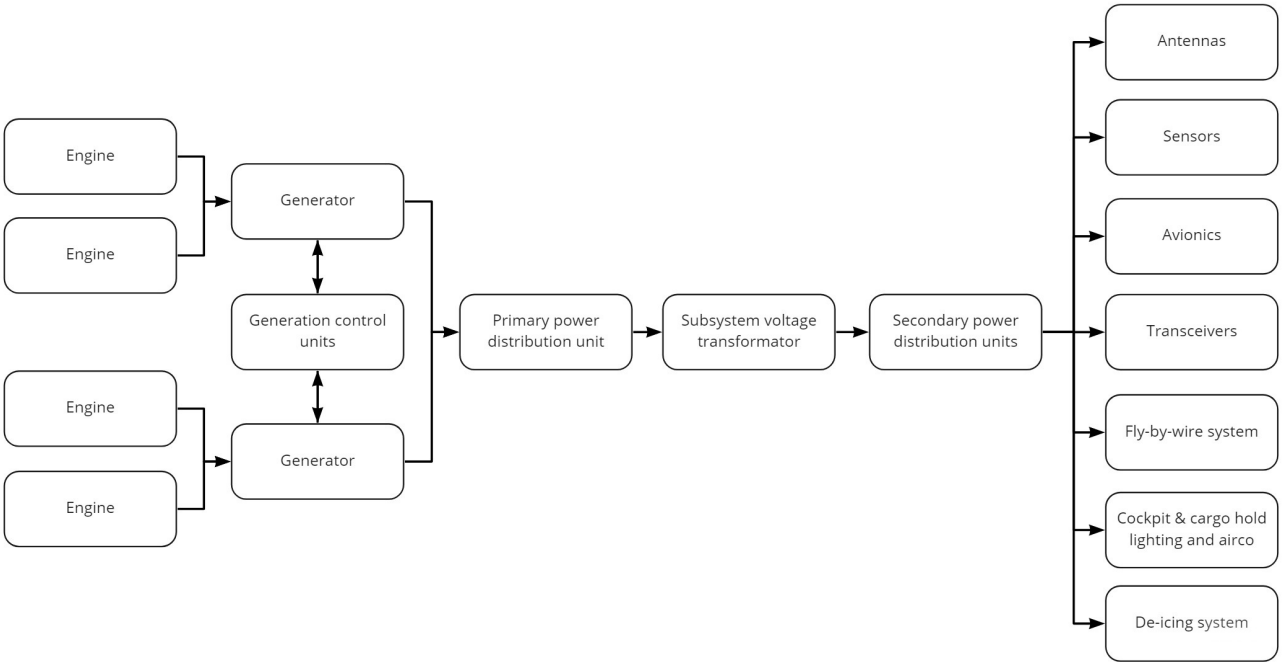

Figure 11.5: Electrical block diagram

12
Sustainability

Firefighting aircraft are very important. They fight fires, and prevent damage to nature and property. Furthermore, it must be noted that in the event of a fire, a firefighting aircraft will always be deployed regardless of its emissions footprint. This is due to the fact that the damage is far larger if the aircraft is not deployed. Nevertheless, it is important to think about sustainability improvements on such an aircraft. The approach to sustainability is described in Section 12.1. After that, the sustainable decisions incorporated into the design are summarised in Section 12.2. These are further elaborated in the respective chapters. Finally, some future opportunities are discussed in Section 12.3. Here, some future design improvements are discussed.

12.1. Approach to sustainability

A brief overview of the sustainability approach is provided. This includes an overview of the steps taken to come to a sustainable design mentioned in the project plan report[65]. First, the current market is analysed to make observations on improvements, or the current state of affairs regarding the design. This is explained in Section 12.1.1. Then, in Section 12.1.2 and Section 12.1.3, a recap is provided of the sustainability paradigm, the sustainability principles and the sustainability vision established. Finally, a quick overview is provided of the sustainability tools used during the design process. This is done in Section 12.1.4.

12.1.1. Market Analysis

The state of the current market is very important for a design. Knowing who are costumers, and how to adapt to their needs is crucial. Especially for a specialised aircraft such as a water bomber, considering that there are only limited uses for such an aircraft and that the amount of buyers is very limited. It is also important to realise that a design that has no buyers, is a waste of invested design time and resources. Therefore, it is decided to make the aircraft not only a good fire fighter, but also multi-purpose, by allowing it to be capable of performing secondary missions such as search & rescue, medical evacuations and cargo transportation.
In Chapter 2, the market analysis is described. This includes an analysis on mission areas as well as the direct competitors of the designed aircraft.

12.1.2. Sustainability Paradigm

In the project plan[65], the sustainability paradigm is introduced. This paradigm is a set of disciplines that needs to be accounted for when making a sustainable design. These disciplines were identified as environmental, social and economical. To the social aspect of the design, emissions (such as noise or air pollution) or safety can be counted. Economical aspects of the design all regard to the cost-effectiveness of the design. This can be performance or maintenance, although emissions could count to this as well if the operating country has emission taxes. The environmental aspect of the design mainly has to do with the emissions of the aircraft. However, the end of life of the aircraft can not be ignored. This could include the use of recyclable materials in the design. A detailed analysis of (noise) pollution, types of propulsion systems and the use of recycled materials can be found in the midterm report[5].

12.1.3. Sustainability Principles and Vision

During the early design stage, sustainability principles and a sustainable vision was developed. The sustainability principles are as follows:

1. “In order to achieve sustainable development, environmental protection shall constitute an integral part of the development process and cannot be considered in isolation from it.” [66]
2. The safety of the operators of the aircraft must be guaranteed.
3. The absence of specialised equipment in remote areas should be considered.
4. The cost-effectiveness of the aircraft should be considered.
5. Environmentally friendly alternatives should be identified and adopted when considered appropriate.

These principles have been guide lines throughout the entire design process so far and every aspect of the design adheres to these principles, as can be found in Section 12.2.
The sustainability vision was established to be as follows: "*The vision of the development team is to develop a cost-effective aircraft that uses recycled materials where possible.*"[65]. Since the design explained in this report is still rather preliminary, it is clear that this vision has not been achieved. However, some steps have been taken towards this vision. For example, the aircraft's structure is made entirely from aluminium. This is done to keep enable future crews to disassemble the aircraft, and reuse the aluminium of the structure.

12.1.4. Sustainability Tools

Next to the establishment of sustainability principles and a vision, explained in Section 12.1.3, some tools are used to guide the sustainable design process. Especially the approach to decision making was set in place. This included a trade-off method to come to a decision. The propulsion system choice, explained in Chapter 7, is a good example of this.

12.2. Sustainability within MANTÆ

This section will provide an overview of the sustainable decisions taken during the aircraft design. First, the performance of the aircraft and the propulsion system are discussed in Section 12.2.1. Section 12.2.2 covers the environmental impact of the aircraft.

12.2.1. Performance

In this section, decisions made regarding not only the performance of aircraft itself, but also the performance of the propulsion is system mentioned.

Aircraft Performance

It has been decided that the aircraft is a high capacity aircraft that can carry $15,000L$ in its four water tanks stored in the hull of the aircraft. With its maximum speed of $130m/s$ during cruise, this means that the aircraft is capable of delivering roughly $31,500L/h$ to a drop site $250km$ away from main base, and $30km$ away from the nearest lake. This is about 2.1 times more than for instance the Canadair CL-415, which is capable of delivering around $15,000L/h$ to such a drop site. At a cost of 48.48 million dollars, it is very cost effective. Compared to the Canadair CL-415, it has a 17% better performance to cost. The performance to cost break down can be found in Section 16.2.

Engine Performance

Four Pratt & Whitney PW150A engines have been selected as the power plant of the aircraft. This engine was chosen largely for its performance to weight. It must however be noted that the noise and emission characteristics of the engines are advantageous. The emission characteristics are good largely due to the PW150A being an efficient turbo-prop engine, but it's capability to run on bio fuels allows it to be also sustainable in the future. See Section 7.7 for more detail on the sustainability of the propulsion system.

12.2.2. Environmental

The environmental impact of the design is summarised in this section. Here, the environmental impact of the power plant is discussed, as well as the environmental impact of production and the recyclability of the aircraft.

Power Plant

As mentioned in Section 12.2.1, the engine is capable of operating on bio-fuels and has very good noise characteristics. In Section 7.7, the sustainability of the propulsion system is explained. In this section, calculations are provided with respect to fuel consumption, emissions and noise levels. It is found that the noise of the propulsion system is in the order of $80dB$, which is far lower than comparable engines. The emissions of the aircraft are also lower compared to jet engines, with a reduction in emissions of up to 50% on short haul flights.

Extinguishing system

During the design of the fire extinguishing system, sustainability is also taken into account. For example, a study has been conducted on the environmental impact of different types of fire retardants. Furthermore, the decision is made to make the water tank structure out of aluminium, which can be recycled easy. Finally, the shape of the extinguishing system is kept rather simple. This is done to ease production. The full analysis on the different types of flame retardant, as well as the material choice of the tanks and the shape can be found in Chapter 8.

Recycling

Most individual components have not been sized yet, and therefore don't have a specific material. The main structure, on the other hand, does already have a material choice. For the structure, aluminium alloys have been chosen, which have good recyclability characteristics. This is beneficial for the end of life sustainability of the aircraft. For more detail on the structural design of the aircraft, see Section 4.4.1.

12.2.3. Maintenance

Extinguishing System

The extinguishing system is designed with maintenance in mind. The water tanks each have 2 access holes that are used by retardant concentrate tanks during operations, and can be removed for inspections. For a complete inspection, the doors of the tanks can be opened for someone to climb into.

Height from Ground
The aircraft has a ground clearance of $0.5m$. It was decided to have the aircraft low to the ground specifically for ground operations such as refilling and maintenance on the water tanks. Due to the aircraft being close to the ground, maintenance crew can easily crawl under the aircraft and perform maintenance on the fire extinguishing equipment. The height of the wing on the other hand makes maintenance of the wing from the ground somewhat more difficult. It is, however, not possible to place the wing lower due to the required clearance for water landings. Also the fact that the engines are placed high up on top of the fuselage makes them difficult to reach. This could be problematic, especially, when maintenance scaffolding is not available. Also the length of the struts of the main landing gear are rather long. This might make maintenance on the main landing gear mechanism more difficult. However, it should be possible to walk on the wing, especially along the wing spars. This makes access to the engines and wing easier, especially when on the water, allowing access to these when there is no ground to walk on. Placing scaffolding on the wing would require careful thought, and potentially a special removable scaffolding that attaches to purpose built connection points on the top of the wing would be needed.

Power plant
The powerplant chosen is the PW150A engine. This is a well-known and reliable turbo-prop engine. And was also picked partly for this reason. This shall make maintenance on the power plant relatively easy.

12.2.4. Safety
Safety is a very important aspect of any aircraft. Therefore, the aircraft comes equipped with a collision avoidance system and a TAWS, explained in Section 11.1.4. Also, a fly-by-wire system is added, as explained in Section 9.3.

12.3. Future Design
As of now, there is a concept for an aircraft that could be further developed in the future. Therefore, some improvements could be made considering sustainability. One of the major downsides of this aircraft could be the complex shape that has to be manufactured and assembled. Therefore, more research could be done to either reduce the complexity of the shape of the aircraft, or to find better manufacturing methods that ease the production of the aircraft.
Also, as mentioned in Section 12.2.3, the current engine placement is not ideal for maintenance. They are placed very high up which makes engine maintenance difficult. In the current design, the engines will have to be placed on top of the wing due to splash-up of water during water landings and take-offs. A better hull design that reduces water splash, could mean that the engines are placed on the upper side on the leading edge, making them far more accessible. Changes in the hull could also mean that the main landing gear would fit inside the hull of the aircraft, making not the struts not only shorter, but it also makes the landing gear more accessible to maintenance crew. Therefore, a better hull design should be investigated.
Finally, when bringing more detail to the aircraft, renewable materials should still be considered, as was done for the aircraft structure.

13
RAMS Characteristics

In this section an analysis on the reliability, availability, maintainability and safety characteristics of the aircraft is performed. The reliability of an aircraft is maximised by minimising the probability of failure, this is explored in Section 13.1. When an aircraft fails it must be repaired and if it is prone to failure it must be regularly checked, both of this actions affect the aircraft's availability, which is described in Section 13.2. To maintain the aircraft's integrity and airworthiness it must undergo preventive and sometimes corrective maintenance procedures, these are elaborated upon in Section 13.3. Finally, the aircraft must comply by safety standards in the design and its operational life. For this certain requirements are imposed. An overview of the safety characteristics of the aircraft is performed in Section 13.4. All of these concepts are interrelated and often, improving one leads to the improvement of other and can be achieved by methods and strategies discussed in this chapter. Their interdependence is illustrated in Figure 13.1.

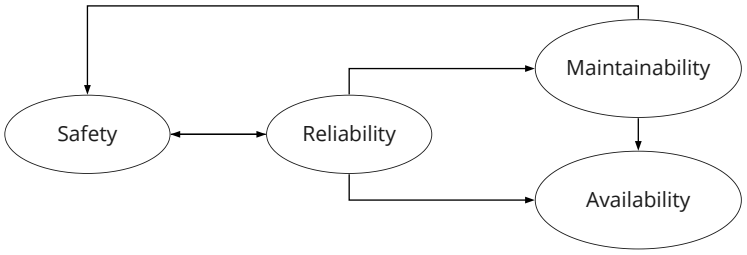

Figure 13.1: Relationship between RAMS criteria[67]

13.1. Reliability

There are several concepts involved with the reliability of an aircraft. One of them is related to the probability of the system (or subsystem of the aircraft) to perform in a satisfactory manner, i.e not fail, for a given period of time. This type of reliability is generally represented by Equation 13.1[67].

$$R(t) = 1 - F(t) \tag{13.1}$$

Where $F(t)$ is the probability that the aircraft will fail within time t. The developed firefighting aircraft is a complex system, counting with multiple subsystems, which must act in the predefined manner if the aircraft is to perform the intended mission. Such complexity comes inexorably with a series of probability of failures. When a certain subsystem or component is dependant on another one to function properly, a series network is generated. Although this is a streamlined process this is intrinsically reducing the reliability of the system. The reliability in a system in series is expressed in Equation 13.2. For this reason, it is important to count with redundancy in the components. Such redundancy increases the overall reliability of the system since, as the name suggests, it allows the same process to be done through different ways. The reliability of a redundant system is a parallel network and the expression is shown in Equation 13.3[67].

$$R_s = \prod_{i=1}^{n} R_i \tag{13.2}$$

$$R_p = 1 - \prod_{i=1}^{n} (1 - R_i) \tag{13.3}$$

It is for the increase in reliability and decrease in probability of failure that requirements are set on the design for redundancy. These requirements, **FA-S&R-002**, **FFA-S&R-006** and **FFA-S&R-007**, state that redundancy is required in some of the components of the aircraft: the propulsion and avionics subsystems. Other subsystems, such as the air frame structure of the aircraft, is developed with a safety factor in mind for a reason of reliability as well as safety for the aircraft. The main components of an aircraft which are designed for redundancy are the engines, avionics (fly-by-wire) and the hydraulic actuators[68].

13.1.1. Redundancy in Propulsion System

Firstly, following requirements **FA-S&R-002** and **FFA-S&R-007**, the aircraft counts with redundancy in the number of engines used. It counts with four turboprop engines. The control surfaces as well as the power delivered by the engines allow it to fly with one engine inoperative. Additionally, as mentioned on the propulsion subsystem's risk analysis in Section 7.8, there are multiple possible malfunctions of the system. These are mainly related to the engine, the fuel system, oil system and propeller system[69]. The propulsion systems must count with several features to increase the reliability. Auto-feathering of the propeller blades reduces the windmilling drag that occurs from an inoperative engine. However, feathering requires oil. For this reason, there has to be an auxiliary oil pump system to feather the propellers in case an oil leak or oil pump failure occurs. Negative torque sensing, overspeed governor pitchlock and other features prevent the propeller blades from being subject to high strain and stress conditions. In the case of an inoperative engine it is also necessary to cut the fuel feeding system to it. This is also necessary in case if an engine or tailpipe fire, since the fuel can increase the danger. For this reason there has to be redundancy in the closing valves from the fuel tank to the engine and in the fuel flow sensors to determine if there is a leak in the system[48].

13.1.2. Redundancy in Avionics

As stated in requirement **FFA-S&R-006**, the aircraft should also count with redundancy in the avionics systems. As mentioned in Section 11.1, the aircraft counts with communication, navigation, flight management, collision avoidance and computing systems. Given the imperative of the requirement for counting with double redundancy it is necessary to carry three copies of the avionics system than what is required for airworthiness and a safe operation. This redundancy reduces the probability of failure of the avionics subsystem and increases the reliability of it providing the aircraft with the required information[70].

13.1.3. Redundancy in Actuators

Similarly to the case with the propulsion and avionics systems, the actuators that are in charge of the control surfaces on the aircraft must also count with redundancy for a reliable operation of the aircraft. This is achieved through a high redundancy actuation concept which is a fault tolerant concept that allows the aircraft to have a graceful degradation. This allows the aircraft to still be controllable even if some actuators have stopped functioning[70].

13.2. Availability

The aircraft's availability refers to the probability that the aircraft will be ready when it is required to be operational. If the aircraft's components have high failure rates then it must spend more time being maintained. Additionally, if the periodic or corrective maintenance procedures on the aircraft take significant amount of time or cannot be performed, the aircraft's availability is lower. In this sense, availability can be considered to be a result of the reliability and maintainability of the aircraft, also reflected on Figure 13.1. There are three main types of aircraft's availability[67]. These are:

- *Inherent Availability(A_i):* This parameter takes into account the repair and failure rates of the aircraft. It does not take into account the scheduled or preventive maintenance procedures, or the logistics time for the aircraft mission. To increase the aircraft inherent availability the probability of failure should be minimised. This can be done by counting with redundant systems as mentioned in Section 13.1.
- *Achieved Availability(A_a):* This parameter takes into account the repair, failure rates as well as the scheduled or preventive maintenance procedures. This availability can be increased by improving the maintainability of the aircraft. This is discussed further in Section 13.3. However it does not take into account logistics or administrative delay.
- *Operational Availability(A_o):* The operational availability takes into account all aspects which allow the aircraft to be ready for a mission. This includes not only maintenance procedures but other aspects that can be related to logistics delays.

These types of availability can be expressed mathematically as shown in Equation 13.4, Equation 13.5 and Equation 13.6. The availability which ultimately allows the aircraft to perform a mission is the operational one because it is the one that takes all factors into account. It can also be expressed in terms of $downtime$, or time during which the aircraft cannot be operated, and $uptime$, which is the service and standby time of the aircraft. This relation can be seen in Equation 13.7.

$$A_i = \frac{T_{MBF}}{T_{MBF} + T_{MTR}} \quad (13.4) \qquad A_a = \frac{T_{MBM}}{T_{MBM} + T_{MTM}} \quad (13.5) \qquad A_o = \frac{T_{MBM}}{T_{MBM} + T_{MTM} + T_{MLD}} \quad (13.6)$$

$$A_o = \frac{Uptime}{Uptime + Downtime} \quad (13.7)$$

Table 13.1: Symbols used for Equations 13.4-13.6.

Symbol	Description
T_{MBF}	Mean Time Between Failures
T_{MBM}	Mean Time Between Maintenance
T_{MTM}	Mean Time To Maintain
T_{MTR}	Mean Time To Repair
T_{MLD}	Mean Logistics Down Time

From this it can be gathered that a maximisation of the aircraft's availability is achieved by:
- Minimisation of the probability of failure of the components. This is already taken into account when the aircraft is designed for maximising reliability. The procedures to do this were described in Section 13.1
- Improving maintainability methods. There are strategies that are used in the design of the aircraft and maintenance operations that minimise the required maintenance of the aircraft. These are described in detail in Section 13.3
- Achieving a stream-lined operation. This prevents logistic or administrative delays. For a firefighting aircraft, which needs to have a quick response to a fire, fast and efficient operations should be achieved. The operations of the aircraft are described in further detail in Chapter 15.

13.3. Maintainability

The aircraft's maintainability is an inherent characteristic of the aircraft and is defined as "(Maintainability) pertains to the ease, accuracy, safety, and economy in the performance of maintenance actions"[67]. There are two types of maintenance that must be taken into account. These are: preventive maintenance and corrective maintenance. An illustration of the maintenance types is shown in Figure 13.2

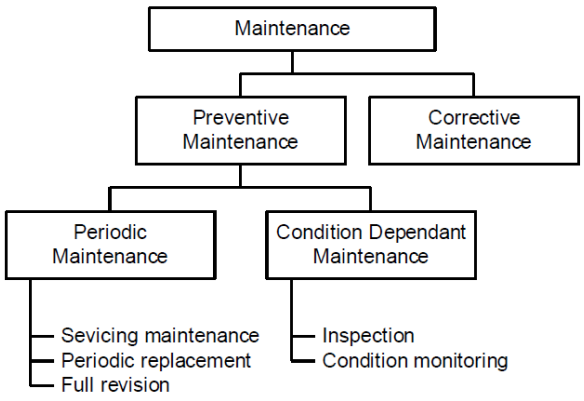

Figure 13.2: Types of maintenance [67]

13.3.1. Preventive Maintenance

This type of maintenance is done to maintain the aircraft's standard and, as it suggests, to prevent a malfunction from happening during the operation of the aircraft. A preventive maintenance should be done periodically and can also be done if the condition of the aircraft suggests that it requires one. The maintenance steering group 3, or MSG-3, has identified four main objectives for the scheduled maintenance of an aircraft. These are[71]:

1. To ensure realisation of the inherent safety and reliability levels of the aircraft.
2. To restore safety and reliability to their inherent levels when deterioration has occurred.
3. To obtain the information necessary for design improvement of those items whose inherent reliability proves inadequate.
4. To accomplish these goals at a minimum total cost, including maintenance costs and the costs of resulting failures.

As it is with the reliability, the maintainability of the aircraft is also affected by the complexity of an aircraft. The most relevant part of the preventive maintenance procedures is the inspection of parts. For this reason, a system with more complex parts requires a more thorough inspection. The main objective from a maintenance point of view is for the aircraft to only need to visit the hangar on scheduled maintenance procedures. For this, routine procedures are performed. Strategies to make this procedure more streamline have been done[72]. These are

- *Redundancy:* this allows the failure of a system or component to not affect the aircraft's airworthiness. This gives time for the aircraft to continue operating until the scheduled date for the maintenance comes.
- *Line Replaceable Units (LRUs):* this are modular components that lead to a fast replacement. This operation can be done while the aircraft is in service, meaning that it does not have to undergo general maintenance for such a change to occur.

- *Minimum Equipment List:* this is a list of the components that must be operational for the aircraft to be airworthy. Keeping track of such a list allows the aircraft to also operate while some components have failed.

Such strategies also support the availability of the aircraft, which was discussed in Section 13.2. Although these strategies are intended to minimise the downtime of the aircraft, it is still necessary to perform the routinely maintenance to bring the aircraft back to a fully operational state. A routinely done maintenance of an aircraft usually includes the following tasks[71]:

- Cleaning the aircraft and its main Avionic components.
- Avionics Maintenance.
- Application of corrosion prevention compound.
- Parts lubrication and overhaul.
- Draining of leaked fluids and checking the trouble shooting fuel systems.
- Servicing of hydraulic and pneumatic systems.
- Replacing rotables and *LRUs* as per guidelines.
- Inspecting and checking for general wear and tear.

In addition to this tasks, given the particular mission of the firefighting aircraft, other tasks must be added to the routine maintenance. To determine this it is important to understand which special environments and situations will the aircraft encounter during its operation. The aircraft will encounter water environments when it is scooping water. The aircraft will also experience high temperature when in close distance to the fire, this also includes smoke and ashes particles. For this reasons the aircraft also counts with systems that other aircraft do not include, such as the hull and the extinguishing system. Tasks that must be performed in a preventive maintenance therefore also include:

- Inspection of the wear and possible cracks of the hull. The hull must not allow water to enter through the crevices, and so should not have cracks also for a structural integrity perspective, since it must resist landing loads on water.
- Inspection of the hydraulics and actuator systems in the water and retardant tanks. These are specially important parts to be checked, since if these are faulty the aircraft would not be able to perform the mission.
- Corrosion preventive measures. The most basic one is to hose the aircraft after operation. This should be done more regularly than on the scheduled maintenance checks. However, there are more corrosion preventive measures to be taken. Anti corrosion coating should be applied regularly in the most affected places. Crevice, galvanic and other forms of corrosion should be checked for in parts that are in constant contact with water, such as the water/retardant tank.
- The probe ends of the extinguishing system are under high pressure when loading the water on the tanks. For this reason they should be checked for any form of failure such as cracking, but also other failure mechanisms can occur. Modularity, or *LRU*, is a good feature to give the probe ends to allow for an easier maintenance.
- The high temperatures can affect any part of the aircraft. The general integrity of the parts must be checked taking into account that high temperatures can decrease their material properties.

13.3.2. Corrective Maintenance

The corrective maintenance of the aircraft is carried out when there is a faulty component of the aircraft which doesn't allow it to fly. This type of maintenance is what a preventive maintenance tries to avoid. This can be a problem with the air frame, engine or components. The maintenance life cycle of each of the parts is relatively similar. This cycle consists of the following steps[73]:

- **Plan and Schedule Work.** This process consists of arranging the necessary things for the beginning of work on the aircraft.
- **Manage Aircraft Configuration.** This consists on getting to know the aircraft's layout and the part that must be worked on.
- **Conduct Engineering and Work Package Design.** This refers to getting to know the requirements that must be complied by the part and the aircraft.
- **Manage spare parts and material.** The necessary parts and material to maintain the aircraft must be procured.
- **Execute Maintenance Work.** The maintenance work is performed.
- **Certify Maintenance Work.** The aircraft must be approved by airworthiness authorities, testing might need to be carried.

It is important for the aircraft to be as easily maintained as possible. This increases the aircraft's availability, as explained in Section 13.2, which in turn allows it to perform the missions on shorter notice. It is for this reason also that the aircraft is required to be equipped with a well-known power plant, as stated by **FFA-Oth-001**. The engine's manufacturer, Pratt & Whitney offer maintenance, repair and overhaul services and facilities in over 40 locations[74]. This improves the maintainability of the aircraft.

13.4. Safety

The aircraft's safety is defined as "the freedom from hazards to human and equipment"[67]. As illustrated in Figure 13.1, it is closely related to the reliability of the aircraft and is ensured by a proper maintenance. There are several measures that are taken into account during the design of the aircraft to ensure that the design is safe. This measures are translated into requirements, that can be both imposed by the stakeholder or design team for the design

or by certification authorities on aircraft generally.
The requirements from the **Safety and Reliability** category are the ones ensuring a safe design. The aircraft counts with collision avoidance systems, the engines, avionics and other components are redundant, a conservative estimation on the flight loads experienced, including a safety factor is used for the sizing of structural components, fatigue cycles are taken into account and the aircraft complies by safety regulations of authorities. These safety regulations are discussed on their corresponding chapters. These include power plant sizing requirements, so that the aircraft can achieve a minimum screen height, minimum climb gradients, climb rates, etc. Performing a risk analysis for the different subsystems brings out what are the possible ways of failure, and their impact on the aircraft. The safety parameters that are included in the aircraft are a way of mitigating these risks of failures of different parts in the aircraft. The preventive maintenance of the aircraft also aims to mitigating the risks of the aircraft to encounter failure during its operation. Additionally, the aircraft as a whole is exposed to different risks while performing the mission. This risks and the mitigation strategies to reduce their impact and likelihood are discussed in further detail in Chapter 14.

14
Risk Assessment

For a safe and reliable design a risk assessment should be performed. Risk can be defined as the likelihood of failure times the impact. The risk assessment can be obtained in Table 14.1, table 14.2 and table 14.3. First risks are identified into relevant categories, each categories containing one or multiple risks. Then the identified risk is described and rate on likelihood, impact and risk with each having their own colour code. After this is done for every category, mitigation starts. Risk mitigation can be done by for example creating procedures, improving communication and maintenance. Lastly, the mitigated risk are again rated on likelihood, impact and risk. Note that if high risks still occur after mitigation (marked by a red box), then the risks should be frequently monitored. Additionally, the risk risk migration should be review every year to have as goal lowering the risk. Note that the risk analysis presented in Table 14.1, table 14.2 and table 14.3 is based on the complete mission and not containing specific subsystem risks. For subsystem risk mitigation please go to the subsystem sections.

Table 14.1: Risk Assessment part 1

Risk Assessment									
			Before Mitigation				**After Mitigation**		
Category	**ID**	**Description**	**Likelihood**	**Impact**	**Risk**	**Mitigation strategy**	**Likelihood**	**Impact**	**Risk**
Environment	En1	Unavailable fuel	Low	High	High	Frequent fuel consumption observations using relevant metering systems (flight time, fuel capacity, fuel rate).	Very low	Moderate	Low
	En2	Flying in military area with collision as consequence	Moderate	High	High	Before flight identify together with the flight service which area are active. Next, keep in contact with ATC about the activity when entering a new flight zone.	Low	High	Moderate
	En3	Accidental leaking of fuel or chemicals from bottom of the aircraft	Low	High	High	Anti-leaking strips will be installed together with tests during the maintenance period	Very low	Low	Low
	En4	Not communicated change in approved retardant list	Moderate	Moderate	Moderate	Pre-flight briefing including latest update on retardant use within drop region	Very low	Moderate	Low
Secondary Missions	SM1	Malfunction in rescue equipment	Low	Moderate	Moderate	Pre-flight checklist will be setup for secondary mission equipment. Additionally, the equipment will be frequently tested before approved on flight	Very low	Low	Low
	SM2	Poor accessibility to rescue equipment	Moderate	Moderate	High	Rescue equipment (such as a rescue boat) will be place in cooperation with the rescue crew. So, accessibility can be optimised	Low	Low	Low
	SM3	Weather conditions are beyond rescue equipment's (especially for the rescue boat)	Low	Moderate	Moderate	Up-to-date weather forecast will be analysed to make better operation decisions	Very low	Low	Low

Table 14.2: Risk Assessment part 2

Risk Assessment									
			Before Mitigation				**After Mitigation**		
Category	**ID**	**Description**	**Likelihood**	**Impact**	**Risk**	**Mitigation strategy**	**Likelihood**	**Impact**	**Risk**
Crew (Pilot, Copilot, Navigator)	Cr1	Pilot fatigue due to noise, vibration and lack of autopilot	Low	Moderate	Moderate	Set up regulation for maximum flight time and monitoring by mission manager.	Very low	Moderate	Moderate
	Cr2	Crew operates while using medications or alcohol	Low	Moderate	High	Pre-flight registration including several visual tests and a personal record including current medication.	Very low	Moderate	Moderate
	Cr3	Insufficient flying skills	Moderate	Moderate	High	Establishment of specific aircraft training programs. First missions for new pilots will be with an additional experienced pilot.	Low	Moderate	Moderate
	Cr4	Conflicting personalities	High	Moderate	High	Do pre-flight briefings to address current relation issue. Attain honest feedback and motivate to maintain positive attitude.	Low	Moderate	Moderate
	Cr5	Pilot not being updated about changed operating procedures standards	Low	Moderate	Moderate	Clarify and report operation changes and make sure the personal is notified about the changes.	Very low	Moderate	Moderate
Maintenance Crew	MC1	Improper maintenance of the aircraft (fatigue, lack of motivation etc)	Moderate	High	Very high	Implement managerial tasks that include fit-for-duty tests. Provide personal improvement course for better employer performance.	Low	Moderate	Moderate
	MC2	Improper maintenance tracking	Low	High	Moderate	A third party will check maintenance report and validate them will the performance maintenance.	Very low	Moderate	Moderate
Distractions	Di1	Pilot distracted by social device that are not mission related	Moderate	Low	Moderate	Strict regulation about secondary device use.	Very low	Low	Low
	Di2	Mission related controls in inconvenient location	Low	Moderate	Moderate	In the design of the cockpit panel cooperate the flight crew for advises.	Very low	Low	Very low
Operation Limits	OL1	The aircraft is being used beyond its capabilities	Moderate	High	Very high	Before accepting a dispatch the aircraft limits are revised.	Low	Moderate	Moderate
	OL2	Aircraft request without looking into specifications	High	Moderate	High	Aircraft performance charts need to be used to determine if the aircraft is able to perform the mission.	Low	Moderate	Moderate
Tactical Support	TS1	Unable to accurately/realistically determine the severity of the fire conditions for aerial drops	Moderate	High	Very high	Setting up representative flight profiles for the aircraft such that better dispatch decisions can be made .	Low	Moderate	Moderate
Aerial Drops	AD1	Personal or property damage due to drop unintentional	Low	Moderate	Moderate	Flight route should be determined beforehand to minimise congested areas. Drop height should within a safe amount .	Very low	Low	Low
	AD2	Personal or property damage due to failure of drop system	Low	Moderate	Moderate	Scoop areas should picked such that congested areas are avoided.	Very low	Low	Very low

Table 14.3: Risk Assessment part 3

Risk Assessment									
			Before Mitigation				**After Mitigation**		
Category	**ID**	**Description**	**Likelihood**	**Impact**	**Risk**	**Mitigation strategy**	**Likelihood**	**Impact**	**Risk**
Mission Profile	MP1	Collision due to small distance to other mission related aircraft	Low	Very high	Very high	The aircraft will be equipped with a highly reliable traffic avoidance system. Additional mission will be properly planned. Addition of tactical commands will reduce confusion and add clarity. Enable the air manager to posting flight restrictions.	Very low	Moderate	Moderate
	MP2	Flying into building, trees, power lines etc	Low	Moderate	Moderate	Frequency updated hazard map will be provided at the pre-flight briefing. Aerial supervising aircraft need to provide feedback on their visuals on the flight route and low flight is only allowed when confident in the flight region.	Very low	Low	Very low
	MP3	Accident due to visibility caused by smoke, sun glares and deceiving shadows	High	High	Very high	Missions should be timed such that visibility's are optimal. Additional aerial supervision aircraft feedback actual flight conditions to make timing more accurate.	Moderate	Moderate	High
	MP4	Pre-approved waterway become unusable due weather or environmental conditions	Moderate	Moderate	High	Waterways will be approve before takeoff by the pilot.	Low	Low	Low
	MP5	Collision while flying on a waterway	Low	High	High	The aircraft will be equipped with an air-horn for warnings. Other than that will the pilot be trained to perceive traffic on the waterway .	Very low	High	High
	MP6	Animal collision to aircraft	Moderate	Moderate	High	In the operation plan wildlife is addressed, so scooping regions will prevent animal encounters. Next, the pilot will be trained to spot wildlife that can cause harm to the aircraft. Also, the use of air-horn warning will scare of wildlife.	Low	Moderate	Moderate
	MP7	Loss of control while on the waterway	Moderate	High	High	Design adaptation for more stable and manoeuvrable aircraft. Next to that, pilot will be specifically trained for water operation.	Low	High	Moderate
	MP8	Loss of control while in the air	Moderate	High	High	Pilot will be tested and trained frequently. Additionally, pre-flight briefing help to prepare the pilot for what is coming such that they can remain calm in case of an emergency	Low	High	Moderate
	MP9	Water containing minerals can cause damage to engines and aircraft structure when cleaning aircraft	Moderate	High	High	For cleaning the aircraft water filter are going to be installed.	Very low	High	Moderate
	MP10	Corrosion causing failure of engines and aircraft structures	Moderate	Very high	High	Yearly inspection will be performed by the FAA for corrosion inspection. Next, the materials can be replaced by non-corrosive materials.	Low	Very high	High

15
Operations and Manufacture

In this chapter the operations of the aircraft are discussed. Takeoff and landing are discussed in Section 15.1. The primary mission, firefighting, is discussed in Section 15.2. Secondary missions are discussed in Section 15.3. The ground operations are discussed in Section 15.4. Delivery and end-of-life of the aircraft are laid out in Section 15.5. Finally, a manufacturing approach is discussed in Section 15.6. A general Operations and Logistics Chart that shows the operating steps and collaboration between different parties is shown in Figure 15.1.

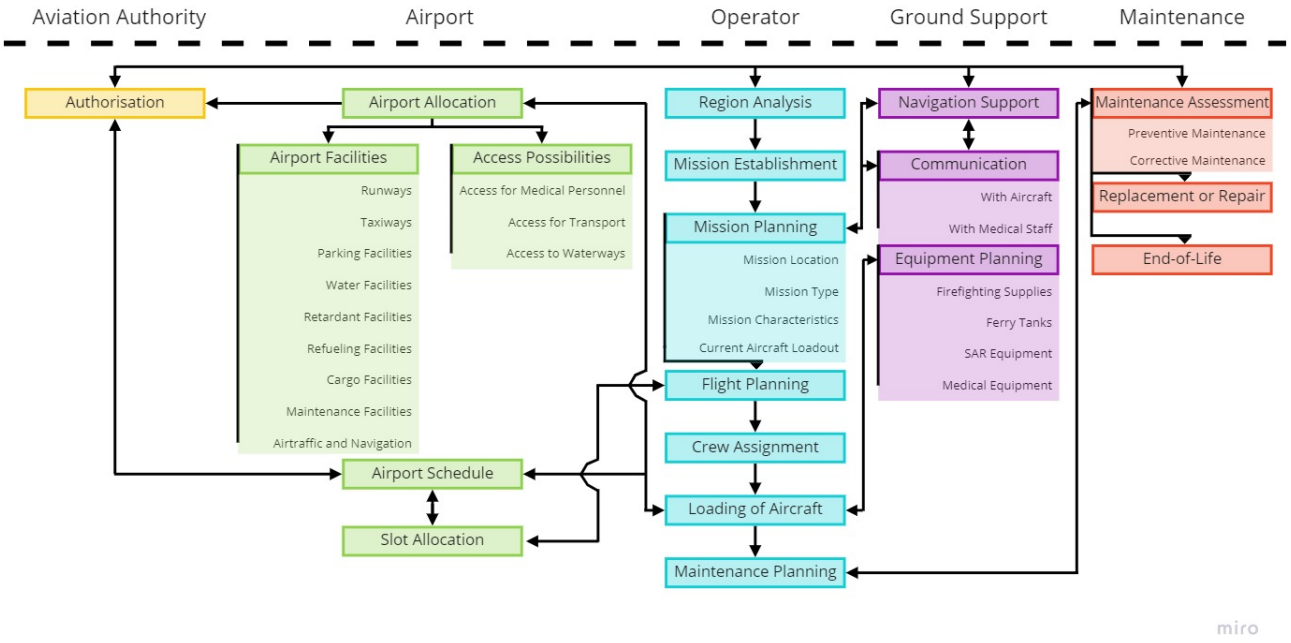

Figure 15.1: Operations and Logistics Chart of the Aircraft

15.1. Takeoff and Landing

As the aircraft can take off and land from both land and water separate operational plans have to be developed for this. These are discussed in the next sections.

15.1.1. Operating from an airfield

Operating from an airfield is not very different from conventional planes, as all the normal regulations have to be followed, like following the lead of air traffic control (ATC)[75]. At towered airports pilots must get clearance before taxiing on the runway. For non=towered airports pilots should state their plan on the common traffic advisory frequency (or that airports equivalent system). Pilots should also visually check that the airfield is clear. Before taking off all the checks described in Section 15.4.1 have to be performed.

The take-off procedure has to be adapted for the conditions of the field and the pilots should look up the current conditions in the performance chart. The aircraft should be able to take off from any field based on its performance but the size of the margin between takeoff length and field length will differ because of temperature, altitude, field conditions, and the weather. If the field is 1-1.2 km there might not be a lot of margin and the aircraft should taxi to the absolute end of the runway before attempting a takeoff. During this takeoff the pilot can brake until the engines reach the maximum RPM, only attempting a takeoff with all engines providing max thrust. In most other cases the takeoff will not cause problems as the aircraft is designed with short, unhardened runways in mind.

During the takeoff regulations should be followed with respect to engine failures. If an engine fails during takeoff but after the decision point the opposing engine can be shutdown for controllability (depending on the conditions) as there is enough power for a turnaround. For a takeoff with crosswind the pilot will have to limit skipping and apply a rudder correction once the aircraft leaves the ground. For a takeoff from a soft field the pilot may want to exploit

ground effect in order to limit the ground drag. This can be done by lifting the nose, becoming airborne, and picking up speed in ground effect before rotation, leading to less time spent on the airfield and better take-off performance.

When landing the pilots should again contact ATC for instructions regarding approaches and holding patterns. If there isn't ATC at an airfield pilots are expected to observe traffic and follow the pattern. In the case that there is no traffic the pilots should check ground indicators to determine which runway and traffic pattern direction to use. Before landing pilots should again check for a clear runway. As they approach, high lift devices should be deployed and the approach speed should be lowered to 1.3 times the stall speed (which depends on temperature and altitude). While a 3° approach is officially preferred for shorter airfields a bigger angle (up to 10°) can be used to limit the approach distance. Again, for crosswinds and soft fields special precautions have to be taken during landing. Once the pilot gets close to the runway they should perform a flare to reduce the speed, after which the aircraft will touchdown. Braking and reverse thrust should immediately be applied upon touchdown in order to limit the field length. The braking procedure should be adapted from the performance chart, although it can be assumed for now that the pilots can apply the full braking force and a computer will limit skidding. Once the aircraft has sufficiently slowed down the thrust reversers can be disabled and the final deceleration can be done on brakes alone. After this the aircraft can be taxied to where it needs to be in order to be refilled with fuel or retardant or be parked until the next operation.

15.1.2. Operating from water

As there are no airfields on the water pilots are theoretically free to choose in which direction they want to takeoff. However, in practice a pilot should always takeoff and land against the wind in order to lower the takeoff speed. Before taking off it is necessary to taxi through the takeoff path in order to make sure it is clear. Like on an airfield it is also important to make sure that the path is clear and will stay clear, as sudden deceleration is not possible during a takeoff on water. In this takeoff run there will be 3 clear phases; displacement, pre-planing and planing. In the displacement phase the aircraft will handle like a boat and it can be steered by differential drag from the belly flaps or differential thrust from the engines in order to line it up for a takeoff. Before attempting the run the belly flaps must be up in order not to crash because of them creating a pitching moment because of water resistance. Once the run has begun the resistance from the water will increase until the aircraft begins planing on the step, after which it decreases. During the planing the plane must be trimmed in order to limit porpoising. Once fully planing will be less drag and thus more power available. This makes the aircraft accelerate quickly again, lifting itself more and more out of the water until the aircraft can be supported by aerodynamic lift (not hydrodynamic lift, which supports it at a lower speed) at which point it will take off. Once in the air the aircraft needs to stay in ground effect in order to pick up the speed needed for climb. After rotation, operations can resume as normal. Waves have a big impact on the takeoff, but if the waves are significant enough to compromise takeoff there will also be a lot of wind, leading to a shorter takeoff and less impact of the waves[1].

Like takeoff, landing a seaplane is also not controlled by ATC like a landing at an airfield (although a pilot may have to report to ATC). Because of this it is extremely important to circle over the landing run in order to confirm it is clear and there are no floating objects in the water. Additionally, it is important to confirm that the gear is not deployed while landing on water, as this will cause a crash. Like mentioned before, landing into the wind is strongly preferred. This direction can be visually confirmed by smoke, flags, or lines on the water. Unlike landing on land the belly flaps should not be extended, as contact with the water at high speed will lead to a crash. Apart from this, the landing is relatively similar to a landing at an airfield. The approach speed has to be about 1.3 times the stall speed and the approach angle 3-10° (although shallower angles are preferred due to a better transition to planing). Once the pilot is close to the water, they should flare to reduce speed and slowly touch down on the water, where the aircraft will begin planing. Brakes cannot be used, but reverse thrust should be used in order to slow the aircraft down until it stops planing, after which it will sink in the water and the hydrostatic and hydrodynamic drag of the displacement regime will further slow the aircraft down. In the displacement regime the belly flaps can be deployed for differential steering. Waves can be a problem if the aircraft doesn't land into the wind. However, as waves form lines perpendicular to the wind direction and as the bow of the hull has increase deadrise, waves (up to the maximum wave height the aircraft is certified for) will not pose a problem since the aircraft will "cut" through the lines when landing.

15.2. Firefighting

Firefighting is the main mission of the aircraft and is split up in three phases: cruise, scooping, and the drop. All of these phases are described in the following sections. A general overview of a firefighting circuit can be seen in Figure 15.2.

[1] http://www.pilotfriend.com/training/flight_training/seaplanes/takeoff.htm

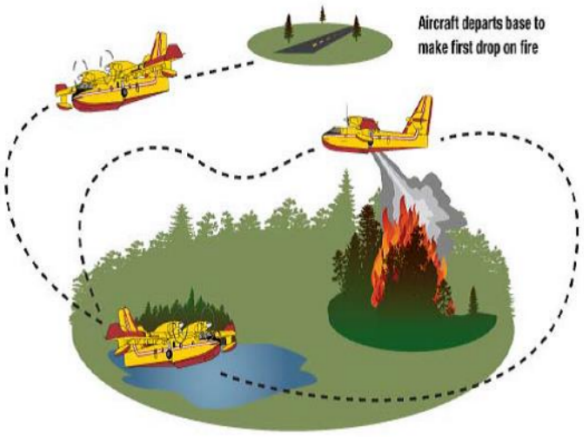

Figure 15.2: Basic overview of the mission of a water scooper. Taken from [76]

15.2.1. Cruise
During the cruise phase of firefighting the aircraft is travelling to -or from- a water source or fire. In this phase it will periodically have to be trimmed depending on the change in center of gravity because of fuel consumption or carrying water. As mentioned in Section 7.2 cruise speed is $130 m/s$. CG will stay relatively constant during cruise, only shifting forward small amounts with fuel burned.

15.2.2. Scooping
Scooping operations are directly related to landing procedures. Once again, it is vital to circle over the scooping body of water to check for obstacles. After this the approach can be made, but instead of slowing down during the landing the scoopers are deployed and power is applied during scooping to correct for drag and the added weight in the aircraft. Once the tanks are full, after about 14 seconds, the aircraft should be able to pitch up, exit planing, and gather altitude, returning to cruise. As mentioned in Section 10.2.2 the minimum skimming speed is 52.7 m/s. During skimming the pilot should slowly apply more throttle to counter for the increased weight. The CG position will change from 32% to 29% MAC with full fuel and 27% to 25% MAC with no fuel. Real values will lie somewhere in between.

15.2.3. Approach to Drop
Once the aircraft gets close to the drop site it is picked up by a lead plane. This plane stays in the air around the fire to monitor how it spreads. The drop coordinator in this aircraft decides where to drop the water/retardant. The lead plane will fly ahead of the aircraft and will let it know when to drop its payload. Alternatively, if no lead plane is present (which might be the case at a direct attack of a new fire), the pilots can plot their own drop. This is however not recommended without good knowledge of the area and its terrain. After the aircraft is picked up by the leadplane it will approach the drop zone, slowly reducing altitude and airspeed.

15.2.4. Drop
Once the aircraft reaches the drop site the doors can be opened and the payload can be dispersed over the selected area. This drop can either be a direct attack, where water/retardant is directly dropped on a fire, or indirect attack, where an aircraft drops water/retardant ahead of the fire in order to establish or strengthen a control line. As discussed in Section 10.2.3 the drop speed will be 70 m/s. Once the tanks are fully drained the drop phase is finished. During the drop the CG will shift backwards; from 29% to 32% MAC with full fuel and 25% to 27% MAC with no fuel. Again, real values will lie somewhere in between.

15.2.5. Flight after Drop
After the drop the aircraft will have lost a significant amount of weight. Because of this it will directly and suddenly gain altitude, something that can be mitigated by decreasing the throttle. After dropping the payload the aircraft can return to the water source to scoop and refill the payload or return to the airfield.

15.3. Secondary Missions
Apart from the primary mission, the aircraft also has to fulfil secondary missions. These include ferrying the aircraft to regions struck by fires, search and rescue, medical evacuation, and transportation of cargo.

15.3.1. Ferry Flights
As the aircraft has a ferry range with tanks of 5,000km+ it can be located all over in the world in a couple of days. For example, if the aircraft is stationed in Sacramento, Ca. (like the current fleet of CalFire) Europe and South America can be reached in 2-3 days and Africa, Australia and Siberia can be reached in 3-4 days.4 A map of this is shown in fig. 15.3. Before ferrying the aircraft the ferry tanks need to be installed. Flexible tanks from Turtle-Pac were chosen as they only

weigh $8kg$ per 1,000L of fuel contained[2]. These tanks can be removed and stored on the ground/in the aircraft when not in use. Apart from this, ferry operations are not that different from regular operations, but authorities of airports meant to land at should be notified of this and asked for landing permission before beginning the ferry flight.

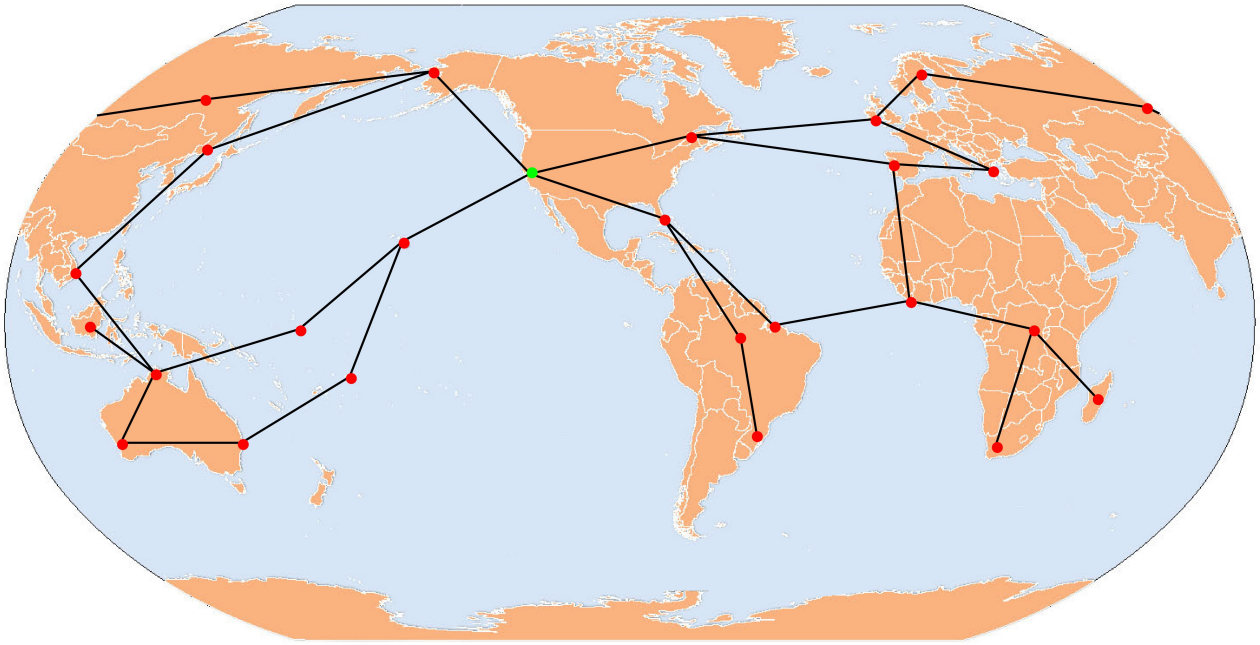

Figure 15.3: Ferry flight map, centered at Sacramento

15.3.2. Search and Rescue

As the aircraft can land on water and has good endurance and range it is possible to use it in Search and Rescue (SAR) missions. In SAR survivors of water landings or problem stricken ships are located, retrieved, and flown to safety. In order to do this the aircraft is fitted with a boat that can be deployed when landed on the water. The cabin layout in this configuration can be seen in Figure 15.4. In general this mission proceeds as follows; first crews are alerted of a possible wreck. Next they will take of from land/water and fly towards the suspected area. Once here they will circle the area and look for survivors. Once survivor(s) are located the aircraft will land, after which the boat will be deployed through the cargo door. As this door is a little above the water line deployment and retrieval is easy. Once the boat is deployed it will drive towards the survivor(s), put them in the boat and get back to the aircraft. The survivor(s) and boat are retrieved and the aircraft will take off again and return to circling or return to the base, depending on condition of the aircraft, survivor(s) and if there are more survivors in the water. After returning to base the survivors are brought to a hospital.

15.3.3. Medical Evacuation

As the aircraft has the ability to land on unprepared runways it can help in disaster-struck areas by evacuating people who need medical help that is not locally available. In order to do this beds and equipment will have to be fitted in the cargo hold and qualified air ambulance staff will have to be flown in. In order to complete this mission, the refitted aircraft will have to fly to an area with people who need to be evacuated. Once there patients will have to be boarded on the plane, preferably over the cargo ramp. Once all patients have been stabilised by the staff the aircraft will take off and fly towards an airfield close to the hospital. Transport should be ready for when the aircraft lands. Once landed, all patients will be loaded into ambulances towards the hospital, after which the aircraft can refuel or redo the mission.

15.3.4. Cargo Flights

The aircraft will also be able to do cargo flights. As the hold will be split by the central spar the cargo capacity decreases. Nevertheless, it can carry either 11 LD-3 containers or 6 LD-9 containers, about half the cargo capacity of the 737 Classic. The layout for this can be seen in Figure 15.5. Cargo can be loaded either through the cargo door or over the cargo ramp, but a lift is needed to load cargo through the cargo door.

[2] https://www.turtlepac.com/products/collapsible-aircraft-ferry-tanks/

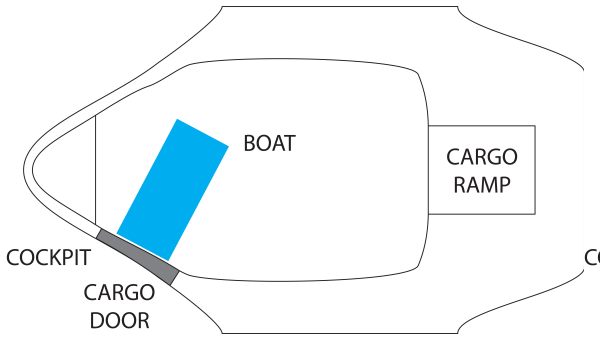

Figure 15.4: Layout of cargo hold for SAR missions

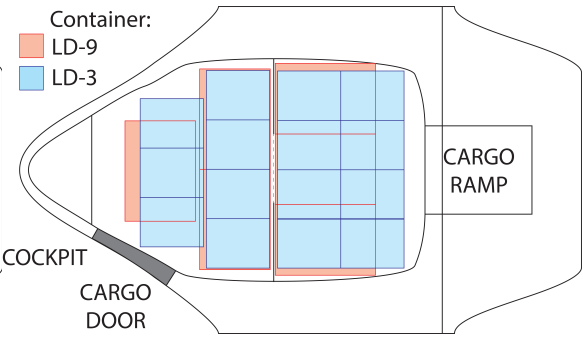

Figure 15.5: Layout of cargo hold for cargo missions

15.4. Ground Operations

Apart from operations with the aircraft flying ground operations are also a vital part of operations. These include startup, refilling the aircraft during a mission, and maintenance.

15.4.1. Startup

All startup and pre-takeoff checklist items should be completed before taxiing anywhere. This checklist includes an inspection of the aircraft, all subsystems, instruments and controls. Once the checklist has been cleared the engines can be started. As the engines can be started electronically no APU is needed to start in advance.

15.4.2. Refilling

When the aircraft returns to base during a mission it is to get fuel, retardant or a combination of both. "Hot loading", where both are refueled at the same time with the engines running, can be permitted based on the airfield and operator, but a separate certification needs to be granted. As discussed in Section 8.5.1 the water tanks of the aircraft can be reloaded on either side. The integrated fuel tanks in the wings need to be refueled separately, as there is no direct distribution mechanism for this present on the plane. This can be done in parallel. Also, a distribution system may be added in the future. Once the aircraft is done refuelling it can continue with its mission.

15.4.3. Maintenance

As discussed in Section 13.3 there generally are 2 types of maintenance, preventive and corrective. Preventive maintenance schedules should be followed and if the aircraft will be on a mission for a long time supplies should be carried to the base of operations so that the schedule can be continued. If a serious malfunction happens the damage will have to be analysed by a mechanic. If the plane is stranded at an airport where maintenance can not be performed there are 2 options; field repairing the aircraft to prepare it for a flight to another airport, and flying in personnel and equipment in order to repair the aircraft. Which option is preferred is dependent on the repair needed.

A special type of maintenance is maintenance after water operations. As the aircraft has come into contact with corrosive liquids (especially salt water) it needs to be cleaned. The easiest way to do this is to spray it down with fresh water. The extinguishing system also needs to be flushed and cleaned in order to remove wildlife and limit the spread of wildlife between water sources.

15.5. Delivery & End-of-Life

When the aircraft rolls out of the factory there are 2 options for the customer: picking the aircraft up at the factory or having it delivered. Customer pick-up of the aircraft is preferred as the customer can inspect the aircraft at the factory. In case of delivery the customer will have to sign documents stating they waive their inspection right.

A pre-delivery inspection is planned to take a few days. On the first day the outside and inside of the aircraft can be expected with the plane still on the ground. The engines can also be checked on this day. On the 2nd day the aircraft can be flight tested by the customer. After these tests modifications can be performed if the customer does not accept the aircraft. When the customer accepts the after (after testing or after modifications) the Airworthy Certificate is issued, the deed of the plane is signed over to the customer and the ferry flight to the new homebase of the aircraft is prepared.

When the aircraft reaches end-of-life it can either be stored in a corrosion free environment or flown to an airfield where it is broken down into its components. This breaking down and reuse of components of material has been researched and is currently applied in only a few places in the world. It is expected that by the time the aircraft reaches end-of-life it is common practice. Once at a processor, reusable items can be stripped and the aluminium airframe can be recycled for a new use.

15.6. Manufacturing

Manufacturing the aircraft will need to be done in such a manner that safety and reliability is maintained, while minimising costs. To this end, the manufacturing process will aim to primarily use tried and tested production methods, with minimal tooling. Production numbers, based on market data, are expected to be too low for mass production benefits. Therefore, part specific machinery and other high investment machines are likely to be unsuitable.

The primary material for the aircraft is aluminium, which is a commonly used material, so a lot of tooling can be found off-the-shelf. The thickness of the spars and skin of the wingbox is such that this will likely be made using rolled or stamped sheets of aluminium. Stiffeners are also expected to be sufficiently thin to use the same process, rather than extrusions. Extrusion does allow for more complex stiffener geometries, however it will require specific heavy machinery, including a die through which to push the aluminium. In comparison, the process of rolling and stamping sheets allows for quick and relatively cheap manufacture of thing aluminium parts. While this process will also require a profile die, it will only require a single die per part assuming a flexible press floor. Furthermore, this process can be used for everything from the panels to the stiffeners, all using the same machine, simply by swapping out the die, whereas extrusion would only be applicable to stiffeners and possibly spars. This means that a press machine will always be necessary, in addition to an extrusion machine. More modern alternatives, which are not part specific, such as additive manufacturing techniques, do exist for aluminium parts, however, they require very expensive machines, that are often very limited in terms of part size. These machines are more suitable to complex parts requiring high performance materials that are difficult to manufacture.

Assembly of the various parts will need to be done via riveting and bolts. Alternatives such as glue are generally used in composites where other options are less attractive, as it requires a minimum surface area to work effectively, and provides a lower load bearing capability in most scenarios. Furthermore, due to the amphibious nature of the aircraft, special care would have to be taken to ensure any such glue would not be adversely affected by humidity or contact with salt water. Welding is another potential alternative, however, welding is often inconsistent, unless done by specific purpose built welding machines. Weld quality is so critical to the strength and longevity of a weld that expensive machines would be required to perform the weld, and also analyse the weld for defects. The thin plates that will make up the main fuselage structure, and even the hull are also detrimental to a welding process. In particular for materials such as aluminium, which has a poor thermal conductivity relative to steel, welding thin plates often results in warping due to variations in temperatures along the plates while welding, catastrophically affecting the final part. Riveting is a common assembly method within the aerospace industry, especially with thin aluminium plates, and requires little tooling. It is often reliable, and can be designed for using various methods that have been proven with years of experience. The only downside is that riveting does not allow for easy disassembly and reassembly, and should therefore only be used in parts that are expected to remain fastened together throughout the lifetime of the aircraft. Where disassembly may be required, for operation or maintenance reasons, bolts are a suitable fastening method. Bolts are also commonplace within the aerospace industry, and can therefore be considered to be a tried and tested method. Furthermore, the use of standardised bolts can be expected to lower production and maintenance costs, as sourcing these mass produced bolts from a manufacturer can be done easily, cheaply, and importantly for this design, can be done anywhere in the world. The ability to remove and reattach parts with minimal and conventional tooling is critical to the cost and speed of maintenance, which bolts are easily able to provide, with only a small weight penalty relative to rivets. Removing a rivet requires the rivet to be drilled out or cut away, meaning that a new rivet will have to be put in place. A bolt however can simply be reused, giving significant gains in the sustainability of the maintenance and operation of the aircraft.

Parts of the aircraft can be manufactured from composites. Composites are commonly used for control surfaces, and will require some investment in machinery. The primary cost will be the composites themselves, and the autoclave required to cure the composite parts once they are made. Making the parts will require a mould, however these moulds can be produced in a simple manner. Depending on the manufacturing method, the manufacturing of the composite parts may produce a quantity of waste in the form of vacuum bags and bleed sheets used to ensure the flow of resin between the fibre in the infusion process, or will require the pre-preg composite to be stored in a freezer during transfer and prior to use in production. This comes with an associated cost to the sustainability of the manufacturing process. However, the process of producing composite parts does not generate the metal waste associated with production of metal parts, which is often shipped back to a processing plant to be recycled. Efforts to reduce this waste by using tape laying machines are possible. These machines would increase the rate of manufacture, with high quality results and minimal waste. However, these machines are very expensive, and would require detailed programming of the entire part production.

Significant attention will have to be paid to the layout of the production floor. Optimising the use of the production floor can speed up production, but more importantly reduces the space required for production. This will in turn

reduce cost. The availability and location of equipment will be a deciding factor of this layout. However small parts start, it is highly unusual to mount all the parts together on one piece. Often times, separate sections, such as the wing, fuselage, and empennage are assembled separately, before being joined together. This assembly of large parts will require heavy lift equipment. This sort of heavy equipment is expensive, and often not available over the entire production floor. Note that this equipment also needs to be capable of smooth and accurate movement, to avoid damage to any assemblies or parts during the production phase. This damage can come from collision between parts, but also from improper handling and lifting of parts. It is therefore necessary to consider how to move parts such that the loads applied do not exceed those that the part was designed for. In a worst case scenario, this might even require a redesign of parts such that these parts can be assembled. Depending on the size of the assembly, it is sometimes possible to use jigs. These jigs are often used when precision assembly of multiple parts is required, and can also be beneficial in terms of time spent on the assembly. These jigs do however have the disadvantage that they require an initial investment, and, although they are reused on every aircraft that is produced, are effectively wasted material in that they are not a part of the aircraft itself.

It should be noted that these considerations apply when deciding to produce the aircraft "in-house", with no prior equipment. The presence of prior machinery, or the availability of extended experience in one or more production methods can have a significant impact on the production methods and decisions. The prior availability of extruders, tape laying machines, or employees experienced with composite manufacturing is something that will decide the final production method of various parts.

Careful consideration must be given to outsourcing production of parts, or aspects of it. Specialised companies exist, which have experienced workers and expensive equipment to produce a wide variety of parts using one or more production methods that would be inefficient to use on a limited amount of parts of an aircraft. This extends beyond manufacturing of parts to the coatings applied to final assemblies. High performance coatings such as heat resistant ones can require complicated expensive machinery such as plasma spray systems. Purchase of such machinery is not economically viable for small scale production of one type of aircraft, but outsourcing to a company specialising in this can achieve better results at a reasonable price. In this manner, the availability of outsourcing should be considered, as it enables the use of methods and can improve quality at a viable price. Care should be taken however, as the risk of outsourcing is potential delays in deliveries, and the sustainability impact of transporting parts over long distances should be considered. Although these can both be reduced by adequately locating of the production and assembly plant near such companies, or with easy access to means of transportation.

16
Resource Allocation

16.1. Weight breakdown

In this section a more detailed breakdown of the total weight of the aircraft is described. The three main parts of the weight are the operation empty weight, the payload weight and the fuel weight. Combining those will result in a maximum take-off weight.

16.1.1. Operation Empty Weight Allocation

In Chapter 4, the structural weight of the design was calculated. Also some weight penalties were taken into account. However, during the design process some of these weight penalties became redundant as the exact weight was calculated, for exampe on the landing gear. A overview of all the component of the Operational empty weight of the aircraft is shown in Table 16.1.

Table 16.1: The operation empty weight breakdown of the aircraft.

Main structure	**Weight[kg]**
inboard wing	11,000.00
outboard wing	3,760.94
crew floor	133.00
apertures	363.00
Sub systems	
Landing gear	1,709.90
Hull	3,800.00
Aircraft systems	
flight control system	255.74
actuators	176.16
hydraulics and electric system	532.40
oxygen system	21.41
air-conditioning and anti-icing system	51.62
Propulsion	
engines	2,867.60
pylons	800.00
Extinguishing system	
water tank 1	350.92
water tank 2	343.24
water tank 3	343.24
water tank 4	350.92
extinguishing equipment	520.00
Other	
furnishing	92.63
paint weight	125.71
Total	27,598.43

After combining the different components of the operation empty weight, the total weight is 27600 kg. From the class I, an operation empty weight was determined of 25108 kg in Chapter 4. Between Class I and Class II was a increase of 9 % which is acceptable as most of the data for the class I weight estimation was based on conventional amphibious aircraft and passenger blended wing body. There ware no data for an aircraft which is comparable with our design and therefore a higher discrepancy is expected.

16.1.2. Payload allocation

The payload weight between the class I to the class II weight estimation only changed regarding the increase of water capacity from 14,000 L to 15,000 L. This also resulted in a increase of total payload weight of 6 % for this reason. The total payload weight breakdown can be seen in Table 16.2

Table 16.2: The breakdown of the payload weight.

Payload	
Payload weight	**Weight[kg]**
Water	15,020
Rescue rib	1,650
Medical evacuation equipment	410
Retardant concentrate	140
Total	17,720

16.1.3. Maximum Take-Off Weight

After combinding the Operation empty weight and the payload weight with the fuel weight calculated in Chapter 7, the final Maximum Take-off Weight can be determined. The breakdown of the Maximum take off weight is shown in Table 16.3.

Table 16.3: The final breakdown of the class II weight estimation.

Component	Weight [kg]
Operation Empty Weight	27,598.43
Payload Weight	17,220.00
Fuel Weight	14,079.50
Maximum Take-Off Weight	58,897.93

The class I weight estimation concluded to a Maximum Take-Off weight of 54000 kg described in Chapter 4. The class II weight estimation resulted in a Maximum take-off weight of roughly 59000kg. So between the class I weight estimation and the Class II weight estimation is an increase of 8% of the Maximum Take-Off Weight, which is acceptable as the class I was mostly estimated on statistical data of conventional amphibious aircraft.

16.2. Cost Breakdown

The cost of the aircraft is highly import for the impact of our aircraft on the market. A too high price will be devastating for the application of the aircraft. Therefor driver requirement **FFA-Cos** was defined to make our aircraft competitive on the market. To make a first estimation of the market price of the aircraft, Equation (16.1)[1] was used to calculate cost due to the operation empty weight.

$$C_{aircraft} = 10^6(1.18 \cdot M_{oew}^{0.48} - 116) \tag{16.1}$$

As can be seen from Table 16.1, the Operational Empty Weight is estimated to be 27600 kg which leads to a first estimate of 43.8 million dollars, 39 million euro. However this cost estimation is purely based on conventional cargo aircraft and therefore a better approximation is needed. For this estimation, different parts of the aircraft are considered as well as the expected amount of sales. Combining the estimated costs with the sale prospect, the market price of the aircraft can be determined.

16.2.1. Airframe

First the airframe material costs are estimated. Most of the main airframe is made of Alluminium alloys and therefore the average price of alluminium 7075-t6 per kg is used, which is 2.8 euro per kg. [1]

[1] `https://www.globalsources.com/Aluminum-sheet/7075-aluminum-sheet-1172516161p.htm#1172516161` [cited: 25-6-2020]

Table 16.4: The cost breakdown of the airframe with the weights of each element

Main structure	**Cost [Euro]**
Inboard wing	30,800
Outboard wing	10,530.63
Crew floor	372.4
Apertures	1,016.4
Sub systems	
Landing gear	1,800,000
Hull	10,640
Aircraft systems	
Actuators	480,000
Hydraulics system	40,000
Oxygen system	800
Air-conditioning and anti-icing system	400
Extinguishing system	
Water tanks	3,887
Extinguishing equipment	5,000
Other	
Furnishing	300
Paint	1,000
Total (120%)	2,861,696

In Table 16.4, the cost estimation of the materials needed for the different compartments of the airframe is described. The main structure, hull and water tanks are made primarly from aluminium so their weight was factored by the price of aluminium per kg. The Landing gear cost are compared to the landing gear costs of the A320. [2]. The A320 has a higher Maximum Take-Off weight, which can compensate the sizing for unpaved landing strips. The costs for the actuators is assumed to be around 10,000 euro per actuator. As explained in Chapter 9, the aircraft is expected to have 48 actuators. This resulted in a total actuator cost of 480,000 euros. The hydraulic systems is estimated to cost around 40,000 euros as it contains around 10 hydraulic pumps which cost around 4,000 euro each. [3] The oxygen system of our aircraft contain of two oxygen containers of 400 euros each. [4] For the cost of the air-conditioning and anti-icing system, a source was not found and therefore it is expected to be around 400 euro's. The extinguishing equipment contains many different components and the cost are estimated to be 5000 euro's. Lastly, the other part of the aircraft cost breakdown. These furnishing is estimated to be around 300 euro's. Be aware, when buying the aircraft the rescue rib and medical evacuation equipment is not included. As a water resistant paint is used, the cost are expected to be around 1000 euro's. This results to a material airframe cost of 2,860,000 euros, included with a contingency of 20 % due to inflation and uncertainties for the cost of the Air-conditioning and anti-icing system, furnishing and paint.

16.2.2. Propulsion

As mentioned in Chapter 7, the cost per engine ise 1.3 milion dollar per engine. However, to convert to euros the conversion rate of 1 dollar is equal to 0.89 euro is taken.[5] Next to the engines, pylons are needed to attach the engines to the airframe. These will be pure aluminium and therefore the price of aluminium per kg of 2.8 is used for calculation the pylon costs. This will result in a total costs of 5.1 million euro including a 10% contingency for inflation, which can be seen in Table 16.5.

Table 16.5: The total costs of the engines

Engine cost [Euro]	1,157,000
Pylon cost [Euro]	2,240
Total cost (110%) [Euro]	1,275,164

[2] https://sassofia.com/blog/aircraft-landing-gear-shop-visit-repairs-and-overhauls/[Cited:25-6-2020]
[3] http://www.aerospacengineering.net/aircraft-hydraulic-system/[cited:25-6-2020]
[4] https://www.aircraftspruce.com/pages/ps/oxygen_0systems/aeroxsys.php[cited:25-6-2020]
[5] Conversion rate of 22-6-2020 https://www.wisselkoers.nl/dollar-euro

16.2.3. Avionics and Electronics

The avoinics described in Chapter 11 are used to approximate the avionics and electronics of the design. All prices from the two breakdowns come from `https://www.airteam.eu/` and the amount of avionic and sensors used are determined in Chapter 11. This will result in a estimated cost for the avionics of 65,000 euros, which is shown in Table 16.6. 57,000 euros is the estimated cost of the eletronics shown in Table 16.7. In both systems there is a 10% contingency implemented due to inflation over time.

Table 16.6: The cost estimation of the avionics

Avionics	**Cost [Euro]**
ADS-B	4,212.31
ELT	594.47
TAWS	7,492.2
Glass cockpit	15,959.72
Airdata system	5,247.82
AHRS	4,460.64
CVBR	21,450
Total (110%)	65,358.88

Table 16.7: The cost estimation of the Electronic system

Electronics	**Cost [Euro]**
AoA sensor	5,340
Pitot tube	4,500
GPS reciever	260
VOR antenna	440
Flow sensor	5,376
Level sensor	280
Force and torque	24,000
Position & displacement sensor	7,200
Proximity sensor	3,000
Temperature	1,200
Total (110%)	56,755.6

16.2.4. Manufacturing

The manufacturing cost has the highest share in the total cost of the design. It is splitted in six different aspects of manufacturing, shown in Table 16.8.

Table 16.8: The estimated cost breakdown of the Manufacturing

Manufacturing	**Cost [Euro]**
Development costs	3,000,000
Labour costs	1,200,000
Logistical costs	500,000
Certification	1,500,000
Testing	2,000,000
Quality control	500,000
Total costs(120%)	10,440,000

The first aspect of the manufacturing is the development cost. These are rather high as the design contains a very complex shape. This challenges the way of manufacturing in comparison with conventional streamlined built-up processes. The labour cost is expected to take 30 weeks to build the aircraft with normal workdays.[6] The employees working on the aircraft is expected to be 50 people with an average hourly salary of 20 euro. This leads to a estimated labour cost of 1.2 million euros. The logistical cost are incoporated as the engines come from a different factory than the main frame. The total logistical cost are estimated to be 0.5 million euros. As the blended wingbody is a rather rare and unconventional aircraft, more certification is needed than for conventional aircraft.[7] Therefore the estimated certification is 1.5 million euros. The testing cost are estimated to be 2 million euros as the design requires a long testing phase. The long test phase is needed as this type of design has never been tested. And finally, quality control is integrated in the manufacturing process to avoid failures due to malfunctioning machines and the estimated cost for this are 0.5 million. This leads to a final manufacturing cost estimation of 10.4 million euros with 20 % contingency as most of these numbers can contain more unforseen costs as this manufacturing process has never been done and therefore there is no data to compare this process with. The 20 % contingency also accounts for inflation.

16.2.5. Operations

The cost breakdown regarding operations is shown in Table 16.9. The costs for the payload is purely for the retardant. The cost of retardant per drop is 8,000 euro explained in Chapter 8, so for a mission with 10 drops the total payload cost result in 80,000 euros. The labour costs consist of a crew which loads the aircraft and the actual pilots flying the aircraft. The payload loading crew is assumed to be 5 people who take 5 hours to make the aircraft ready with a salary of 30 euro per hour. The flight crew consists of 3 people who fly for 4 hours wit a salary of 30 euro per hour. This will result in 660 euros. The fuel costs are the amount of fuel needed mentioned in Chapter 7, which is 13,552.35 L factor with the jet fuel price. Currently, the oil industry is affected by the corona pandemic and this dropped the price of

[6] Five work days a week and working for 8 hours a day.

[7] `https://generalaviationnews.com/2012/09/09/the-cost-of-certification/` [cited: 25-6-2020]

jet fuel per litre to €0.20. However, this number will rise again and therefore the price per litre before the pandemic is used for the cost estimation, which is €0.65 per litre. Lastly Airport fees are also taken into account in the cost breakdown. This consists of parking, take-off, landing fees and are estimated to be 2,000 euro per operation.

Table 16.9: The estimated cost breakdown of operations

Operations	**Cost[Euro]**
Payload	80,000
Labour	660
Fuel	8,809.03
Airport fees	2,000
Total cost(110%)	1,00,615.93

16.2.6. Maintenance

For maintenance, there are certain regulations the aircraft has to uphold. These regulations are mostly focussed on the preflight check, the 100 hour inspection and the annual inspection.[8] It is decided that this aircraft also needs a 50 hour inspection due to its missions containing a higher risk of damages than airliners. The annual cost estimation of the maintenance can be seen in Table 16.10.

Table 16.10: The estimated cost breakdown of the Maintenance per year.

Maintenance	**Costs[Euro]**
Preflight checks	24,750
50 hour inspection	9,900
100 hour inspection	26,400
Annual inspection	4,800
Repairs	50,000
Uninsured repairs	20,000
Total costs (120%)	138,020

The preflight checks will be performed by the flight crew of 3 people with a hourly rate of 30 euros. It will take the flight crew approximiatly one hour to do the preflight checks. It is determined that the aircraft will perform 275 mission per year and therefore the preflight checks cost 24,750 euros. For the cost calculation of the 50 hour inspection, it is assumed that the average mission time is 4 hours. This results in 22 50 hour inspections where 11 merge with the 100 hour inspection and 11 can be seen as purely 50 hour inspections. During 50 hour inspections five maintenance workers work for 6 hours on the aircraft with an hourly rate of 30 euros. For the 100 hour inspection the maintenance workers increase to 8 and the time inspecting the aircraft increases to 8 hours to do a more intensive inspection. There is also one annual inspection, where 10 people inspect the aircraft for 16 hours. During these inspections, some repairs are needed. Some of these repairs can be insured, where the manufacturer has to provide the new part free from charge due to malfunction. However, there can also be some repairs which were cause by own fault. These are expected to cost around 20,000 euros per year. This concludes to a total maintenance cost of 139,000 euros with a contingency of 20 % contingency due to inflation and unforeseen costs which are prominent during maintenance.

16.2.7. Total costs

After calculating the cost for the materials and the manufacturing, the cost of one aircraft can be determined. This contains the aircframe, propulsion, avionics, electronics and manufacturing cost. It also takes into account the insured repairs the manufacturer has to pay when the operator finds a malfunction. This results in a final cost per aircraft is shown in Table 16.11.

Table 16.11: The total cost estimation

Component	**Costs[Euro]**	**percentages of total**
Airframe	2,861,696.07	14.66
Avionics & Electronics	122,114.48	0.63
Engine	5,090,800.00	26.09
Manufacturing	10,440,000.00	53.50
Maintenance	1,000,000.00	5.12
total price(105%)	20490341.08	105

[8] `https://doublemaviation.com/aircraft\protect\discretionary{\char\hyphenchar\font}{}{}maintenance/#:~:text=Aircraft%20that%20are%20flown%20for,be%20changed%20every%2050%20hours.` [Cited: 22-6-2020]

For the estimation of sales of this design, a market analysis was done on the two main competitors of the design, the CL-415 and the Be-200. The main difficulty of determining the demand of the market is that the majority of the suppliers are government agencies with limited financial resources. Therefore it is utmost import to design a financial attractive aircraft as well. The Cl-415 produced in total 91 aircraft in a span of approximate 20 years.[9] For the Beriev 200, currently 17 are built from 2003.[10] Considering these two statistics, it is planned to built 40 aircraft in 20 years as the market of firefighting aircraft is growing due to the growth in forest fires. Due to the unpredictability of the market, the aim is to break even quite early after the start of production. Therefore it was chosen to break even after 22 aircraft were sold. This resulted in a market price of 38 million euros.

16.3. Performance-to-cost comparison

As discussed in Section 2.3.2 the main competitors of the MANTÆ are the Canadair CL-415, the Beriev Be-200 and the Shinmaywa US-2. The characteristics of these aircraft, which were shown in Section 2.3.2, are shown in Table 16.12 together with the characteristics of the MANTÆ.

	Canadair CL-415	Beriev BE-200	ShinMaywa US-2	MANTÆ
Capacity (L)	6,136	12,000	15,000	15,000
Cruise Speed (m/s)	93	167	134	130
Firefighting Range (km)	1,850	2,100	2,300	1,100
MTOW (kN)	195	400	540	590
Configuration	Propeller, 2 engines	Jet, 2 engines	Propeller, 4 engines	Propeller, 4 engines
Cost (million $)	27	70	103	42

Table 16.12: Characteristics of the MANTÆ and competitor aircraft

Performance per unit cost with varying distance to the airfield and water can be seen in Figure 16.1 and Figure 16.2 respectively. Figure 16.1 varies the airfield distance with a constant water source distance of 30 km, the distance from the design mission. Likewise, Figure 16.2 varies the water source distance with a constant airfield distance of 250 km. High values are a better performance per unit of cost. As it can be seen in the figures, the MANTÆ is the most cost-effective firefighting aircraft up to 370 km distance from the airfield. At this point it is surpassed by the Beriev because of its larger operational range (2,100 and 1,100 km). The large drops in Figure 16.1 are the distances at which the aircraft is no longer able to make the same number as drops as before, significantly reducing performance.

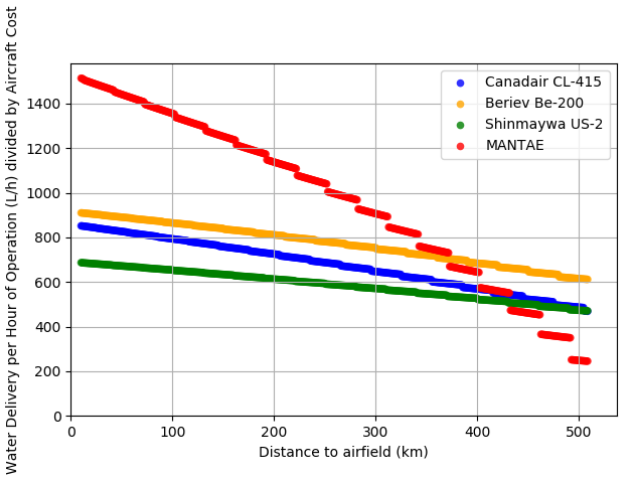

Figure 16.1: Aircraft performance per unit cost for varying distance to the airfield and 30 km distance to a water source.

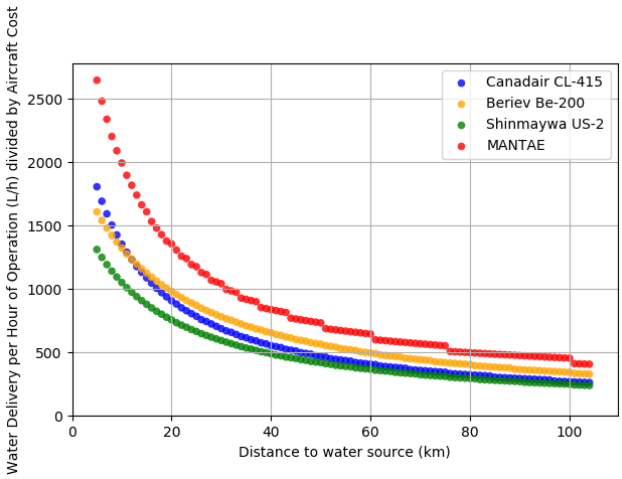

Figure 16.2: Aircraft performance per unit cost for varying distance to water and a 250 km distance to the airfield.

As can be seen in the graphs, the MANTÆ has the best performance per cost when operating close to airfields or water sources. As the range is fairly limited compared to its competitors it drops below their performance at 3-400 km. A way to increase performance would be to carry a ferry tank for the flight towards the water source, making sure that the tank is empty when reaching the water source in order to not exceed MTOW. Graphs for this situation can be seen in Figure 16.3 and Figure 16.4. Nevertheless, when operating at lower ranges the performance to cost ratio is not equalled by its competitors.

[9] `http://www.deagel.com/Private-Aircraft/Bombardier-415_a000081001.aspx#:~:text=Description%3A%20The%20Bombardier%20415%20multi,215s%20have%20been%20sold%20worldwide.` [Cited: 25-6-2020]

[10] `https://russianplanes.net/planelist/Beriev/Be-200` [Cited: 25-6-2020]

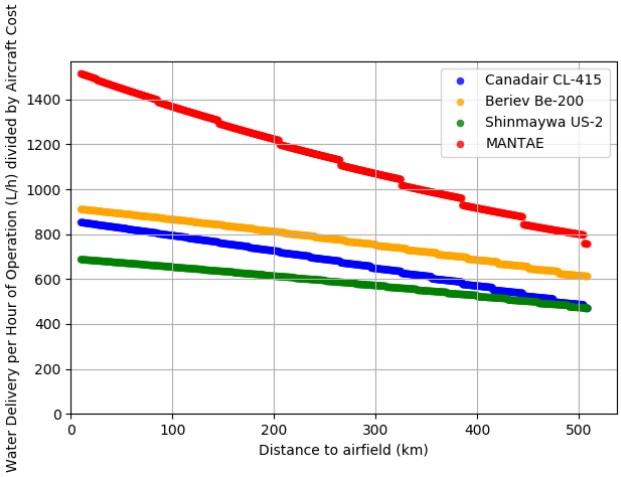

Figure 16.3: Aircraft performance per unit cost for varying distance to the airfield and 30 km distance to a water source with a one-way ferry tank.

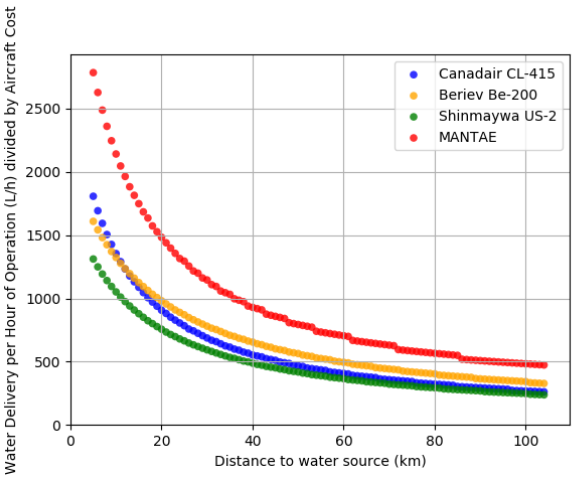

Figure 16.4: Aircraft performance per unit cost for varying distance to water and a 250 km distance to the airfield with a one-way ferry tank.

17
Sensitivity Analysis

Now that the subsystems have been designed and performance has been analysed, it is important to conduct a sensitivity analysis to determine how the aircraft performance varies with changing parameters. This chapter analyses the effect of airfoil choice and changing costs on the performance of the aircraft, since these are parameters that could realistically change if the development of the MANTÆ were to continue past this design phase.

17.1. Airfoil Selection

In the current design, integration of the hull with the fuselage results in substantial wetted surface area. An airfoil with a flatter underside could facilitate the hull integration and reduce drag. If a different airfoil is indeed chosen for the aircraft centre section, this could have significant effects on the performance and result in a substantial change in interior layout. In the current MANTÆ design, the centre section and the wings consist of differing airfoils. However, the Trefftz plots in Figure 17.1 and Figure 17.2 illustrate the lift generated by the aircraft with the airfoil MH78 used across the entire aircraft compared to the current airfoil used, the Workman 69.

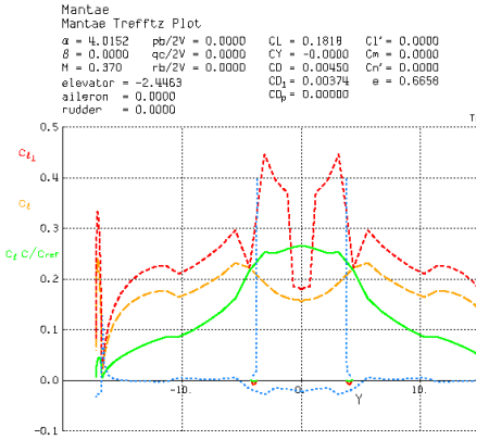

Figure 17.1: Lift distribution at cruise with the current airfoil

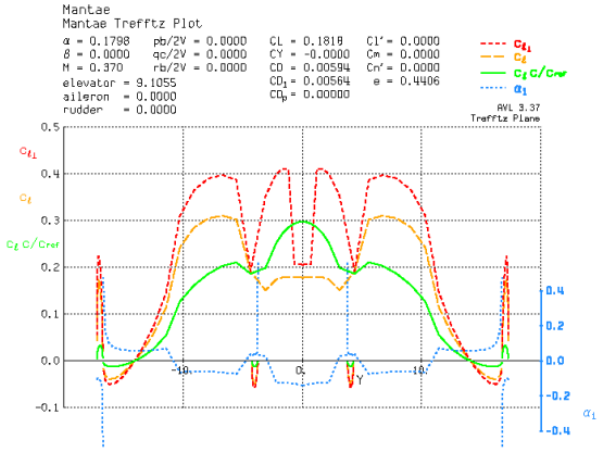

Figure 17.2: Lift distribution at cruise using only the MH78 airfoil

For a geometry that is prominently three-dimensional with varying chord and sweep, the orange C_l curve is the most indicative of the real-life lift distribution. The graphs illustrate that, the MH78 airfoil is able to generate more lift and thus needs an AoA of only 0.18° at cruise, compared to 4.01° for our original design. The lower angle of attack results in a smaller wetted area of the aircraft S_{wet} and consequently a reduction in drag. However, in order to achieve a zero pitching moment and keep the aircraft flying straight and level, an elevator deflection of +9.10° is required. This is undesirable as the pilots would need to push the control stick forward in order to keep the nose pointing up, as explained in Section 9.2.2. This factor, combined with the increase in trim drag due to the greater elevator deflection, eliminate the aerodynamic advantage of the airfoil and make it less desirable for pilot control.

Additionally, the change in airfoil results in an increased C_{Lmax} from 0.90 to 1.21. Consequently, a new flight envelope diagram can be generated. This is illustrated in Figure 17.3.

The flight envelope illustrates that the maximum and minimum design loads of the aircraft are the same as for the flight envelope generated in Section 4.4, since the gust envelope is still contained within the manoeuvre envelope. However, the quadratic stall curves are steeper, and thus the aircraft is able to fly at lower speeds. At drop speed, the aircraft must be able to sustain loads of $2g$, and for this flight envelope that is equivalent to a speed of $61 m/s$. This is a reduction in drop speed of almost $10 m/s$, which could result in an increase in retardant effectiveness to around 60%, as explained in Section 8.5.3. It would also allow the pilot to perform tighter manoeuvres at low speed to avoid collisions or align correctly with the fire.

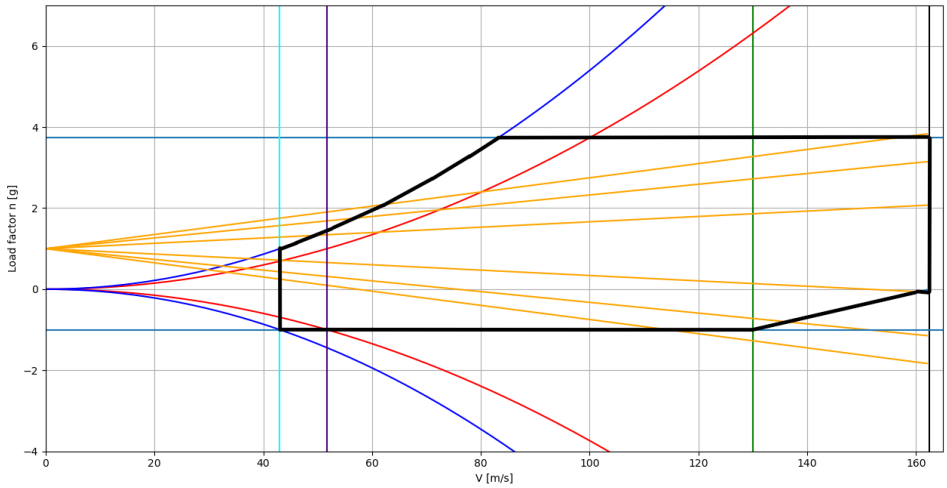

Figure 17.3: Overall flight envelope for the modified centre section airfoil

17.2. Costs

The costs calculated in Section 16.2 are made based on information from the current economy. However, the costs of manufacturing the aircraft may rise drastically due to extra testing needed and extensive certification periods, and this must be considered in the evaluation of total costs. Hence, the manufacturing costs have been increased by 50% to observe the impact that this has on meeting the performance to cost requirement. The performance to cost ratio has been plotted against distance from the fire and distance from the lake in Figure 17.4 and Figure 17.5 respectively.

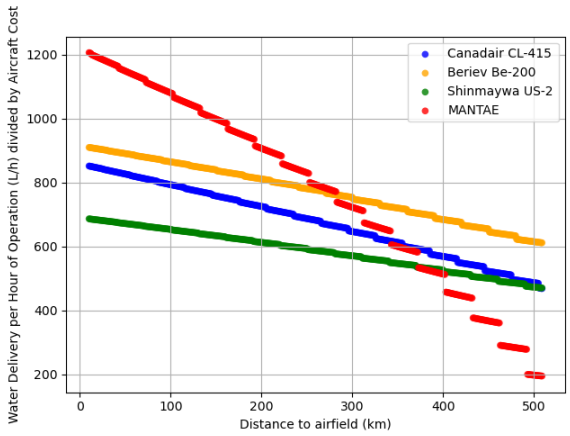

Figure 17.4: Aircraft performance per unit cost for varying distance to the airfield and 30 km distance to a water source, with a 50% increase in manufacturing costs

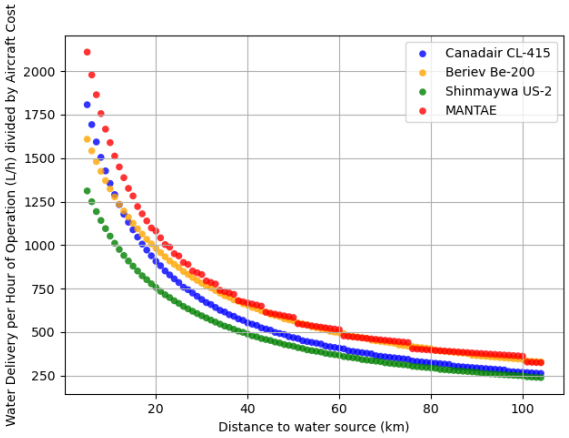

Figure 17.5: Aircraft performance per unit cost for varying distance to water and a 250 km distance to the airfield, with a 50% increase in manufacturing costs

Observing the first diagram, the MANTÆ aircraft has a better performance to cost ratio until a distance of 282 km from the aircraft base to the fire. Previously, this distance was equal to 370 km. Additionally, the MANTÆ performs better than competitors until a distance of 50 km from the water source, where previously the aircraft performed better at all water distances. Overall, this means that for the main mission of 250 km to base and 30 km to water, the MANTÆ aircraft is still the most cost efficient choice, even with an increase in manufacturing costs of 50%. However, only for the missions in Siberia and Africa, the Beriev Be-200 becomes a more cost efficient choice.

18
Verification and Validation of the Design

There are two types of verification and validation procedures that are relevant in the design of the aircraft. These are: verification and validation of numerical and computer models and verification and validation of the design. The former type of procedures is set for the tools that are developed in order to automatise or perform faster calculations. These procedures are discussed in their respective chapters throughout the report, after their formulation and application on the design has been covered. The latter type of procedures is the one discussed in this chapter.
Once the design is finished, it is necessary to go back to the initial requirements used to develop it. It is important to determine whether the developed aircraft is able to meet the requirements. This is the verification of the design and it is evaluated through a compliance matrix, which can be seen in Section 18.1. Finally, it is important to determine if the aircraft is able to perform its mission. The ability to meet the mission need and stakeholder requirements is evaluated through the validation of the design and is performed in Section 18.2. What is evaluated and compared within a verification and validation process is illustrated by the V-diagram in Figure 18.1[67]. The ability of the product of satisfying the requirements and needs, determined by a verification and validation, proves that the product can be used for its intended purpose[67].

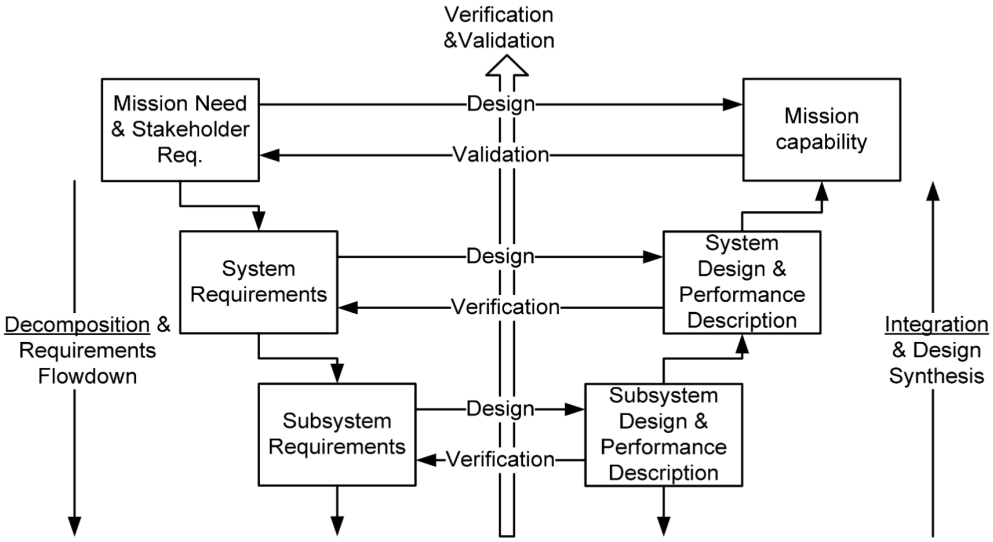

Figure 18.1: V-diagram for systems engineering[67].

18.1. Verification

As previously mentioned, the verification of the design consists of determining if the requirements have been met. To meet some requirements it is necessary to include a certain component, others determine the size of certain part. All of this was taken into account during the design process, and now it is up to verification methods to evaluate whether or not they have been met successfully.

18.1.1. Verification Methods

There are four main methods of verification of requirements. These are:

- Review of design
- Analysis
- Inspection
- Test

Review of design This method consists of reviewing the documentation of the design process to establish if the requirements are met. This is for example determining whether the design counts with a certain component needed to meet the requirement. It also refers to the process of following a design method and determining whether a step determined by a requirement has been followed.

Analysis The analysis method establishes, through mathematical or other modelling techniques and analysis, if a certain requirement has been met. For analysis verification different options can be used. These are:

- **Performance analysis:** this can include a simulation tool to determine whether with the current aircraft characteristics it is able to meet a certain requirement on its performance. Performance analyses have been performed in Chapter 7 and Chapter 10.
- **Structural analysis:** this type of analysis can include a finite element method simulation, although, for the purpose of this design other simpler analytical or numerical methods can be used. These include a boom idealisation to determine whether a certain force can be sustained by the structure. Essentially, a similar tool that the one used for designing can be then used for verifying. Structural analyses have been performed in Chapter 4.
- **RAMS analysis:** this is a qualitative analysis on the reliability, availability, maintainability and safety characteristics of the design. It is mainly used to determine whether the *Safety & Reliability* requirements have been met. A RAMS analysis has been done in Chapter 13.
- **Cost analysis:** this is a breakdown of the costs relevant to the the different stages of the aircraft. It can be performed through estimating methods or specific cost identification. This is performed in Chapter 2.
- **Aerodynamic analysis:** This analysis of the design determines the aerodynamic characteristics of the aircraft. It can be done through CFD analysis, however, similarly to with the structural analysis, other tools based on potential flow or vortex lattice method can be used used, in this case, AVL. This is performed in Chapter 6.

Inspection & Test These verification methods are intended for a physical product. They consist on the examination and scrutiny over the final product and on the testing of components or the entire aircraft. For this reason, these verification methods are not applicable for the final design which has not been produced. There are requirements which are currently verified through a review or analysis that could later on - if possible - be inspected or tested to determine with a higher certainty if the requirements have been met.

18.1.2. Compliance Matrix

With the described verification methods all of the previously stated requirements are verified. If they have been met then the compliant is marked as "Yes", if they have not it is marked as "No". From Table 18.1 to Table 18.6, the compliance matrix is shown, specifying the compliant, verification method, description and reference in the report for each of the requirements.

Table 18.1: Compliance Matrix - 1/6

Requirement ID	Requirement	Compliant	Verification Method	Description	Reference
FFA-Per-001	The aircraft shall be capable of delivering an average of 15 tonnes of water per hour of operation on a fire taking place 250km away from the airfield and 30km away from the nearest usable body of water.	Yes	Analysis	The amphibious aircraft is able to deliver water taken from a body of water. Given the water capacity, fuel performance and speed of the aircraft it is able to reach the water delivery performance.	See Chapter 10, Chapter 7 and Chapter 8
FFA-Per-002	The aircraft shall be able to be deployed 20,000km from its main base within one week.	Yes	Analysis	Given the ferry range of the aircraft, its cruise speed and operations it is able to cover the distance in a shorter time.	See Chapter 10, Chapter 7 and Chapter 8
FFA-Per-003	The aircraft shall be able to take-off from a 2,000m runway at sea-level and standard atmosphere conditions.[1]	Yes	Analysis	The power available by the aircraft is able to deliver enough to take-off from a 1000m runway given its maximum take-off weight.	See Chapter 10and Chapter 7
FFA-Per-004	Secondary missions such as search and rescue, medical evacuation and equipment transport shall be applied if possible.	Yes	Review of Design	The aircraft counts with space for storage, a boat for rescue and medical evacuation.	See Chapter 15 and Chapter 4
FFA-Per-005	The aircraft shall have a rate of descent of at least 20 m/s.	Yes	Analysis	The aircraft is able to meet 23 m/s during the water drop manoeuvre.	See Chapter 10
FFA-Per-006	The aircraft shall have a rate of climb of at least 12 m/s. [2]	Yes	Analysis	The aircraft can reach a rate of climb of over 13m/s.	See Chapter 10 and Chapter 7.
FFA-Per-007	The aircraft shall have an operational range of 1250 km.	Yes	Analysis	The aircraft's fuel tanks allow for 2184 km of operational range.	See Chapter 10 and Chapter 7.
FFA-Per-008	The aircraft shall have a capacity for six persons of maximum length 2.0m and average weight of 80kg while performing search and rescue.	Yes	Analysis	The aircraft has 12 space for medical beds capacity and can carry more people in the fuselage.	See Chapter 15 and Chapter 4

Table 18.2: Compliance Matrix - 2/6

Requirement ID	Requirement	Compliant	Verification Method	Description	Reference
FFA-Per-009	The aircraft shall be able to transport 4000 kg of cargo.	Yes	Analysis	The aircraft can use part of its payload weight for cargo.	See Chapter 15 and Chapter 4
FFA-Per-010	The aircraft shall be able to drop a supply package of 4000 kg .	Yes	Analysis	The aircraft can use part of its payload weight for supply package.	See Chapter 15 and Chapter 4
FFA-S&R-001	The platform shall be equipped with collision-avoidance systems to guaranty flight safety at low altitude and in mountainous areas.	Yes	Review of Design	The avionics subsystem of the aircraft counts with these systems	See Chapter 11
FFA-S&R-002	Engines and systems shall be redundant.	Yes	Review of Design	There are four engines and other systems are designed redundant.	See Chapter 7 and Chapter 11
FFA-S&R-003	The airframe shall be sized to sustain harsh operating conditions, such as high loads from fire updraft and extreme manoeuvres.	Yes	Review of Design	The load factors and manoeuvres loads are taken into account when sizing the internal structure of the aircraft.	See Chapter 4
FFA-S&R-004	Airframe fatigue shall be accounted for when sizing the aircraft.	Yes	Review of Design	Fatigue cycles that reduce properties of the structure are taken into account when sizing through the safety factor included.	See Chapter 4
FFA-S&R-005	The aircraft shall comply to the safety regulations set by authorities.	Yes	Review of Design	The aircraft follows guidelines set by authority EASA, following CS25 regulations	On all chapters.
FFA-S&R-006	The aircraft shall have double redundancy in the avionics.	Yes	Review of Design	The aircraft counts with redundancy on avionic systems	See Chapter 11
FFA-S&R-007	The propulsion shall have single redundancy.	Yes	Review of Design	The aircraft counts with four engines and the control surfaces take into account an IOE situation.	See Chapter 7 and Chapter 11
FFA-Sus-001	Recycling used civilian or military aircraft shall be considered.	Yes	Review of Design	The recycling of existing aircraft was taken into consideration as a conversion option.	See Chapter 3
FFA-Sus-002	Use of recycled material shall be maximised.	Yes	Review of Design	When selecting materials the use of recyclable metals is maximised for sustainability	See Chapter 4 and Chapter 12.

Table 18.3: Compliance Matrix - 3/6

Requirement ID	Requirement	Compliant	Verification Method	Description	Reference
FFA-Sus-003	Propulsion using biofuel shall be used if possible.	Yes	Review of Design	The engines are compatible and have been tested to fly on biofuels	See Chapter 7 and Chapter 12.
FFA-Sus-004	The aircraft mission-specific subsystems shall be adaptable to different mission profiles.	Yes	Review of Design	The aircraft is able to be used on different mission profiles and secondary missions.	See Chapter 15.
FFA-Sus-005	The aircraft subsystems shall be adaptable to future upgrades.	Yes	Review of Design	The aircraft has space to be adaptable for other operations.	See Chapter 15
FFA-Sus-006	Parts of the aircraft shall be reusable at the end of its life.	Yes	Review of Design	The use of recyclable materials is maximised for after life purposes.	See Chapter 12.
FFA-EnB-001	The trade-off shall be achieved between acquisition cost, maintenance cost, projection capabilities, sustainability and operational performances.	Yes	Review of Design	During the concept selection these criteria were taken into account	See Chapter 3.
FFA-EnB-002	In-flight water refilling capabilities (such as an amphibious plane) shall be traded off against a platform allowing airfield refill only.	Yes	Review of Design	During the concept selection these criteria were taken into account	See Chapter 3.
FFA-EnB-003	There shall be a trade off between designing a purpose-made aircraft or converting an existing platform (with permanent or temporary modifications).	Yes	Review of Design	During the concept selection these criteria were taken into account	See Chapter 3.
FFA-Cos-001	The price relative to performance of the developed aircraft shall not exceed current platforms (25 million Euros for the CL415).	Yes	Review of Design	The cost of the aircraft relative to its water delivery performance exceeds the one of other firefighting aircraft.	See Chapter 10, Chapter 2 and Section 16.2.
FFA-Cos-002	The manufacturing costs shall be 20 million Euros.	Yes	Review of Design	The manufacturing costs of the aircraft meet the requirement.	See Section 16.2.
FFA-Cos-003	The maintenance costs for general maintenance shall be 20 million Euros over the first 10 years.	Yes	Review of Design	The maintenance cost are estimated to be around below this value for this period of time	See Section 16.2.

Table 18.4: Compliance Matrix - 4/6

Requirement ID	Requirement	Compliant	Verification Method	Description	Reference
FFA-S&M-001	The parts of the aircraft exposed to water shall be corrosion resistant.	Yes	Review of Design	During the concept selection these criteria were taken into account	See Chapter 5 and Section 13.3.
FFA-S&M-002	The aircraft structure shall be able to perform 5500 of flights.[3]	Yes	Analysis	The airframe is sized to sustain the fatigue loads related to the flight cycles of the aircraft.	See Chapter 4.
FFA-S&M-003	The aircraft structure shall withstand temperatures of up to 200°C.	Yes	Analysis	The selection of materials of the aircraft is based on this temperature limit and scheduled maintenance ensures the structure integrity	See Chapter 4.
FFA-S&M-004	The aircraft structure shall be able to withstand gust winds of 20 m/s.	Yes	Analysis	The airframe is sized to endure the loads and the control surfaces sized to maintain the aircraft controllable and stable	See Chapter 4 and Section 9.3.
FFA-S&M-005	The aircraft structure shall withstand a load factor of +3.75g, -1.5g.	Yes	Analysis	The load factor is taken into account for the sizing of the airframe.	See Chapter 4.
FFA-S&M-006	The landing gear shall be capable of withstanding landing load.	Yes	Analysis	The landing gear is sized to sustain landing loads	See Section 9.2 and Section 9.3.
FFA-Ctrl-001	The aircraft shall be controllable.	Yes	Analysis	The aircraft's control surfaces allow it to be controllable	See Section 9.2 and Section 9.3.
FFA-Ctrl-002	The aircraft shall be stable.	Yes	Analysis	The aircraft's c.g location, neutral point and other properties make it stable	See Section 9.2 and Section 9.3.
FFA-E&A-001	The aircraft shall be equipped with a Global Navigation Satellite System (GNSS).	Yes	Review of Design	This system is part of the avionics of the aircraft	See Chapter 11.
FFA-E&A-002	The navigational parameters shall be monitored and displayed to the pilot(s).	Yes	Review of Design	The navigational parameters are obtained and displayed.	See Chapter 11.
FFA-E&A-003	The primary flight parameters shall be monitored and displayed to the pilots in accordance with regulations set by airworthiness authorities.	Yes	Review of Design	The regulations by authorities are taken into account for internal system communication	See Chapter 11.

Table 18.5: Compliance Matrix - 5/6

Requirement ID	Requirement	Compliant	Verification Method	Description	Reference
FFA-E&A-004	The aircraft shall be equipped with a weather detection system.	Yes	Review of Design	This system is part of the avionics of the aircraft	See section in avionics
FFA-FOp-001	The aircraft shall have a ferry range of 2700 km.	Yes	Analysis	The aircraft fuel tank allow it to reach a ferry range over 5000 km	See Chapter 7 and Chapter 10.
FFA-GrO-001	The aircraft shall have a turn radius of 20 m while on the ground.	Yes	Analysis	The aircraft, based on the landing gear positioning can reach under 10 m turn radius.	See Section 9.1.
FFA-GrO-002	The normal maintenance policy of the aircraft shall comply to the regulations given by the authorities.	Yes	Review of Design	The maintenance operations of the aircraft are performed according to authorities	See Chapter 15.
FFA-GrO-003	The aircraft's systems shall be accessible to maintenance crew.	Yes	Review of Design	The aircraft's layout counts with space to perform maintenance operations.	See Chapter 15 and Section 13.3.
FFA-GrO-004	The total turnover time of the aircraft shall be maximum 60 mins.	Yes	Analysis	This turnover time allows the aircraft to deliver the estimated performance.	See Chapter 15.
FFA-GrO-005	Refuelling shall take place at a rate of 350 L/min.	Yes	Analysis	This condition allows the aircraft to operate as required for mission performance.	See Chapter 15 and Chapter 7.
FFA-GrO-006	Refilling retardant tanks shall take at a rate of 2000 L/min.	Yes	Analysis	This rate is allows by the design of the fire extinguishing system.	See Chapter 8.
FFA-GrO-007	Refilling concentrate tanks shall take at a rate of 500 L/min.	Yes	Analysis	This rate is allows by the design of the fire extinguishing system.	See Chapter 8.
FFA-Com-001	The aircraft shall be equipped with a transponder.	Yes	Review of Design	This system is part of the avionics of the aircraft.	See Chapter 11.
FFA-Com-002	The pilots shall be able to communicate to ATC and other aircraft.	Yes	Review of Design	This system is part of the avionics of the aircraft.	See Chapter 11.
FFA-Com-003	The pilot(s) shall be able to communicate with the Fire Brigade.	Yes	Review of Design	This system is part of the avionics of the aircraft.	See Chapter 11.

Table 18.6: Compliance Matrix - 6/6

Requirement ID	Requirement	Compliant	Verification Method	Description	Reference
FFA-Com-004	The pilot(s) shall be able to send data regarding fires.	Yes	Review of Design	This system is part of the avionics of the aircraft.	See Chapter 11.
FFA-Com-005	Communication with the ground shall function when a natural obstruction, such as terrain, is present.	Yes	Review of Design	The selected components are certified to function in this condition.	See Chapter 11.
FFA-Com-006	Communication with the ground shall function in the presence of expected atmospheric disturbances.	Yes	Review of Design	The selected components are certified to function in this condition.	See Chapter 11.
FFA-Com-007	The bandwidth of the communication system shall be between airband limits.	Yes	Review of Design	The communication system allows the bandwidth to be between this limits.	See Chapter 11.
FFA-Oth-001	The platform shall be equipped with a well-known power plant model to ease maintenance work in remote locations where spare parts may be scarce.	Yes	Review of Design	The powerplant is well-known and the manufacturer company has MRO service globally for maintenance.	See Chapter 7 and Section 13.3
FFA-ExS-001	The aircraft shall have a retardant tank.	Yes	Review of Design	A retardant tank is part of the extinguishing system.	See Chapter 8.
FFA-ExS-002	The aircraft shall have a concentrate tank.	Yes	Review of Design	A concentrate tank is part of the extinguishing system.	See Chapter 8.
FFA-ExS-003	The aircraft shall have a retardant mixing system.	Yes	Review of Design	A retardant mixing system is part of the extinguishing system.	See Chapter 8.
FFA-ExS-004	The retardant tanks shall be refilled on the airport.	Yes	Review of Design	This is possible by the ground fill adaptor located on the extinguishing system.	See Chapter 8.
FFA-ExS-005	The retardant tank shall store commercially available liquid fire retardant.	Yes	Review of Design	This is a possibility by the design of the extinguishing system.	See Chapter 8.

18.2. Validation

As a final step, it is necessary to determine if the developed design is able to achieve what is determined by the mission need.

As previously mentioned, the mission need statement reads:

"Develop the next generation firefighting aircraft, able to outperform and replace an ageing fleet, to improve aerial support during firefighting operations".

As mentioned in Chapter 2 the developed MANTÆ aircraft is the best performing option for a firefighting mission. This includes not only a water delivery performance, but also performance to cost parameter. Taking this into account, the aircraft is most likely to be considered as an outperforming option for the ageing firefighting fleet. A mission simulation of the aircraft with its aerodynamic, performance, propulsion and structural characteristics is performed in Section 7.6.6 and Chapter 10. With this developed tool it is determined that the aircraft reaches the required mission. On addition to this, the aircraft is able to perform secondary missions such as search and rescue, medical evacuation and cargo transport as explained in Chapter 15. This also shows an improvement in the aerial support that the aircraft offers in addition to firefighting operations.

As mentioned in Chapter 12, it is a most important feature of future generations of aircraft to have sustainable properties that ensure the possibility of being used today without compromising the situation of future generations. For this reason the MANTÆ aircraft is developed to be as sustainable as possible. This is reflected in the selection of materials for the airframe in Chapter 4. The aircraft also has a high fuel efficiency and is able to use bio-fuels. This allows the aircraft to reduce the overall CO2 emissions which make it a more sustainable choice. This feature give the aircraft an additional advantage over the ageing fleet and proves it to be truly a next generation aircraft capable of outperforming the current fleet of firefighting aircraft.
It is important to mention that the lack of other amphibious blended wing-body aircraft limits the possibility of comparing the aircraft's performance and the amount of validation data. So far, a mission scenario test was performed, the output was shown in Chapter 10. Additional validation procedures that should be performed further into the development of the MANTÆ are testing and simulations. These can be done through the production of specific parts or of a smaller model to do wind tunnel testing.

19 Conclusion

19.1. Conclusion

To conclude, the MANTÆ aircraft is an aircraft that will be capable of delivering $31,500 L/h$ to a fire that is $250 km$ away from the main base, and $30 km$ away from a usable water source. It can operate in remote areas with runways that of low quality (dry grass or hard sand) and has a maximal operational range of $2184 km$ and a ferry range of up to $5224 km$[1] enabling it to cover a distance of up to $78,624 km$ per week[2].

Precautions have been made, such that secondary missions can also be performed. This includes search and rescue, cargo transport and medical evacuations. To cater for these needs, a rescue rib is included, as well as space for a medical bay and a large cargo door through which cargo could be placed into the aircraft.

The estimated cost of the aircraft is equal to 48.5 million dollars. This gives the MANTÆ a performance relative to cost higher than that of the Canadair CL-415, it's performance-wise closest competitor (17% better performance to cost).

A 3D render and a top down view of the aircraft is provided below in Figure 19.1 and Figure 19.2.

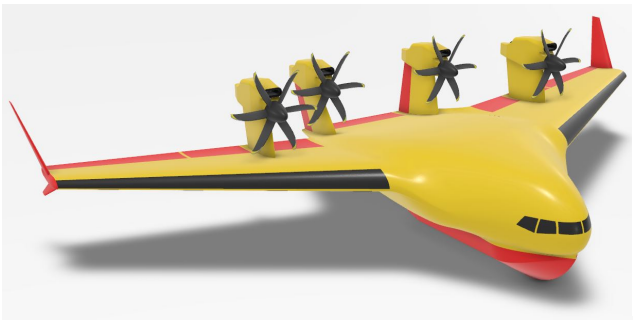

Figure 19.1: 3D rendering of the MANTÆ aircraft

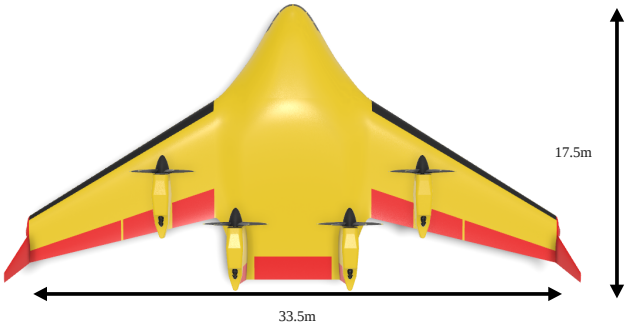

Figure 19.2: Top-down view of aircraft including wing span and aircraft length.

19.2. Recommendations

This report is by no means the final optimal design of such an aircraft. Throughout the design procedure, notably due to time constraints, various options were eliminated, as conducting a proper investigation would require too much time, to the detriment of other aspects of the design. It is important that the reader realises that this also means that a number of assumptions and conclusions were made, which were based on literature and general knowledge. While these were verified and validated as much as possible, they should by no means be taken as absolute, especially when considering the rapid rate of technological advancements.

19.2.1. Design Choices

Throughout the process of this DSE, a number of decisions and trade-offs were performed, based on knowledge at the time. With the knowledge gained since a number of decisions warrant reevaluating. Very early on in the design process it was decided to go with turboprop engines, as these were more efficient than jet engines and promised better acceleration and performance at the speeds and altitudes common to firefighting. While those criteria have not changed, other aspects were not taken into account, such as the ease of mounting. The penalty of mounting turboprop engines with their required propeller clearance was not taken into account. Furthermore, propfan engines were not considered due to the lack of mass produced engines of this type. This follows from the requirement to use a common mass produced engine to ensure that spare parts are cheap and readily available. Should this requirement change, or should a mass produced version of this engine hit the market, it should definitely be considered.

During the initial design of the hull, research was done into the various requirements of the hull, and the design considerations used to meet those requirements. Research focused on existing previous flying boats. This meant

[1] With ferry tanks, without ferry tanks, the ferry range is 2350 km

[2] Not taking into account landings and take-offs, constantly flying at a cruise speed of 130 m/s

that little to no information was found on catamaran and trimaran configuration. This lack of information meant that these configurations were eliminated, despite the potential advantages they might bring, as these were heavily dependent on assumptions. The trimaran configuration in particular should be evaluated, as the central hull still allows for a balanced internal tank layout and scooping mechanism, while potentially offering a reduced aerodynamic impact and improved stability on water.

Furthermore, as the hull was designed using empirical formulas its design can't be directly verified and validated. This should still be performed. Verification can be performed by recreating the hull in integrated naval architecture tools like MAXSURF, while validation can be performed with a drag test of a scaled model.

The airfoil choice was based upon the results of the AVL program used to analyse the combined result of having different airfoils on the inner and outer sections of the wing. This program however is based on the vortex lattice method, which cannot model flow separation. A constant source of trouble was this lack of capability, which in turn engendered problems, with AVL at times not providing values at all, resulting in the elimination of the airfoil. It must therefore be recommended that each airfoil be tested with a more accurate program. Furthermore, the final chosen airfoil was particularly thick, and may have airflow separation at low angles of attack. This airfoil was chosen as it performed best, notably in stability, at the end of a number of iterations. However, due to time constraints, no further iterations could be made, and only a relatively small number of airfoils could be analysed. This leads to the recommendation of adding more airfoils to test.

The limited range of the aircraft is what makes it perform worse on long-ranged missions compared to its competitors. As shown in the chapter, a one-way ferry tank for flying towards the mission site will eliminate this deficiency. If this method is chosen the operations need to be adapted in order to make full use of this.

As a result of the combination of hull design and aerodynamics, a final planform was settled upon. However, this planform has significant impacts on the viability of various airfoils and hulls, and the reverse is also true. It is therefore recommended, as it was previously recommended to further experiment with other airfoils and untested hulls, to experiment with the planform. Notable mentions are that width and length of the centerbody for a trimaran configuration, and wing sweep for airfoil choice and stability calculations.

The previously mentioned limits of the AVL program are a feature common to other programs and calculations. A number of simplifications were made in the calculation of the structure of the aircraft. The final design is simple, and based on general conservative assumptions. It is therefore reasonable to expect that significant weight reductions can be achieved with a more detailed analysis and design, notably using Finite Element Analysis (FEM) to optimise the design. This can also validate the current design, and model more complex loading scenarios. A more in depth design would also be beneficial. Currently, due to time constraints, stringers and ribs to prevent buckling are planned, but not sized according to calculations. Furthermore, due to the clear issues AVL had in calculating drag, and the general shape of the wingbox, it was assumed that drag would not be the critical load scenario, and so the wingbox was not sized for the moment generated by drag. However, this assumptions may not be valid with combined loading. The design of the integration of the hull to the fuselage load bearing structure was also not fleshed out due to time constraints. These issues could prove problematic, notable under combined loading scenarios that are complex to analyse, and computationally expensive. A better aerodynamic analysis combined with a FEM analysis would be needed to ensure no failure occurs.

A number of calculations are based on partial inexact data. The previously mentioned conservative structure calculations and aerodynamic calculations are prime examples. Further calculations stemming from this carry these errors forwards. The cost and performance calculations are therefore not final, and will vary. This will need to be further refined with a more detailed calculation once such values become available that it is possible.

Bibliography

[1] Rashid Ali & Omran Al-Shamma. A comparative study of cost estimation models used for preliminary aircraft design. *Global Journal of Researches in Engineering: Automotive Engineering*, 14, 2014.

[2] Edward Keating. Air Attack Against Wildfires: Understanding U.S. Forest Service Requirements for Large Aircraft, 2018. URL https://www.rand.org/pubs/monographs/MG1234.html.

[3] US Forest Service. Interagency Standards for Fire and Fire Aviation, 2009. URL https://www.nifc.gov/policies/red_book/archive/2009RedBook.pdf.

[4] H H Erwich, I. H. de Boer, P. A. Decormis Leon, D. J. Hélant Muller, F. V. Hoogeboom, L. M. Middendorp, M. A. J. Maurer, J. N. P. Post, H. M. Rutten, and K. B. Wessendorp. Next Generation Firefighting Aircraft Baseline Report. Technical report, Delft University of Technology, 2020.

[5] H H Erwich, I. H. de Boer, P. A. Decormis Leon, D. J. Hélant Muller, F. V. Hoogeboom, L. M. Middendorp, M. A. J. Maurer, J. N. P. Post, H. M. Rutten, and K. B. Wessendorp. Next Generation Firefighting Aircraft Midterm Report. Technical report, Delft University of Technology, 2020.

[6] Daniel P. Raymer. *Aircraft Design: A Conceptual Approach*. American Institute of Aeronautics and Astronautics, 6 edition, 1989. ISBN 1624104908, 9781624104909. URL https://books.google.nl/books/about/Aircraft_Design.html?id=3G1uuwEACAAJ&source=kp_book_description&redir_esc=y.

[7] Steve Hall. Consolidation and Analysis of Loading Data in Firefighting Operations Analysis of Existing Data and Definition of Preliminary Air Tanker and Lead Aircraft Spectra, 2005.

[8] BEAD-air. BEAD-air-S-2005-013-A. Technical report, French Ministry of Defence, 2008.

[9] Ger J.J. Ruijgrok. *Elements of Airplane Performance*. Delft Academic Press, Delft, 2 edition, 2009.

[10] CONAIR. 2018 Transport Canada Delegates. Conference Presentation, 2018.

[11] Joris Melkert and Calving Rans. Lectures slides week 5: Holes and cut-outs, 2020. URL https://brightspace.tudelft.nl/d2l/le/content/213463/viewContent/1586092/View.

[12] R. M. Ajaj & M. I. Friswell & D. Smith & A. T. Isikveren. A conceptual wing-box weight estimation model for transport aircraft. *Aeronautical Journal*, 177(1191):533–551, May 2013.

[13] D Howe. Blended wing body airframe mass prediction. *Proceedings of the Institution of Mechanical Engineers, Part G: Journal of Aerospace Engineering*, 2001. ISSN 09544100. doi: 10.1243/0954410011533329.

[14] Glynn Garlick. Plane sailing: the seaplane of the future?, 2015. URL https://www.theengineer.co.uk/plane-sailing-the-seaplane-of-the-future/.

[15] A G Smith, B Sc, J E Allen, B Sc Eng, and A M I E Mech. Water and Air Performance of Sea- plane Hulls as affected by Fairing and Fineness Ratio Water and Air Performance of Seaplane Hulls Affected by Fairing and Fineness Ratio. *Reports and Memoranda 2896, Aeronautical Research Council*, 1950.

[16] Y. Staelens. Study of belly-flaps to enhance lift and pitching moment coefficient of a blended-wing-body airplane in landing and takeoff configuration. *PhD Thesis*, 2007.

[17] Geoffrey M. Lilley David P. Lockard. The Airframe Noise Reduction Challenge, 2004. URL https://ntrs.nasa.gov/archive/nasa/casi.ntrs.nasa.gov/20040065977.pdf.

[18] Zhang Dejiu Li Yong, Wang Xiunnan. Control Strategies for Aircraft Airframe Noise Reduction, 2012.

[19] David P. Lockard Craig L. Streett. Aerodynamic Noise Reduction for High-Lift Devices on a Swept Wing Model, 2006. URL https://arc.aiaa.org/doi/abs/10.2514/6.2006-212.

[20] European Union Aviation Safety Agency. Certification Specifications and Acceptable Means of Compliance for Large Aeroplanes, 2020.

[21] Pratt & Whitney. General Aviation Engines, 2020. URL https://www.pwc.ca/en/products-and-services/products/general-aviation-engines.

[22] Pratt & Whitney. Regional Aviation, 2020. URL https://www.pwc.ca/en/products-and-services/products/regional-aviation-engines.

[23] Honeywell. TPE331 Engines, 2020. URL https://aerospace.honeywell.com/content/dam/aero/en-us/documents/learn/products/engines/brochures/N61-1491-000-000-TPE331-10TurbopropEngine-bro.pdf?download=true.

[24] Rolls Royce. Aerospace Defence AE2100, 2020. URL https://www.rolls-royce.com/{~}/media/Files/R/Rolls-Royce/documents/customers/civil-aerospace/ae2100-tcm92-5742.pdf.

[25] Rolls Royce. Aerospace Defence T56, 2020. URL https://www.rolls-royce.com/products-and-services/defence/aerospace/transport-tanker-patrol-and-tactical/t56.aspx{#}section-overview.

[26] General Electric. GE H-Series, 2020. URL https://www.geaviation.com/sites/default/files/HSeries{_}datasheet.pdf.

[27] European Union Aviation Safety Agency. CT7-series engines, 2019. URL https://www.easa.europa.eu/sites/default/files/dfu/TCDSIME010Issue7.pdf.

[28] Europrop. The TP400-D6, 2020. URL http://www.europrop-int.com/the-tp400-d6/.

[29] Ichvenko Progress. Al-20 engines, 2020. URL http://ivchenko-progress.com/?portfolio=ai-20{&}lang=en.

[30] Ichvenko Progress. Al-24, 2020. URL http://ivchenko-progress.com/?portfolio=ai-24{&}lang=en.

[31] Ichvenko Progress. TV3 engine, 2020. URL http://ivchenko-progress.com/?portfolio=sbm1{&}lang=en.

[32] Pratt & Whitney. PW100/150, 2020. URL https://www.pwc.ca/en/products-and-services/products/regional-aviation-engines/pw100-150.

[33] European Aviation Safety Agency. TYPE-CERTIFICATE DATA SHEET PW150A. Technical report, European Aviation Safety Agency, 2014.

[34] R. I. McCormick E. Hosking, D. P. Kenny and A. A. Smailys S. H. Moustapha, P. Sampath. The PWlOO Engine: 20 Years of Gas Turbine Technology Evolution. Technical report, Pratt & WHitney, Quebec, 1998.

[35] Forecast International. The Market for Aviation Turboprop Engines, 2010. URL https://www.forecastinternational.com/samples/F641{_}CompleteSample.pdf.

[36] Colin Cutler. How A Constant Speed Propeller Works, 2017. URL https://www.boldmethod.com/learn-to-fly/aircraft-systems/how-a-constant-speed-prop-works/{#}:{~}:text=Constantspeedpropellersworkbyvaryingthepitchofthepropellerblades.{&}text=Atthesametime{%}2Cmore,andtheenginespeedsup.

[37] Hunt, Hugh Harrison, U.S. Navy Naval Air Systems Command. *Aerodynamics for Naval Aviators.* Ravenio Books, 1 edition, 1965.

[38] FlyRadius. Bombardier Q400 Propeller - Dowty R408, 2015. URL https://www.flyradius.com/bombardier-q400/propeller-dowty-r408.

[39] European Union Aviation Safety Agency. R408 series propellers Datasheet. Technical report, EASA, 2008.

[40] Modern Transport and Environment. ATR: The Optimum Choice for a Friendly Environment, 2016. URL https://web.archive.org/web/20160808173542/http://web.fc.fi/data/files/ATR{_}TheOptimumChoice.pdf.

[41] International Civil Aviation Organization. Annexes 1 to 18. Technical report, The Convention on International Civil Aviation, 1974. URL https://www.icao.int/safety/airnavigation/nationalitymarks/annexes{_}booklet{_}en.pdf.

[42] Peter Henley. Quiet revolution. *FLight Global*, 2000. URL https://www.flightglobal.com/quiet-revolution/31793.article.

[43] Graham Warwick. Turboprop- and proud of it. *FLight Global*, sep 1998. URL https://www.flightglobal.com/turboprop-and-proud-of-it/22922.article.

[44] European Union Aviation Safety Agency. TYPE-CERTIFICATE DATA SHEET FOR NOISE. Technical report, European Union Safety Agency, 2019. URL https://www.easa.europa.eu/sites/default/files/dfu/EASA.IM{_}.A.191Issue6.pdf.

[45] European Union Aviation Safety Agency. Type-Certificate Data Sheet for Noise - A320. Technical report, European Union Safety Agency, 2020. URL https://www.easa.europa.eu/sites/default/files/dfu/TCDSNEASA.A.064.3Issue26.pdf.

[46] SkyNRG. Porter Airlines Operates Bombardier Q400 Aircraft in Canada's First Biofuel-Powered Revenue Flight, apr 2012. URL https://skynrg.com/wp-content/uploads/2019/03/20120417{_}Press{_}Release{_}Porter-Biofuel-Powered-Flight{_}EN.pdf.

[47] PTI. SpiceJet operates India's first biofuel powered flight, aug 2018. URL https://economictimes.indiatimes.com/industry/transportation/airlines-/-aviation/spicejet-operates-indias-first-biojet-fuel-flight/articleshow/65560105.cms?from=mdr{#}:{~}:text=Thenearly45-minuteflight,ataround1150hourshere.{&}text=However{%}2Cuseofbiofuelforregularflightswouldtakesometime.

[48] Cast Safety. PROPELLER OPERATION AND MALFUNCTIONS BASIC FAMILIARIZATION FOR FLIGHT CREWS, 2020. URL https://www.cast-safety.org/pdf/4{_}propeller{_}fundamentals.pdf.

[49] Mike Kloch. AIRPLANE TURBOPROP ENGINES BASIC FAMILIARIZATION, 2018. URL https://mikeklochcfi.files.wordpress.com/2018/08/airplane-turboprop-engines-basic-familiarization.pdf.

[50] All Agencies. Chapter 16 Aviation Operations and Resources. *Redbook 2020*, pages 323–356, 2020.

[51] Kevin Merill. Amphibious Water Scooper Aircraft, Operations Plan 2016. *United States Department of Agriculture*, 2016.

[52] I T Loane and J S Gould. Aerial suppression of bushfires: cost-benefit study for Victoria. *National Bushfire Research Unit*, 1986.

[53] Kevin Merrill. Water Enhancers for Wildland Fire Management. Technical report, Us Forest Service, 2019.

[54] Joe Madar. Foam vs fire. Technical Report October, National wildfire coordinating group, 2019.

[55] Edward Goldberg, Fire Safety, and Phos-chek Fire Retardant. Use of Fire Chemicals in Aerial Fire Fighting, 2010.

[56] Charles George and Fred Fuchs. Improving Airtanker Delivery Performance. *Oxford University*, 52(2):31–39, 1986. URL https://books.googleusercontent.com/books/content?req=AKW5QaeZb8cCzWl4I5L5LPrBClSJJgAXxJxciOIe9Nj7iGbkyHgkrSKm9{_}f{_}eQZBmoPJ-LQQeri7eZdQbiBrACMUvmaqh8k

[57] Kohyu Satoh, Iwao Maeda, Kunio Kuwahara, and K. T. Yang. A numerical study of water dump in aerial fire fighting. *Fire Safety Science*, pages 777–787, 2005. ISSN 18174299. doi: 10.3801/IAFSS.FSS.8-777.

[58] The Goodyear Tire & Rubber Company. Global Aviation Tires, 2020. URL https://www.goodyearaviation.com/resources/pdf/databook-6-2018.pdf.

[59] A.C. in 't Veld. *AE3212-I: Aerospace Flight Dynamics & Simulation*. TU Delft, 2019.

[60] Eduardo D. Sontag. *Mathematical Control Theory*. Springer, New Brunswick, NJ 08903, 1998. ISBN 0-387-98489-5.

[61] Daniel Alazard Clément Toussaint Gilles Taquin Yann Denieul, Joël Bordeneuve-Guibé. Multicontrol Surface Optimization for Blended Wing–Body Under Handling Quality Constraints. *Journal of Aircraft, American Institute of Aeronautics and Astronautics*, pages 1–14, 2017. ISSN 0021-8669. doi: 10.2514/1.C034268.

[62] MOOG. Actuation and Motion Systems, 2010. URL https://www.moog.com/content/dam/moog/literature/MCG/actprodguide.pdf.

[63] Brown, M and Vos, Roelof. Conceptual Design and Evaluation of Blended-Wing Body Aircraft. In *AIAA Aerospace Sciences Meeting*, Delft, 2018. AIAA. doi: https://doi.org/10.2514/6.2018-0522. URL http://resolver.tudelft.nl/uuid:e080bf9c-cf06-4fd6-9cd1-26c79f66388b.

[64] U.S. Department of transportation. *Advanced Avionics Handbook*. Federal Aviation Administration, 2009. URL https://books.google.nl/books?id=7EbJo-lI6KAC&printsec=frontcover&hl=nl#v=onepage&q=author&f=false.

[65] H H Erwich, I. H. de Boer, P. A. Decormis Leon, D. J. Hélant Muller, F. V. Hoogeboom, L. M. Middendorp, M. A. J. Maurer, J. N. P. Post, H. M. Rutten, and K. B. Wessendorp. Next Generation Firefighting Aircraft Project Plan. Technical report, Delft University of Technology, 2020.

[66] National Research Council. *Sustainability and the U.S. EPA*. The National Academies Press, Washington, DC, 2011. ISBN 978-0-309-21252-6. doi: 10.17226/13152. URL https://www.nap.edu/catalog/13152/sustainability-and-the-us-epa.

[67] M.J.L. van Tooren Ir. R.J. Hamann. *SYSTEMS ENGINEERING & TECHNICAL MANAGEMENT TECHNIQUES*. Delft University of Technology, Delft, 2006.

[68] Flight Safety Systems. Redundancy, 2020. URL https://sites.google.com/site/flightsafetysystems/home.

[69] Poente Technical. AIRPLANE REDUNDANCY SYSTEMS, 2020. URL https://www.poentetechnical.com/aircraft-engineer/airplane-redundancy-systems/.

[70] Ellis ; Hitt and F. Dennis Mulcare. Fault-Tolerant Avionics, 2001. URL https://www.cs.unc.edu/{~}anderson/teach/comp790/papers/fault{_}tolerance{_}avionics.pdf.

[71] Varaprasadarao Manda. AIRCRAFT SERVICING, MAINTENANCE, REPAIR & OVERHAUL-THE CHANGED SCENARIOS THROUGH OUTSOURCING. *International Journal of Research in Engineering and Applied Sciences*, 7(5), 2017.

[72] Anant Sahay. An overview of aircraft maintenance. *Leveraging Information Technology for Optimal Aircraft Maintenance, Repair and Overhaul (MRO)*, pages 1–14, 2012. doi: 9780857091437.1. URL https://www.sciencedirect.com/science/article/pii/B9781845699826500017.

[73] Anant Sahay. Aircraft maintenance paradigm. *Leveraging Information Technology for Optimal Aircraft Maintenance, Repair and Overhaul (MRO)*, pages 33–114, 2012. URL https://www.sciencedirect.com/science/article/pii/B9781845699826500030.

[74] Pratt & Whitney. Pratt & Whitney GTF™ Engine MRO and Repair Network Has Global Reach, 2019. URL https://newsroom.prattwhitney.com/2019-10-14-Pratt-Whitney-GTF-TM-Engine-MRO-and-Repair-Network-Has-Global-Reach.

[75] Federal Aviation Administration. Airplane Flying Handbook. *U.S. Department of Transportation*, page 348, 2016. doi: https://www.faa.gov/regulations{_}policies/handbooks{_}manuals/aircraft/airplane{_}handbook/media/FAA-H-8083-3B.pdf. URL http://scholar.google.com/scholar?hl=en&btnG=Search&q=intitle:Airplane+Flying+Handbook#1.

[76] USDA Forest Service. Amphibious Water Scooper Aircraft Operations Plan. *United States Department of Agriculture*, pages 1–39, 2016. URL https://www.fs.usda.gov/sites/default/files/media_wysiwyg/amphibious_water_scooper_aircraft_operations_plan_final_2016-_041316.pdf.

A
Statistical Data for the Weight Estimation

Table A.1: The statistical data which was used in the weight estimation

Aircraft	Capacity [L]	MTOW [kg]	OEW [kg]	Fuel weight [kg]	Type
Air Tractor Fire Boss	3084	7254.999572	4080.606045	1150.4	Amphibious
Beriev Be-12P	6000	35988.99083	24491.63354	7500	Amphibious
Beriev Be-200	12000	40987.46177	27590.57492	7500	Amphibious
Beriev Be-200ES	12500	42986.85015	27590.57492	7500	Amphibious
CL215(T)	5455	20518.04567	12155.8475	4728	Amphibious
CL415	6136	19883.23761	13603.35303	4650	Amphibious
ShinMaywa US-2	15000	55129.45973	25621.24766	12000	Amphibious
Martin Mars	27255	79353.72538	34267.29413	19640	Amphibious
BWB150	-	72000	38000	-	BWB
Small bussiness jet BWB	-	44300	24400	-	BWB

B
Turboprop Engine Choices Considered

Table B.1: Power Information of Turboprop Engines.

Engine Manufacturer	**Engine Family**	**Engine Name**	**Equivalent Power Take-Off Peq ($ESHP$)**	**Shaft Power Take-Off Pbr (SHP)**	**Shaft Power Take-Off, Pbr (kW)**	**# of engines required**	**# of engines ≤ 4**
Pratt & Whitney	PT6A	PT6A' Small' (A-11 to A-140)	600-1075	500-900	671.09	20	no
		PT6A 'Medium' (A-41 to A-62)	1000-1400	850-1050	671.09	20	no
		PT6A 'Large' (A-64 TO A-68)	1400-1900	700-1900	671.09	20	no
	PT6E	PT6-E series	1825-1845	1100-1200	671.09	20	no
	PW100-150	PW150 Series	6,200.00	5,000.00	3,728.25	4	yes
		PW127 Series	3,200.00	2,750.00	2,050.54	7	no
		PW123/124 Series	3,000.00	2,400.00	1,789.56	8	no
		PW120 Series	2,400.00	2,100.00	1,565.87	9	no
		PW118 Series	2,180.00	1,800.00	1,342.17	10	no
Honeywell Garret	TPE331	TPE331-10	944.00	940.00	700.91	19	no
		TPE331-14	1,833.00	1,650.00	1,230.32	11	no
Rolls Royce	AE2100	AE2100 A/P	4,774.80	4,152.00	3,096.00	5	no
		AE 2100D2	5,332.55	4,637.00	3,458.00	4	yes
		AE2100 D3	5,332.55	4,637.00	3,458.00	4	yes
		AE 2100J	5,279.65	4,591.00	3,423.00	4	yes
	T56	T56-A-7	4,830.00	4,200.00	3,133.00	5	no
		T56-A-14	5,290.00	4,600.00	3,433.00	4	yes
		T56-A-15	5,279.65	4,591.00	3,425.00	4	yes
		T56-A-425	5,290.00	4,600.00	3,433.00	4	yes
		T56-A-427	6,037.50	5,250.00	3,920.00	4	yes
		T56-A-427A	5,865.00	5,100.00	3,806.00	4	yes
	M250	M250 turboprop	N/A	380-450	335.54	39	no
General Electric	GE H-Series	GE H75	862.50	750.00	559.25	24	no
		GE hH80	920.00	800.00	596.54	22	no
		GE H85	977.50	850.00	633.82	21	no
	CT7-9	CT7-9A	2,012.50	1,750.00	1,304.92	10	no
		CT7-9B	2,012.50	1,750.00	1,304.92	10	no
		CT7-9C	2,012.50	1,750.00	1,304.92	10	no
Europrop	TP-400	TP-400-D6	12,650.00	11,000.00	8,202.37	2	yes
Ichvenko Progress	Al-20	AI-20K	4,000.00	3,478.26	2,593.63	5	no
		AI-20M series 6	4,250.00	3,695.65	2,755.74	5	no
		AI-20D series 4	5,180.00	4,504.35	3,358.76	4	yes
		AI-20D series 5	5,180.00	4,504.35	3,358.76	4	yes
		AI-20D series 5M	4,750.00	4,130.43	3,079.94	5	no
	Al-24	AI-24 series 2	2,550.00	2,217.39	1,653.44	8	no
		AI-24VT	2,820.00	2,452.17	1,828.51	8	no
		AI-24T	2,820.00	2,452.17	1,828.51	8	no
	TV3	TV3-117VMA	2,500.00	2,173.91	1,621.02	8	no

C
Stability Coefficients

All the stability coefficients used in Section 9.3.1 and Section 9.3.2 are listed down below in Table C.1 for the cruise and the drop phase. These coefficient have been obtained from AVL. Note that the derivatives w.r.t. control surface deflection (derivatives with a δ) have been multiplied by a factor equal to $\frac{180}{\pi}$, since AVL outputs those derivatives as a function of the deflection in degrees, whereas the derivatives as a function of the deflection in radians is required. Coefficients K_X, K_Y, K_Z and K_{XZ} are the radius of gyration of the aircraft. These are calculated using the mass moment of inertia of the aircraft. The chord c and the span b are also predefined given the aircraft's planform.

Table C.1: Stability coefficients used for dynamic stability analysis for cruise and dropping condition.

Force coefficients			Moment coefficients			Other		
	Cruise	Drop		Cruise	Drop		Cruise	Drop
C_{X_0}	0.0159	0.0717	C_{l_β}	-0.0305	-0.0655	K_X	0.1588	0.1683
C_{X_u}	-0.0069	-0.0154	C_{l_p}	-0.3000	-0.2909	K_Y	0.0865	0.1209
C_{X_α}	0.2716	0.4978	C_{l_r}	0.0094	0.0367	K_Z	0.1789	0.2050
C_{X_q}	0.1411	0.2959	$C_{l_{\delta_a}}$	-0.1377	-0.1327	K_{XZ}	0.0865	0.1209
$C_{X_{\delta_e}}$	0.0386	0.0665	$C_{l_{\delta_r}}$	0.0004	0.0002			
						μ_c	17.2974	8.6832
C_{Y_β}	-0.1204	-0.1167	C_{m_u}	0.0098	0.0204	μ_b	5.3978	2.7097
$C_{Y_{\dot{\beta}}}$	0.0000	0.0000	C_{m_α}	-0.1299	-0.1408			
C_{Y_p}	0.0801	0.1507	$C_{m_{\dot{\alpha}}}$	0.0000	0.0000	C_L	0.1928	0.3709
C_{Y_r}	0.0703	0.0731	C_{m_q}	-0.8623	-0.8833			
$C_{Y_{\delta_a}}$	-0.0001	-0.0013	$C_{m_{\delta_e}}$	-0.3000	-0.3016	c	10.454	10.454
$C_{Y_{\delta_r}}$	0.0685	0.0650				b	33.5	33.5
C_{Z_0}	-0.2093	-0.4895	C_{n_β}	0.0278	0.0364			
C_{Z_u}	-0.1134	-0.2389	$C_{n_{\dot{\beta}}}$	0.0000	0.0000			
C_{Z_α}	0.5745	3.3970	C_{n_p}	-0.0456	-0.0869			
$C_{Z_{\dot{\alpha}}}$	0.0000	0.0000	C_{n_r}	-0.0158	-0.0177			
C_{Z_q}	-3.5219	-3.6209	$C_{n_{\delta_a}}$	-0.0062	-0.0087			
$C_{Z_{\delta_e}}$	-0.0685	-1.0157	$C_{n_{\delta_r}}$	-0.0171	-0.0167			

D
Mission Scenarios

Table D.1: Distances assumed for different mission types and their comparable location on the world.

Mission	Distance Fire (km)	Distance Water (km)	Comparable to
A	100	15	Southern Europe, North America
B	250	30	South-East Asia
C	250	45	Australia
D	350	15	Amazon Forest
E	350	45	Siberia, Africa